12th International Corrosion Congress

PRECEEDINGS

September 19-24, 1993

Volume 6

Houston, Texas USA

ELECTRIC POWER INDUSTRY

NACE International

CORROSION CONTROL FOR LOW-COST RELIABILITY

12th International Corrosion Congress

PRECEEDINGS

VOLUME 6

ELECTRIC POWER INDUSTRY

The manuscripts in this volume have been printed from camera-ready copy and have been accepted without editing by NACE International.

Neither NACE International, its officers, directors, members thereof, nor instructors accept any responsibility for the use of the methods and materials discussed herein.

Any goods, products, and/or services mentioned are mentioned as items of information only. Such mention does not constitute an endorsement by NACE International.

The information is advisory only, and use of the materials and methods is solely at the risk of the user.

ISBN: 1-877914-65-7

Published by

NACE International
P.O. Box 218340
Houston, TX 77218-8340

NACE International

PRECEEDINGS CONTENTS

Paper # Page #

VOLUME 1

PLENARY LECTURES

COATINGS ON STEEL

COATINGS

METALLIC COATING AND SURFACE TREATMENTS

NON-METALLIC COATINGS ON STEEL SUBSTRATES

VOLUME 2

ATMOSPHERIC CORROSION

CHEMICAL PROCESS INDUSTRY WORKSHOP

HIGH TEMPERATURE CORROSION

VOLUME 3B

INHIBITORS

Paper # Page #

LOCALIZED CORROSION/CREVICES

LOCALIZED CORROSION/PITTING

PASSIVITY AND BREAKDOWN

VOLUME 4

CATHODIC PROTECTION

HYDROGEN EFFECTS

OIL AND GAS PRODUCTION AND REFINING WORKSHOP

PIPELINE CORROSION

RELIABILITY AND CORROSION CONTROL OF WELDMENTS/CORROSION RESISTANT ALLOYS

VOLUME 5A

AIRCRAFT

AUTOMOTIVE/ACCELERATED TESTING

CORROSION IN CONCRETE

ELECTRONICS

EXPERT SYSTEMS

SURFACE ANALYSIS TECHNIQUES

NUCLEAR ENERGY AND WASTE STORAGE

Cutting the Costs of Corrosion and Fouling by Real-time Performance Monitoring

P.S.N. Stokes
CAPCIS MARCH Ltd
Manchester, UK

W.M. Cox
CAPCIS MARCH Ltd
Manchester, UK

M.A.Winters
Amoco Corporation
Naperville, Illinois

P.O. Zuniga
Amoco Chemicals Company
Alvin, Texas

Abstract

Excessive fouling and under-deposit corrosion of heat exchangers in cooling water service impede heat transfer and cause equipment failures, resulting in substantial operating costs associated with lost productivity, repair/replacement and on-going maintenance. Reliable on-line monitoring of fouling and corrosion under representative heat exchangers operating conditions is key to successful cooling water system operations. Traditional monitoring tools were inadequate , focusing separately on fouling and corrosion, and tracking corrosion without heat flux. To redress these shortcomings, a combined fouling and corrosion monitoring system has been developed incorporating state-of-the-art electrochemical corrosion monitoring methods with proven deposit on monitoring technology.

Keywords:

Fouling, under-deposit corrosion, on-line performance monitoring, cooling water systems.

INTRODUCTION

Instrumentation Needs

Corrosion of fouled heat exchangers equates to lost revenue in the power generation, nuclear, refining, petrochemical and chemical industries. These losses are incurred directly by reduced thermal efficiency and throughput, and indirectly due to wall penetration, lost plant availability, product contamination, environmental pollution, replacement tube maintenance and inspection. For a major operator the total cost can be considerable.

Conventional monitoring tools have focused separately on fouling or corrosion appraisal. Fouling monitors have been invariably designed for ease of use and simplicity. Recent developments in this field have focused on developing instrumentation which is sensitive to changes in water treatment programs and their effect on fouling at the heat transfer surface. This has given an indication of the heat transfer efficiency of the unit. On-line corrosion monitoring techniques have relied upon information obtained from unheated probes. These only give an indication of the corrosivity of the bulk water and will not give an indication of the corrosion activity of a fouled, heated surface.

A biofilm monitor has recently been developed[1] which is capable of detecting biofilm activity on cooling water components. The monitor uses electrochemical methods to detect corrosion associated with biofilm activity, although in the absence of heat transfer.

Corrosion activity under heat flux differs from corresponding surfaces without heat flux in two ways: First higher temperatures increase the rate of corrosion reaction kinetics. Secondly, non-uniform scales or fouling deposits are not protective and insiduously promote localized under deposit attack rather than uniform corrosion. As such, the presence of scale will often exacerbate damage rather than prevent it.

In recent years it has become increasingly apparent that the simultaneous measurement of corrosion and fouling tendency under heat transfer conditions is necessary to verify the management and performance quality of the chemical treatment packages used in cooling water systems.

The need to upgrade the degree of control and efficiency of cooling water treatment programs has been accentuated by the move to non-chromate treatments using blends of zinc, phosphate, molybdate and/or organic inhibitors. These packages are not only more prone to fouling/deposition but also are less forgiving than the old chromate inhibitors; all of which requires a high level of performance monitoring control.

A recent improvement on the monitoring methods employed has been the development of a combined corrosion and fouling monitoring system. The system is based upon a proven fouling unit , originally designed by the fouling group at Montana State University[2] . The design has been augmented to incorporate state-of-the-art electrochemical methods of corrosion assessment under heat flux. These modern corrosion evaluation

techniques can be used to obtain real-time information on localized attack and under-deposit attack, the most frequent causes of failure in cooling water systems.

Unless a real-time indication of corrosion under heat transfer is monitored, the vicious cycle of cooling water problems, as schematically illustrated in figure 1, will be difficult to break.

MONITORING INSTRUMENTATION AND METHODS

The combined monitoring system comprises a miniature heat exchanger, an electronic flow meter, heat control unit and a data collection device that is linked to storage. The heat exchanger uses a segmented heat exchanger tube (user specified but typically carbon steel) that is coated with heat transfer paste and mechanically clamped in an electrically heated block. A side stream of cooling water is fed through the exchanger and a paddle-wheel flow meter enables the flow to be maintained between 0.30 and 4.6 ms^{-1} and can be kept within ± 0.02 ms^{-1} of the set value. Heat transfer rate can be set between 1000 and 5000 BTU hr^{-1} equating to a typical skin temperature between 38 to 93 °C. At a fixed heat transfer rate the wall temperature will rise to maintain it as deposits form on the heated surface. The skin temperature may also be set but is less commonly used in the field.

Platinum resistance temperature detectors (RTD's) measure the temperature of the fluid and the block outside the tube. Theoretical inside wall temperature, T_W, is calculated by the following equation:

$$T_W = T_b - HI \times Constant$$

Where

T_b = block temperature, °F

HI = heat input, Btu/hr

A mathematical analysis of the entire heat exchanger system determines a constant for zero heat transfer resistance. Convective and conductive resistance is subtracted from overall resistance to yield changes in fouling heat transfer resistance only.

$$HTR_{fouling} = HTR_{overall} - (HTR_{conductive} - HTR_{convective})$$

$HTR_{fouling}$ is output continuously to give an indication of the fouling tendency.

In conjunction with the fouling tendency, the corrosion information is obtained using recently developed electrochemical techniques[3,4] . These techniques address the requirements a monitoring system must have in order to operate effectively in conditions of localized attack such as pitting, crevice or under-deposit corrosion. The electrochemical noise analysis has proven to be powerful in this respect, especially when augmented by impedance measurements. Moreover, the application of these techniques under heat flux, presents a powerful tool for tracking corrosion in a heat exchanger or other environments

where fouling is prevalent. The noise techniques are particularly sensitive to localized corrosion and to the threshold onset of attack. In part this is because they do not rely on an electrochemical response from polarization of a corrosion cell , but evaluate spontaneous signals generated on the electrode surface by the corrosion process itself. Pitting and crevice corrosion give individually distinct traces from the traces obtained from uniform attack.

Electrochemical noise measures the low frequency, low amplitude random and spontaneous fluctuations in potential and current which occur during a corrosion process. Such corrosion processes involve stochastic events, small bursts of activity, which contribute to the overall process. These events produce the noise which is of theoretical and practical interest. The electrochemical potential (EPN) noise technique is highly sensitive during the onset of attack and at fairly low rates of corrosion. At higher rates the potential fluctuations tend to merge, and it is therefore useful to use an instrument which also incorporates electrochemical current noise (ECN) analysis. ECN is the fluctuations on the coupling current between two nominally identical electrodes. The ECN signal also characterizes the type of corrosion attack. Evaluation of the coupling current between the same two electrodes, by zero resistance ammetry (ZRA), also gives a general indication of the corrosion trends at moderate and high corrosion rates. A fourth electrochemical technique, either linear polarization resistance measurement (LPRM) or simple electrochemical impedance spectroscopy (EIS) is also utilised to track generalized corrosion. The combination of the two noise signals, resistance noise (R Noise), where resistance noise is the correlation of the standard deviation of the noise signals (δEPN/δECN), may be used to estimate the corrosion rate from the Stern-Geary relationship[5]. The noise techniques can avoid problems associated with other techniques i.e. the conductivity of the electrolyte, the presence of films, etc. do not effect the noise techniques. ZRA and LPRM or EIS are selected to track generalized corrosion. EIS is more effective in low conductivity media than LPRM, which has limited use on fouled surfaces or in low conductivity electrolytes. A combination of techniques are used since no single technique is capable of giving a complete appraisal of all modes of corrosion attack.

INSTALLATION, COMMISSIONING AND MAINTENANCE OF THE SYSTEM

The system is relatively simple to install and commission and would typically take one technician/engineer 2 to 3 days depending on the site application. The system is based upon the principle of feeding a sidestream of the cooling water through the miniature heat exchanger and flow controller as illustrated schematically in figure 2. The instrumentation and data acquisition hardware are housed in a suitable enclosure or cabin adjacent to the miniature heat exchanger and flow controller. Once the system has been commissioned only periodic checks are required (typically not more than once a week). The system gives a continuous indication of the fouling and corrosion status in the form of easy to interpret bar chart displays of the heat transfer resistance, pitting tendency (defined as the mean ECN value divided by the mean ZRA value) and the general rate of corrosion. In addition 24 hour time records of all raw and analysed data are saved automatically, as illustrated in figure 3. The system can also been interrogated to display historical data while logging real-time data continues. Time records, in a report ready format, are produced by a separate analysis package.

Routine cleaning of the heat exchanger tube is necessary although this is not typically more than once every two weeks. The frequency of cleaning, however, depends on the degree of fouling in the system. On these occasions the heat transfer resistance (HTR) value of the system is re-zeroed. The frequency of cleaning the unit is effected by the operating conditions, ie low flow rates and high heat inputs, which encourage fouling will increase the cleaning requirements. However, if the monitor is run under the same conditions as the plant heat exchanger, then the cleaning schedule for the monitor should be the same as the plant heat exchanger, in order to give representative data.

Once the system has been installed, and with a minimal amount of on-site training during installation, the day to day running of the system is non-labour intensive and can be interrogated and supported according to the requirements and time constraints of site personnel.

MODES OF OPERATION

In the conventional "monitoring system" used to track corrosion and fouling in a cooling water system the fouling monitor is usually operated under conditions which promote a "positive" and significant fouling trend in a short period of time. This mode of operation is satisfactory in terms of detecting fouling and conditions which influence fouling. This mode of operation is known to be sensitive to small changes in water treatment chemistry, pH etc in terms of immediate changes in the fouling tendency which may occur[6]. However in terms of representative corrosion information, this system has limited use as all corrosion information is derived from a non-heat flux surface. Any changes in corrosion behavior due to changes in the fouled condition of the heat transfer surface will not be detected.

When using the combined corrosion and fouling system the system should not be run in the same manner as the conventional system. The operating parameters, i.e. flow and heat input, should be set to mimic as closely as possible the risk operating condition of the unit. This will allow the corrosion reading to be used as an alarm for both corrosion and fouling changes, as the corrosion readings are sensitive enough to be a good indication of minute changes in fouling behavior. If operated under heavy fouling conditions the system is likely to indicate high rates of corrosion which are not representative of the heat exchanger unit. However the "positive fouling mode" operation may be acceptable if the water treatment inhibits under-deposit corrosion, otherwise the information can be misleading.

PLANT TRIALS

A combined corrosion and fouling monitor was installed in a recirculating water system at Amoco's Chemical Plant, Chocolate Bayou, Texas. The plant utilized river water make-up to the cooling towers and, historically, had suffered severe under deposit corrosion caused by particulate settlement and oxygen-induced attack. Over the years, remedial measures had been taken to minimize the fouling and corrosion tendency of the cooling water but problems were still evident due to low flow rate and/or high temperature

conditions in the system. In order to monitor the situation, the plant has used conventional monitoring technology: heat exchanger fouling monitor, corrosion coupons and a LPR corrosion probe without heat flux. Based upon the plant history, the high level interest on site and the availability of a comprehensive conventional monitoring capability, it was selected as the best site to field test the combined system. A schematic illustration of the field set up is given in figure 4.

Initially, in line with established practice, conditions were set to promote fouling on the heat capability of the system. Subsequently, the effectiveness of typical chemical treatment packages in combating and/or preventing fouling and corrosion was investigated. The final part of the trial was used to assess a number of passivation/inhibitor tests. During occasional pH excursions and chlorine overfeed, the response of the combined monitor provided valuable information on corrosion behaviour at the heat transfer surface.

The combined monitor exhibited good correlation with observed fouling behaviour from an adjacent fouling monitor. However, both monitors were being operated under conditions which promoted significant fouling in a short period of time; these conditions are more severe than the target operating conditions in the plant exchangers. For the detection and control of fouling behavior this has been found to be a good way to operate a fouling monitor. However this mode of operation causes heavy deposition on the heat transfer surface, and therefore the surface chemistry is altered and corrosion rates are much higher than would be anticipated. During the field trial, corrosion rates as high as 100 mpy were indicated under these conditions. Confidence in these rates was only obtained once confirmatory metallographic examination of the sensors had been carried out by the client.

It was found that initial resistance to the installation of the surveillance instrumentation was dissipated, once a degree of scepticism in its capability had been overcome. Subsequently however, confidence weakened when unexpected high levels of localized corrosion activity, contradictory to both expectation and data generated by traditional instrumentation, were revealed by the new equipment. Nevertheless, when post exposure destructive metallography, undertaken by the client, confirmed the predictions obtained from the new corrosion instrumentation, and an improved result display format had been developed (giving both real-time indications of general and localized corrosion) which was better suited to the needs of cooling water system appraisal, the user response was very positive from site personnel, contracting suppliers and the R & D group which supervised the project. During the trial each monitoring instrument did give reliable corrosion data in the environment being monitored. However the major diiferences in the corrosion data obtained from the new and traditional equipment were due to the differing corrosion behavior beneath a fouled heat transfer surface and a relatively clean non-heat transfer surface.

The results of the trial illustrated the high sensitivity of corrosion attack to the formation of fouling deposits on heat transfer surfaces. In the past there has been a tendency to consider that scaled heat transfer surfaces are protected by the presence of the scale itself and that observed damage took place at some other time, perhaps when the unit was out of service. These assumptions were shown to be erroneous. Fouling has an immediate and significant impact on the surface corrosion condition. Localized/non-

uniform deposits clearly impede the performance of corrosion inhibitors and create differential aeration cells to promote under deposit oxygen-induced corrosion. More detailed results of the trial and there implications have been reported elsewhere[7].

COST BENEFITS OF SYSTEM

Equipment Integrity - Underdeposit corrosion is an insidious problem which inevitably manifests and progresses before detection and/or failure. Real-time detection of UDC offers significant cost benefit and revenue savings in 1) Circumventing equipment deterioration/failure, 2) Optimizing chemical treatment program, and 3) minimizing shutdown for equipment repair, maintenance and replacement.

Heat Transfer - The primary objective of the water treatment program is to maximise the heat transfer in the heat exchangers. Improved thermal efficiency has a high cost-benefit and minimises the necessity to design heat exchangers with excess capacity to allow for the shortfall in performance caused by fouling.

Performance Control - The combined system allowed precise monitoring of water treatment programs to establish their effectiveness in prevention or reducing corrosion in heat exchangers to an acceptable level.

Lower Chemical Costs - Revenue savings can be achieved by optimizing the selection and verifying the quality of the management of a chemical treatment program.

Minimize Downtime and Improve Reliability - A proven cause of major expenditure for an operator is the maintenance and refurbishment costs of the heat exchanger and cooling water circuits. These costs can be minimised, and production, availability and reliability maximized by improved plant condition surveillance.

REFERENCES

1. G. Licina, G. Nekoksa and R.L. Howard, EPRI Service Water System Corrosion Seminar, Claerwater, Fl., April 1992.

2. F. Roe, N. and W.G. Characklis, Intech, September 1985 (pp 91-94).

3. K. Hladky and J. L Dawson, Corr. Sci., 23, p231 (1982).

4. D.A. Eden and A. N. Rothwell, Corrosion 92, Paper No. 292, Nashville, TN, 1992.

5. Stern and A.L. Geary, Journal of Electrochemical Society, 104 (1957) : 56.

6. P.O. Zuniga, K. Miller and M.A. Winters, Chemical Processing, April 1990.

7. M.A. Winters, P.S.N. Stokes, P.O.Zuniga and D.J. Schlottenmier, Corrosion 93, Paper No. 392, New Orleans, Louisiana.

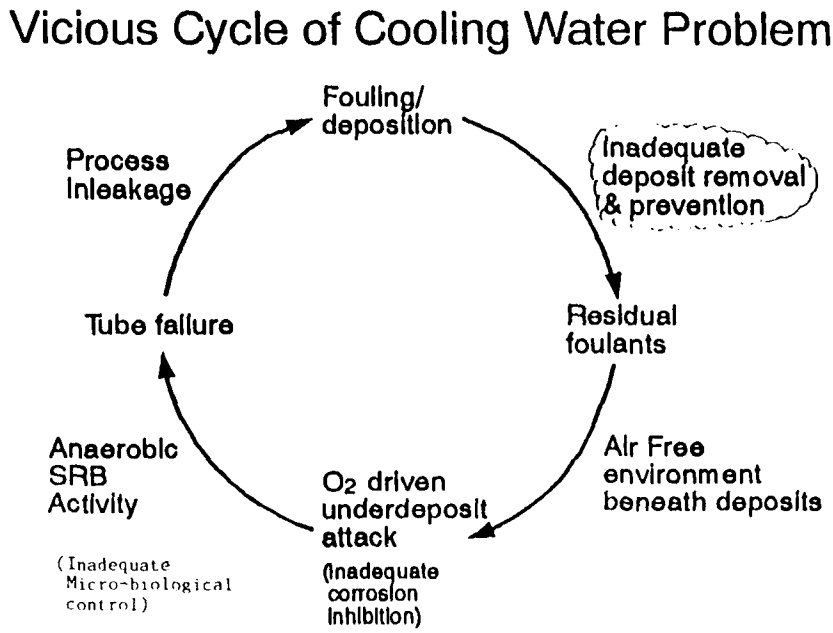

The Vicious Cycle of Cooling Water Problems.

Figure 1 The Vicious Cycle of Cooling Water Problems.

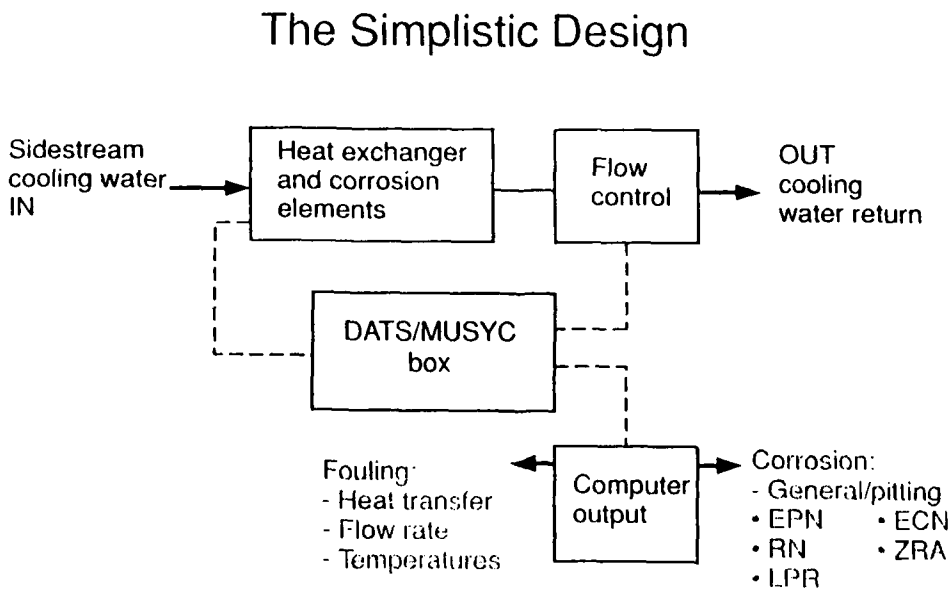

The Simplistic Design of the Combined Fouling Monitor. DATS is defined as Deposit Accumulation Testing System and MUSYC is defined as Multi-Sytem Corrosion Monitor.

Figure 2 The Simplistic Design of the Combined Fouling Monitor. DATS is defined as Deposit Accumulation Testing System and MUSYC is defined as Multi-System Corrosion Monitor.

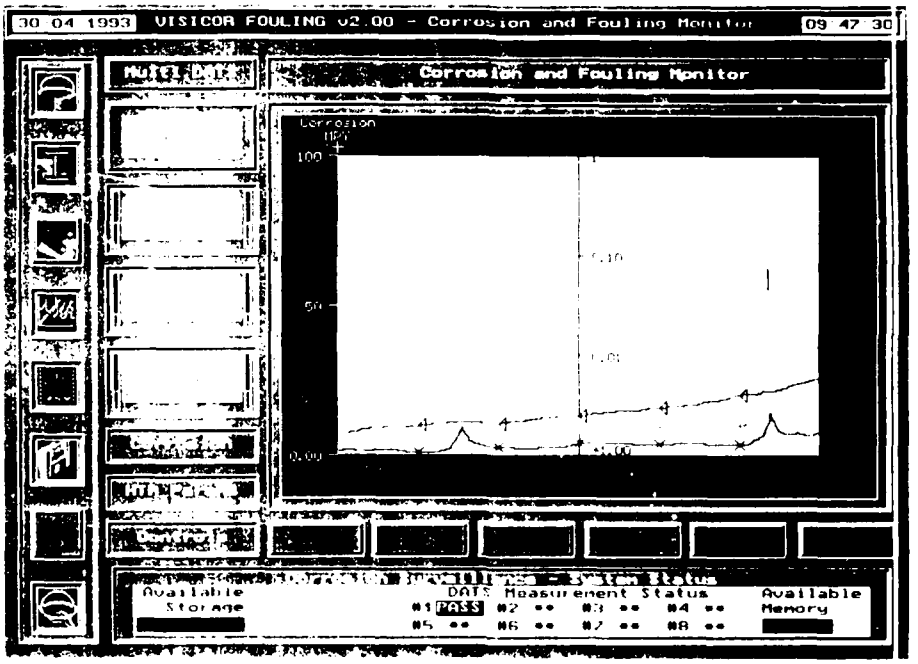

Figure 3 Example of 24 time record of heat transfer resistance, pitting tendency and general rate of corrosion.

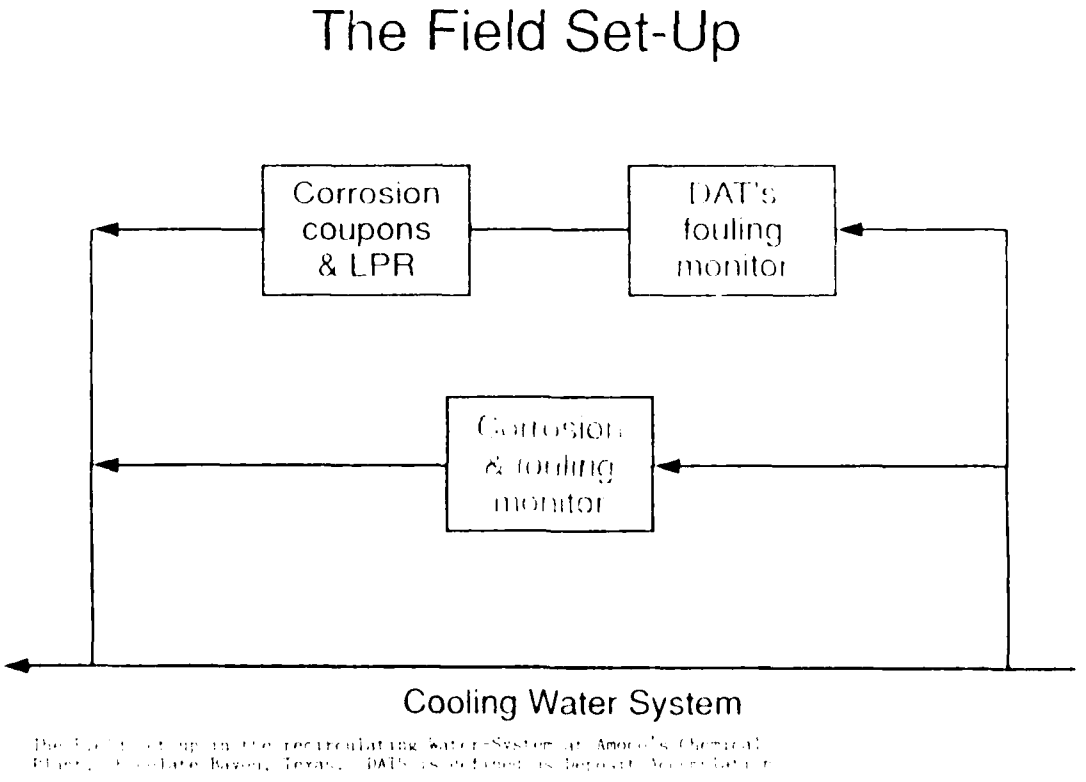

Figure 4 The Field Set-Up in the recirculating Water-System at Amoco's Chemical Plant, Chocolate Bayou, Texas. DATS is defined as Deposit Accumulation Testing System.

Service Water Electrochemical Monitoring Development at Ontario Hydro

A.M. Brennenstuhl
Ontario Hydro Research Division
800 Kipling Avenue
Toronto, Ontario
Canada, M8Z 5S4

Abstract

Ontario Hydro (OH) is currently investigating the feasibility of using electrochemical techniques for the corrosion monitoring of service water systems. To date all evaluations have been carried out in a field simulator. The studies include examining the effects of; system startup after periods of stagnation, sodium hypochlorite injection, and zebra mussel settlement on metallic surfaces. Carbon steel and Type 304L stainless steel have been evaluated. Electrochemical potential noise (EPN), electrochemical current noise (ECN) potential and coupling current were semi-continuously monitored over a period of up to one year.

Data obtained from the electrochemical noise monitoring has given us valuable insights into the mechanisms of degradation in service water systems. The high sensitivity of the electrochemical noise technique, particularly to localized corrosion has proved to be the major attraction of the system.

Introduction

Failures of components exposed to untreated natural freshwater in OH's power plants has resulted in a number of research programs aimed at preventing such occurrences in the future. While much of the research has been conducted in the laboratory a significant portion has also been performed in the field using equipment simulators and the same water employed in the plants. A very important aspect of the field simulations has been corrosion monitoring. Corrosion monitoring was introduced into our service water research program with two main objectives in mind. The first of these is the need to assess the utility of corrosion monitoring for determining the effects of changes in the chemical, physical, and biological conditions of the systems under study. The second is to better characterize the systems in order to provide information for the design of a practical accelerated test.

Corrosion monitoring has been carried out to determine the effects of i) hypochlorite injection for zebra mussel and biofilm control, ii) zebra mussel attachment to metal surfaces, and iii) stagnation followed by equipment startup. Type 304L stainless steel and carbon steel (ASTM A53 Grade B) have been evaluated.

The techniques employed for monitoring corrosion have included electrochemical potential (EP), zero resistance ammetry (ZRA), electrochemical potential noise (EPN), and electrochemical current noise (ECN).

This paper describes the corrosion monitoring studies carried out in the field simulators. Details of the equipment and corrosion probe designs are given, problems that were encountered are discussed and test results and their interpretation are presented.

Test Programs and Background

Three test programs will be detailed in this paper. The work involves determining the following effects:

i) hypochlorination on the corrosion of Type 304L stainless steel and ASTM A53 Grade B carbon steel.

ii) zebra mussel settlement on the corrosion of Type 304L stainless steel and ASTM A53 Grade B carbon steel, and

iii) stagnation followed by startup on the corrosion of Type 304L stainless steel.

The effects of hypochlorination were investigated because OH has recently been forced into employing this chemical to prevent zebra mussel attachment. Hypochlorite is a cathodic depolarizer ($OCl^- + H_2O + 2e^- \longrightarrow Cl^- + 2OH^-$) which may accelerate corrosion of carbon steel. In addition the noble redox potential for the $HOCl/OCl^-$ reaction suggests that passive alloys may be susceptible to pitting and/or crevice corrosion if pit activators such as Cl^- and $S_2O_3^{-2}$ are present. While the freshwater employed in OH's power generation plants is relatively benign fouling of equipment surfaces leads to the creation of environments very different from the bulk water[2]. Reduced sulphur species and chloride become concentrated in the deposits and are available as corrosion activating species.

Zebra mussel attachment to metallic substrates is a concern because of the potential development of a habitat for the growth of anaerobic sulphate reducing bacteria (SRB). These microorganisms can accelerate the corrosion of carbon steel and Type 304 stainless steel[3]. In addition it has recently been found that the zebra mussel bissle pad material contains a high concentration of a sulphur species, this may become available for reaction with the substrate to which the mussel is attached[4].

Stagnation followed by startup is a concern. Much of OH's equipment is left full of water after valving out of the system during periods of repair. Some freshwater cooled heat exchangers (HX's) tubed with stainless steel and nickel alloys are subjected to this treatment. Leaks due to underdeposit corrosion is a problem in this equipment. During the period of isolation the water contained in the systems becomes stagnant, anaerobic SRB grow and produce H_2S which continues to buildup while the bacteria remain viable. This condition is not expected to lead to corrosion because of the uniform low redox conditions which result[3]. However, when operation of the systems is resumed, the stagnant H_2S containing water is exposed to fresh oxygenated water. Thiosulphate, an established pit activator[4] is believed to be a product of exposure to dissolved oxygen. The stagnation/startup investigation was aimed at determining whether or not this cycle is deleterious to the tube material.

Experimental

Test Facility and Test Conditions

Testing was conducted in a specially built facility which was located at the Nanticoke Power Generating Station on the shores of Lake Erie. Figure 1 is a schematic of the test setup. Three 130 mm diameter polyvinyl chloride (PVC) spool pieces were employed for the hypochlorination experiment. The test samples (electrodes) were contained in these spool pieces. Untreated water which was taken from the station intake, the composition of which is given in Table 1, was passed over the samples at a nominal rate of 0.6 litres per minute. Water temperature was continuously monitored and ranged from 3°C-22°C. Sodium hypochlorite was injected into the water passing through two of the spool pieces. Two chlorination regimes were investigated, a continuous treatment at a residual level of 0.5 ppm and a shock treatment resulting in a 2 ppm residual for thirty minutes once every twelve hours. Both ASTM A56 Grade B carbon steel and Type 304L stainless steel were exposed to hypochlorate.

The spool piece through which untreated water was allowed to flow (the control) was also employed for the stagnation/startup investigation.

Smaller spool pieces (50 mm in diameter) were utilized for the zebra mussel attachment investigation. The tube diameter was reduced to minimize the PVC surface area relative to that of the test samples. Zebra mussels prefer to attach to PVC spool piece surface.

The stagnation experiment consisted of closing the inlet and discharge valve (outlet) of the spool piece for a period ranging from two days to two weeks. After allowing the lake water to stagnate the inlet valve only or both the inlet and outlet valves were opened. An identical routine was also carried out with the samples contained in the spool piece through which water treated with 0.5 ppm hypochlorate was passed. Microbiological analysis of the water contained in this tube indicated that it was essentially sterile.

Sample Design

Figure 2 illustrates the type of sample employed for the hypochlorite and stagnation/startup studies. Each sample comprised of three identical metal electrodes 2.5 mm in diameter giving a total surface area of 7.9 mm^2 only, one surface was exposed to the test environment. Potential and currents were measured between pairs of electrodes, one of the electrodes was common. The electrodes had a connecting lead spot welded to the back surface. The connecting leads were sheathed in polypropylene tubing. Epoxy resin was employed to prevent the coupons from making contact during exposure to the lake water stream and to maintain an equal separation between them for the duration of the test. To reduce crevice formation due to poor adhesion at the metal/epoxy interface the resin was vacuum degassed during the curing stage of the fabrication process. Removal of the residual epoxy on the metal surface was achieved by abrading the surface with 40 grit silicon carbide paper.

Tube samples were used for the zebra mussel attachment experiment, see Figure 3. The electrode assembly was composed of three tube coupons each having a surface area of 27 cm^2. Electrical isolation was achieved with polymethyl methacrylate (PMMA) insulators. Epoxy resin joined the coupons and the insulators. Electrical leads were spot welded to each coupon. The welds and the outer surface of the coupons were then coated with epoxy paint.

The electrical leads attached to the coupons exited the spool pieces through rubber fittings and were attached to the terminals of the corrosion monitoring equipment.

Electrochemical Monitoring

Critical components of the electrochemical monitoring setup are shown in Figure 4.

Monitoring was performed using a CAPCIS-MARCH DENIS (digital electrochemical noise integration system) instrument. This instrument collects, stores and performs summary statistics on the raw time data. The summary statistics are comprised of the following information:

i) Potential between two of the three metal electrodes.

ii) Electrochemical potential noise (EPN) this is the standard deviation of the electrochemical potential. EPN is usually of low amplitudes (<1 mV) and of low frequency, in the range of 1 Hz and below. It is claimed that signatures for uniform corrosion, pitting, corrosion, crevice attack and stress corrosion cracking can be differentiated with this technique[6].

iii) Coupling current, here the current between two of the electrodes is measured with a zero-resistance ammeter (ZRA). Coupling the two electrodes through the ZRA forces their potentials together, hence the difference in rates are observed as a current flow.

iv) Electrochemical current noise (ECN), with this technique fluctuations in the coupling current between two similar electrodes, are evaluated. These fluctuations are generally less than 1 μA.

v) Degree of localization was arrived at by dividing the ECN by the RMS coupling current. This parameter is used to broadly classify the corrosion process occurring on the sample surface. Values between 0.1 and 1.0 are an indication of a poisson type process, i.e. an unstable system such as pitting, crevice corrosion or stress corrosion cracking. Values less than 0.1 are generally associated with general attack.

vi) Resistance noise (Rn) is derived from the potential noise divided by the current noise and is analogous to polarization resistance (R_p) and charge transfer resistance (Rct) obtained by linear polarization resistance measurements and impedance spectroscopy respectively[7].

The degree of localization was used to assess corrosion of the stainless steel and the resistance noise was employed to obtain relative information from the carbon steel.

The monitoring system was mutiplexed to interrogate up to twelve samples on a semi-continuous basis. Each interrogation period consisted of collecting one thousand and twenty four data points each separated by an interval of four seconds before moving on to the next sample. The time domain information was stored on the hard drive of the logging computer. This cycle continued for the duration of the tests which ranged from six months to one year.

The data generated can be transformed into frequency domain for mechanism identification.

All of the test samples were biofilmed prior to testing. This treatment involved exposing the samples to untreated lake water of a period of two weeks. During this exposure period a relatively thick deposit comprised of lake sediment and biomass formed on the surface of the sample.

RESULTS AND DISCUSSION

Hypochlorination Experiments

ii) Type 304L Stainless Steel

Typical degree of localization versus time output for the Type 304L stainless steel at the start of the initial chlorination experiment are given in Figure 5. The data for the control and the 0.5 ppm treatment are quite similar. Low amplitude meta-stable events were evident. These data contrasted quite sharply with results for the "shock" treatment, where the degree of localization is significantly greater than for the control and 0.5 ppm tests.

At the start of the "shock" treatment the introduction of hypochlorite into the system resulted in an increase in potential this was accompanied by very little difference in coupling current but a decrease in ECN, see Figure 6. This observation is taken to infer that the addition of hypochlorite to the system has effectively increased the protectiveness of the passive layer by moving the potential further into the passive region. However, this behaviour was short lived. After this initial passivation, a sudden increase in the degree of localization occurs, see Figure 7. The potential plot indicates that hypochlorite injection again results in an increase in potential, however, unlike at the start of the experiment, potential noise is evident. An increase in the current noise can above seem to coincide with the change in potential.

When the "shock" treatment samples were removed from the spool piece a large proportion of the electrode surfaces was covered with deposit and the surface resembled that of the untreated control. Evidently, the "shock" treatment was unable to completely prevent the fouling which concentrates anodic activating species.

Clearly, under these circumstances hypochlorite can increase corrosion activity by raising the potential between the anode and cathode. This was not the case with the sample exposed to the continuous 0.5 ppm treatment; they remained deposit free for the duration of the experiment.

It should be pointed out that the outputs obtained for the "shock" treatment suggested metastable pitting only. Dissolution is immediately followed by repassivation. There was no indication of stable pit formation. While this must be kept in mind, it should be remembered that piping in actual plants often has a surface area of many thousands of square meters, and therefore the probability of one of the very large number of metastable pits becoming a stable propagating pit is greater than is the case with our small sample.

ii) Carbon Steel

A typical potential/coupling current output for a carbon steel sample is shown in Figure 8. The coupling current is much higher than was observed with the Type 304L stainless steel and as a consequence the EPN and ECN were less apparent. Initially, very little difference was seen between the samples exposed to hypochlorite and the control. As the exposure time increased it became evident from the resistance noise data that the "shock" hypochlorite treatment may have a beneficial effect, see Figure 9. Although these data were scattered, the resistance noise for the "shock" treatment was generally higher than that for the others. Careful examination of the "shock" exposure outputs revealed a cyclic pattern to the resistance noise values. When hypochlorite was injected into the system the resistance noise values increased and then gradually decreased with time until hypochloride was added to the system again. This observation suggests that the increase in redox potential of the solution a result of the introduction of hypochlorite moves the corrosion potential in to a more protective domain. This protection is not permanent, it gradually decreases until hypochlorite in introduced again.

No clear difference was apparent between the control and the continuous 0.5 ppm hypochlorite treatment.

The results of the hypochlorination trials thus far suggest that corrosion is unlikely to reduce the life of Type 304L stainless steel and carbon steel provided that continuous treatment at a residual level of 0.5 ppm is employed to prevent zebra mussel attachment. Rather, continuous hypochlorination will eliminate the underdeposit corrosion we have experienced in our systems by preventing the establishment of a biofilm on the metal surface[2]. This however, is not the case with the "shock" treatment. The combination of deposits and an increase in the potential between the anodic and cathodic sites appears to promote attack.

Effects of Zebra Mussel Settlement

Prior to the introduction of zebra mussels into the spool piece there was very little difference in the electrochemical outputs from the control test samples and the test samples which were later to be seeded with zebra mussels. Figures 10(i) shows a typical output for the Type 304 stainless steel. However, as time progressed the electrochemical signals from the spool piece containing the zebra mussels indicated a reduction in the degree of localization relative to that for the samples not exposed to zebra mussels, see Figure 10(ii). Similar behaviour was noted with the carbon steel (see Figure 11i and ii). A possible explanation for this behaviour was that the presence of zebra mussels had reduced flow in the spool piece to the extent that a uniform layer of deposit had formed on the surface of the coupons. The deposit which was comprised of lake sediment and biomass leads to the development of low redox conditions at the deposit metal interface due to anaerobic bacteria activity. The absence of an oxygen cathode or other cathodic depolarizing species leads to a reduction in the corrosion rate. When the samples were removed for inspection it was found that very thick deposits were present in the zebra mussel containing spool piece. This simulation therefore did not represent what may be happening in a large diameter pipe as it was intended to do, it more closely simulates a small diameter pipe such as would be used for a fire protection system.

During this experiment, we had difficulties in getting the zebra mussels to attach to the surface of the stainless steel and carbon steel, they preferred the PVC pippes. To overcome this difficulty the spool piece was saturated with with zebra mussels which had the unfortunate effect of significantly reducing the flow through the spool piece. In future attempts will be made to reduce the surface area of the PVC relative to the sample surface. This should increase the probability of mussels attaching to the metal surface without having to saturate the system. Several pump failures occurred and this lead to the development of stagnant conditions in the spool piece and the death of the mussels. The attachment and the pump problems significantly reduced the duration of monitoring with mussels attached to the surface of the samples. A backup pump system will be employed in future studies.

Effects of Stagnation Followed by Start-up

Figure 12 shows a time domain plot for stagnant conditions followed by exposure to oxgenate lake water. The initial part of the plot, Region [I], represents the stagnant condition, all electrochemical outputs were low in this region. When the inlet valve was opened, a relatively rapid increase in potential immediately occurred. The potential peaked decayed slightly then increased again, reached another peak and then decayed sharply, see Region [II] This reduction in potential was followed by a period of relative stability. However, during this period of

"stability" the potential displayed high frequency fluctuations (metastable pitting) which appear to decrease in frequency with time. This is Region [III] of the time domain plot. The current noise output contrasts with the potential noise output. Initially a decrease in current was observed; this was followed by a rapid recovery. A slight increase then occurred followed by a decay to a value similar to that observed before the valve was opened. Approximately twelve minutes after the inlet valve was opened a sharp increase in the current occurred. This coincided with a drop in potential. The current then reached a relatively high value and like the potential signal exhibited large fluctuations in the current.

The results obtained during this study add further support to the observation that uniform anaerobic conditions are not conducive to corrosion. Electrochemical noise and coupling current monitoring suggest very little corrosion of the sample exposed to stagnant untreated lake water. Corrosion is however, enhanced when the stagnant water comes into contact with oxygenated water. Initially potential appears to be particularly sensitive to oxygen ingress. The potential increases almost immediately, if this is a redox response it would seem the oxygen is able to diffuse to the sample surface very rapidly.

The coupling current and ECN observations contrast with the potential and EPN results. Apart from a very short initial transient current, it is almost potential independent until approximately twelve minutes into the exposure. Clearly, the changes in the environment necessary for increased corrosion are not as quick as those seen for the potential. Such a change might be explained by the sluggish rate of oxidation of metabolic products produced by the SRB. Whatever these changes are, they lead to an environment which increases the coupling current and results in meta-stable pitting on the surface of the sample.

During the winter months the activity described above is relatively short lived. This is possibly due to a drop in the temperature of the water in the spool piece (at 16°C-18°C) when it makes contact with the lake water which is at a temperature of 2°C. Pit propagation was sometimes observed when this experiment was conducted during the summer when the lake water temperature was 15-20°C indicating that temperature is a very important factor.

The behaviour described here became evident after two days of stagnation. The amplitude and duration of the signals was found to increase with stagnation time.

When the inlet valve is closed part way through the exposure the activity gradually ceases but could be restarted by opening the inlet valve again. Opening both the inlet and outlet valve thus allowing rapid fluid exchange leads to a sudden rise in potential and an increase in coupling current. These changes were of a much lower magnitude than was the case when a limited quantity of

oxygen was allowed to enter the system. This behaviour was taken to infer that the corrosion precursor (H_2S) was quickly purged from the system.

This behaviour was not observed when the water contained in the spool piece was sterilized; this phenomenon has therefore been attributed to microbiological activity[1].

The information obtained during this investigation highlights the importance of i) preventing the growth of anaerobic sulphate reducing bacteria during shutdown periods, and ii) flushing the system rapidly when valves are opened and has helped with the development of a laboratory based accelerated test.

Conclusions

Electrochemical monitoring of materials exposed to untreated freshwater has led to valuable insights into the effects of hypochlorination, zebra mussel attachment in small diameter tubes, and stagnation followed by startup. The effects of changes in the chemical, physical and biological conditions of the systems under study were obtained. In addition, in the case of the effects of stagnation followed by start-up experiment, important information which can be employed for a laboratory test was also revealed.

References

1. A.M. Brennenstuhl and T.S. Gendron, "The Use of Field Tests and Electrochemical Noise to Define Conditions for Accelerated MIC Testing", ASTM International Symposium on Microbiologically Influenced Corrosion (MIC) Testing, November 16-17, 1992, Miami, Florida.

2. A.M. Brennenstuhl, T.S. Gendron and P.E. Doherty, "Fouling and Corrosion of Freshwater Heat Exchangers", Fifth International Symposium on Environmental Degradation of Materials in Nuclear Power Systems - Water Reactors, August 25-29, 1991, Monterey, California.

3. R.C. Newman, B.J. Webster and R.G. Kelly, "The Electrochemistry of SRB Corrosion & Related Inorganic Phenomena", ISIJ International, Vol. 31, No. 2, pp. 201, 1990.

4. A.M. Brennenstuhl and A. Robertson, "Micro-analysis of Zebra Mussel Bissle Pads", Ontario Hydro Research Division Report, #M93-29-K, May 1993.

5. A. Gamer, R.C. Newman, Corrosion'91 paper 186, Cincinnati, Ohio, 1991.

6. D.M. Farrell, "Electrochemical Noise Process", Industrial Corrosion, Vol. 9, No. 5, pp. 7, 1991.

7. D.A. Eden, et.al., Corrosion 86 paper number 274, March 17-21, 1986, Houston, Texas.

Table 1

Water Chemistry Parameters at Nanticoke, Lake Erie

pH	8.10
Cl (mg/L)	20.50
SO_4 (mg/L)	25.0
Alkalinity (mg $CaCO_3$/L)	99.00
Total Iron (mg/L)	0.08
Specific Conductivity (mS/cm)	293.10

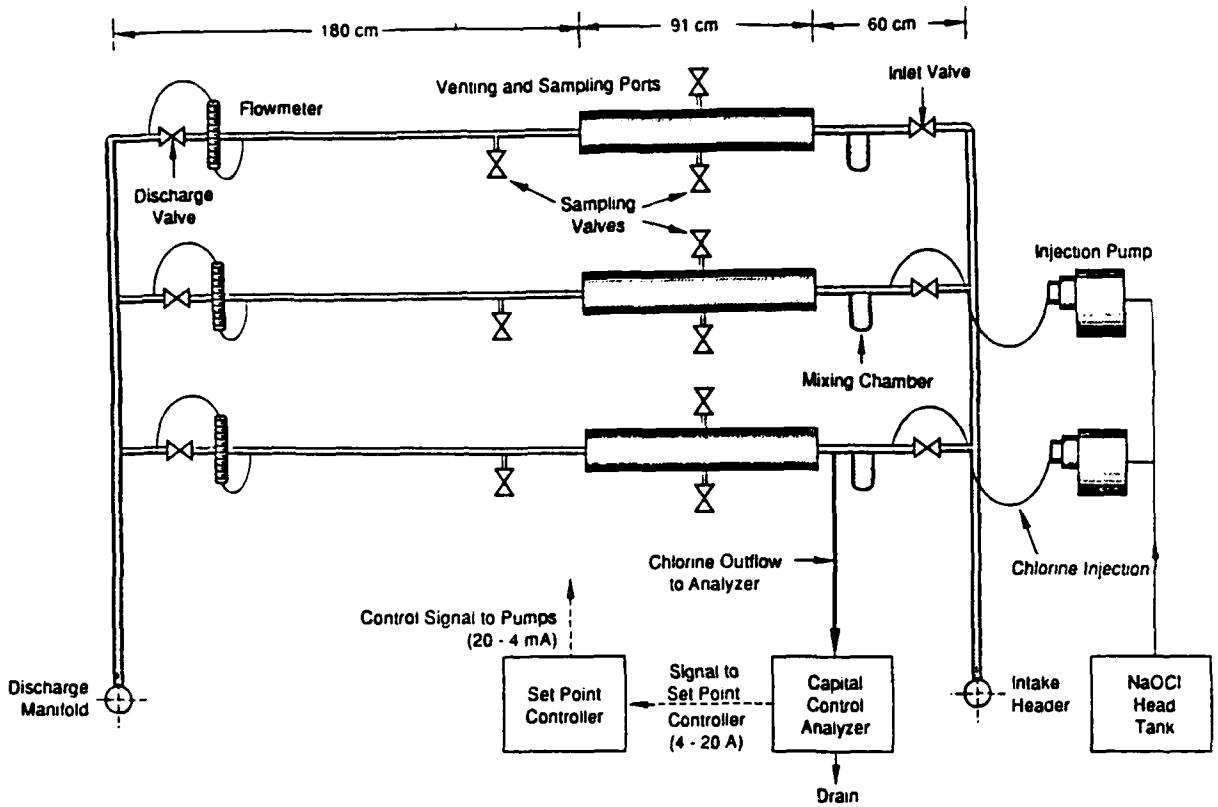

Figure 1. Schematic of the field setup.

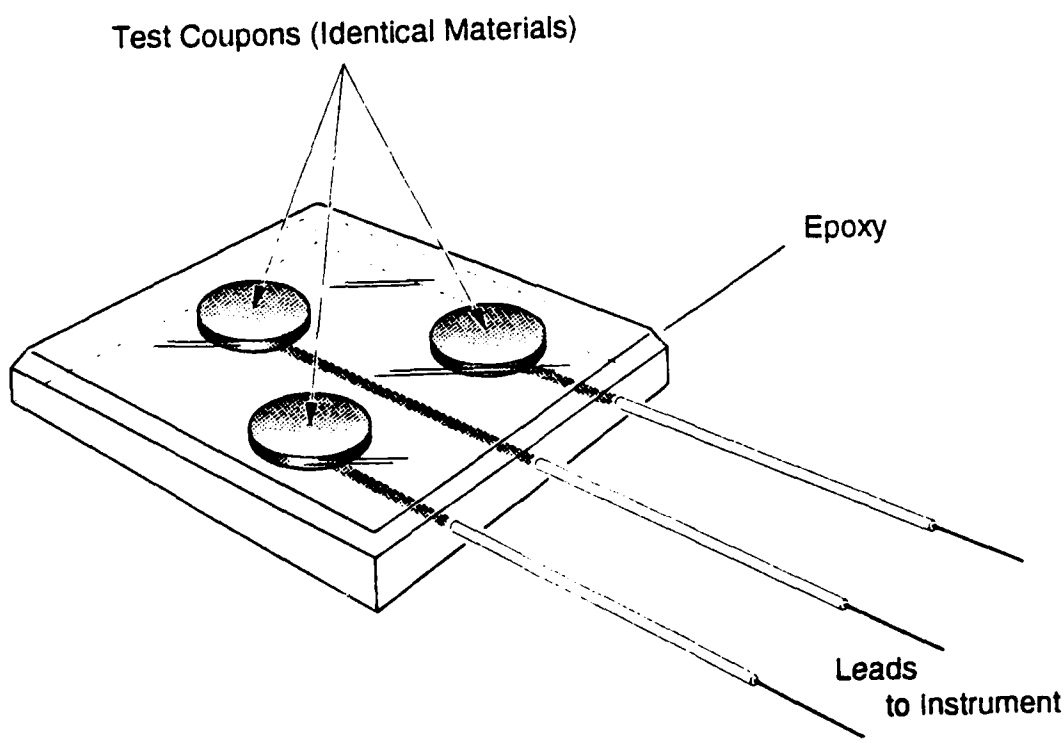

Figure 2. The three electrode sample used for sodium hypochlorite and effects of stagnation evaluations.

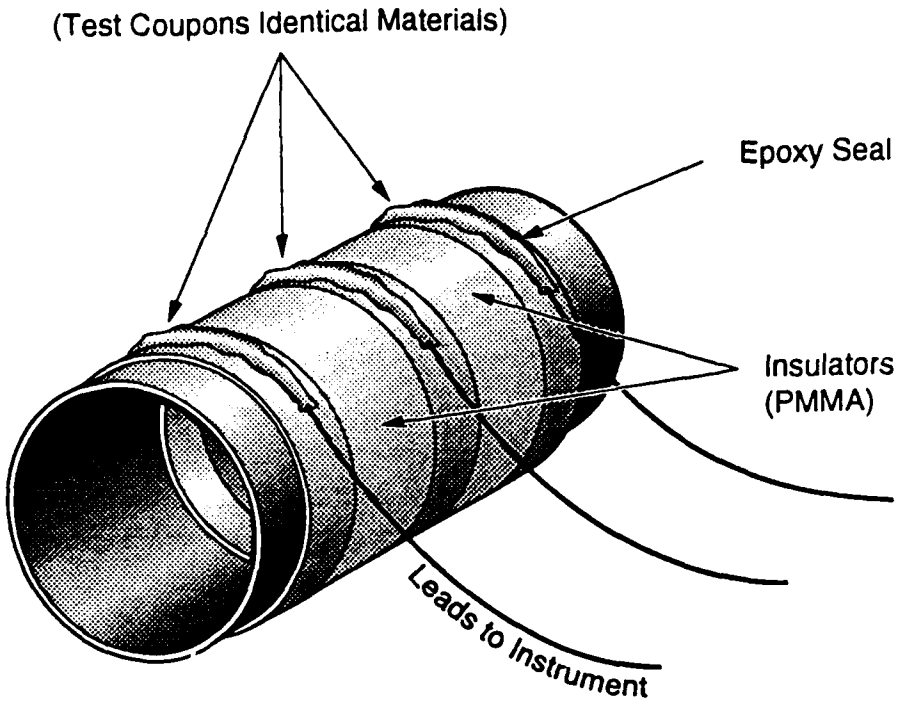

Figure 3. The three electrode tube sample employed for the effects of zebra mussel attachment study (arrows show insulators).

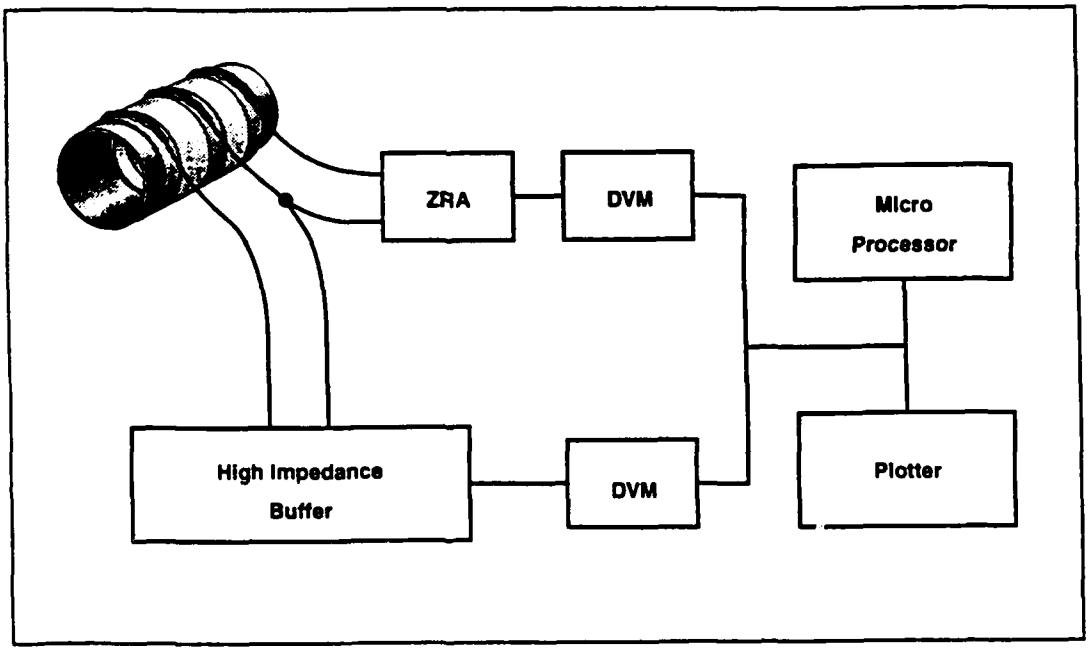

Figure 4. The essential features of the digital systems - employed for the experiments (note; DVM refers to digital volt meter).

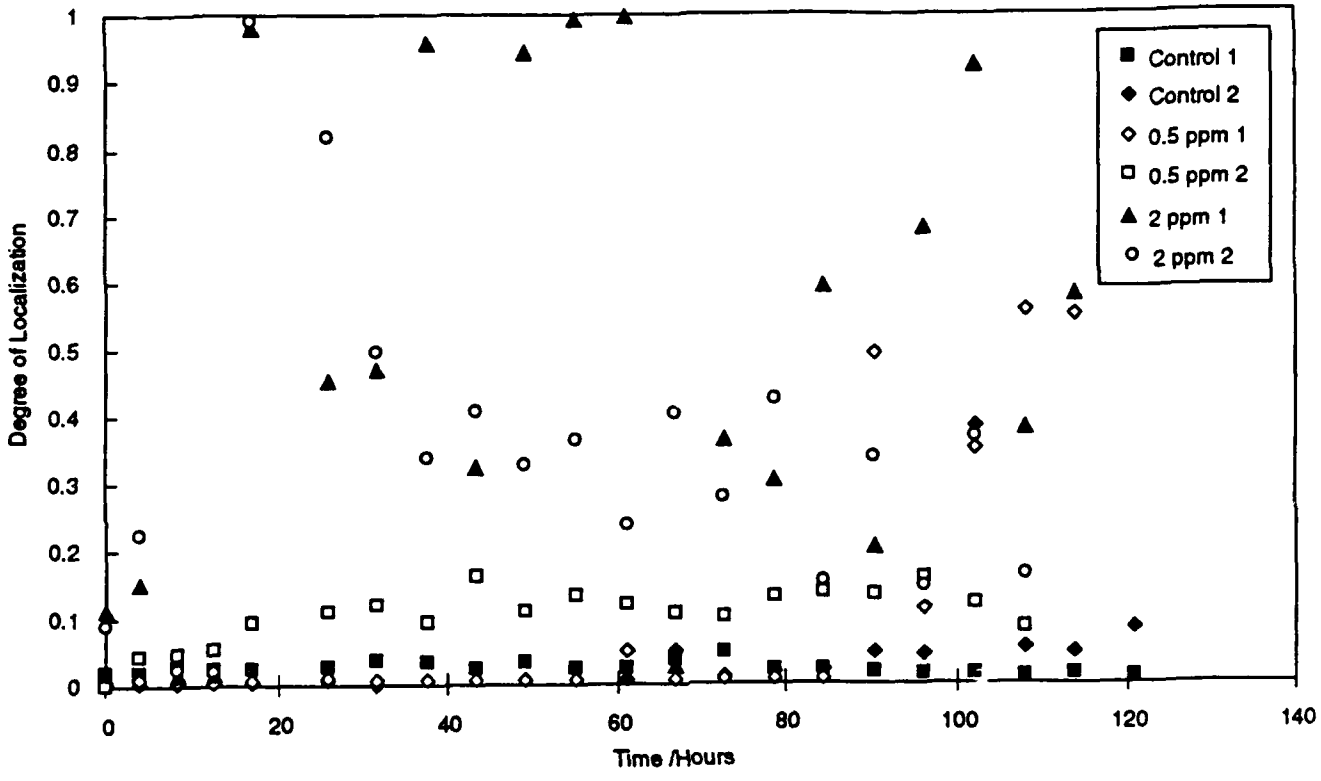

Figure 5. Data for the Type 304L hypochlorite study at the start of the test.

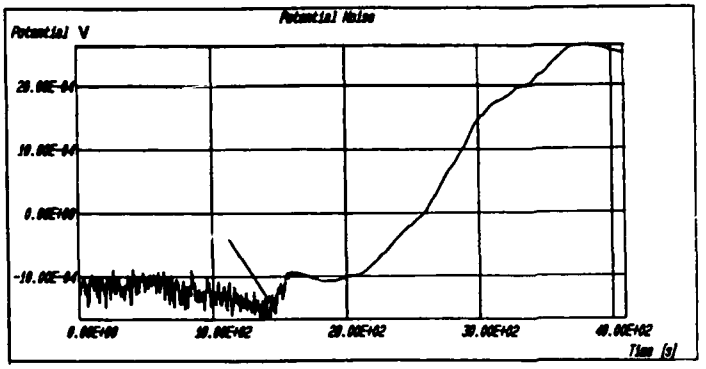

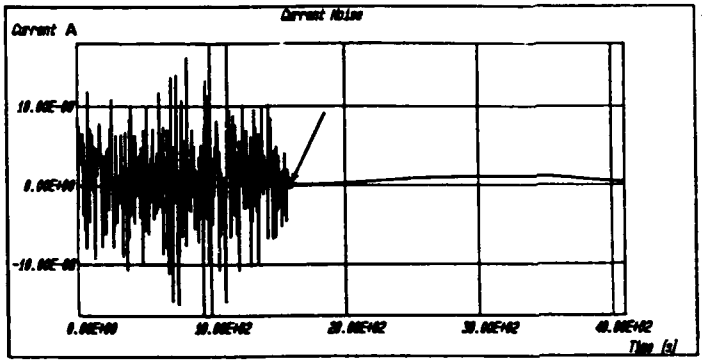

Figure 6. A time domain plot for a sample subjected to the "shock" treatment. The arrow indicates when hypochlorite was introduced into the system. This response was only observed at the start of the exposure.

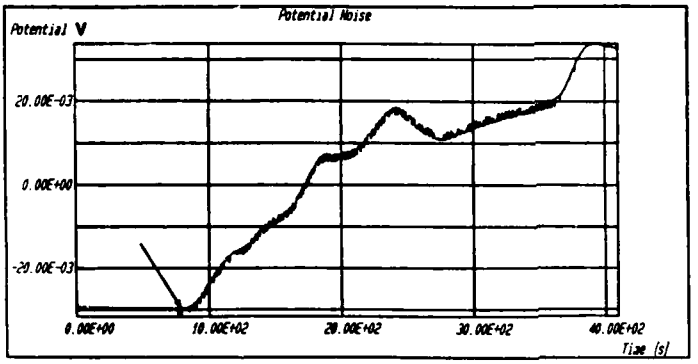

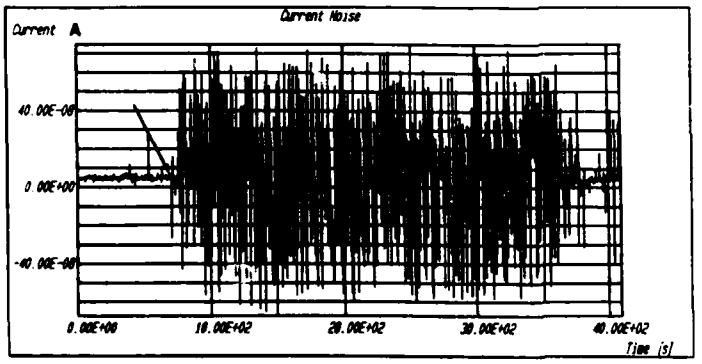

Figure 7. A time domain plot for a sample subjected to the "shock" treatment. The arrow shows when NaOCl was injected into the system. This response was observed after several days had elapsed.

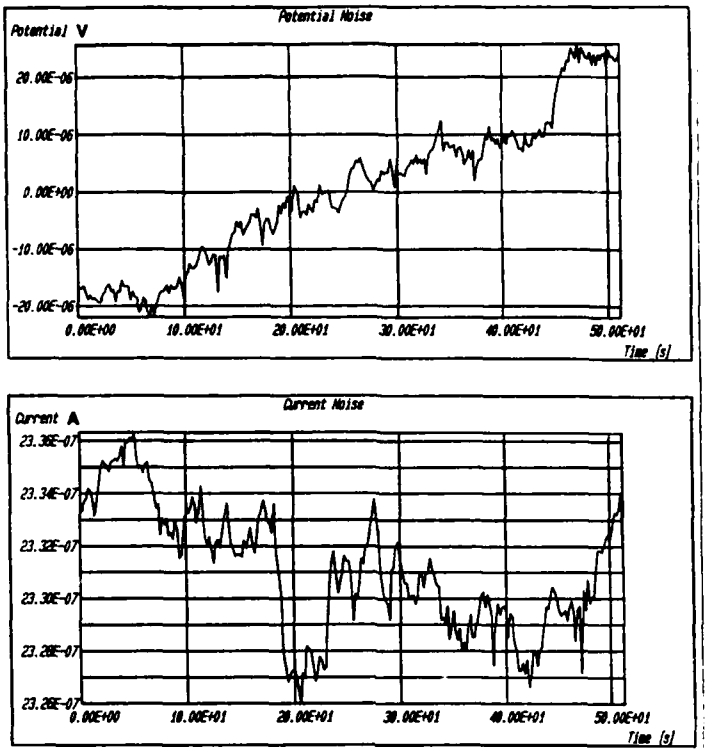

Figure 8. A typical time domain output for carbon steel

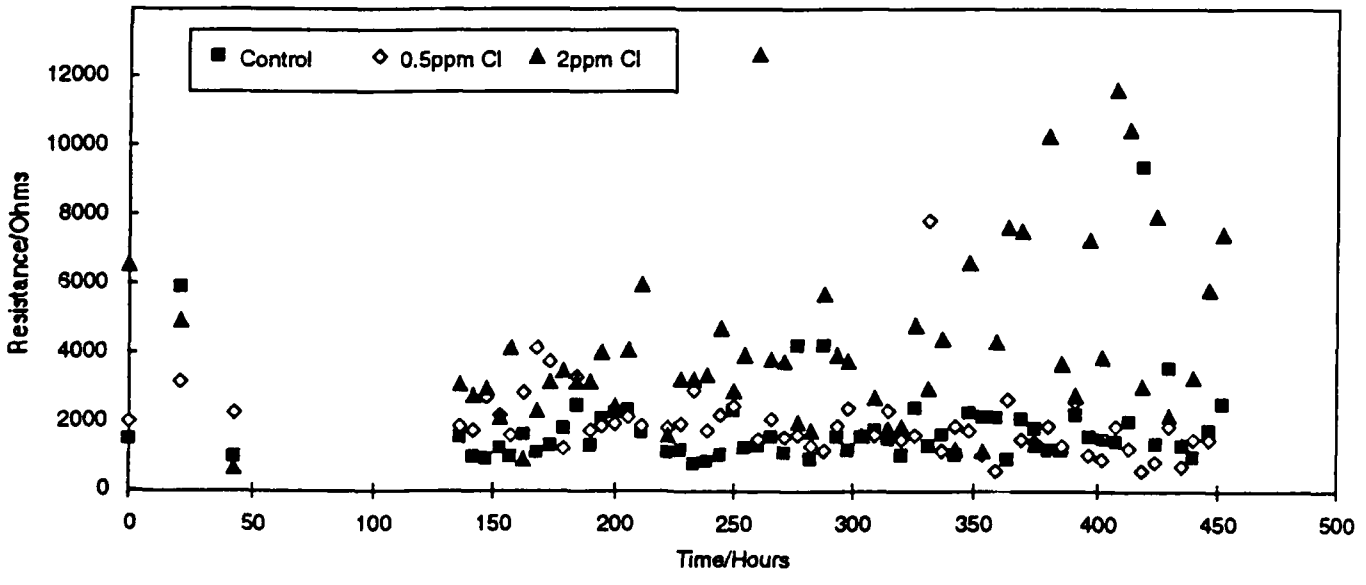

Figure 9. A resistance noise plot versus time for the carbon steel, showing the effect of hypochlorination after nine months of exposure.

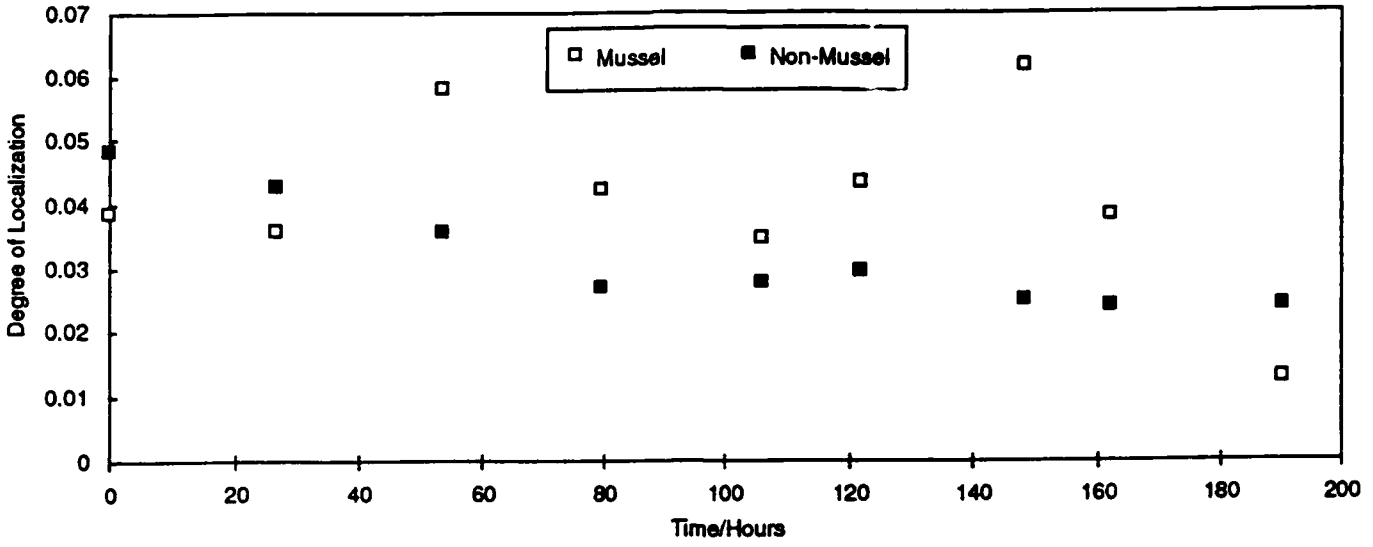

(i)

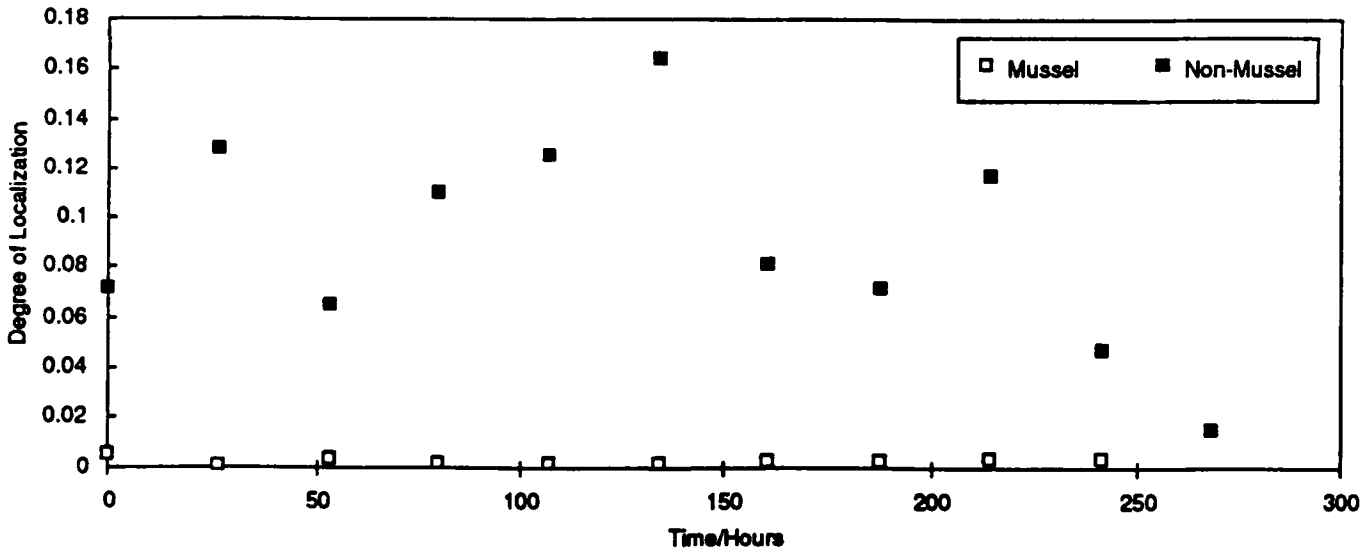

(ii)

Figure 10. A typical plot for i) degree of localization of the Type 304L before the addition of zebra mussels and ii) after introduction of zebra mussels.

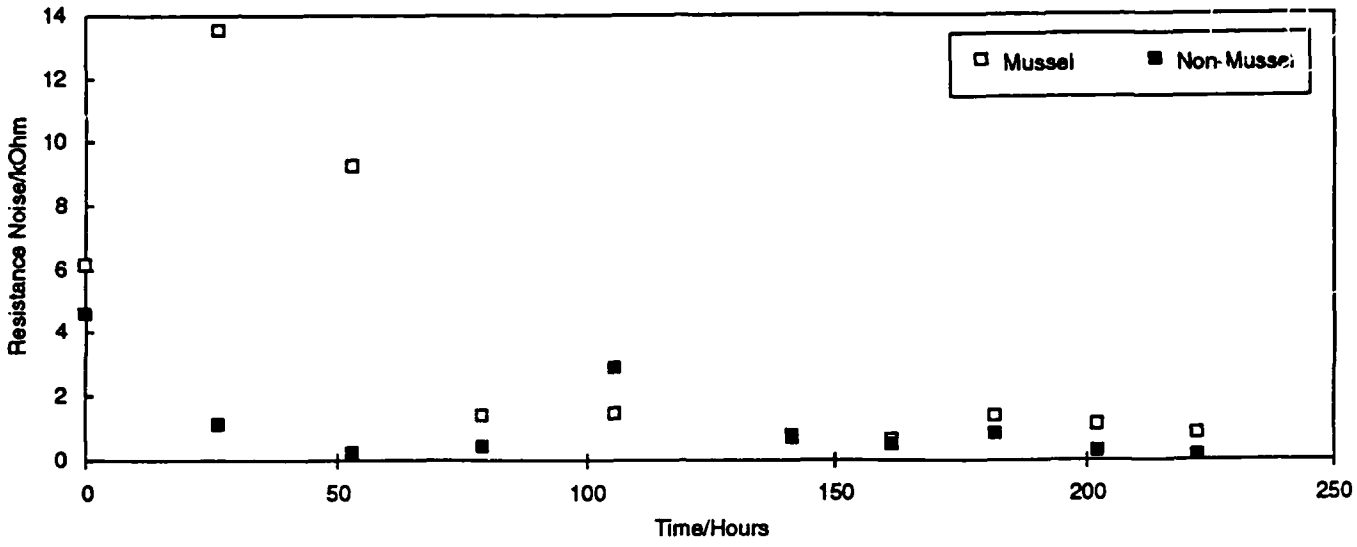

(i)

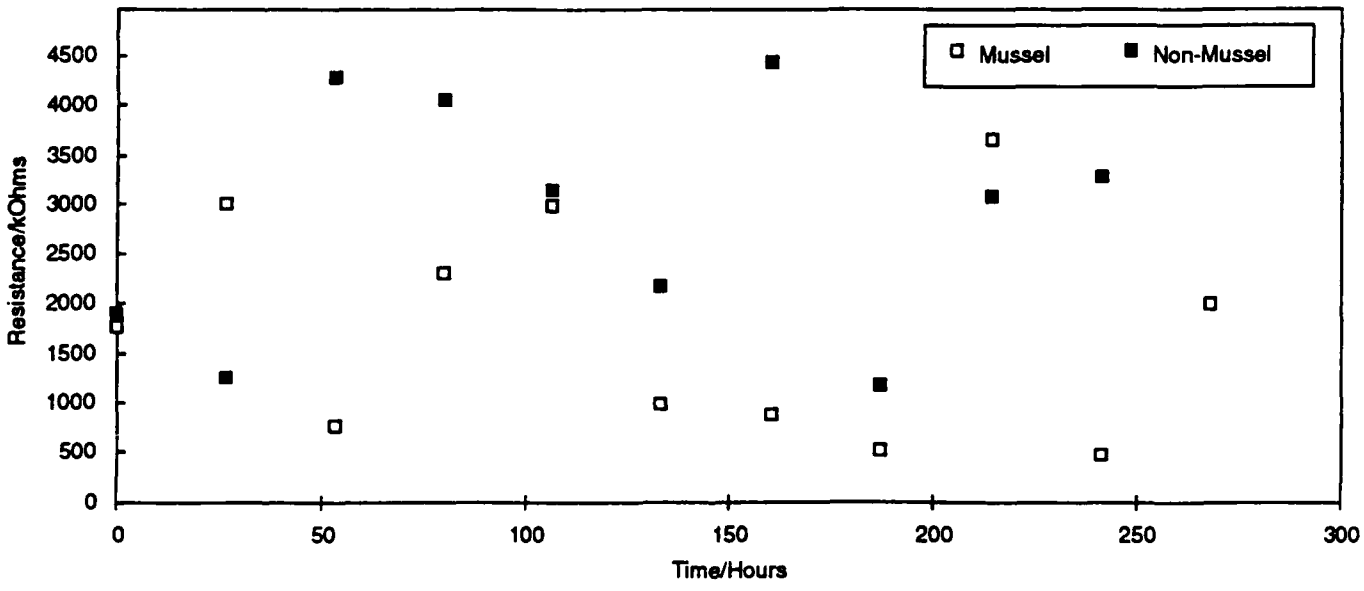

(ii)

Figure 11. A typical plot for i) resistance noise outputs for carbon steel prior to the addition of zebra mussels and ii) resistance noise after the introduction of zebra mussels.

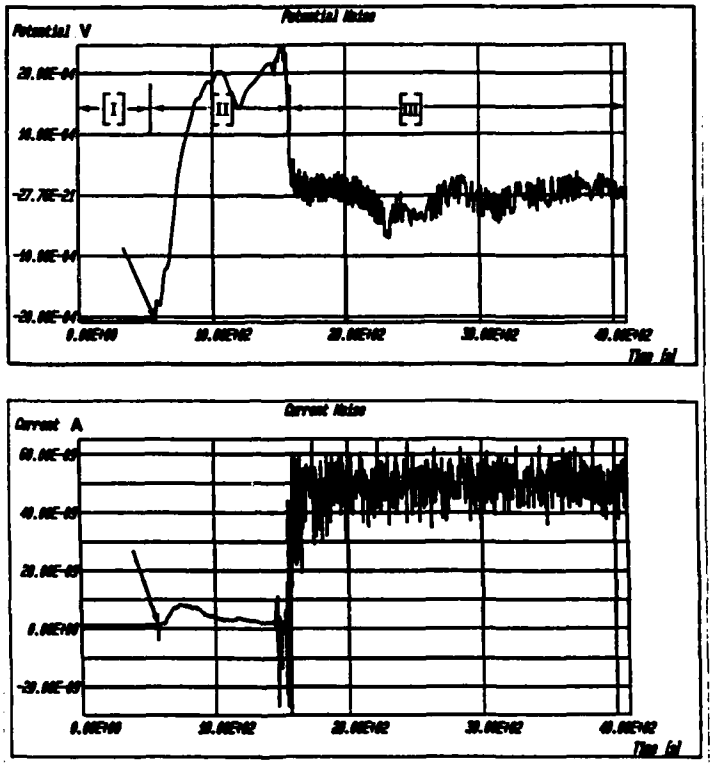

Figure 12. A time domain plot showing the effect of allowing a limited amount of oxygen to enter the system after a period of stagnation. The arrow indicates when the inlet valve to the spool piece was opened.

Monitoring of Corrosion in a Spray Dryer Absorption FGD Plant

Niels Henriksen
Faelleskemikerne
ELSAMPROJEKT A/S
7000 Fredericia
DENMARK

Jon Kristgeirson
ELSAMPROJEKT A/S
7000 Fredericia
DENMARK

Abstract

Electrochemical corrosion monitoring has been used for monitoring corrosion in a flue gas desulphurization plant of the Spray Dryer Absorption type. The corrosion rate of the actual system is low, but the corrosion has caused a serious emission problem due to the exfoliation of corrosion produ ts from the surfaces of the flue gas ducts. The corrosion can be avoided by heating up the flue gas. As reheating of the flue gas is an additional expense it is desirable to minimize the heat input.

By using electrochemical corrosion monitoring techniques it is possible to optimize the heat input. This study has shown that by means of electrochemical noise techniques, corrosion signals are achieved which correlate to relevant operating parameters. The computer technique, neural networks, has been used for processing the large amount of signals which are rather weak due to a low corrosion rate and also difficult to correlate.

Key terms: FGD plant, corrosion monitoring, neural networks

Introduction

ELSAM is the electric utility company covering the western part of Denmark. ELSAM has an installed capacity of 4000 MW and produces 55% of the electricity in Denmark.

Since 1988 ELSAM have commissioned a series of flue gas desulphurisation (FGD) plants. Three different types of FGD plants have been installed: the wet process (F.L.Schmidt/Mitsubishi), the SNOX process (Haldor Topsoe) and the spray dryer absorption (SDA) method (ABB Flaekt/Niro).

Three 350-400 MW units have been equipped with SDA FGD plants. The flue gas is cleaned in an absorber by dispersion of a lime slurry containing a certain amount of recirculated reaction product. The reaction product is dried by the heat of the flue gas. The product is removed at the bottom of the absorber or in the following bag-filter. See figure 1.The FGD product consists mainly of $CaSO_3$ and small amounts of $CaCl_2$, $Ca(OH)_2$ and $CaSO_4$.

A corrosion problem was experienced after approximately 6 months of operation. The corrosion was located in the clean gas duct downstream from the bag-filter and acid flakes of corrosion products were exfoliated from the duct surfaces and emitted into the immediate surroundings. This gave rise to complaints from neighbours, and the local authorities requested this emission to be stopped.

The corrosion was stopped by raising the temperature, however, this method of solving the problem is rather expensive because it impairs the desulphurization process, meaning that the consumption of lime will be increased considerably if an unchanged degree of desulphurization is to be maintained.

Alternative ways of solving the corrosion problem, such as coating the ducts or installing a heat-exchanger after the bag-filter, were considered. It was decided to coat two of the units and to install a heat exchanger in the third unit. The heat exchanger was installed downstream from the bag-filter implying that the heating does not influence the desulphurizing reaction. As the corrosion is assumed to be the result of a combination of several operating parameters and not only of the temperature, it will be possible to reduce the heating requirements for less critical combinations of operating parameters provided that the corrosion has been thoroughly studied.

Therefore, ELSAM has initiated an R&D project with a view to investigate the possibility of using on-line corrosion monitoring for describing the above-mentioned corrosion process in order to isolate significant service parameters. Another purpose of this project has been to test the equipment in a weak corrosion environment and to gain practical experience, the objective being to use this method for other applications.

The Corrosion Process

Based on the results of analyses and various theoretical considerations the corrosion of the SDA plant is expected to be influenced by several operating parameters.

Analyses by B. Sander[1] have shown that the desulphurization product consists mainly of $CaSO_3$ of which a small part is oxidized to $CaSO_4$. Because there is a surplus of $Ca(OH)_2$ in the system, the hydrochloric acid in the flue gas is bound in the form of $CaCl_2$ or, to be more specific, in the form of the double-salt $CaCl_2.Ca(OH)_2.H_2O$. This double-salt is not particularly hygroscopic as it only absorbs water at a critical relative humidity of approximately 60%[2] or higher. The remaining SO_2 in the flue gas reacts with the remaining lime in the layers on the surfaces of the flue gas ducts. However, this reaction will most probably be slow under dry conditions[3]. Under wet conditions the double-salt is expected to react with the SO_2 in the flue gas, thus producing the highly hygroscopic salt $CaCl_2.2H_2O$. This salt will absorb humidity at a relative humidity of above 14% at the normal operating temperature of 68-70°C.

Investigations carried out by the FORCE Institutes (The Danish Corrosion Centre)[4] have shown that corrosion is greatly influenced by the relative atmospheric humidity indicated by the ΔT_{ADSAT} parameter (ΔT_{ADSAT} is the temperature difference between the duct surface temperature and the adiabatic saturation temperature of the clean gas). FORCE has discovered that corrosion is produced at the actual relative humidity of 32-42% or above, depending on the absorber liquid being either salt or fresh water. The divergence of the theoretical limits from FORCE's results may be due to a combination of two conditions:

- the layers contain a certain amount of $CaCl_2$, implying that water is absorbed. However, for corrosion to occur the layers must contain a

certain minimum water concentration so as to provide the required conductivity.

- FORCE's investigation[4] had a duration of 500 hours, meaning that the results represent an average of different service parameter combinations at presumably different corrosion rates.

Apart from the mentioned service parameters, the following parameters might influence the corrosion:

- The Chloride Concentration

  The composition of various chloride salts will influence the initiation of corrosion because of different hygroscopicity. The total chloride concentration will influence the corrosion rate.

- The SO_2 Concentration

  The degree of desulphurization is a determining factor for the chloride concentration. A high degree of desulphurization produces a low concentration of chloride.

  The SO_2-concentration in the clean gas affects the corrosion directly due to absorption and reaction with the surplus lime, however, provided that the environment is sufficiently humid.

- The Flue Gas Flow

  The flue gas flow influences the depositing of dust particles and the surface temperature of the ducts.

- The Remaining Lime Content

  The remaining lime content of the desulphurization product influences the chemical composition of the chloride salts and raises the pH of the product. A high concentration of lime results from a low efficiency of the desulphurization process caused by a high ΔT_{ADSAT}.

In order to study the corrosion process, a series of signals of relevant process variables describing the above-mentioned parameters is needed for comparison with the corrosion signals. The following signals have been available:

- Probe temperature
- Flue gas temperature
- Absorber temperature
- Flue gas flow
- SO_2 before desulphurization
- SO_2 after desulphurization
- Adiabatic saturation temperature, T_{ADSAT}
- HCl in flue gas
- Conductivity of absorber liquid

Corrosion Monitoring

It was decided to purchase equipment for on-line corrosion monitoring, partly in order to gain experience as regards the equipment and partly to investigate whether it would contribute to an improved understanding of the current corrosion problem.

It was decided to buy equipment from CAPCIS MARCH Ltd. (CML) which had previously been used for corrosion monitoring in wet FGD plants[5]. A multi-technique corrosion monitoring system was purchased. It includes:

- single probe multi-technique analogue corrosion monitors,
- multi-electrode electrochemical probes with the electrodes made in carbon steel and corten steel corresponding to the duct materials and with a total area of approx. 5 cm^2., The electrodes are placed in the end surface of a probe, made of AISI 316L tube (diameter: 100 mm)
- data collection and transmission units,
- computer hardware and software (VISICOR).

The equipment measures the following electrochemical parameters:

- R_s: solution resistance measured by impedance technique at high-frequency AC (approx. 10 kHz).
- R_p: polarization resistance measured by impedance technique is the difference between the low frequency AC (approx. 10 mHz) measurement and the high frequency measurement (R_s).
- ZRA: zero resistance ammetry between two nominally identical electrodes. For actually corroded electrodes this will not be the case. In practice a small current of alternating direction is measured. The absolute value represents the tendency to non-uniform corrosion or most often pitting corrosion. It is a qualitative evaluation because these values cannot be converted into a corrosion rate.
- EPN: electrochemical potential noise is measured by means of a high-ohm voltmeter between two nominally identical electrodes. The measured value should be close to zero; however, a slightly varying voltage is measured.
- ECN: electrochemical current noise is a filtered value of the zero resistance ammetry, from which the DC average value is subtracted.

The equipment was commissioned in January 1991. The installation was carried out by technicians from CAPCIS MARCH together with personnel from the power station. The cost of the equipment amounted to approximately USD 85,000 (1991 price), and on top of this the power station had an additional cost of approximately USD 25,000 for the installation of cabling, cooling-facilities and insulation. A rough estimate of operating the equipment and analyzing the data is USD 100,000.

Data Processing/Artificial Neural Networks (ANN)

As mentioned, several operating parameters influence the corrosion. It is not easy to handle the considerable amount of data resulting from the registration of signals from the corrosion probes and from the registration of the selected service parameters. Thus the finding of correlations between operating parameters and corrosion signals becomes a very demanding task. See figure 2 and 3.

Therefore the data have been processed by the computer technique, neural networks, on an experimental basis.

ANN are computer models inspired by the structure and behaviour of the brain. Like the brain, they can recognize patterns and, most interestingly, they can learn.

In general, ANN are composed of any number of layers, each consisting of any number of processing elements or neurons. The first is designated as the input layer, the last as the output layer, and those in between as the hidden layers. The input layer receives data from the external world (i.e. digitized pad, sampled time series or output from a computer programme). The output layer sends information to the external world. The hidden layers process and store the information presented by the input data. As mentioned above, the ability to learn is one of the distinguishing features of the neural networks. ANN work even when given erroneous information or when information is missing. Information is stored as weights in ANN, not as series of bits as it would in normal computers.

ANN may operate in two phases. The first phase is the training of the network. The user provides the network with a "suitable" number of input and output patterns, if required. The possible presence of output patterns depends on how ANN are trained.

ANN are sometimes called Model-free Estimators, because users need not state how outputs depend mathematically on inputs. Systems which are interpreted as being complex and unknown, uncertain non-linear physical processes, are hard to analyze by means of mathematical tools. ANN have been known to exhibit a number of properties, due to the ability of learning, which make them even better than traditional math tools at approximating complex systems.

Results/Correlation

By using neural networks on different combinations of service parameter values, as far as they lie within the normal variation area, we have succeeded in predicting the electrochemical corrosion signals.

We have used feed-forward network, trained by the back propagation learning algorithm[6], for our research into the performance of ANN regarding finding the correlation between inputs and outputs of the time series. After training, the net was tested on the data shown in fig.2 and fig.3, where the time series in fig.2 are the inputs. Fig.3 shows the training series and net output. As can be seen, the net was good at finding the correlation between input and output, considering the complexity of the time series.

A series of simulations has been carried out based on the results from the neural networks with a view to clarifying the significance of the individual operating parameters for the corrosion process.

One of the simulations was performed by setting the operating parameters to controlled sine functions with maximum and minimum values within the normal range. For some values a constant value has been given. The input values are:

* SO_2-concentration before FGD: 3000 mg/Nm^3,
* SO_2-concentration after FGD: $375\sin(2\pi*t/7)+525$ mg/Nm^3,

* HCl concentration in flue gas: $60\sin(2\pi*t/11)+80$ mg/Nm^3,
* Slurry conductivity: $9\sin(2\pi*t/36)+24$ mS/cm,
* Flue gas flow: 170 Nm^3/s,
* Probe temperature: $10\sin(2\pi*t/24)+65$ °C,

Where t is the time in hours and Nm^3 is m^3 at normal temperature and pressure.

For this set of input functions the absorber temperature has been set to a constant value. The resulting signals of the electrochemical current noise, based on net output for four different absorber temperatures, are shown in figure 4. Evidently the ECN decreases when the absorber temperature is increased. This and other simulations can be used for finding the optimum way of operating the FGD plant without causing corrosion.

A quantification of the corrosion rate has not been performed and will also be rather complicated to carry out as signals will have to be integrated over a very long period of time and correlated to weight coupon measurements, which should be temperature controlled in the same way as the electrochemical probes.

Evaluation of the Method

Just after the commissioning of corrosion monitoring system we decided to add a simple cooling system to the system. Subsequently a series of cooling tests were performed. As previously described, the corrosion of the FGD ductwork is minimal and the electrochemical signals are consequently low. It proved very difficult to interpret these data. However, based on these data and information from the supplier it was concluded that the corrosion was negligible.

Of course, this is a correct statement when focusing on material loss, however, as this investigation was initiated because of severe emission problems caused by minimal corrosion, we continued our efforts trying to get some indication of on-going corrosion and to find a correlation with service parameters.

After a long time and by means of neural networks we found a correlation between the electrochemical signals and the service parameters, which earlier had seemed rather chaotic. This correlation corresponds quite well to our expectations as regards the influence of the individual operating parameters. On this basis we conclude that the probes can detect even very limited corrosion based on noise measurements.

Processing the considerable amounts of corrosion data and operating parameters has proven the greatest difficulty when it comes to getting information from the probes. The data processing has been further obstructed by erroneous signals from the probes which apparently have nothing to do with the corrosion process as they differ some 1-2 decades from the normal level. Errors occur at the change of date and at start-up of the measuring equipment after a standstill period. Considerable efforts have been made to detect and eliminate these erroneous signals.

Time synchronisation proved to be another problem. Actually we have had to discard data because the clock of the PC did not keep pace with the clock of the process computer. For future applications it is evident that better time synchronisation is required.

In our opinion the software design could have been better, but it must comply with the many different requirements of various customers and thus most probably had to be designed the way it was. However, more thorough documentation of the software would have been preferable.

The hardware has not given rise to any real problems. In fact, the only problem has been that the probes without temperature regulation constitute a thermal bridge and thus become colder than the walls of the ducts. This

problem should be considered if the probes are to be used as proper operating instruments without temperature regulation.

The normal operation of the equipment as regards temperature control and operation of the computer is very simple and maintenance is almost negligible, and the monitoring equipment it self implies no risk to the plant. The interpretation of data is fairly demanding and during the test-period, personnel with a wide experience of electrochemistry, knowledge of the actual corrosion problem, the process in question and data processing is needed. After the test-period we expect that the general operating personnel can use the equipment, provided that the results achieved during the test are incorporated in the process control software.

Conclusion

Electrochemical corrosion monitoring has been used for monitoring corrosion in a flue gas desulphurization plant of the Spray Dryer Absorption type. The corrosion rate of the actual system is low, but the corrosion has caused a serious emission problem due to the exfoliation of corrosion products from the surfaces of the flue gas ducts. The corrosion can be avoided by heating up the flue gas. As reheating of the flue gas is an additional expense it is desirable to minimize the heat input.

The corrosion process is dependent on several operating parameters, which vary in a complicated way.

By means of electrochemical noise techniques, corrosion signals are achieved which correlate to relevant operating parameters. The computer technique, neural networks, has been used for processing the large amount of data. Based on this know-ledge it is possible to reduce the heat-input concerning combinations of process parameters resulting in considerable savings.

By using the method some advantages and shortcomings have turned up.

Advantages are:

- the possibility of monitoring the corrosion on-line and install plant regulation equipment to limit corrosion,

- the possibility of analyzing the corrosion problem by advanced computer techniques, e.g. artificial neural networks for obtaining a better understanding of coherence between operation parameters and corrosion.

Shortcomings are:

- a quantitative calculation of the corrosion rate requires difficult calibration to other methods,

- the large amount of data, collected by this method requires extensive data power and well educated personnel

- the measurement is very localized and therefore heavy demands are made for the placing of probes. Removal of probes requires a good deal of work.

Literature.

[1]. B.Sander. Chemical composition of flue gas particles after a Spray Dryer Absorption FGD plant. Internal ELSAM report, 1991.

[2]. B.Sander. Chloride salts hygroscopical properties. Internal ELSAM report, 1992.

[3]. G.Mohr und D.Steinmetz. Korrosionsschåden durch Rauchgaskondensate hinter quasi-trockenen Rauchgasentschwefelungsanlagen (REA), VGB-conference, "Chemie in Kraftwerk 1990".

[4] P. Jansen, V. Hansen and T. Jensen. Corrosion experience with carbon steel in spray absorption FGD-plant. Workshop on Corrosion and Corrosion Protection in Flue Gas Desulphurization Plants. European Federation of Corrosion, Frankfurt, January 1991

[5]. T. Illson, C. Eley, W.Y. Mok, W.M. Cox and D.B. Meadowcroft. Recent initiatives in the use of modern electrochemical instrumentation for FGD corrosion investigation and surveillance. Werkstoffe und Korrosion, 43, 321-328 (1992).

[6] R. Hecht-Nielsen, Neurocomputing, Addison-Wesley Publishing Company. 1990

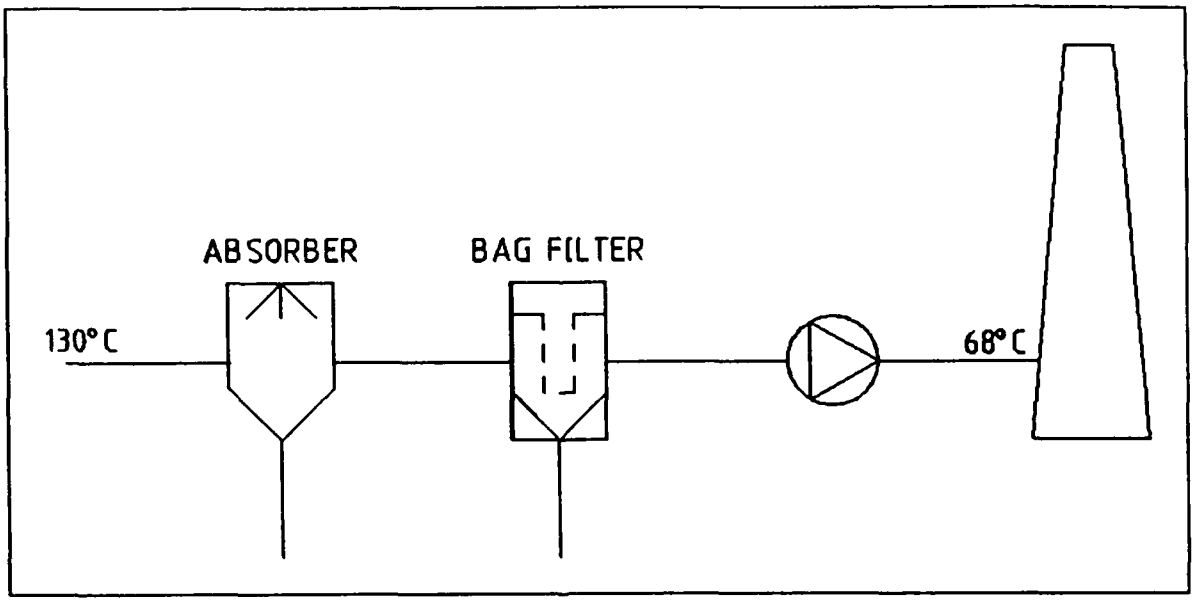

Figure 1: Schematic drawing of the Spray Dryer Absorption FGD process.

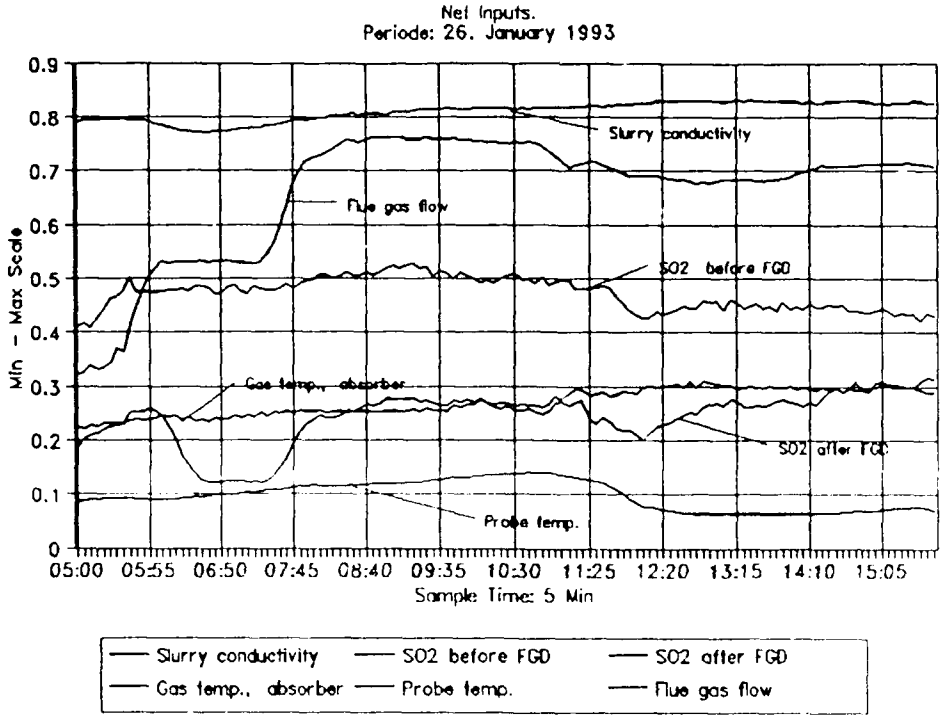

Figure 2: Net input of real process parameters. The unit of Y-axis is a normalized value, where "1" is equal to maximum registered value of the parameter and "0" is the minimum registered value of the parameter. The unit of the X-axis is time of the day (hours: min). Sample time is the logging interval.

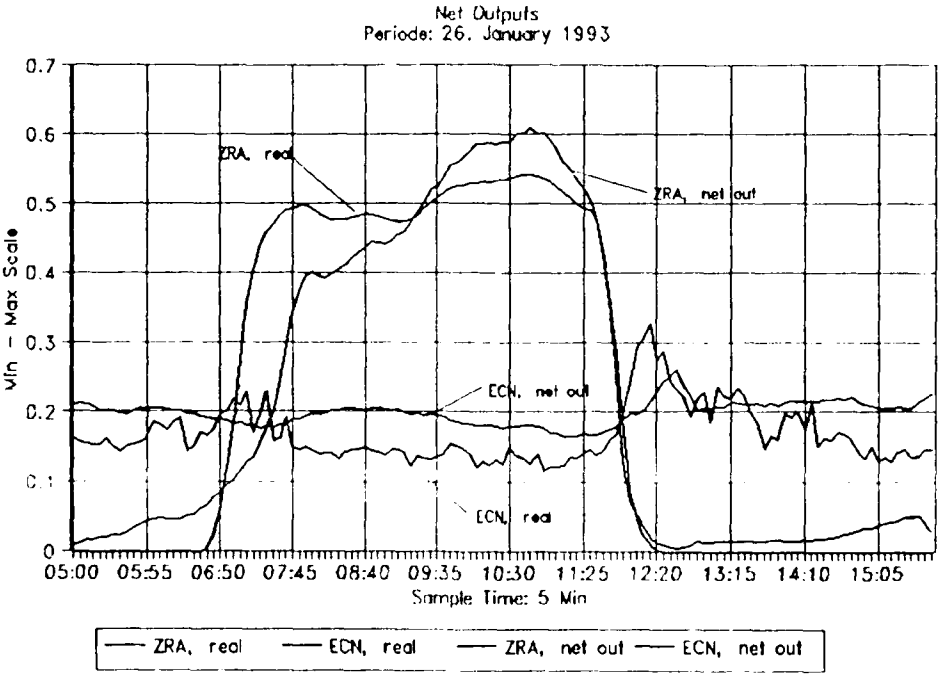

Figure 3: Measured values of ZRA and ECN compared to ANN output values of ZRA and ECN. The unit of Y-axis is a normalized value, where "1" is equal to maximum registered value of the parameter and "0" is the minimum registered value of the parameter. The unit of the X-axis is time of the day (hours: min). Sample time is the logging interval.

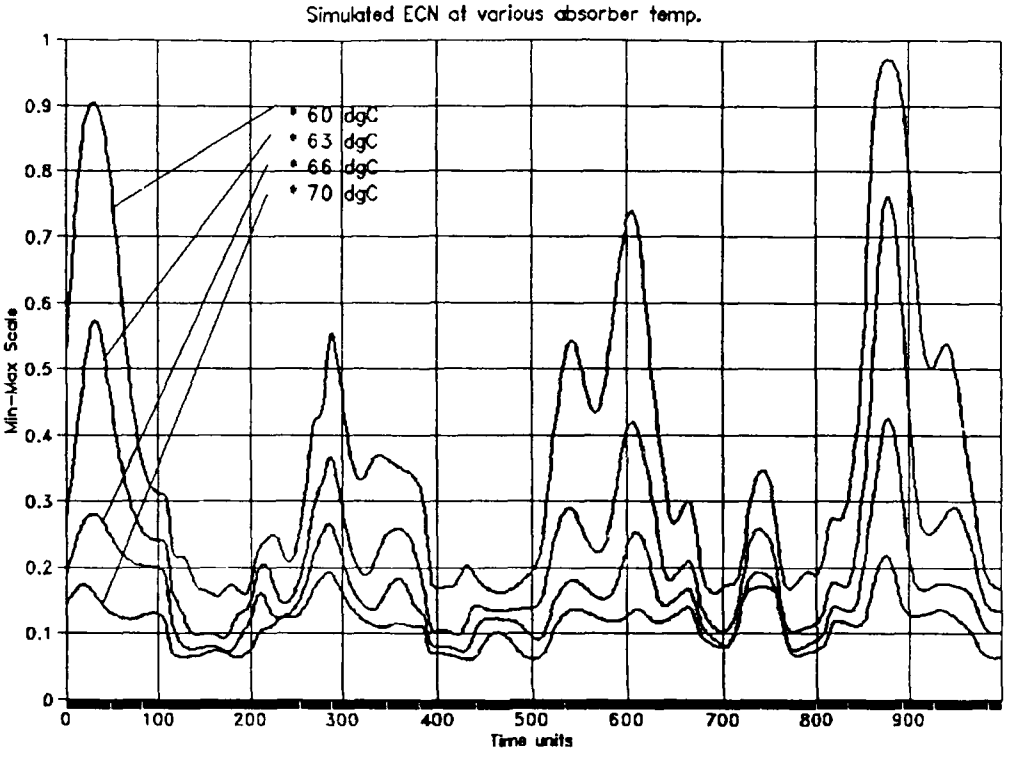

Figure 4: Simulated values ECN compared to ANN output values of ZRA and ECN. The unit of Y-axis is a normalized value, where "1" is equal to maximum registered value of the parameter and "0" is the minimum registered value of the parameter. The unit of the X-axis is minutes.

On-line Monitoring of Fireside Corrosion in Power Plant

David Farrell
Rowan Technologies Ltd
Carrington Business Park, Urmston
Manchester, M31 4DD, ENGLAND
Tel: 61 776 4518
Fax: 61 775 8995

Abstract

There is currently a move towards increasing the efficiency of operation of fossil fuel fired power plant. In the U.K. conventional and ageing pulverised fuel (PF) fired plant are expected to compete with new gas-fired plant. Coal fired boilers are increasingly being operated at higher efficiencies with excess oxygen levels minimized and intervals between scheduled maintenance shutdowns maximized. Typical maintenance intervals are currently 3 years, however the utilities are increasing these; in a few cases to 6 years.

Corrosion, fouling and sometimes failure of heat exchanger tubing in fireside situations is a major obstacle to this aim. Furnace wall corrosion and fouling tend to increase with decreasing excess oxygen concentration. Unscheduled outages for tube repairs are currently of the order of four per year on a typical 500MW boiler; the unit remaining off-line for periods of the order of 2 to 3 days to effect repairs.

Monitoring of the condition of these surfaces has, to date, only been carried out off-line during scheduled maintenance outages. A new corrosion monitoring method, based on a modification of the well established electrical resistance technique, has been developed and evaluated in a 500MW coal fired boiler in the U.K. A fully commercial system is scheduled for installation in a 4GW power station to monitor wastage of furnace wall tubes in vulnerable areas of the boiler. This paper describes the technology behind this new monitoring system and illustrates its use for the condition monitoring of furnace wall corrosion surfaces.

Key terms: fireside corrosion, power plant, corrosion monitoring, high temperature sensors

Introduction

Corrosion of metals exposed to high-temperature gaseous environments, frequently in the presence of deposits, has long been a problem in boilers, furnaces and industrial process plant [1]. The corrosion may be caused by gas-phase oxidation, sulphidation, molten salt attack, carburization or erosion-corrosion type mechanisms. Furnace wall corrosion is caused by low excess oxygen levels resulting in high concentrations of carbon monoxide around the furnace tubes. The attack is reported to be exacerbated in the presence of high flue gas chlorine concentrations [2].

A method for on-line monitoring of the corrosion rate in high temperature systems has not previously been available, although this would be immensely useful to link increases in the severity of the corrosion environment with changes in the unit operation, combustion conditions, fuel composition and additive performance.

In high-temperature environments, corrosion is frequently encountered on heat transfer surfaces or, alternatively, on wall surfaces subject to heat loss; in both of these cases the surfaces are subject to lower temperatures than that of the gas, Figure 1. Corrosion rate is dependent on operating temperature. Conventional corrosion monitoring probes do not have a capability for cooling and, when exposed in a gas system, normally take up a temperature similar to that of the gas. Simulation of the corrosion occurring on a heat transfer surface using a conventional corrosion probe is not therefore possible. During the past few years, corrosion monitoring techniques have been adapted for use in high-temperature plant using suitable ceramic probe sections and cooling systems.

Corrosion Monitoring Techniques

The corrosion monitoring techniques described in this section are complementary. The specific technique employed frequently depends upon the objectives of the corrosion monitoring study.

Weight-Loss Coupon Technique

Weight-loss probes, incorporating either an air or water cooling system, have been used for a number of years to monitor corrosion in boilers and refinery plant. A weight-loss probe incorporating a heat-pipe cooling arrangement has been designed by Powergen for studying furnace wall corrosion in power generation plant [3]. This portable probe allows the medium to long term exposure of a small coupon sample to real furnace conditions.

Weight-loss probes provide valuable information on the type/nature of corrosion attack and the morphology of the corrosion products. However the rate of acquisition of corrosion data is slow because samples are typically exposed for several thousand hours before the metal loss from the coupons can be accurately determined. The corrosion rates are time averaged values giving no appreciation of the short term influence of operational variables on the corrosion process.

Variable Temperature Electrochemical (VTEC) Technique

Electrochemical techniques are used to monitor corrosion at low

temperatures in aqueous systems where the ionic nature of the electrolyte allows the rate of corrosion to be estimated. The polarisation resistance method is used extensively both for on-site corrosion monitoring and for laboratory investigation. The techniques respond rapidly to changes in the rate of attack but determination of an accurate rate of corrosion is sometimes difficult due to other factors which influence the measured electrochemical parameters (eg variable scale or deposit resistance, thermo-electric effects within the probe and variation in the correlation factor).

The ability of the electrochemical techniques to evaluate the corrosion processes is dependent on the ionic transport in the scale or in the deposits formed on the high-temperature surfaces during exposure in-plant [4,5]. Corrosion processes involving molten salt phases or scales with significantly high ionic transport number (t_{ion}) may be monitored using ac or dc electrochemical techniques. Corrosion processes involving simple oxidation, sulphidation or carburization mechanisms produce electronically conductive scales; this prevents electrochemical assessment of the corrosion reactions using simple probe configurations. Electrochemical monitoring techniques rely on the presence of an ionic medium separating the electrodes.

A variable temperature electrochemical (VTEC) ceramic faced probe has been used to monitor corrosion in the furnace walls of power generating boilers [6]. The probe was fitted with three identical carbon steel electrodes set in a ceramic frontface. This allowed three different electrochemical techniques to be used for monitoring the corrosion processes. The techniques used were zero resistance ammetry (ZRA), electrochemical potential noise (EPN) and electrochemical current noise (ECN). The latter two techniques may be used to obtain a polarisation resistance which can be related to the corrosion rate using the Stern Geary equation.

Variable Temperature Electrical Resistance (VTER) Technique

The electrical resistance (ER) technique is the most commonly used method for continuous monitoring of corrosion rate in low-temperature plant. It provides a direct measure of the loss of metal from the exposed test element and also has the ability to monitor corrosion and erosion in both aqueous and non-aqueous environments. The probes typically employ two similar elements; an exposed corrosion element and a protected reference element.

The electrical resistance of a metal is highly dependent on its temperature. The second element is normally contained within the body of the probe and provides compensation for any temperature variation of the exposed element. This temperature compensation system is only effective at relatively low temperatures, ie below 100^{0}C. At higher temperatures a measurable and variable temperature differential exists between the exposed and the protected elements. In addition the conventional ER probe systems are unable to facilitate cooling of the exposed element due to the physical presence of the reference element.

Rowan Technologies has developed a variable temperature electrical resistance (VTER) probe for use in high-temperature plant [7,8]. The increased accuracy and resolution of digital resistance and

temperature measuring instruments now allow accurate and direct monitoring of the resistance of the corrosion element and its temperature to a resolution of 0.1^0C. The resistance of the corrosion element may therefore be temperature compensated using a software package and the element thickness and corrosion rate calculated. This system, comprising resistance and temperature measuring/control instrumentation, data logging system and VTER corrosion probe is shown in Figure 2. CAMERA software is used for data collection and subsequent analysis. The system employs both an 'active' and a 'passive' data acquisition system. The 'active' mode entails high speed monitoring of the probe temperature to determine the optimum time to take a resistance measurement, ie when the rate of probe temperature change around the set-point is at its lowest. This enables a ten fold improvement to be made in the repeatability of consecutive measurements; the 'passive' mode is used when the plant undergoes shutdown. The output is in the form of corrosion rate graphs where the remaining element thickness or change in thickness (corrosion rate) is plotted against time.

Temperature compensation for the VTER element is carried out as follows:

$$R_t = R_{293} (1 + \alpha t) \qquad (1)$$

Where:

R_t = Resistance at test temperature, ohms.
R_{293} = Resistance at 20^0C (293^0K), ohms.
α = Temperature coefficient of resistance, K^{-1}.
t = Test temperature, ^{0}K.

An accurate determination of α is made during commissioning of the probe by scanning through a range of temperatures. Calculation of the remaining element thickness at 20^0C is made as follows:

$$D = \frac{r \times l}{W \times R_{293}} \qquad (2)$$

Where:

r = Resistivity, ohm m.
l = Element length, m.
W = Element width, m.
D = Remaining element depth, m.

On the furnace wall probe the frontface is semi-cooled and typically operates at temperatures in the range 800^0 to 1000^0C in a gas temperature of 1500^0C. A cobalt alloy (Co-20%Cr-15%W-10%Ni) was used for fabrication of this section because of its corrosion resistance. The corrosion element is air cooled and operates at the set-point temperature. The remaining sections of the probe are subject to a high degree of cooling and were fabricated in stainless steel type 316L. The probe utilises a total of six different ceramics and the frontface element insulation comprised a ceramic reinforced fiber.

The design of the probe had to take into account the effect of

thermally induced voltages at the element/electrode lead junctions at high operating temperatures. A thermoelectric compensation (TEC) device, comprising a dummy circuit, is included in the probe to minimize these voltages; the probe was "tuned" during commissioning. The remaining thermally induced voltage was nulled by the instrumentation.

The VTER probe is capable of accurately measuring a change in element thickness of 0.1 micrometer; this relates to the ability of the system to measure a high corrosion rate of 1.6 mm/y (64 mpy) within 0.5 hr, or alternatively, a low corrosion rate of 0.2 mm/y (8 mpy) within 4 hrs. If localised corrosion is prevalent on the probe, then the results will indicate a higher than expected corrosion rate.

On the latest probes the corrosion element has a similar thickness to high temperature heat exchanger tubing (ie 8 to 10mm) and the VTER probe has the added advantage of being able to measure the rate of heat transfer, and thus the rate of fouling, in addition to the corrosion rate. This is achieved by monitoring of the cooling air requirement to the probe.

Results

Examples are given in this section of electrochemical and electrical resistance data from high-temperature corrosion in power generation boilers.

Variable Temperature Electrochemical (VTEC) Techniques

Research of furnace wall corrosion was carried out in collaboration with Powergen [6]. The corrosion trial employed electrochemical monitoring instrumentation and ceramic faced insert probes installed in the furnace wall of a 125 MW power generation boiler. A system was subsequently installed in a 500 MW base-load unit.

The corrosion results, based on 'typical' proportional factors showed reasonable agreement with corrosion rates previously measured by Powergen using a weight-loss probe. A description of the electrochemical techniques used on this trial is outside the scope of this paper [6]. However, an increase in the ZRA and ECN outputs normally indicate an increase in corrosion rate. Representative data from this trial are shown in Figure 3. This data file, at a mean probe temperature of 460^{0}C, illustrates the effect of small excursions in plant operation on corrosion behavior. The probe had been installed in the furnace wall some five days previously and was still undergoing conditioning (initial scale/deposit formation on the corrosion element). Steady corrosion behavior was observed at the start of the data file. At approximately 22:30 hrs, a decrease in probe temperature was identified, possibly as a result of temporary boiler load change. The corrosion monitors (ZRA and ECN) indicated a simultaneous sharp increase in corrosion attack. When the probe temperature returned to its previous value, some two hours later, the rate of attack returned to its previous level. A second boiler operational variation occurred some four hours later and again a sharp increase in corrosion activity was detected. These results illustrate the sensitivity of the corrosion behavior to changes in boiler operation. Identification of the precise cause of the operational

variation was not possible although the timing of the events was similar to that for steam sootblowing of the boiler.

Variable Temperature Electrical Resistance (VTER) Technique

The VTER system was initially installed in a Babcock Robey, chain grate fired, shell boiler installed at the British Coal Research Establishment (CRE), Cheltenham [9]. The boiler was rated at 12,000 lb/hr and the gas temperature was typically around 900^{0}C. The probe was installed in the reversal cell after the first pass (furnace tube) and the element was maintained at a temperature of 400^{0}C. This shakedown test provided the corrosion rate data and probe performance data required to design the second commercial system for the power generation boiler. These boilers operate at considerably higher temperatures and involve heat fluxes as high as 500kWm^{-2}.

The VTER system was subsequently installed in the furnace wall (side wall - 70 foot level) of a 500MW PF fired boiler (Foster Wheeler John Brown) equipped with 'low NOx' burners, Figures 4 and 5. The probe required conditioning (initial scale formation on the carbon steel corrosion element) prior to full insertion (flush with the furnace wall tubes). This was carried out by inserting the clean probe some 75mm back from the front tube position for a period of six days [10]. After this conditioning period, the probe was capable of maintaining a temperature of 400^{0}C in the fully inserted position (gas temperature range 1200^0 to 1500^{0}C). A number of gas thermocouples were used in conjunction with the VTER probe; these rapidly failed due to the extreme conditions in this section of the boiler.

The reduction in thickness of the 3mm thick probe element (at a high metal temperature of 500^{0}C) during the 51 day test is shown in Figure 6. The resistance measurements were temperature compensated and the remaining element thickness at 20^{0}C was recorded. An example of fouling, and the resulting effect of boiler cleaning in the furnace zone is shown in Figure 7. A water lance was used for cleaning in this region. The condition of the probe at the completion of the test is shown in Figure 8.

Discussion

Monitoring of the condition of high-temperature process plant has to date, normally comprised visual inspections carried out during plant shutdowns. This has been because suitable on-line monitoring probes and instrumentation have not been available. However, systems are now available to monitor and allow control of the operation of high temperature plant.

Electrochemical probes and associated instrumentation are available for use in high-temperature plant. The electrochemical systems can be useful for identifying periods of high and low corrosion activity due to their rapid response to change. However, the electrochemical parameters associated with the corrosion reaction are influenced by a number of factors and the accuracy of the measured corrosion rate is frequently poor. In addition, the techniques rely on the presence of an ionic path between the electrodes and are not effective in erosion situations. In the presence of essentially electronically conductive scales, only the

resistance of the scale will be measured.

The variable temperature electrical resistance probe and associated digital instrumentation is now being used to monitor corrosion at metal temperatures up to 800^{0}C and in gas streams up to temperatures of 1500^{0}C. The resistances of scale or deposits which can build up on the probe are significantly greater than that of the probe element and they do not interfere with the measurements. The system has the capability of monitoring wastage due to corrosion, erosion and erosion-corrosion. In addition, the probe incorporates a fouling measurement capability to enable the efficiency of the heat transfer surfaces to be monitored. This facility is useful for indicating the requirement for boiler cleaning.

Tubular probes, suitable for use in superheater zones, are currently being evaluated in-plant. The VTER system presents no significant risk to the boiler when used in a fireside situation. It has been designed to operate with little or no maintenence in the environment around a fossil fuel fired boiler. The basic VTER system (including instrumentation, probe, temperature control facility, data handling system and software) costs around US $17,000. Additional channels (including probes) can be added at a cost of US $6,000. The system can be inserted in furnace or superheater zones susceptible to attack to give an indication of the remaining life of heat exchanger tubes. Alternatively, the VTER system can be used to optimize the operation of the boiler (trimming the excess air) without causing a significant increase in fireside corrosion.

Future research needs include a demonstration of the system on a boiler optimization program to assess the efficiency gains to be made from use of this and other high temperature sensor systems in coal fired boilers. In addition, the system may be used for studying high temperature corrosion processes in-plant. A high pressure version of the probe will be required for use in the nuclear or steam applications. Large temperature variations, of the order of ±300^{0}C, have been found in-plant around the furnace walls. Research is currently being initiated to improve temperature measurement systems for use in furnace environments.

Conclusions

1. Electrochemical probes are capable of monitoring short-term variations in corrosion rate in some high-temperature plant. They may not be used in situations where electronically conducting scales are present. The accuracy of the corrosion rate estimations can sometimes be poor.

2. Variable temperature electrical resistance probes are capable of monitoring short-term and also long-term corrosion in high-temperature plant. The characteristics of the scale, and/or surface deposits, do not affect the accuracy of the measurement. The system has the additional capability of monitoring heat flux and fouling in high temperature plant.

3. The VTER system is currently being used for monitoring wastage by both erosion and corrosion in high temperature boiler plant. A full commercial system has now been installed in a

660MW coal-fired power generation boiler.

4. The VTER system should find additional use in power generation, refinery and process plant where condensation corrosion at lower temperatures is prevalent.

Acknowledgements

The author expresses his thanks to the Department of Trade and Industry, British Coal, National Power PLC, ENEL-CRTN (Italian Electricity Generating Authority) and Esso Engineering Europe Ltd who are supporting this work. The author also expresses his thanks to Len Pinder (Powergen) for his assistance with the VTEC work and Mathew Lee of Ferrybridge Engineering Centre (National Power) for his assistance with the VTER on-site tests.

References

1. W.D. Halstead, Progress Review No. 60: Some chemical aspects of fireside corrosion in oil-fired boilers, J. Inst. Fuel, July 1970.

2. T. Flatley and C.W. Morris, Control of fuel ash corrosion in coal fired boilers, U.K. Corrosion 83, Birmingham, November 1983.

3. P.J. James and L.W. Pinder, Electronically controlled variable capacity heat pipe probes for furnace wall corrosion studies in coal-fired boilers, CEGB, OED Report, 1988.

4. D.M. Farrell, F.H. Stott, G. Rocchini and A. Colombo, Electrochemical aspects of high-temperature corrosion reactions in combustion systems, U.K. Corrosion 91, Manchester, October 1991.

5. D.M. Farrell, F.H. Stott, G. Rocchini and A. Colombo, The influence of electrochemical processes on high temperature corrosion reactions in combustion systems, Materials at High Temperatures, February 1992.

6. D.M. Farrell, W.Y. Mok and L.W. Pinder, On-line monitoring of furnace wall corrosion in a 125 MW P.F. boiler, 2nd Int. Symp. High Temperature Corrosion, Les Embiez, France 1989.

7. D.M. Farrell, U.K. Patent App. No. 9126881.3, Dec. 1991.

8. D.M. Farrell, U.S. Patent App. No. 990459, Dec. 1992.

9. D.M. Farrell, Corrosion Monitoring in High-Temperature Environments, Conf. Condition Monitoring and Corrosion Prevention in Refineries and Petrochemical Plant, BSI, London, June 1992.

10. D.M. Farrell, Corrosion Monitoring in High Temperature Systems, U.K. Corrosion 92, Manchester, Oct. 1992.

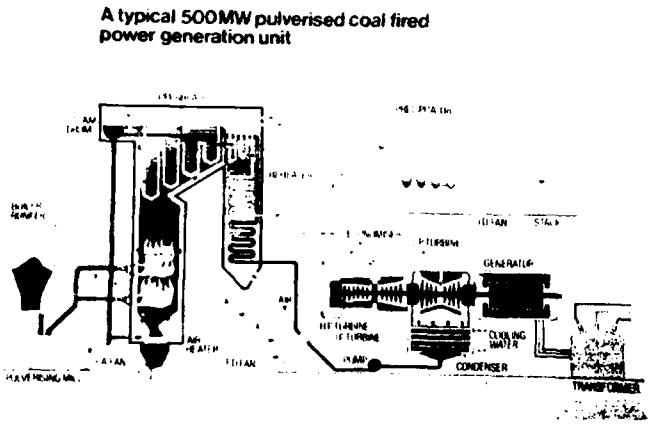

Figure 1. Schematic Diagram of a 500MW Power Generation Boiler.

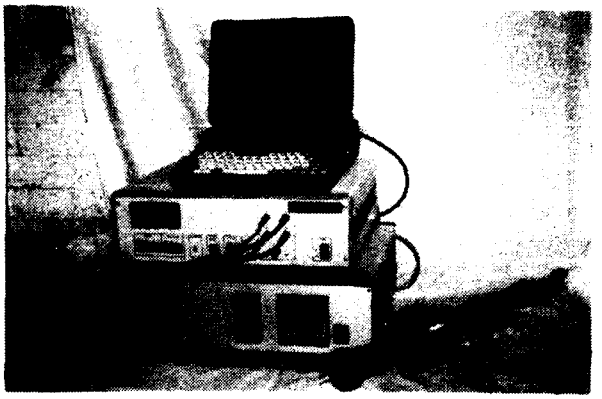

Figure 2. Variable Temperature Electrical Resistance Probe and Instrumentation.

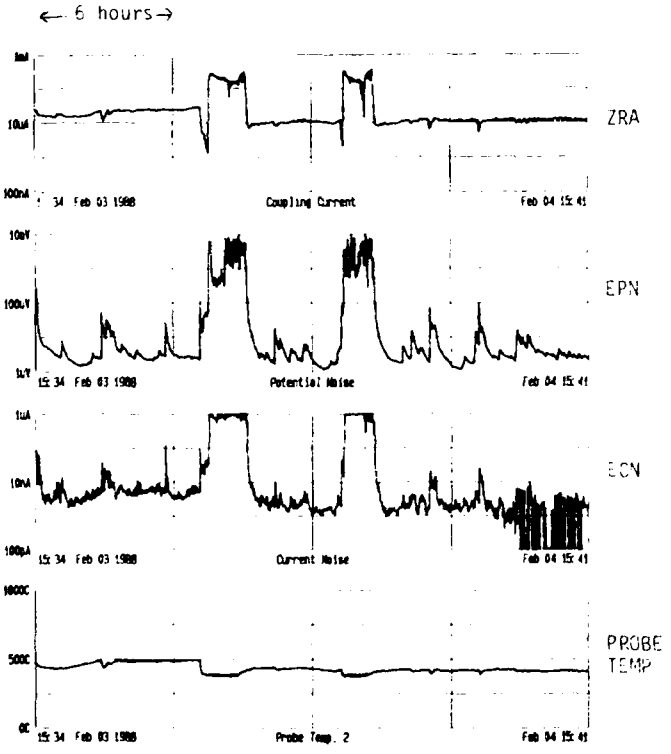

Figure 3. Illustration of Corrosion Behavior using the Variable Temperature Electrochemical Technique.

Figure 4. Probe Port installed in a Door of a 500MW Boiler.

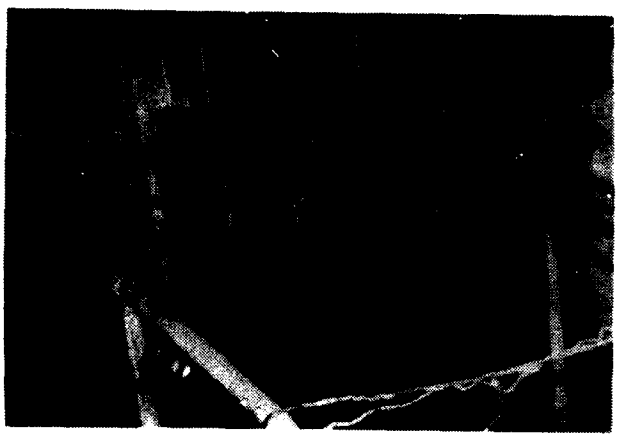

Figure 5. Variable Temperature Electrical Resistance Probe Installed in the Furnace Wall.

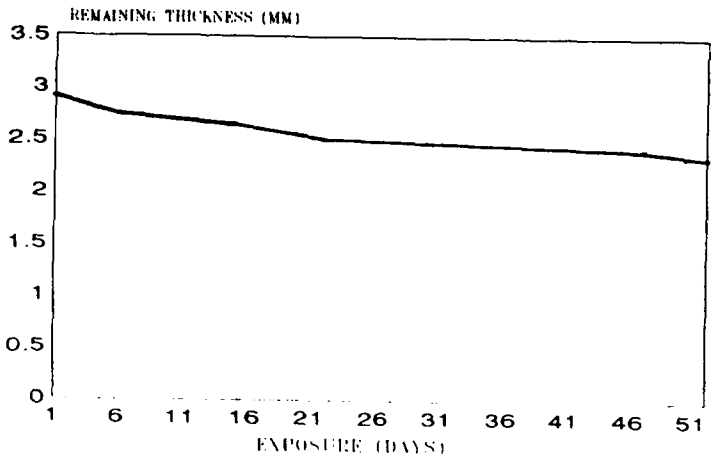

Figure 6. Reduction in Thickness of a 3mm probe element installed in a furnace wall at a temperature of 500^{0}C.

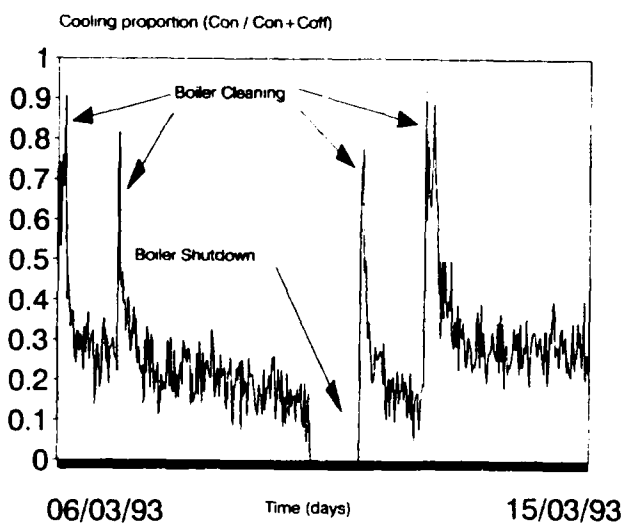

Figure 7. Example of Probe Cooling Data illustrating the Influence of Boiler Cleaning.

Figure 8. Condition of the VTER Probe at the Completion of the Test.

FSM – A New and Unique Method for Monitoring of Corrosion and Cracking Internally in Piping Systems and Vessels

Roe D. Strommen, Harald Horn, Kjell R. Wold – CorrOcean as, Trondheim, Norway

Abstract

Over the last couple of decades there has been a substantial growth worldwide in the number of plants for generation of power, mainly electricity. As the plants grow older, the need for inspection and monitoring becomes ever more important to ensure a safe and non-interrupted operation of these plants. At the same time it is a challenge to optimize inspection and monitoring programs to reduce the expenditures for such programs.

This paper describes a new technique known as the FSM – the Field Signature Method, that offers a means of continuous monitoring of the condition of pipes, pressurized vessels etc. of such plants, and of any corrosion, pitting or cracking that might take place, and of the remaining wall thickness at any time of a pipe or a vessel. It is claimed that this new FSM technique combines the advantages of corrosion probes and NDT/inspection: It offers high sensitivity and responds to changes in corrosion of the actual pipe wall in real time. This combines with an ability to cover relatively large areas of the actual structure.

FSM removes the need for access fittings, for replacement of probes and for retrieval operations, reducing costs and improving safety.

The System requires virtually no maintenance nor replacement of consumables. The service life of an FSM System equals that of the pipe work itself.

FSM is therefore an excellent technique for monitoring any piping system, pressure vessels etc, and in particular inaccessible areas like buried and subsea pipelines and hazardous areas in nuclear power stations.

Introduction

With the strong growth over the past years in the number of, and often also in the size of, power stations, process plants, chemical and petrochemical plants, the continued, safe operation may become a challenge. As the plants grow older, corrosion, pitting and cracking, e.g. in welds and in the HAZ may represent a threat to the safe and non-interrupted operation of the plant.

To reduce the risk of failure, and to optimize maintenance of the plants, measures are taken to protect the plants and components against corrosion. Monitoring and inspection programs are instigated with the objective of having early warning of failure, allowing for optimization of maintenance programs, and secondly with the purpose of controlling corrosion mitigation programs. Such mitigation programs may involve e.g.

inhibitor injection or simply a strict control of the process parameters like the product chemistry, temperature, flowrates etc.

While many of the traditional NDT and inspection techniques may represent excellent tools for assessment of the condition and integrity of a piping system or a pressure vessel, the sensitivity of these methods may not be adequate for monitoring the performance of an inhibitor or to produce feedback on unacceptable changes in the process parameters that cause corrosion. In this latter case a monitoring method is required with a high sensitivity, and data collection with a frequency high enough to produce reliable trends, e.g. on a weekly basis.

It is thought that the FSM technique combines the advantages of corrosion probes and NDT/inspection: It offers high sensitivity and responds to changes in corrosion of the actual pipe wall in real time. This combines with an ability to monitor the condition, i.e. the actual pipe wall thickness of relatively large areas of the actual structure. FSM may therefore offer a means of designing an optimized and economical inspection and monitoring program for a plant.

FSM – The Field Signature Method was developed and patented by Center for Industrial Research (SI) in 1985/86.(1). CorrOcean as, which has acquired all rights from SI for worldwide commercial exploitation of the FSM technique, has spent in excess of 3.5 Million USD over a 4–year period developing this technique, and is presently in the process of adapting this technology for applications subsea.

For internal corrosion monitoring, the FSM represents a non–intrusive technique. This means that the sensing electrodes and all other equipment is placed on the outside of the pipes, tanks or vessels to be monitored. In comparison with traditional corrosion monitoring methods (probes), the FSM therefore exhibits operational advantages as listed below:

* There are no components being exposed to the corrosive, abrasive, high temperature and high pressure environment often found in process piping.

* There is no danger for introduction of foreign objects in the piping.

* There are no consumables. The complete monitoring system can be designed for a service life comparable with the piping, tank or vessel itself.

* There is no danger for leaks in access fittings or due to unsuccessful retriever operations.

* Measurements are done on the wall of the pipe, tank or vessel itself, not on a small probe or test piece.

* The sensitivity and reliability is better than for most NDT techniques.

The FSM Principle

The FSM method is based on feeding an electric direct current through the selected sections of the structure to be monitored, and sensing the pattern of the electrical field by measuring small potential differences set up on the surface of the monitored object. By proper interpretation of these potential differences, or rather changes in potential differences, conclusions can be drawn e.g. pertaining to general wall thickness reduction. Local phenomena can be monitored and located by performing a suitable number of potential measurements on a given area. Figure 1 gives an illustration of the principle: By inducing an electrical current into a selected section of a structure like a pipe, this current will spread out into a pattern which is determined by the geometry of the structure and the conductivity of the metal. This pattern is represented by current flow lines and equi–potential lines at normal angels to the current flow, as shown in fig. 1.

Any corrosion whether localized or general, will cause a change or distortion in this field pattern, which reflects the size, shape and location of the corrosion defect. This is indicated in figure 2. In order to assess in detail the location, size or severity of localized or general corrosion phenomena, computer models have been developed to calculate or estimate changes in the electrical field pattern for known corrosion patterns.

The FSM is unique in that all measured electric potentials are compared with initial values measured when monitoring of the object started. These values represent the initial geometry of the object, and may be regarded as the object's fingerprint. Hence the name of the method.

Figure 3 illustrates a typical arrangement for internal corrosion monitoring of a pipe. The monitored area is located between two electrodes for feeding the excitation current. Any potential measurement between two selected electrodes in the matrix is compared to a measurement between two reference electrodes and to the corresponding initial values when monitoring started, i.e. the fingerprint.

The so-called Fingerprint Coefficient (FC) is calculated according to the expression as follows for each set of measurements:

$$FC_{Ai} = (B_s/A_s * A_i/B_i - 1) * 1000 \text{ (ppt)}$$

FC_{Ai} = Fingerprint Coefficient for electrode pair A at time i
A_s = Voltage for electrode pair A at startup
B_s = Voltage for reference pair B at startup
A_i = Voltage for electrode pair A at time i
B_i = Voltage for reference pair B at time i

The FC is the parameter which is used for analysing corrosion rates and accumulated corrosion. The FC is expressed in parts per thousand (ppt) and corresponds to reduction in wall thickness in ppt when monitoring general corrosion or erosion. When monitoring starts, the FC values are always zero.

The reference pair of electrodes is located in the vicinity of the monitoring electrode matrix, however at an area where corrosion will not occur. This is necessary in order to achieve effective compensation for (small) fluctuations in temperature and excitation current. Different practical arrangements have been developed for securing sufficiently small temperature gradients between reference and monitoring electrodes. The more common practical solution is to transmit the electric current through a reference plate fitted to the pipe wall, to ensure that the temperature is similar for the two elements. The reference plate is furthermore electrically insulated from the pipe wall and well coated/embedded to ensure adequate corrosion protection.

Figure 3 illustrates schematically the instrument setup. By use of statistical filtering techniques, very high sensitivity is achieved. This facilitates high resolution monitoring even when measurements are performed on the opposite side of the corroding wall as will be the case for internal corrosion monitoring. Resolution figures obtained in practice represents less than 0.05% (0.5 ppt) of the wall thickness.

Arrangement of Sensing Pins

When designing an NDT or inspection program, the inspection engineer will select critical locations of a pipeline or a structure where the risk of corrosion, erosion or cracking are high, or serious hazards might arise in the event of failure. Similar principles are utilized in the case of FSM. Typical areas chosen for monitoring are:

* Girth welds of pipes and pipelines.

* Bottom sections, e.g. at 4–7 o'clock position in horizontal pipes where corrosive water may be deposited.

* Combinations of the above, and areas subject to corrosion induced by CO_2, H_2S or biological activity.

* T–joints of pipes where there is a risk for erosion/corrosion.

* Pipe bends and welds.

* Structural node corners.

* Tank bottoms, inlets and outlets of tanks and vessels, critical and stressed welds.

The selected area is fitted with the current induction transformer and the minimum number of 24 sensing pins. This number may however, be increased in multiples of 8 pins up to a maximum of 64 pins for one FSM spool and instrumentation module. A typical arrangement is shown in figure 4.

The sensing pins may be distributed in a matrix over the critical area where the matrix spacing or pin–to–pin distance may vary typically from 2–3 cm (1 inch) up to 10–15 cm (4–6 inches), depending on the sensitivity required for detection of smaller pits. With a matrix spacing of 2–3 cm the system has a proven capability of detecting and monitoring the growth of pits in welds as small as 1–2 mm in diameter and depth. A matrix spacing of 10–15 cm is used in the case of uniform corrosion, or when wide and shallow pitting is expected. Typical surface area covered per instrument module may range from 0.1 to 1.1 m^2 (1–10ft^2)

Status and Test Results

Since the development of this technology was completed some two years ago, a number of 15–20 installations have been completed or are in the process of being completed. Two of these projects are for installation on pipelines subsea, to be done in 1994.

In addition to fairly extensive laboratory tests some of these projects have offered good opportunities for testing and evaluation of this technique, by comparison with data obtained from other inspection methods or from inspection after retrieval from the plants of test sections of pipes fitted with FSM instrumentation. One of these tests were conducted on a spool piece installation on Shell Expro's Dunlin Platform in the North Sea. In this case, corrosion was localized to welds or HAZ in piping carrying crude oil with a fairly high water cut and some 4% CO_2. The FSM proved able to detect and present the actual corrosion trends on a weekly basis, and variation in its severity around the circumference of the pipe in and around the weld zone. Since the sensitivity of the FSM is 1 ppt of the wall thickness, this means in practical terms that a corrosion rate of 10 mpy on a 1/2 inch wall can be concluded in approx 2 weeks time. For further details, refer to reference 2.

Applications

FSM represents both a supplement and a cost effective alternative to existing NDT and corrosion monitoring techniques. The method combines the advantages of NDT inspection, that can cover fairly large surface areas of an actual structure, with those of corrosion probes, which offer high sensitivity and a quick response to changes in the corrosivity. This can be utilized to improve the long term cost efficiency of corrosion monitoring and inspection programs, of an inhibitor control program etc.

There are many applications for the FSM in the industry. Examples comprise :

* Offshore topside petroleum production and process equipment.
* Subsea production units and pipelines.
* Onshore petroleum production.
* Petrochemical plants and refineries.
* Paper and pulp production.
* Other process industries.
* Nuclear power plants.

Typical examples of defects that can be monitored and located by the FSM are:

* General corrosion.
* CO_2 corrosion.
* Localized corrosion or pitting.
* Bacterial corrosion.
* Cracking in welds/HAZ.
* Erosion.

As already stated the FSM may have a particular attraction for internal corrosion monitoring in pipelines, piping systems and vessels. FSM can monitor internal corrosion from the outside, and cover fairly large surface areas of piping, pipe bends, pressure vessels etc. The non-intrusive nature of the FSM offers a number of advantages:

* It produces high quality data on the condition of a plant, at the same time reducing the need and cost of UT/NDT and intelligent pigging.

* There is no need for replacement of probes/consumables as the lifetime of an FSM installation depends mainly on the remnant lifetime of the pipewall itself. FSM does not require access fittings, or retrieval operations. This can significantly reduce costs and improve safety.

* Since FSM generates the same information provided by UT/NDT measurements as well as additional data, the UT/NDT program and its costs can often be reduced while improving the quality of the data produced, both locally and overall.

Corrosion and Crack Monitoring in Inaccessible Areas

An important feature of the FSM technology is that the system requires virtually no maintenance, nor is there a need for replacement of consumables. This is a feature that makes the FSM particularly attractive for remote monitoring at inaccessible locations. Examples comprise internal corrosion monitoring of buried, onshore pipelines, and corrosion and crack monitoring in the hazardous areas of nuclear power plants, where radiation limits human access.

Structural Corrosion and Crack Monitoring

Examples from numerous applications comprise : bridges, crane pedestals, node corners of offshore platforms, tendons of tension leg platforms, aircraft, spacecraft etc.

Internal Corrosion Monitoring of Subsea Pipelines and Subsea Completions

Internal corrosion monitoring of subsea pipelines and satellites/templates based on the FSM represents potentially exciting applications, particularly as there are virtually no other practical monitoring methods available today.

In combination with intelligent pigs, FSM represents the only reliable alternative to internal corrosion monitoring subsea. Correlation of intelligent pigging results and FSM readings may allow less frequent pigging runs to be done.

With FSM there are no sensors to be replaced, and the complete monitoring system can be designed for the same service life as the subsea pipework.

In addition the FSM can monitor corrosion accurately at relevant locations subsea, at actual temperatures and flow conditions. It can monitor the performance of inhibitors, also the influence of scale formed on the pipe wall, actual corrosion and erosion rates in-situ. This information can be transferred without delay to the surface, allowing the corrosion engineer to take immediate action.

Particularly in the case of multiphase transport of corrosive petroleum products, the FSM may offer an adequate tool for controlling inhibitor treatment of the subsea line. In some cases the only alternatives might be either failure and replacement of a carbon steel pipeline, or the use of alloyed steel at considerable expense. FSM stations subsea can produce detailed and reliable information on the condition of your pipeline and pipework. FSM improves the safety, while at the same time reducing the costs, e.g. by reducing the required frequency of intelligent pigging.

Instrumentation

Depending on the type of application, four different instrumentation concepts are possible for the FSM:

Portable FSM Interrogator

The portable system consists of the following components (See also figure 7):

* The instrumented section of the structure or pipe including the current excitation arrangement, the sensing pins with wires and connectors and a protective cover normally made in stainless steel.

* A portable interrogator unit which can be used on any number of instrumented sections. When this instrument is hooked up to an instrumented section, it can run on command the measurements and store the results along with time, date and any tag no. or identification.

* FSMTrend software for use with a PC. This accepts downloading of the readings from the portable FSM meter, and takes care of historical file storage, data analysis, graphing, printing and plotting.

FSM Station for Continuous Logging

As an alternative to the use of a portable meter, the FSM can be supplied as a stand alone battery powered logging station. See figure 8. The equipment comprises :

* The instrumented FSM section with current feeding transformer, sensing pins with wires and connectors, and the protective cover.

* A self-contained, battery powered logging station, preprogrammed for automatic interrogation at regular intervals, and storage capacity for several months of operation based on one reading per day.

* A data retrieval unit for downloading the readings directly to a PC.

* The FSMTrend software package.

On-line Monitoring System.

Permanent instrumentation systems for on-line monitoring are based on FSM Stations to be fitted locally, one at each location, and connected via a field bus system to a Master unit in a control room. The Master unit can handle up to 15 FSM Stations, and is controlled by a version of the FSMTrend for on-line monitoring, installed on a standard PC. The components that go into this system comprise (see figure 9):

* One or more FSM Stations with field bus interface, as described above.

* Master unit, to be installed in the control room, and connected to a PC.

* Field bus cable system, a cable consisting of two pairs linking in series the FSM Stations to the Master unit.

* The FSMTrend software, automatic version.

Instrumentation for Subsea and other Remote Monitoring.

FSM Systems are being designed as ready made spools for subsea completions and subsea pipelines. (See figure 10) Suitable concepts for instrumentation comprise :

* Spools located close to subsea completions. Power supply and data communication can be routed through cables run back to the subsea electronics control module, and transmitted to an onshore station or platform via the umbilical. The system can be set up for remote polling via the umbilical.

* Battery powered systems with hydro accoustic communication to the surface, either to a fixed installation within 15-20 km distance, or via surface ship or a buoy supplied with satelite communication.

* Battery powered FSM system with an ROV or diver retrievable datalogger. Battery is made integral with the data pack to simplify retrieval.

Conclusions

The FSM has proven to be a reliable and flexible means of monitoring corrosion, erosion and cracking. Based on its principles and from testing it can be concluded as follows:

* FSM can be installed on steel and other metal structures, piping systems and vessels of virtually any geometry.

* FSM combines the advantages of corrosion probes and NDT/inspection: It offers high sensitivity and responds to changes in corrosion of the actual pipe wall in real time. This combines with an ability to cover relatively large areas of an actual structure.

* The readings are conclusive. FSM shows on the screen the actual condition of the plant, corrosion rates and trends, location and severity of pits and cracks.

* From a number of lab tests and field installations it has been concluded that FSM can monitor accurately the internal condition of pipes and vessels from the outside.

* FSM removes the need for access fittings, for replacement of probes and for retrieval operations, significantly reducing costs and improving safety.

* The System requires virtually no maintenance nor replacement of consumables. The service life of an FSM System equals that of the pipe work itself.

* FSM is therefore a technique suitable for monitoring inaccessible areas like buried pipelines, hazardous areas in nuclear power stations, subsea pipelines and structures.

References

1. HÅREK HOGNESTAD (SI): Several in-house reports on the FSM technique. Norwegian patent no.150.136, dated 19 April 1982

2. ROE D. STRØMMEN, HARALD HORN, K.R. WOLD: Paper no 7, NACE Corrosion/92

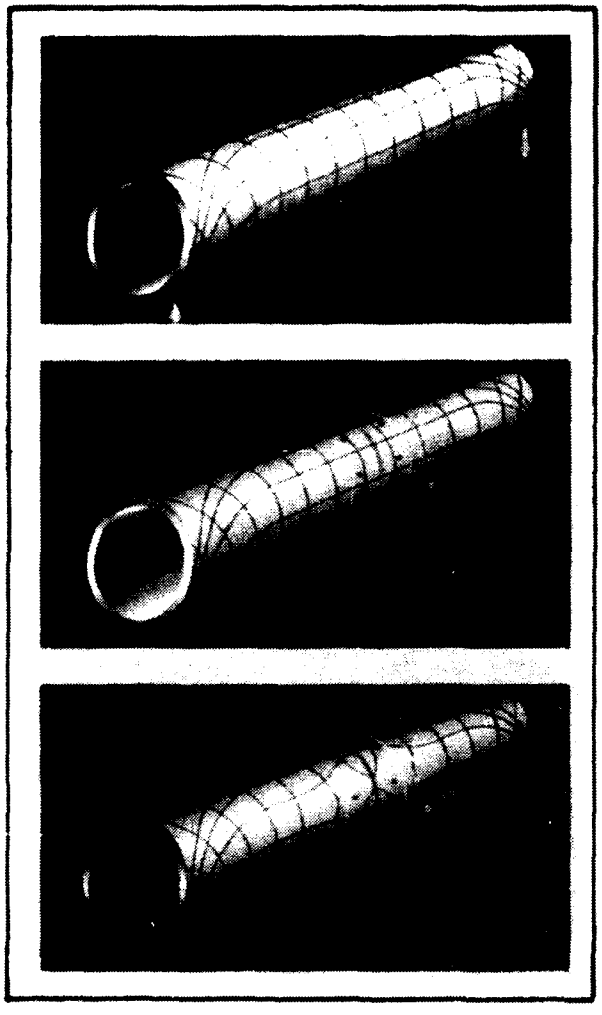

FIGURE 1 – By inducing an electrical current in flawless pipe, an "ideal" field pattern is generated, as shown on the top two sections. Initiation and growth of pits, cracks or other corrosion phenomena will cause a distortion in the field pattern as shown on the bottom pipe section.

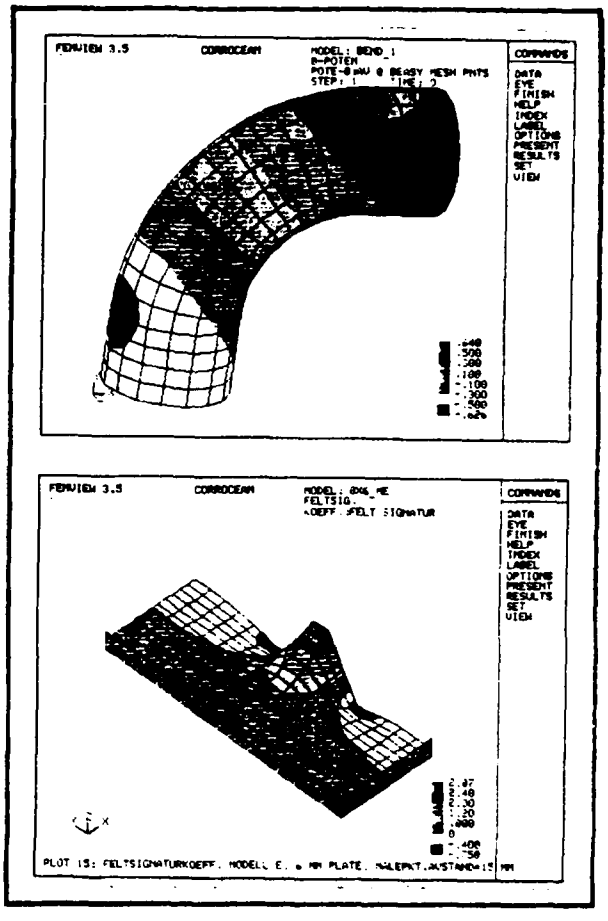

FIGURE 2 – Computer models have been developed to estimate distortions in the electrical field pattern and the corresponding corrosion attack.

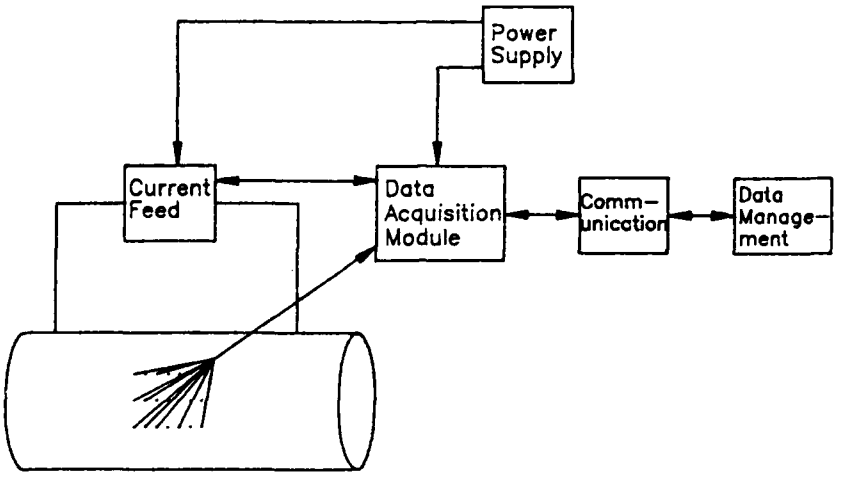

FIGURE 3 – Schematic of instrumentation for the FSM, including current feed source, sensing pins, data acquisition module and data management system.

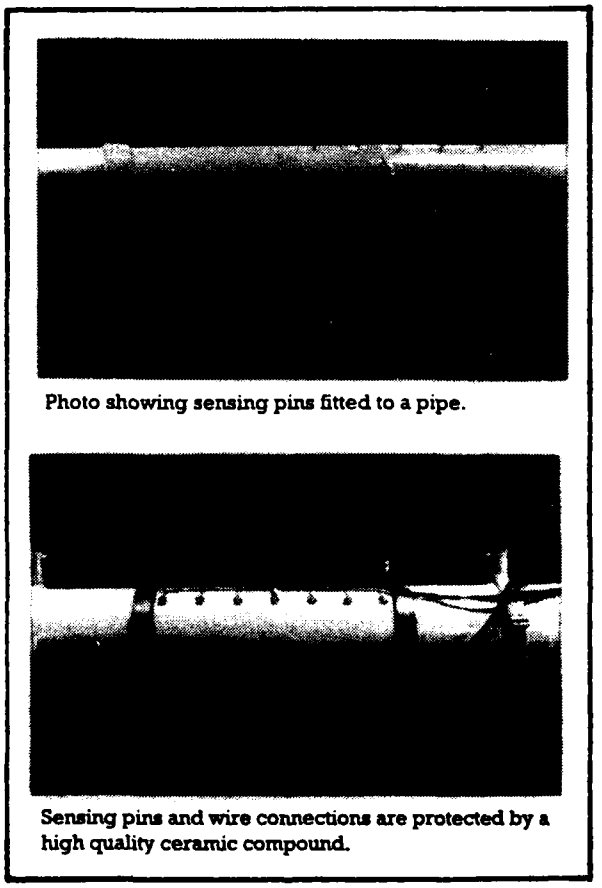

FIGURE 4 – Up to 64 sensing pins can be fitted to the monitored sections by studwelding (top) and hardwired back to an electrical connector (bottom).

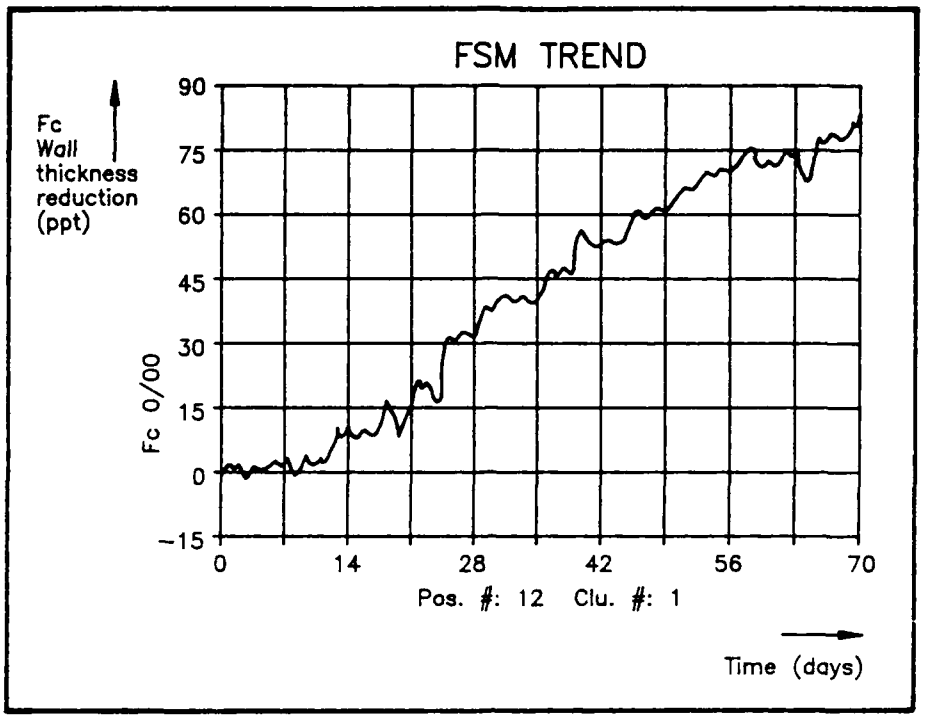

FIGURE 5 – This graph shows the increase with time in the FC-value, i.e. in accumulated corrosion (in ppt) of original wallthickness between one selected pin pair on a carbon steel piping subjected to corrosion in a test. At the end of this test approx 8% of the wallthickness was lost.

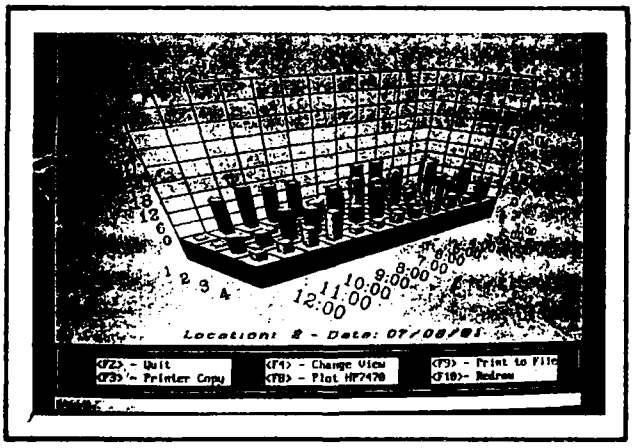

FIGURE 6 – A software package has been developed to display accumulated corrosion for all the pin-pairs fitted in a monitored section.

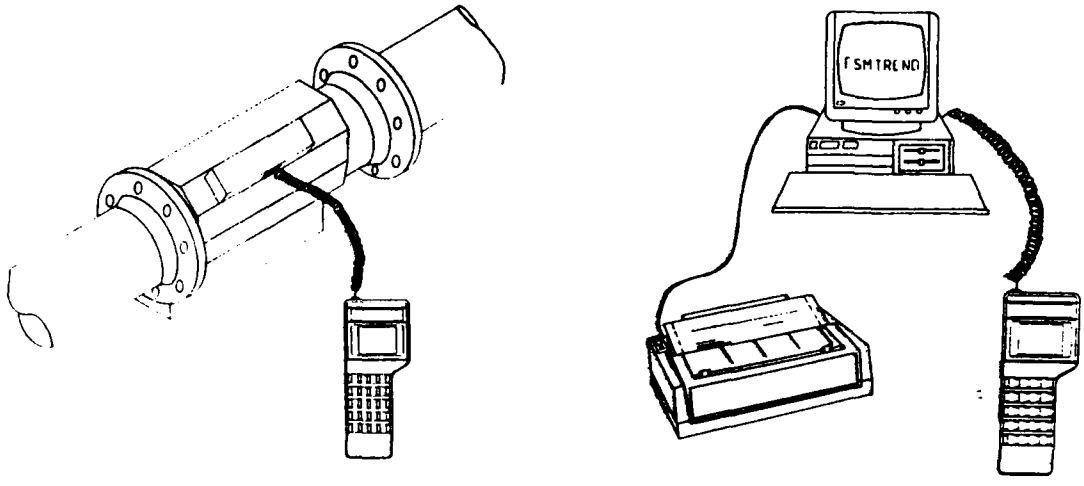

FIGURE 7 – Readings can be obtained with a portable instrument on an FSM-fitted section, for later downloading to a PC.

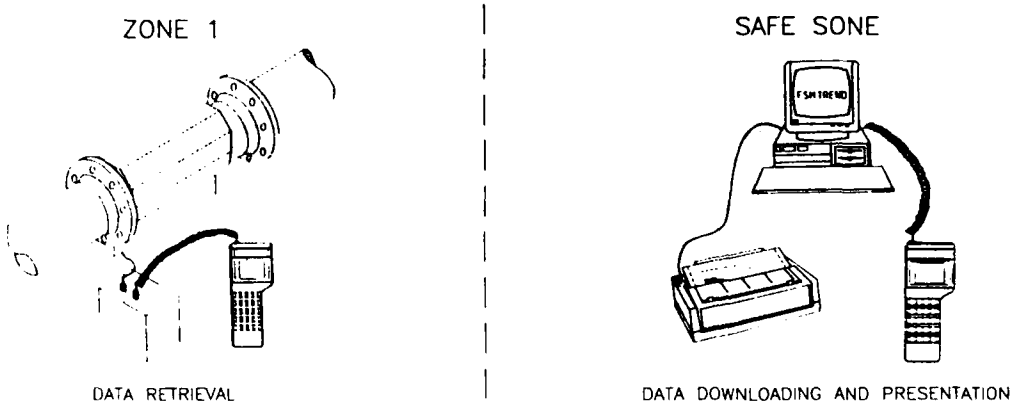

AUTONOMOUS FSM STATION FOR Ex ZONE 1

FIGURE 8 – Optionally, an autonomous logging station can be used for automatic logging of instrumented sections, also designed for data retrieval by a portable device and later downloading to a PC.

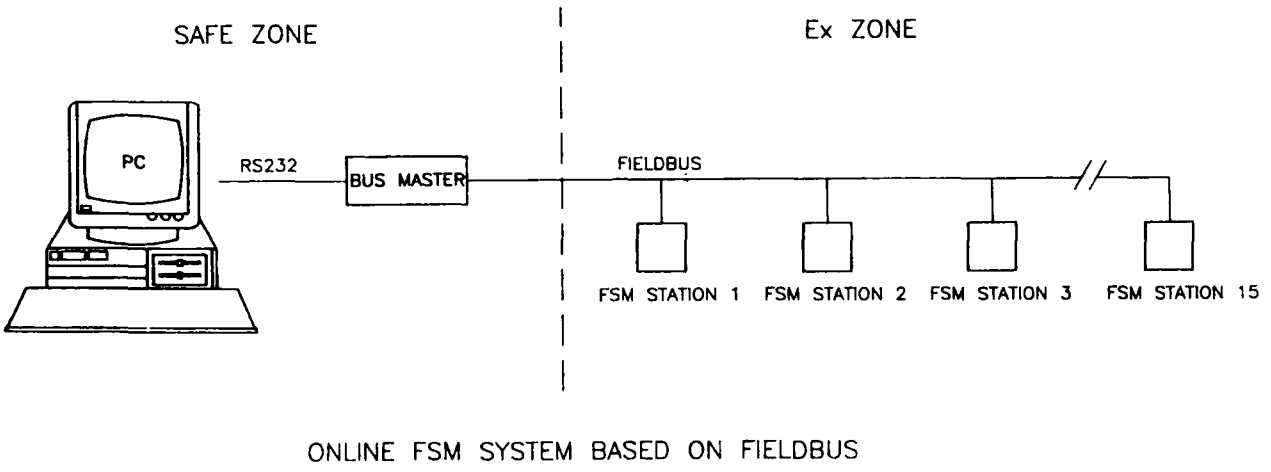

FIGURE 9 – A fully automatic logging station can be used for interrogation of up to 15 local FSM stations via a field bus system.

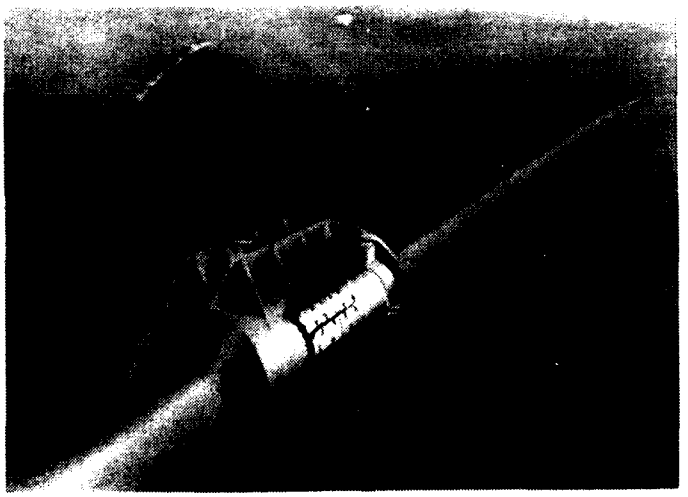

FIGURE 10 – This "cutaway" FSM section shows the obvious advantages of the non –intrusive nature of the FSM when used on subsea pipelines. In this case data communication is done by hydro acoustics.

Experience with Neutron Activation for Real-Time Corrosion Monitoring in a Urea Plant

Giel Notten
Mechanical Plant Services, DSM
PO Box 18, 6160 MD Geleen, The Netherlands

Johan Thoelen
Mechanical Plant Services, DSM
PO Box 18, 6160 MD Geleen, The Netherlands

Hans Verhoef
Mechanical Plant Services, DSM
PO Box 18, 6160 MD Geleen, The Netherlands

Robbert van Sluijs
Radioisotope Applications and Support, DSM Research
PO Box 18, 6160 MD Geleen, The Netherlands

Abstract

Reprocessing in a urea plant of ammonium carbamate from two melamine plants was feared to cause variations in the redox potential of the urea synthesis solution. Such variations may reduce the corrosion resistance of the material of construction of the high pressure process equipment, i.e. type UNS S31603 (AISI 316L urea grade) and UNS N08310 (X2CrNiMoN 25 22 2). An on-line corrosion monitoring system was felt to be necessary for early detection of corrosion, so assuring plant safety and performance reliability.

We opted for a radioactive monitoring technique (i.e. neutron activation), because this technique does not require insertion of probes through the wall of the high-pressure equipment. Basically, the method operates by measuring the decrease in gamma radiation of an active coupon exposed to the corrosive environment.
Experience gained with this on-line corrosion monitoring technique is explained, the following aspects being highlighted:

- method of measurement
- method of activation
- system setup for industrial application
- safety regulations
- interpretation of results

Introduction

Urea plants according to the DSM stripping process use ammonia and carbon dioxide as feedstock. Equipment exposed to the process fluids in the high-pressure area of the urea synthesis section is made either in UNS S31603 (urea grade AISI 316L) or UNS N08310 (X2CrNiMoN 25 22 2). The temperature of the ammonium carbamate solution in this area of the process is approx. 180°C. Passivity, and so corrosion resistance, of the stainless steels is maintained by adding oxygen to the gaseous CO_2 feed stream. In this way, a redox system is created which ensures that the corrosion potential of the stainless steel remains in the passive region of the current vs. potential curve, where corrosion is low. Experience over many years and many plants all over the world has shown that the corrosion rate is typically 0.05 - 0.10 mm/year.

At the DSM plant in Geleen, Netherlands, the waste stream of a melamine plant is added to the feedstock. Before being supplied to the urea reactor, the ammonium carbamate is concentrated in the tie-in stage. This addition of waste carbamate causes an increased corrosion rate in the urea plant: 0.10 - 0.15 mm/year is the result of several years of experience.

A reduction of the redox potential (due to, for instance, insufficient oxygen being added) may cause the stainless steel to become active.[1,2] A simplified representation of active and passive corrosion of stainless steel with various amounts of oxygen is given in Figure 1. In Figure 1a, the central curve shows the relation between the current and potential of a sample electrode in a urea synthesis solution without oxygen. This current actually is the algebraic sum of two partial currents: the positive current (a) that corresponds to the anodic dissolution (oxidation) of the metal and the negative current (c) that corresponds to the cathodic formation of hydrogen (reduction of the liquid). Only at the active corrosion potential E_a, do the two currents cancel each other and the resulting current is zero. Without external current being applied the metal will adopt this potential and active corrosion occurs. When some oxygen is present (Figure 1b), the cathodic current is larger (more negative), as oxygen is reduced too. There exist two potentials where the net sum current is zero: at the active potential E_a and at the more positive passive corrosion potential E_p. When active, the metal cannot pass the current peak (which is typical for passivatable stainless steels) and remains active. When the metal is passive and the conditions do not change, the metal remains passive. By supplying the carbamate stream from the melamine plant process conditions change. The consumption of oxygen by this carbamate stream increases the passive corrosion rate and even may cause activation. When a high amount of oxygen is present (Figure 1c), only one zero current potential exists in the passive region: the metal is in a stable passive state and the corrosion is low.

Because the waste carbamate of a second melamine plant was to be added to the feedstock, so that the ammonium carbamate waste stream was to be substantially increased, it was feared that the redox potential might diminish so much as to allow corrosion, especially of UNS S31603, to develop. Experience is that the active corrosion rate of these steels in ammonium carbamate can be as high as 10 to 30 mm/year. Therefore, a real-time corrosion monitoring system was installed.

The main purpose of the monitoring was to alert in the case of active corrosion. Additionally, we were interested in measuring the passive corrosion rate as a function of process conditions, i.e. the waste carbamate stream. The reliability of the plant, operating at high temperature and pressure, was in no way to be endangered.

The Corrosion Monitoring Technique

Since the plant operates at pressures of about 15 MPa, insertion of probes or electrodes through the wall of the equipment was out of the question.
Being one of the most reliable non-intrusive methods, a method based on ionising radiation was chosen for the corrosion monitoring. The method had proven its applicability at DSM earlier.[3]

Corrosion monitoring based on a radioactive material utilizes the loss of radionuclides as a measure of surface loss brought about by corrosion or corrosion-erosion.[4] Radionuclides are formed by activating the material under test; this may be a coupon of the material to be tested or a particular spot on the pipeline or piece of equipment under investigation.
For direct weight loss measurement of the material under test it is essential that gamma radiation emitting radionuclides be formed. Gamma radiation is only partly absorbed by material and can, within certain limits, be detected from outside of the process. The intensity of the gamma radiation is proportional to the amount of radioactivity and is measured with a NaI detector. Of course, the measuring signal needs to be corrected for radioactive decay of radioisotopes. The resulting signal is directly proportional to the thickness of the test coupon.
Another requirement for proper performance of this technique is that corrosion products be removed so they cannot interfere with the measurement.

The material can be activated by bombarding it with either high energy charged particles (in the case of thin layer activation; TLA) or with neutrons (in the case of neutron activation; NA),[5] see Figure 2. In principle, most materials can be activated.[6]

Method of Activation

The choice of the method of activation, and thus the level of activity of the main radioisotope formed, is dictated by the required monitoring period, the desired accuracy and the anticipated corrosion rate. Essential differences between TLA and NA are given in Table 1. Table 2 shows the minimum detectable corrosion rates achievable with TLA and NA.

The key data for the monitoring system were as follows:
- overall monitoring period of about 4 years;
- penetration through 20 millimeters of stainless steel;
- anticipated passive corrosion rate approximately 0.1 to 0.15 mm/year.

The duration of the monitoring period meant that the radionuclide to be formed had to have a half life of several years and the energy of the gamma radiation had to be high enough so as not to be completely absorbed by the pipe wall. The absorption of gamma radiation is dependent on the radiation energy. High energy radiation is absorbed to a lesser extent than low energy radiation. For these reasons we opted for neutron activation of the cobalt (^{59}Co), present as a contaminant in the UNS S31603 stainless steel to be tested. On being activated, the ^{59}Co generated ^{60}Co, a radio-isotope with a half life of 5.27 years and emitting two gamma rays with energy levels of 1173 and 1330 keV, each with a yield of approx. 100%.

Another argument for choosing NA was the required radioactive layer thickness based on the average passive corrosion rate of 0.15 mm/year. Because of the homogeneous activation of the test coupon, any wall thickness could be chosen so long as the accuracy was not unduly impaired.

In spite of the relatively poor sensitivity, the accuracy of the method was expected to be good enough, since the monitoring system was intended to detect passive corrosion over a longer period of time and active corrosion within a few hours (see Table 2).

Irradiation of the target material must not adversely affect its corrosion resistance. Huey-testing to Stamicarbon Material Specification revealed no difference in the corrosion resistance of UNS S31603 before and after being irradiated with neutrons. The relevant literature, too, suggests that at the expected corrosion rates irradiation is unlikely to affect corrosion resistance.[7]

System Setup

The corrosiveness of the urea synthesis solution can best be measured at the top of the reactor or in the line from the reactor to the stripper. Since gamma rays are absorbed by steel, the thickness of steel intervening between the coupon and the detector should not be more than, say, 30 to 40 mm. Therefore, the monitoring system was installed in the line to the stripper (adjacent to a flange, see Figure 3).

In November 1989, two UNS S31603 coupons, whose chemical analysis, microstructure and Huey test performance were in accordance with Stamicarbon specifications, were irradiated with neutrons in the BR No. 1 reactor of SCK (StudieCentrum voor Kernenergie, Nuclear Energy Research Centre) at Mol, Belgium.

Approximately six months after irradiation, the short-lived nuclides had decayed, leaving only ^{60}Co, resulting in a level of activity of approx. 5 MBq. With the NA method, the whole coupon is activated. Since field welding of a radioactive material calls for special precautions, two non-radioactive strips were welded to the test coupon. This was done in the Nuclear Energy Research Center in Belgium. The welder was specially instructed and the welds were radiographed before mounting in the plant. The coupon with the best welds was chosen. Field welding was done using a special device to protect the radioactive coupon and to keep it in place during welding. The coupon was mounted in the pipe during a plant shutdown in May 1990 and was welded as shown in Figure 4, allowing the flow of fluid to remove all corrosion products from the test coupon. The second coupon was kept, but not to date used, for reference purposes.

The detector used was an industrial NaI scintillation detector giving pulses whose frequency is directly proportional to the measured gamma radiation intensity. The detector had to be very reliable over a long period of time and was cooled with water. The pulses generated by the detector are counted by a counter and then converted for readout of the surface loss or corrosion rate in the control room of the plant. This was done by means of an industrial PC and a purpose-made software program (see Figure 5). Readings, stored on hard disk, are corrected in terms of natural decay and background radiation (less than 1 % of the

measured level of activity). Figure 6 shows the setup of the monitoring system in the plant; the computer and associated hardware are shown in Figure 7.

Safety Regulations

As far as safety regulations are concerned, the NA monitoring system falls in the same category as industrial radioactive measurements for level and density. An important distinction is that the radioactive source is in direct contact with the process fluid, corrosion products may cause low-level radioactive contamination of the product or waste streams. For the government licence this meant that the system comes under the heading of tracer applications. This involved the following additional requirements:

- the NA monitoring system must be reported to the authorities;
- the level of the source activity must not exceed a given limit;
- product contamination must not exceed the maximum allowable concentration specified in the license;
- the source may be handled only under supervision of qualified personnel.

Performance

The system was started up in May 1990 after a two-yearly maintenance shutdown of the urea plant. It was inspected during the next shutdown in May 1992. We took that opportunity also to compare the then remaining wall thickness with the data generated by the on-line NA monitoring system.

The software enables the collected data to be plotted at hourly intervals. Average monthly corrosion rates are computed from the slope of the curves (the coupon surface loss being proportional to the decrease in activity). The first derivative with respect to time yields the corrosion rate. These calculations can, in principle, be done automatically in the control room to trigger an alarm when a predetermined value is exceeded. On the other hand, interference from, for instance, other radioactive sources might hamper proper interpretation of the data and cause false alarms.

Figure 8 shows the relative activity versus time from May 21, 1990 to December 31, 1991. Figure 9 shows the data from January 1, 1992 to December 31, 1992.

The figures show positive and negative spikes. In the period from October 8, 1990 to December 31, 1990, a new plant was under construction not far from the urea plant. The positive spikes observed during this period are due to radiography of field welds. The negative spikes, however, cannot be explained as yet. For the used data processing however, these spikes do not interfere.
Initially, at around July 16, 1990 the plant was down for a brief period, when the reactor-to-stripper line was flushed. This was done again in 1991 and late 1992. Increased levels of activity were measured during these three periods as there was no urea synthesis solution in the pipeline and, so, no absorption in the fluid. This is shown in the figure as relatively broad peaks.

A couple of weeks later, early 1992, the curve showed a stepwise loss of activity, which could not be explained. All system components were checked and even the detector was replaced. A temperature measurement had been added to the system in late 1991 in order to study the effect of temperature on the corrosion rate. Eventually, we found that the data processing section got upset on receiving faulty temperature values and so produced erroneous data. Omitting the temperature measurement solved the problem.

The shutdown period in May 1992 is easy to recognise by the higher level of activity. After the shutdown the level was somewhat higher than previously.
This difference is due to installation of the replacement detector: both the distance to the coupon and the detector sensitivity were different. However, this makes no difference since the measurement is a relative one.

The rough data in Figure 8 and Figure 9 can not be used directly for corrosion rate calculations. The data first were subjected to a smoothing program based on moving average. The corrosion rate is calculated from the decrease of activity during a period of time (after compensation for the natural decay). In Figure 9 the calculated slopes for three corrosion rates are shown.
A short measuring period yields a relatively large noise in the results. For the detection of active corrosion this causes no problem. The decrease in a period of, say two hours, is expected to be much larger than the scatter. However, for accurate measurements of the passive corrosion rate a much larger period is required. An accuracy of 10 μm can be obtained with a measuring period of three days.

Figure 10 shows the average monthly corrosion rates. Process conditions during the first six months may be assumed to have been constant; daily review of these conditions revealed no significant changes. Yet, the corrosion rate of the material was increasing. The explanation is that the passive oxide layer, which had been there ever since fabrication, had slowly broken down under the given process conditions. A less stable dynamic oxide layer was formed. This oxide layer is maintained by oxygen present in the process fluid. Variations in the process conditions are readily detectable in the case of passive corrosion, due to the dynamic nature of the oxide layer. Depletion of the oxygen in the urea synthesis solution would lead to active corrosion in very short time.

The next period we did see varying rates of passive corrosion. This was found to be due to changes in the carbamate flow from the melamine plant. An increased carbamate flow corresponds to an increase in corrosion rate.

During the May 1992 shutdown, the coupon was inspected in order to ascertain if the monitoring results were in agreement with the corrosion that had actually taken place. The pattern of attack found on the coupon appeared to correspond with that of the same, but non-activated, material at the top of the reactor. The measured wall thickness loss of the coupon was equal to the loss established by the NA technique. It is added here that the micrometer readings need to be corrected with respect to the surface topography of the coupon. The micrometer yields peak-to-peak readings whereas measurements of the radioactivity reveal integral material losses regardless of the surface condition.

Future Research

The software used in the NA monitoring technique is purpose-written. For commercial equipment the system can be simplified by replacing some of the software by hard software. It is further advantageous to integrate statistics in the software for easier and quicker interpretation.
In our applications the radioactive monitoring technique is applied to iron-based alloys. It might be interesting to investigate whether this technique is suitable for metals like titanium or non-metals.

Conclusions

1. Corrosion monitoring by neutron activation is well able to show the effects of changing process conditions on the corrosion performance of materials as far as overall corrosion is concerned. It is essential that the corrosion products be carried away by the process fluid. Passive corrosion increased on increase of the carbamate feed stream coming from the melamine plants.

2. Corrosion monitoring by neutron activation revealed passive corrosion of UNS S31603 material exposed to a urea synthesis process. Passive corrosion rates ranged from 50 to 200 μm/year. Active corrosion was not detected, nor did it occur, during the monitoring period.

3. A passive corrosion rate of 10 μm per year can be established in about three days. Active corrosion (at 10 to 30 mm/year) is expected to be detected within two hours.

4. The wall thickness loss of the test coupon measured by micrometer was equal to the loss established by the NA technique. Being highly reliable, this technique might allow plant operators to postpone plant turnarounds without compromising plant safety or performance reliability.

References.

1. R. de Jonge, F. Baraké and J. Logemann, "Corrosion and corrosion prevention in stainless steel urea plants," Chemical Age of India **26**(1975)no.4: pp. 249-260.

2. J.F.M. Leerschool and J.C. Verhoef, "Corrosion Prevention in the Stamicarbon Urea Process," Chem + Tech '80 International Congress (Symposium 3).

3. D.A.W. Bossus and R. van Sluijs, "Corrosion Monitoring by thin layer activation", Proceedings of the 4th Conference on Radioisotope Application and Radiation Processing in Industry, Leipzig, DDR, 19-23 sept. 1988.

4. D.J. Finnigan, K. Garbett and I.S. Woolsey, "The application of thin layer surface activation to the study of erosion corrosion behaviour," Corrosion Science **22**(1982) pp. 359-372.

5. G. Notten, J. Thoelen, K. Verheesen and R. van Sluijs, "Neutron Activation for Real-Time Corrosion Monitoring in a High Pressure Process Plant", NACE, 13-18 sept. 1993, USA

6. J.A. Richardson, "Innovations in techniques for corrosion monitoring. Needs for advances in materials technology for process industries (Prof. Conf.), 29-31 Oct 1984, Atlanta, Georgia, 1985, pp. 200-218, 8609-72-0344.5.

7. D.E. Williams and J. Asher, "Measurement of low corrosion rates: comparison of a.c. impedance measurements and TLA activation methods," Corrosion Science **24**(1983): pp. 185-196.)

Table 1. Main differences between TLA and NA

	TLA	NA
Irradiated surface	beam, approx. 1 cm^2	no beam, whole surface
Irradiated layer thickness	approx. 25 - 300 μm	throughout
Useable in special locations, e.g. pipe bends	yes	no
Activity distribution	depending on particle and energy	homogeneous
Target elements in matrix	often high levels, e.g. Fe or Cr in S.S.	low levels, e.g. Co in S.S.
Suitable radionuclide formed on irradiation of S.S.	^{56}Co T½ = 78 days	^{60}Co T½ = 5.2 years

Table 2. Accuracy and lowest detectable corrosion rates for TLA and NA

Parameter	TLA	NA	Unit
Isotope	^{56}Co	^{60}Co	-
Activity	0.5	5	MBq
Wall thickness	5.0	20	mm
Transmission through walls	0.8	0.4	-
Gamma-radiation factor	0.046	0.035	(mR/h)/(MBq/m^2)
Efficiency	6000	6000	cps/(mR/h)
Distance r	0.15	0.15	m
Count rate at t=0	4900	18700	cps
Initial layer thickness	0.05	2	mm
Absolute accuracy at t=0, RA=100 %			
Monitoring period			
Tm = 1 hour	36	730	nm
Tm = 8 hours	13	260	nm
Tm = 24 hours	7	130	nm
Lowest detectable corrosion rate at t=0, RA=100 %			
Monitoring period			
Tm = 1 hour	0.9	18.2	mm/year
Tm = 8 hours	0.04	0.8	mm/year
Tm = 24 hours	0.005	0.1	mm/year

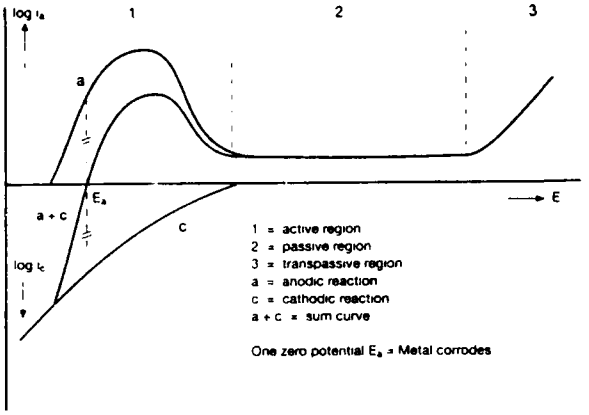

Figure 1a. Current/potential curve of stainless steel with active behaviour in ammonium carbamate

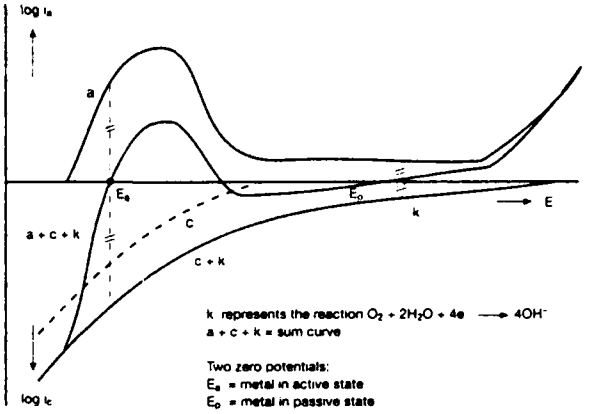

Figure 1b. Influence of oxygen on the current/potential curve

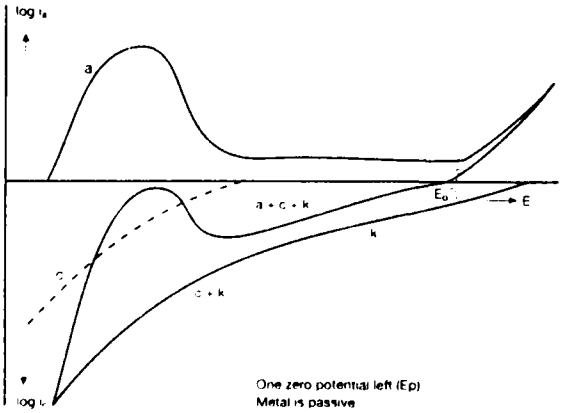

Figure 1c. Influence of an increase in oxygen on the current/potential curve

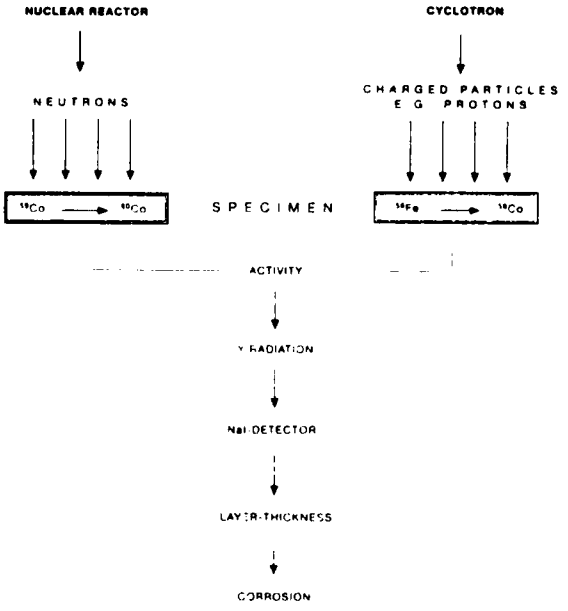

Figure 2. Schematic representation of corrosion monitoring based on TLA and NA

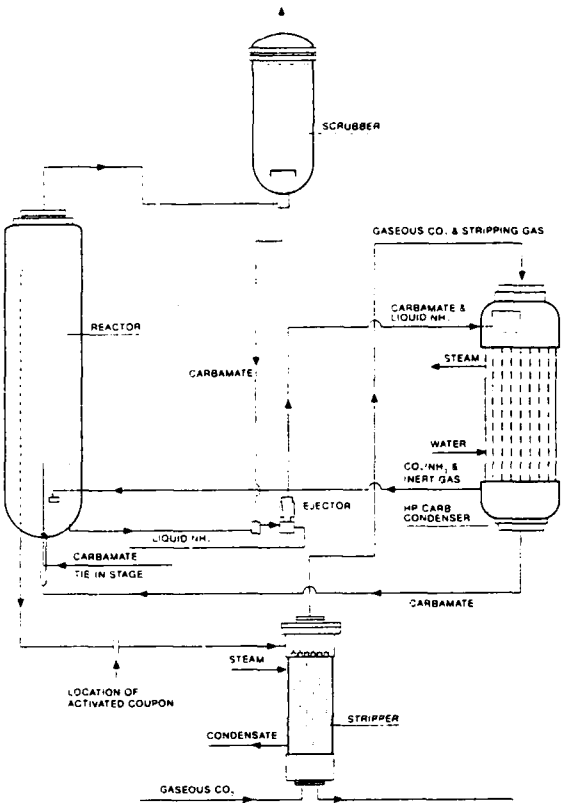

Figure 3. Urea stripping process and location of corrosion monitoring

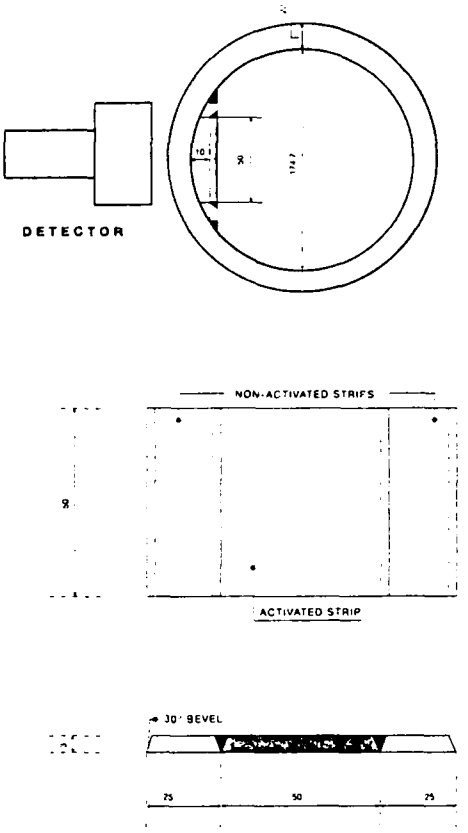

Figure 4. Coupon mounting in pipe

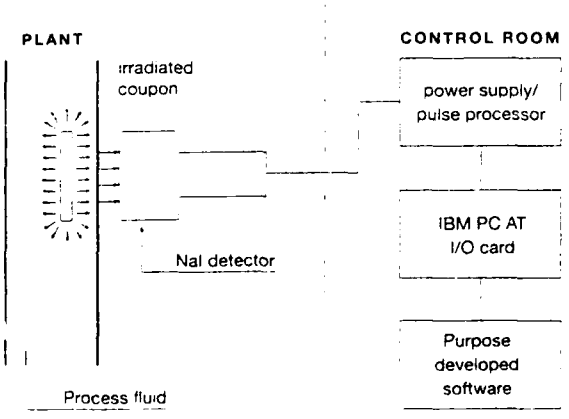

Figure 5. Schematic representation of corrosion monitoring setup

Figure 6. Corrosion monitoring assembly in plant

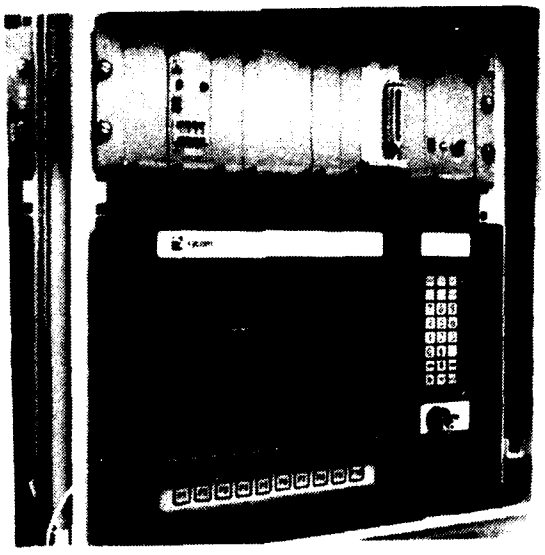

Figure 7. Corrosion monitoring assembly in control room

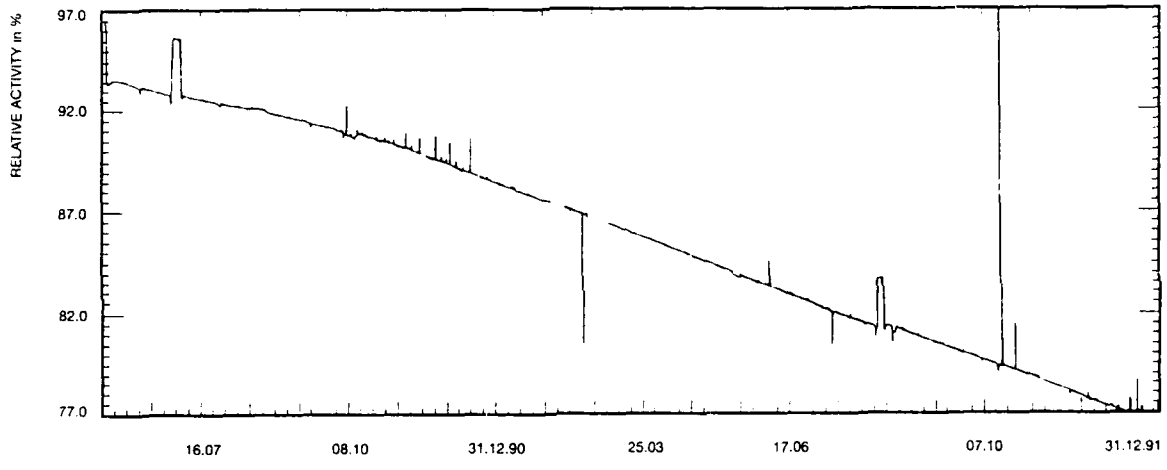

Figure 8. Relative activity versus time, 1990/1991

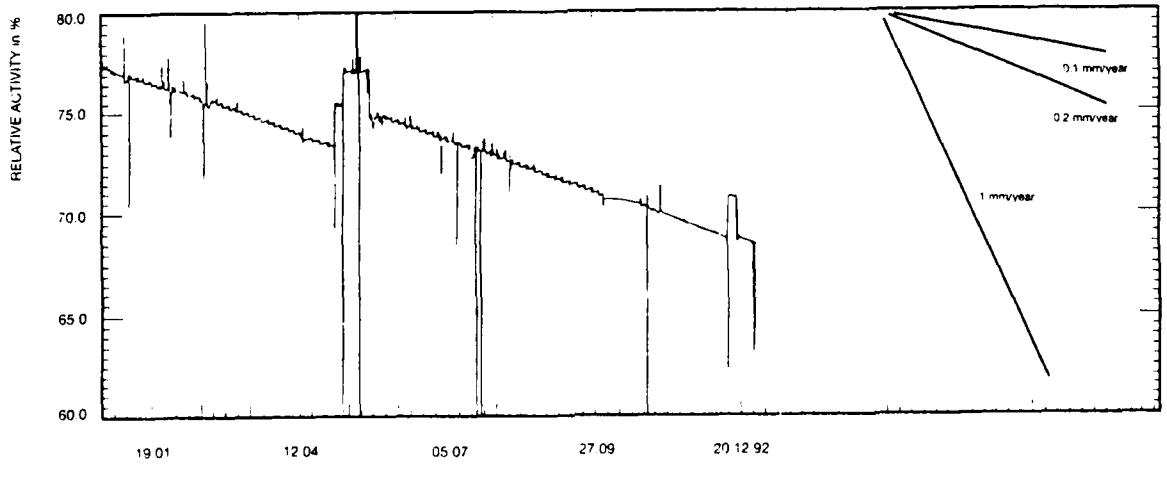

Figure 9. Relative activity versus time 1992; calculated slopes for three corrosion rates

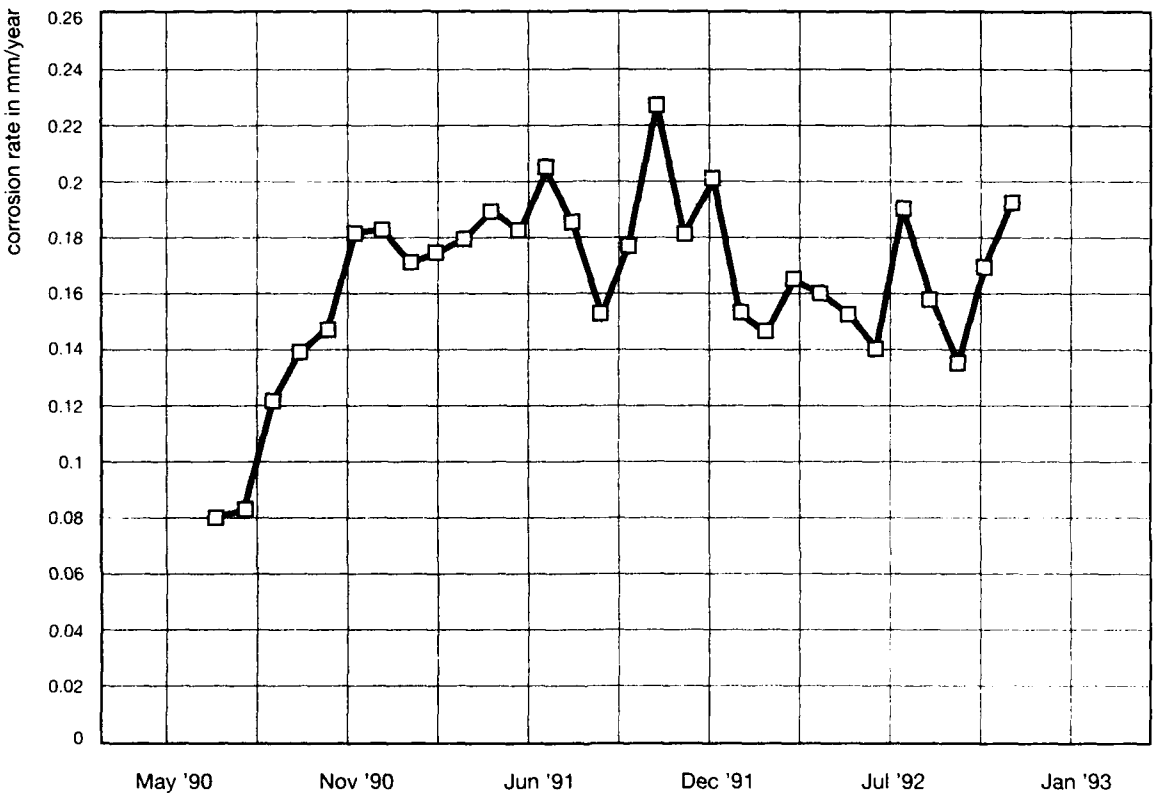

Figure 10. Average corrosion rate per month

Monitoring of Microbiological Activity in Power Plants

George Nekoksa
Corrosion Failure Analysis and Control
209 Gaucho Court,
San Ramon, CA 94583, USA

George Licina
Structural Integrity Associates, Inc.
3150 Almaden Expressway, Suite 145
San Jose, CA 95118, USA

Abstract

Biofouling and microbiologically influenced corrosion (MIC) compromise the reliability of the power plant cooling systems and increase downtime and operating costs. Monitoring of the biofilm activity is an important part of an effective MIC control.

The existing methods for MIC monitoring and biofilm deposition in cooling systems usually rely on batch-type measurements of microbial activity and deposits, monitoring of heat transfer or water pressure changes. These methods are often too slow to permit the equipment operator to apply mitigation methods before biofilms have become established and corrosion attack initiated. Implementation of an effective MIC control program in the power plant requires continuous in-situ monitoring of microbial activity as a supplement to the batch-type methods.

Laboratory monitoring of microbiological activity in soil extracts, rich with microorganisms, indicated that repeated short-term polarization of two-electrode probes changed the bio-activity on the probes and dramatically changed the electrochemical response of the probes. Monitoring of probe electrode potentials versus SCE after intermittent polarization showed characteristic electrode potential/time signatures.

Future research should include correlation of the electrochemical monitoring data with chemical, microbiological and corrosion analyses on the probes and component surfaces.

Key terms: Microbiologically influenced corrosion, monitoring of biofilm activity, biocide effectiveness.

Introduction

Microbially influenced corrosion (MIC) is a problem that pervades all industries. It may account for as much as 10% of the costs associated with corrosion problems [1]. Its importance in degradation of nuclear power plant components has prompted considerable research activity by the regulatory authorities, utility organizations such as the Electric Power Research Institute, as well as by individual utilities.

Development of a successful method and equipment to monitor microbially influenced corrosion (MIC) could prevent costly MIC damage, for instance by operating chlorinators more effectively and by timely scheduling of the service water system cleaning. The MIC monitoring technique must be sensitive enough to signal the necessity for corrective action before thick biofilms are established on the plant components and before any severe corrosion attack have occurred. An increase of the chlorination dose is usually effective only when applied before complex and protective biofilms are deposited.

The existing technology to monitor biofilm activity in power plants requires exposure of rectangular or small button coupons, removal of the coupons for inspection, bacteria cultivation or enzyme analyses. This technology is time consuming and does not provide information fast enough, for instance, to adjust the chlorinators before the biofilm gets established and becomes resistant to chlorine. Other existing methods monitor biofouling in the tubes by heat transfer loss, water pressure drop in tubes or decrease of flow through the tubes. The latter methods are sensitive to the growth of an established biofilm but they cannot be used to monitor biofilm activity as a precursor to the MIC attack.

Existing electrochemical methods, such as linear polarization, corrosion potential monitoring, polarization testing to determine pitting and repassivation potentials, and AC impedance spectroscopy have been used with success for monitoring of general corrosion and an indication of pitting corrosion in the power plants. The effects of biofilm activity on the metal surface electrochemistry and the feasibility of electrochemical methods to monitor the biofilm activity have been investigated by several authors [2-6]. Other investigators have reported on depolarization effects of microbial films on passivating metals [7-11]. Several authors have recommended to use the cathodic depolarization effects as a technique for biofilm monitoring [12,13]. The cathodic depolarization effects result in an increase of the cathodic polarization current required to maintain a preset electrode potential.

The biofilm depolarization effects have been also found in cathodically protected condensers with Ti tubes and stainless steel main circulating pumps. A correlation of the chlorinator outputs with the automatic cathodic protection current outputs have indicated that cathodic protection system operation is very sensitive to chlorinator output and biofilm activity [14]. Large increase of the cathodic protection current demand and rapid fluctuation of potentials have indicated cathodic depolarization after the chlorination had been stopped or the chlorination dose decreased.

Two-Electrode Probe Test Results

The BIoGEORGE(1) probe Type 2 consists of two sets of type 304L stainless steel discs (electrodes), insulated from each other by epoxy. Details of the probe are shown in Figure 1. Two probes of this type were exposed in an electrolyte prepared from organic soil (peat) with a large concentration of sulfate reducing bacteria (SRB). Soil samples were mixed with distilled water in two beakers. The mixing ratio was one part of soil to ten parts of water. One beaker with the electrolyte was boiled for ten minutes to eliminate or reduce the SRB population. The other beaker was considered to contain

(1) Patent pending, Electric Power Research Institute, 1991. Trade name of Structural Integrity Associates.

naturally present bacteria in the soil. Both probes were sterilized with chlorine, washed with distilled water and exposed in stagnant electrolyte for 40 days. The probes were shielded against light. After 40 days, the electrolyte was stirred typically every day for two minutes.

Each probe was controlled by a programmable module. The test sequence for each day was as follows: The programmable module applied 200 mV potential difference between the two sets of the stainless steel discs for 30 minutes. At the end of the 30-minute interval, the polarization current was measured and graphed in Figure 2a as an applied current. After the 30-minute polarization, the probe terminals were shorted for the rest of the day and the current generated by the probe was monitored. The value of the generated current, measured several minutes before the next application of the power source and 200 mV polarization, was plotted in a graph shown in Figure 2b. After 20 days of exposure, the probe terminals were left open for one hour each day and at the end of the one-hour period, the potential difference between the terminals was plotted in Figure 2c. It was noticed that the potential between the terminals was increasing with time.

As expected, there was a good correlation between the three graphs in Figure 2. The applied current increase after the 12th day indicated depolarization. It coincided with substantial increase of the generated current and a large potential difference between the electrodes. The potential difference between the electrodes was causing the generated current flow. After stirring the electrolyte, the applied current returned to its original value, while the generated current and potential difference between the electrodes fluctuated.

The response of the probe with active biofilm can be explained by changes *in* the biofilm and surface chemistry on the electrodes caused by the 30-minutes-per-day polarization. Once the different conditions on the electrodes were established, these conditions persisted for a long time (weeks).

A control test with the probe exposed to boiled electrolyte did not show any increase of applied or generated current. The generated current in the boiled electrolyte was less than 1% of the current in the electrolyte with bio-activity and was rapidly decreasing with time. Both probes were inspected for corrosion after the exposure. Slight corrosion was found on both electrodes of the probe with the biofilm. It is not clear if some corrosion is necessary for the probe to respond to the biofilm. It was however noticed that the corrosion was much smaller that would result from the measured dc current flow.

The selected 200 mV potential difference applied between the two sets of discs simulates potential differences existing on some stainless steel structures at the welds, crevices and inclusions where the MIC attack is usually concentrated. It can be deduced that small potential differences would result in a slower and smaller response of the probe to the biofilm. Large potential differences could deposit alkaline calcareous deposits on the cathodic set of discs and inhibit the bioactivity on the probe.

Several polarization intervals were tested. The one-half and one-hour polarizations each day provided more prominent electrochemical responses to the biofilm than polarization for 23 and half hours each day.

One monitoring system, consisting of a probe and a programmable control module costs approximately $3,500. The test results are easy to evaluate - a technician should be able to interpret the monitoring data from the probe, especially when the data have been compared, at least once, with the results of the structure inspection or with the test results on exposed coupons.

The two-electrode probes with programmable modules were tested in several power plants. The increases of the applied and generated currents with time in the power plants were similar to the laboratory test results. Figure 3 shows results from Browns Ferry Nuclear Plant [15].

Probe Electrode Potential Monitoring

To study the electrochemical behavior of individual probe electrodes, laboratory tests were conducted in different electrolytes. Testing was conducted on Type 2 probes exposed to river water samples with resistivity of 6700 ohm-cm. To determine the effect of an active biofilm on the probes, one probe was exposed in the natural river water sample, and another probe was exposed in boiled and cooled river water sample. After 14 days of exposure, when the applied and generated currents substantially increased, the probe electrode potentials were recorded using a standard saturated calomel electrode (SCE) positioned close to the probe surface and a two-channel recorder. The potential recordings versus a SCE are shown in Figure 4.

After polarization of the probe by application of 200 mV from a power source for 30 minutes, the electrodes were shorted for approximately five minutes and then the electrode terminals were left open for the rest of the test period to record the electrode potential/time signatures. The recording in Figure 4a shows potential response on the probe with biofilm. This response, typical for active biofilm on the probe, shows that the electrode potential recordings crossed each other and the potential of the previously cathodically polarized electrode was changing in the positive direction with time. The electrode potentials on the probe exposed to boiled river water sample showed that potentials of both electrodes slowly decayed to the value of the shorted electrode potentials before polarization (see Figure 4b).

As expected, the electrode potentials correlated well with the generated current because the generated current flow was the result of the potential differences between the electrodes. Generally, after removal of the 200 mV on the terminals, a probe with an active biofilm showed an electrode potential cross-over, increasing potential difference between the electrodes with time and increasing generated current of the same direction as the applied current. A probe without an active biofilm showed decreasing potential between the electrodes with time and an insignificant generated current.

Figure 5 shows an another, more interesting, electrode potential signature. The Type 2 probe was exposed for 36 days in a soil extract prepared from garden top soil mixed with distilled water in a ratio of one part soil and 5 parts distilled water. The corrosivity of this extract was increased by adding ASTM sea salt to the extract so that the final electrolyte resistivity was 160 ohm-cm. The electrode potential cross-over in Figure 5 is clearly visible. However, in this case, the previously cathodically polarized electrode showed potentials much more noble than the shorted electrode potentials before application of the 200 mV polarization. The maximum potential difference between the electrodes was 328 mV and the maximum negative electrode potential change from the shorted potential was 250 mV.

The noble electrode potentials were close to the pitting potential of 304L stainless steel in some soils and waters. This indicates that a cathodically protected 304L stainless steel structure could be susceptible to pitting after the removal of cathodic polarization.

The two-electrode probe does not have a reference electrode and cannot be used in a power plant to monitor individual electrode potentials versus time. A new three-electrode probe, Type 3, was developed to allow long-term monitoring of applied and generated currents, and also the electrode potential signatures in power plant cooling systems. The Type 3 probe is shown in Figure 6. It consists of 304 L stainless steel discs and a zinc reference electrode. The 99.99% zinc electrode usually maintains a stable potential in seawater and in most brackish and fresh cooling waters with and without bioactivity. In polluted waters and in cooling waters with low chloride/sulfate ratios, the zinc electrode potential could drift with time and a frequent calibration versus a more stable reference electrode could be necessary.

Future Development and Testing

Preliminary laboratory results indicated that the electrode potential monitoring versus time after a short-term polarization could provide valuable additional information about the biofilm activity on the electrodes. Long-term testing with the three-electrode probes will be conducted together with other applicable corrosion monitoring methods in a brackish cooling water system with high concentration of microorganisms. To monitor applied and generated currents and also the electrode potential signatures on one probe, a test sequence shown in Table 1 is being considered for future field testing.

Presently, testing is being prepared to obtain data for probes built from different alloys. The main objective of future tests will be to correlate the results of microbiological, chemical and corrosion surface analyses with electrochemical data from the corrosion and biofilm monitoring probes.

Conclusions

The test results showed that a new electrochemical probe can be useful for detection of biofilms and for monitoring of biofilm activity in the power plants. Data from the electrochemical probes indicated biofilm activity before the biofilm was fully established and before any severe corrosion has occurred. The probes can be used for an early warning system to signal changes in demand for biocide or necessity for cleaning the cooling systems.

References

1. "Microbiologically Influenced Corrosion", Material for EPRI NDE Center Training Course, Electric Power Research Institute, Palo Alto, CA, 1990.

2. N.J.E. Dowling, E.E. Stansbury, D.C. White, S.W. Borenstein and J.C. Danco,"On-Line Electrochemical Monitoring of Microbially Influenced Corrosion", 1988 Proceedings of EPRI Microbial Corrosion Workshop, RP 8000-26, Edited by G.J. Licina, Structural Integrity Associates, San Jose, CA for Electric Power Research Institute, Palo Alto, CA, April 1989.

3. G.J. Licina, "Electrochemical Aspects of Microbiologically Influenced Corrosion", 1988 Proceedings of EPRI Microbial Corrosion Workshop, RP 8000-26, Edited by G.J. Licina, Structural Integrity Associates, San Jose, CA for Electric Power Research Institute, Palo Alto, CA, April 1989.

4. S.C. Dexter and G.Y. Gao, "Effect of Seawater Biofilms on Corrosion Potential and Oxygen Reduction of Stainless Steel", Paper No. 377 Presented at Corrosion '87, National Association of Corrosion Engineers, Houston, TX.

5. G. Gundersen, B. Johansen, P.O. Gartland, I. Vintermyr, R. Tunold and G. Hagen, "The Effect of Sodium Hypochlorite on the Electrochemical Properties of Stainless Steels and on Bacterial Activity in Seawater", Paper No. 108 Presented at Corrosion '89, National Association of Corrosion Engineers, Houston, TX.

6. V. Scotto, "Electrochemical Studies of Biocorrosion of Stainless Steel in Seawater", 1988 Proceedings of EPRI Microbial Corrosion Workshop, RP 8000-26, Edited by G.J. Licina, Structural Integrity Associates, San Jose, CA for Electric Power Research Institute, Palo Alto, CA, April 1989.

7. B. Little, P. Wagner, D. Duquette." Microbiologically Induced Cathodic Depolarization Depolarization". CORROSION/87, Paper No. 370, NACE, Houston, Texas, 1987.

8. S.C. Dexter, G.Y. Gao. "Effect of Seawater Biofilms on Corrosion Potential and Oxygen Reduction of Stainless Steel." CORROSION/87, Paper No. 377, NACE, Houston, Texas, 1987.

9. B. Little, P. Wagner and D. Duquette, "Microbiologically Induced Increase in Corrosion Current Density of Stainless Steel Under Cathodic Protection", Corrosion Vol.44, No.5, May 1988, pp 270-274.

10. R. Holthe, E. Bardal, P.O. Gartland." The Time Dependence of Cathodic Properties of Stainless Steels, Titanium, Platinum and 90/10 CuNi in Seawater". CORROSION/88, Paper No. 393, NACE, Houston, Texas, 1988.

11. V. Scotto. " 1988 Proceedings of EPRI Microbial Corrosion Workshop", RP 8000-26, ER 6345. Edited by G.J. Licina, Structural Integrity Associates, San Jose, CA for Electric Power Research Institute, Palo Alto, CA, April 1989.

12. G. Salvago, G. Taccani, G. Fumagalli. "Electrochemical Approach to Biofilms Monitoring". Presented at International Congress on MIC, Knoxville, Tennessee, October 1990.

13. A. Mollica, E. Traverso, G. Ventura. "Electrochemical Monitoring of the Biofilm Growth on Active-Passive Alloy Tubes of Heat Exchangers Using Seawater as Cooling Medium". Proceedings, 11th International Corrosion Congress, Volume 4, pp. 4.341-4.349, Associazione Italiana di Metallurgia, Milano, Italy, 1990.

14. G. Nekoksa and R.T. Hanson, "Effects of Chlorination on Cathodic Protection Current Requirements", Paper No. 286 Presented at Corrosion '89, National Association of Corrosion Engineers, Houston, TX.

15. G. Licina, G. Nekoksa and R.L. Howard, "The BIoGEORGE Probe, An Electrochemical Method for On-Line Monitoring of Biofilm Activity". NSF-CONICET Workshop on Biocorrosion and Biofouling, Mar del Plata, Argentina, November 1992.

Table 1

Test Sequence for Three-Electrode Electrochemical Biofilm Monitoring Probes

Time Period (hrs:min)	Test Sequence	Time*	Data Retrieved for Daily Monitoring
00:00 to 00:30	200 mV applied on the probe terminals	00:25	Applied current
00:30 to 04:30	Probe terminals shorted		
04:30 to 08:30	Probe terminals open	04:30 to 08:30	Electrode potential signature recorded
08:30 to 24:00	Probe terminals shorted	23:50	Generated current

* Indicates time at which measurement is taken for daily monitoring.
Note: See Figure 6 for details of the Type 3 probe.

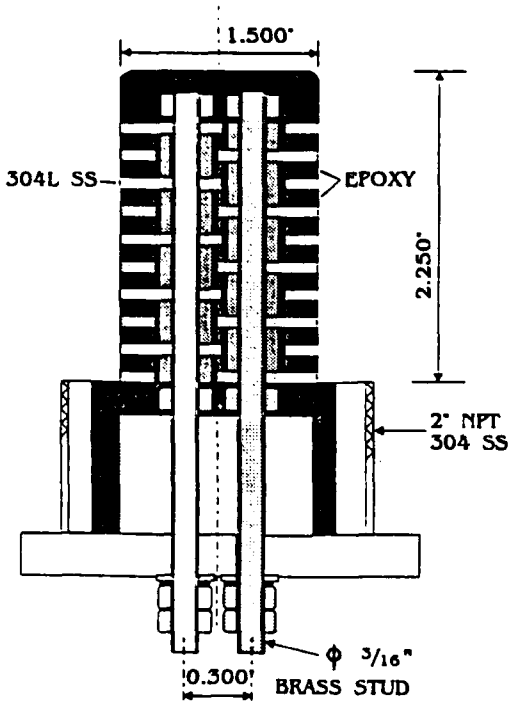

Figure 1. Electrochemical Biofilm Activity Monitoring Probe, Type 2

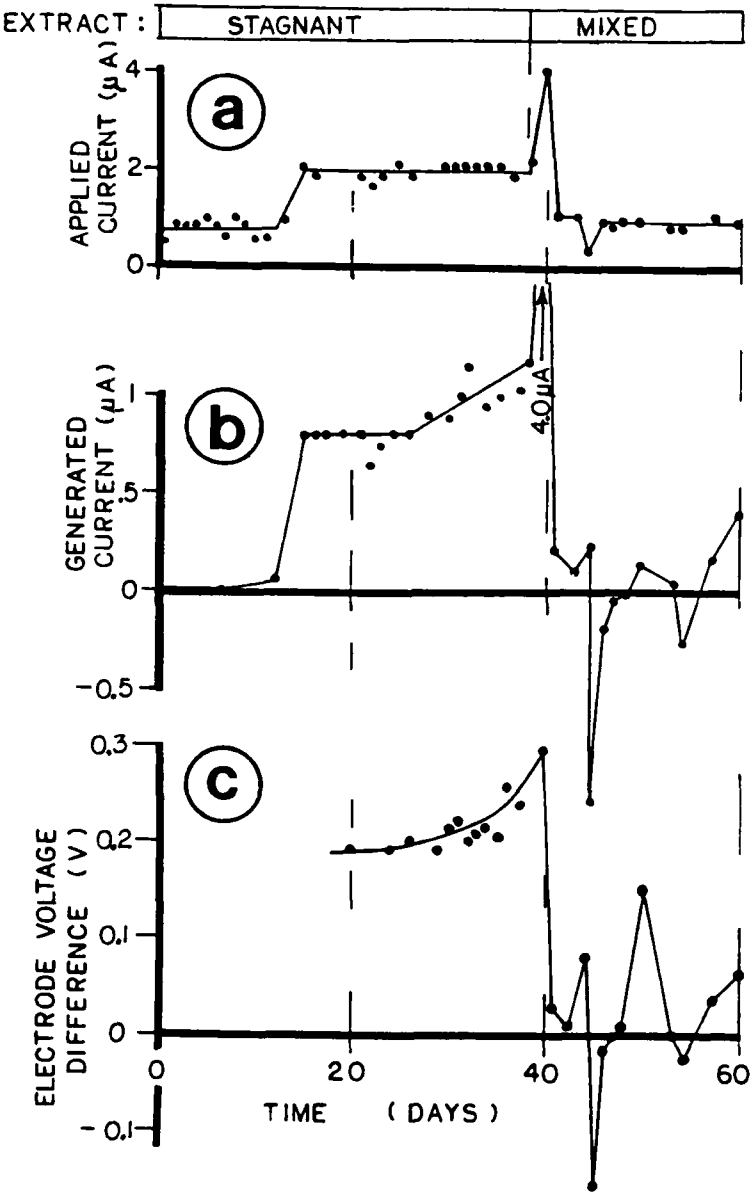

Figure 2. Test Results, Type 2 Probe in Peat Soil Extract.
a. Applied Current vs. Time
b. Generated Current vs. Time
c. Electrode Voltage after Polarization vs. Time

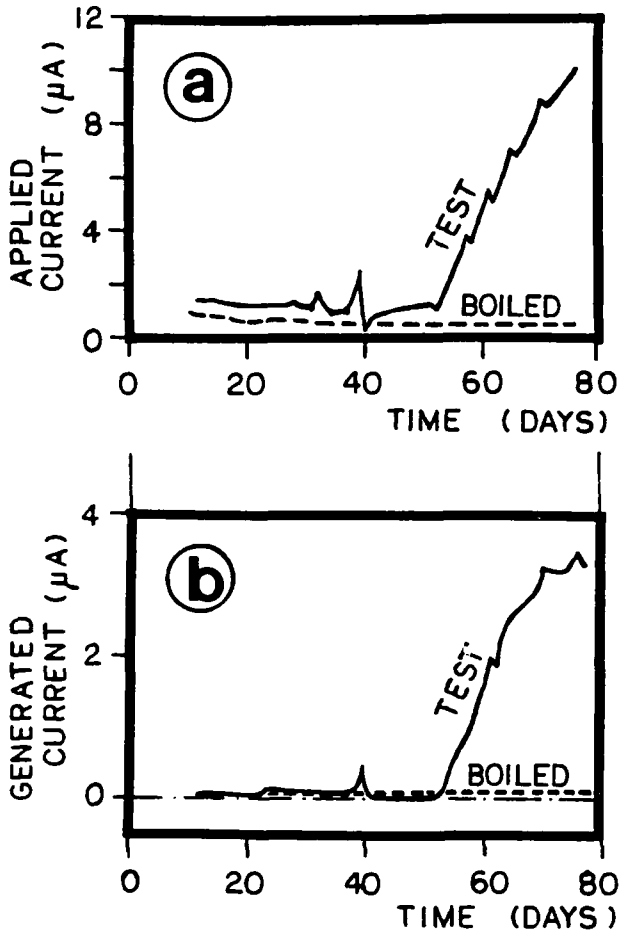

Figure 3. Applied (a) and Generated (b) Currents from Browns Ferry Power Plant

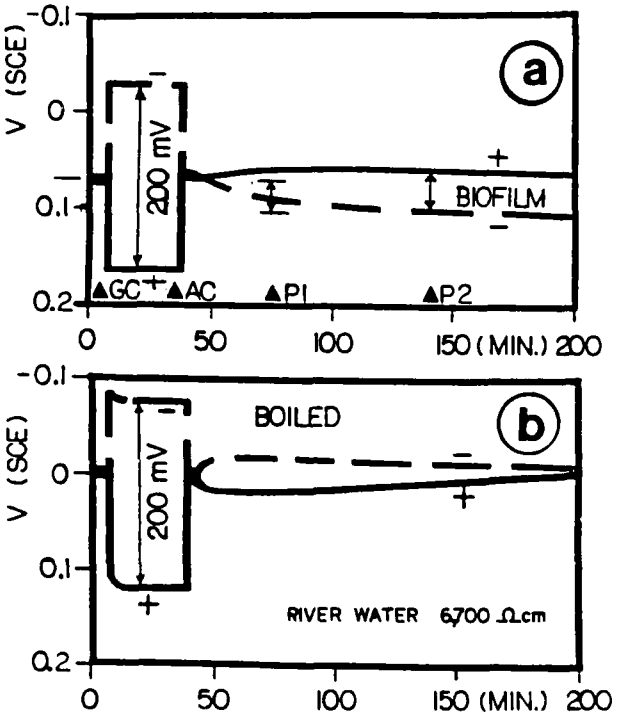

Figure 4. Electrode Potential/Time Signature after 14-Day Exposure in River Water.

Data Points:
GC: Generated Current
AC: Applied Current
P1: Maximum Electrode Potential Change from Shorted Pot.
P2: Maximum Electrode Potential Difference

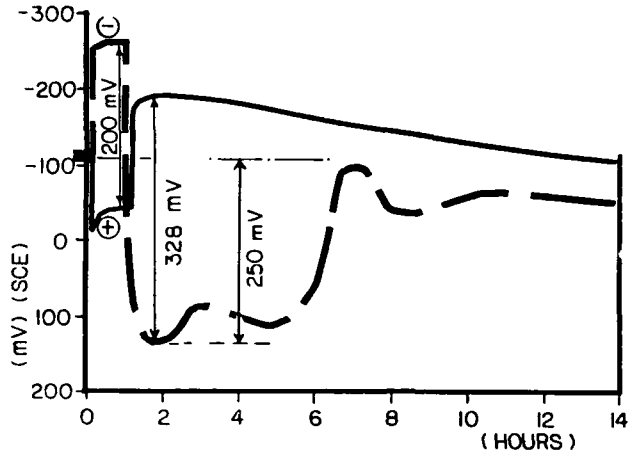

Figure 5. Electrode Potential/Time Signature on Probe Type 2 after 36-Day Exposure in Garden Top Soil Extract with ASTM Sea Salt

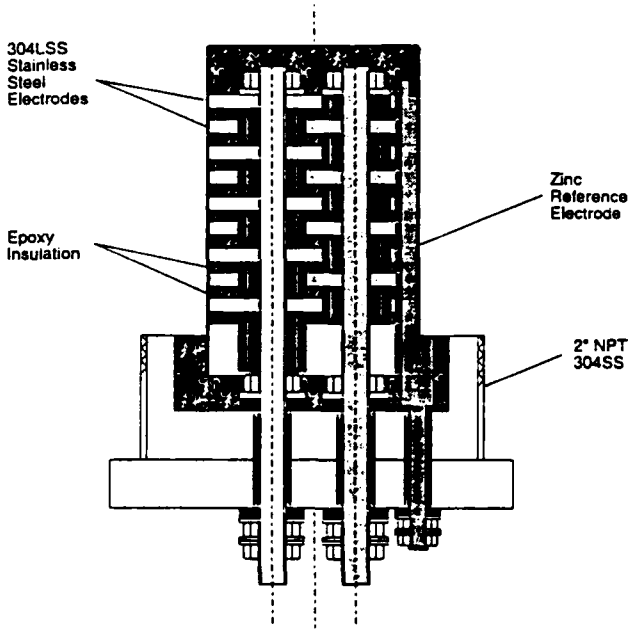

Figure 6. Electrochemical Biofilm Activity Monitoring Probe, Type 3.

Electrochemical Monitoring of Erosion-Corrosion in Multiphase Flows

E. Heitz, I. Ehmann, K. Miers, A. Schnitzler, K. Schroeder, Xiao Shimeng
Karl Winnacker Institute of DECHEMA e.V.
Theodor-Heuss-Allee 25
6000 Frankfurt am Main 15
Germany

Abstract

On the basis of mechanistic considerations of erosion-corrosion various electrochemical sensors for liquids containing particles were developed and tested. The corrosive part of mass loss can be elucidated by well-known methods, such as polarization resistance and potentiostatic measurements. The erosive part can be indirectly correlated with particle rate and flow rate measurements. Prototypes of sensors were tested in pilot loops simulating flow conditions of quencher fluids in flue gas desulphurization plants, conditions in cooling systems, in formation water from oil and gas production and other process waters. Conclusions with regard to the applicability ranges of the sensors are drawn.

Introduction

Flowing multiphase systems with a liquid as the main commponent are of growing interest to various branches of the process industry. Important technologies in which multiphase flows play a major role are: oil and gas production from geological formations containing sand, certain sectors of the conventional energy industry (flue gas desulphurization, cooling loops, hydroelectric power plants), hydraulic transport, offshore technology and, last but not least, chemical technology. The trend towards higher throughput and, therefore, higher flow velocities increases the mechano-corrosive load on plant equipment, piping and particularly on hydraulic aggregates.

When running such plants it is important to evaluate the potential of electrochemical methods with respect to on-line monitoring of erosion-corrosion. Since liquids containing solids generally raise the greatest problems, emphasis is laid on this kind of flow.

Flowing liquids containing particles induce various effects on metal surfaces according to their corrosivity. These processes include the mechanical destruction of passive and corrosion product layers of the base metal as well as healing processes of damaged surface layers. As a consequence the electrochemical kinetics of corrosion differs very much from the behaviour of undamaged surfaces[1].

Taking into consideration the mechanisms of erosion-corrosion in liquids containing particles, it has been found that, among other parameters, such as angle of impingement, particle size, shape and hardness, the rate of attack is proportional to the square of the flow velocity and directly proportional to the particle concentration. This suggests that the kinetic energy of a single particle is the decisive parameter of the mechanical part of attack[2]. This is accompanied by more or less intense electrochemical processes. It is clear that electrochemical measurements can only cover this part of attack.

A number of activities have been initiated to develop continuous corrosion surveillance technology in various branches of industry[3]. Modern approaches are

based on electrochemical potential and current noise, zero resistance ammetry and electrochemical impedance monitoring.

The aim of the investigations presented was to develop and apply sensors for monitoring erosion-corrosion in liquids containing particles.

Methods Applied

Polarization Resistance Measurements

This method can be successfully applied in corrosion systems with actively corroding metals. A typical set-up is shown in Fig. 1. The test section is a sudden pipe expansion with a diameter which is double that of the entrance section. Different rings of test materials (various stainless steels) are electrically insulated by perspex mountings and serve as working electrodes. The design permits simultaneous measurements with different materials as well as measurements with only one kind of material, but under different hydrodynamic conditions. The reference electrode is connected by an electrolyte bridge through a hole in the working electrode. The reference electrode is a pressure-resistant Ag/AgCl-electrode. The inlet or exit parts of the measuring section are the counter electrodes, consisting of stable, corrosion-resistant materials. Such a set-up is designed for higher temperatures and pressures and can be integrated in test loops[1].

If the conductivity of the corrosion system is low, the ohmic drop has to be eliminated. This is done in the usual way: either by an interruptor or an impedance method[4].

Potentiostatic Measurements

Attempts have been made to monitor erosion-corrosion in systems which are seemingly in the passive state, but which are prone to particle impact and, therefore, unstable passivity. The electrochemical basis for such measurements is shown in Fig. 2. This figure exhibits the polarization curves of material X3CrNiMo 17 13 5 in a quencher solution of a flue gas desulphurization (FGD) plant. Such solutions contain gypsum particles, pH values between 2 and 7 and high flow rates. It can be seen that particles added to the medium may induce very different effects. Hard particles (quartz) increase the passive current significantly. It is evident that potentiostatic measurements in the appropriate potential regions give an indication of the effects of impinging particles. Measurements of this kind are made with the set-up shown in Fig. 1.

Particle Rate Sensor

In a medium consisting of a liquid phase with electrical conductivity of roughly 1 mS cm^{-1} or more and a particle content of an insulating material, such as glass, it is possible to determine the existence of particles between two sensor electrodes by means of an amperometric method. The principle of the particle rate sensor is shown in Fig. 3. It consists of two planar electrodes which should approximate the size of the particle to be measured. If a constant voltage is applied, a particle passing the electrodes causes a short drop in the current. The particle rate in the wall region can be determined by counting such signals. A typical working voltage is 1.9 V, giving a signal current in the range of 0.05 mA, converted to the corresponding signal voltage. By treating the signals

appropriately (time derivation and squaring) the evaluation of the signals can be improved[5].

Flow Rate Sensor

A flow rate sensor based on electrochemical limiting current measurements is included in this discussion since flow rate is a decisive parameter of the two-phase flow under consideration. The principal set-up of the flow rate measuring arrangement is given in Fig. 4. All electrochemical systems producing a transport limiting current can be used as flow rate indicators. If oxygen is present, it is convenient to measure the limiting current of cathodic oxygen reduction. This current can be correlated with the flow rate provided there is no change in flow mode or in fluid composition, such as oxygen content or pH value. If the sensor is combined with an oxygen partial pressure measuring device it is possible to allow for correction of oxygen concentration. Further information on this method is given in[5, 6].

Results and discussion

The following results were obtained under practical conditions. This means that the sensors were mounted in test sections of pilot plant loops in which two-phase flows relevant to special industrial applications are produced. These pilot loops can be described as follows:

- a pilot loop for high flow rates (24 m/s in 20 mm diameter pipes) which is constructed from polyvinyliden fluoride parts and applicable up to temperatures of 80°C and pressures of up to 3 bar[7]
- a flow loop simulating district heating conditions, constructed from stainless steel AISI 316 and usable for temperatures of up to 140°C and pressures of up to 10 bar[8]
- a test loop simulating conditions of the sealing gaps of an original centrifugal pump; construction material: duplex steel; maximum temperature 80°C; pressure normally 4 bar, but can be extended to 10 bar; maximum volume flow rate 40 m^3/h; rotation speed 2000 rpm[9].

Polarization Resistances, Polarization Curves, Current Noise

Polarization resistance sensors have been successfully applied in monitoring materials' behaviour in the quencher fluid of FGD plants. Separate measurements reveal B values of approximately 25 mV in the Stern-Geary relationship[10]. A typical result is given in Fig. 5. It shows the reciprocal of the polarization resistance of various materials plotted against the pH value of the fluid. The composition of the fluid is representative of industrial conditions: gypsum 10% weight (particle size 25-30 µm), chloride 30 g/l, temperature 60°C, flow rate 24 and 6 m/s in the sensor device shown in Fig. 1.

In Fig. 6, current signals from a duplex steel (G-X 40 CrNiMo 27 5), polarized potentiostatically to a potential of 0.0350 V (SHE), are plotted vs. the distance along the test section. The experiments were performed in a pilot loop containing seawater with 0.5% by volume sand of 0.4 mm diameter. As can be seen, the current ratings are highly dependent on measuring position and flow rate in the test section, which again is of the type shown in Fig. 1.

Current fluctuations induced by impinging particles, as produced in the preceding experiments are shown in Fig. 7. A quantitative noise analysis is difficult since

there is interference from parasitic signals from the electrical equipment of the flow loop.

Particle Rates in Tap Water Containing Sand

The particle rate sensor was successfully applied in various waters containing sand. A typical example is given in Fig. 8.

Under usual conditions the decrease in the current is about 3% to 5% of the absolute value. The duration of the signals is a few milliseconds. Fluctuations of electrode potential can occur in electrochemical systems and may be caused by electrode poisoning or a change in fluid composition. They lead to an increase or decrease in the current, but, in principle, do not affect the measurements. The current drop caused by a particle lasts only a few milliseconds, whereas the disturbances described above are generally longer. The special shape of the particle signal is used to improve the signal determination by time derivation and squaring. The particle rate is determined by counting the single particle signals. Therefore, the measuring time is very long for small particle rates, but it can be reduced by using more than one electrode couple (sensor array).

Flow Velocity of Industrial Fluids

Fig. 9 shows the diffusion limited current dependence on the average value of the flow velocity at a fixed potential. The sensor was mounted in the pilot loop in the first ring after the pipe expansion in the region of high turbulence and reverse flow (Fig. 1). The result is an almost linear correlation between current and averaged flow velocity. Previous measurements had shown that the mounting place and its hydrodynamic conditions are very important. Therefore it is necessary to carry out a calibration measurement if the sensor is used under partly unknown and partly undefined flow conditions which may occur during application in practice.

Conclusions

- It is possible to measure the electrochemical part of erosion-corrosion by appropriate electrochemical methods, such as polarization resistance and anodic current at a specifically set potential.

- The mechanical destruction during erosion-corrosion can be followed indirectly by determining the particle rate and flow rate at specific positions of the equipment.

- The measurement techniques discussed were tested under conditions simulating practice, including pressure up to 10 bar, temperature up to 140°C and turbulent disturbed flows of aggressive fluids which sometimes contained a solid phase. There is a limit to flow rate measurement at higher velocities. If the mass transfer becomes very high, the reaction is not only mass transfer, but also charge transfer controlled. In addition, IR drop may dominate. This limit was not reached in the present experiments.

- The particle rate sensor can be optimized according to particle size and concentration. In principle not one of the measurement techniques itself is influenced by high pressure or temperature so their application under pressures higher than 10 bar and temperatures over 140°C should be possible.

- For technical applications it is necessary to combine various sensors. For example, if a polarization resistance reading and potentiostatic current

measurements are evaluated together with particle rates and flow velocity it should be possible to obtain a good indication of the erosion-corrosion status of a given system. This is also interesting if differences in local conditions are to be investigated. Developments in this direction are in progress. They are based on the application of multi-sensor arrays.

- On the whole, the combination of measurements can be used on site for qualitative or semi-quantitative surveillance. To quantify erosion corrosion conventional mass loss or wall thickness measurements are necessary.

References

1. I. Ehmann, E. Heitz, A. Schnitzler, Werkstoffe und Korrosion 42 (1991) 520-527

2. E. Heitz, CORROSION 47 (1991) 135-145

3. T. Illson, C. Eley, M.Y. Mok, W.M. Cox, D.B. Meadowcroft, Werkstoffe und Korrosion 43 (1992) 321-328

4. E. Heitz, R. Henkhaus, A. Rahmel, Corrosion Science - an experimental approach, p. 25, Ellis Horwood Publ., 1992

5. K. Miers, E. Heitz, Proc. 3rd Int. Workshop on Electrodiffusion Diagnostics of Flows, Dourdan (France) 1993, in print

6. K. Miers, E. Heitz, J. Appl. Electrochem. (in preparation)

7. W. Blatt, T. Kohley, U. Lotz, E. Heitz, CORROSION 45 (1989) 793-804

8. E. Heitz, N. Sacoph, A. Pereira, publication in preparation

9. K. Schroeder, E. Heitz, Mat.-wiss. u. Werkstofftech. 24 (1993) 65-71

10. R. Grauer, P.R. Moreland, G. Puci, Report for the European Federation of Corrosion Working Party, NACE, Houston, TX, 1982

Acknowledgement

These investigations were kindly sponsored by the Stiftung Stahlanwendungsforschung through the Forschungskuratorium Maschinenbau, VDMA, Frankfurt, and the Bundesministerium für Forschung und Technologie R & D Programme Corrosion and Corrosion Protection (Coordinator: DECHEMA e.V., Frankfurt).

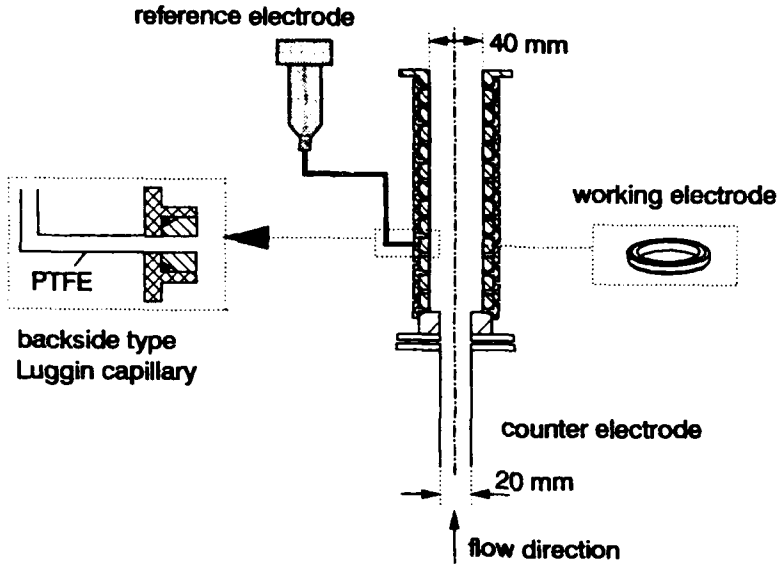

FIGURE 1
Segmented measuring section for electrochemical measurements in liquids containing particles

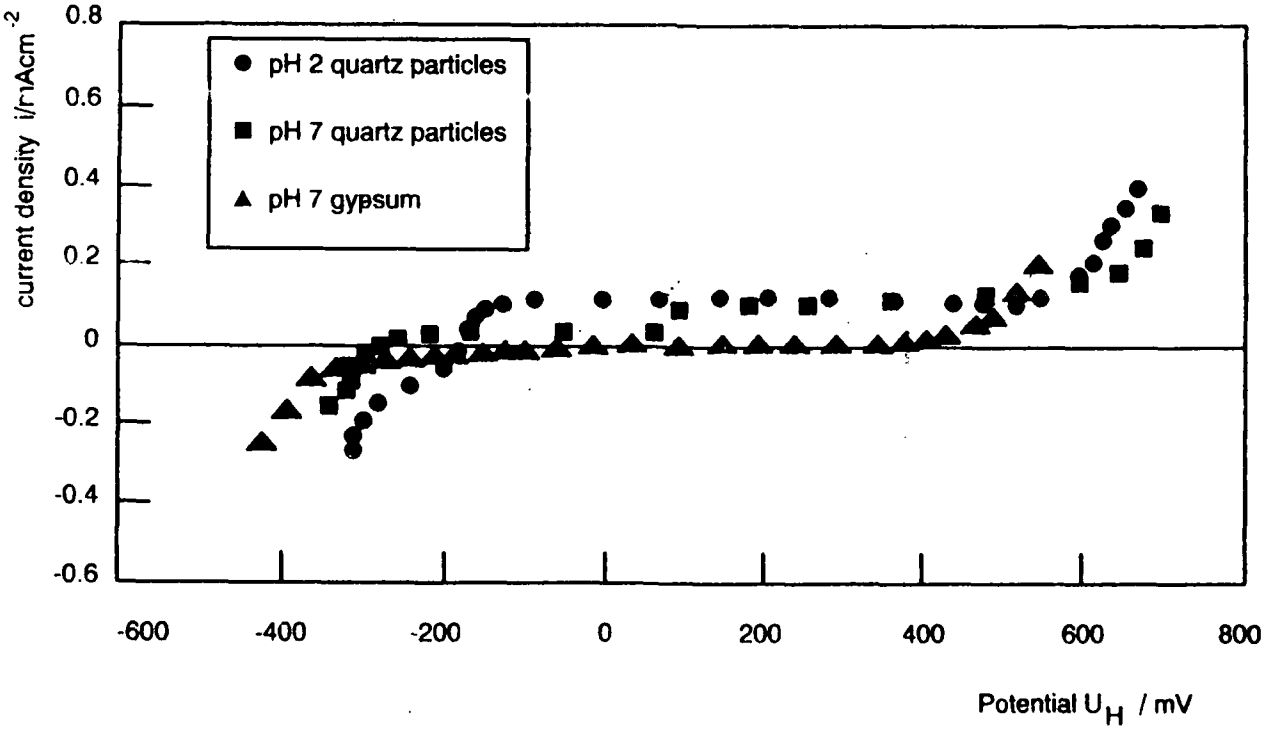

FIGURE 2
Polarization curves of material X3 CrNiMo 17 13 5 in FGD quencher fluid containing quartz or gypsum particles; pH = 7; 12 and 3 m/s flow velocity in the pipe expansion from 20 mm to 40 mm diameter, as shown in Fig. 1

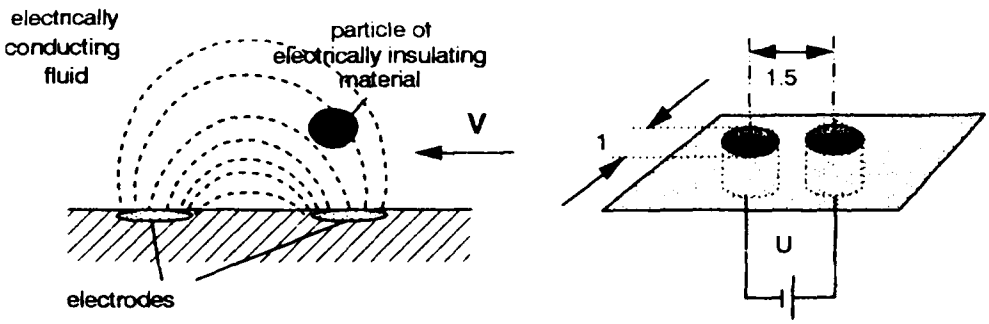

FIGURE 3
Principle of the particle rate sensor

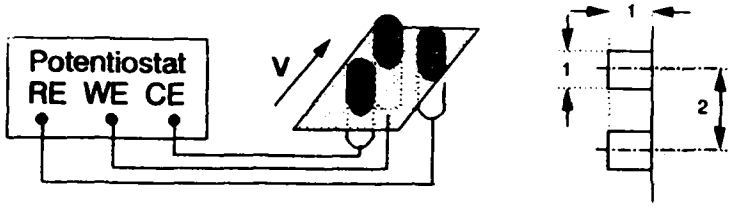

FIGURE 4
Principal set-up of the flow rate sensor

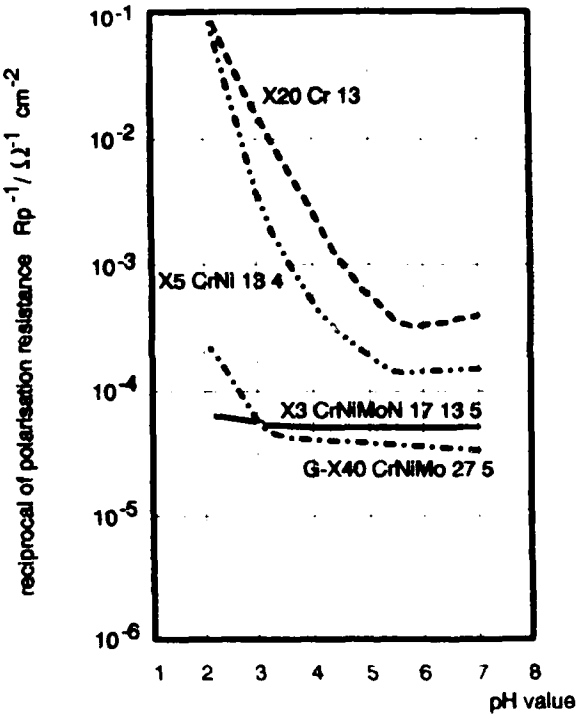

FIGURE 5
Reciprocal polarization resistances of various materials as a function of the pH value in a FGD quencher solution (gypsum 10% weight, chloride 30 g/l, air saturated; temperature 60°C, flow rate 24 and 6 m/s in the pipe expansion shown in Fig. 1)

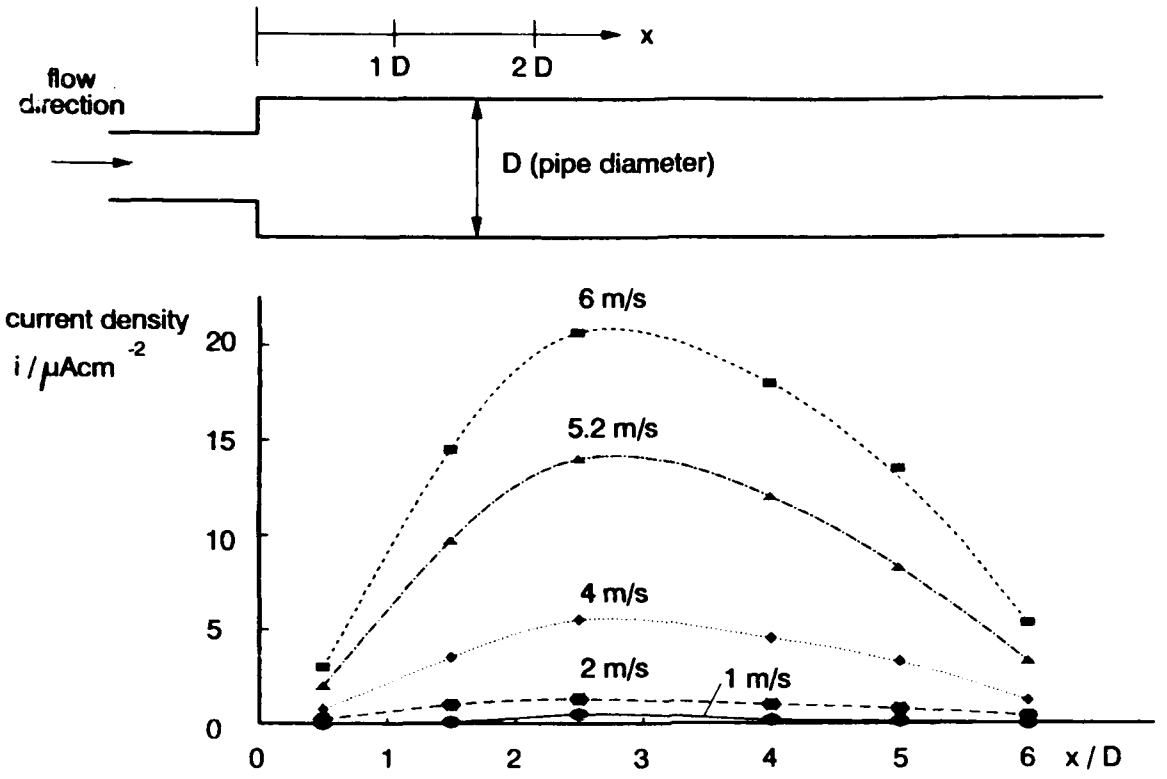

FIGURE 6
Potentiostatic current densities at U_H = +350 mV in 0.5% quartz sand containing sea water as a function of position in the measuring section (Fig. 1); material: duplex steel G X40 CrNiMo 27 5

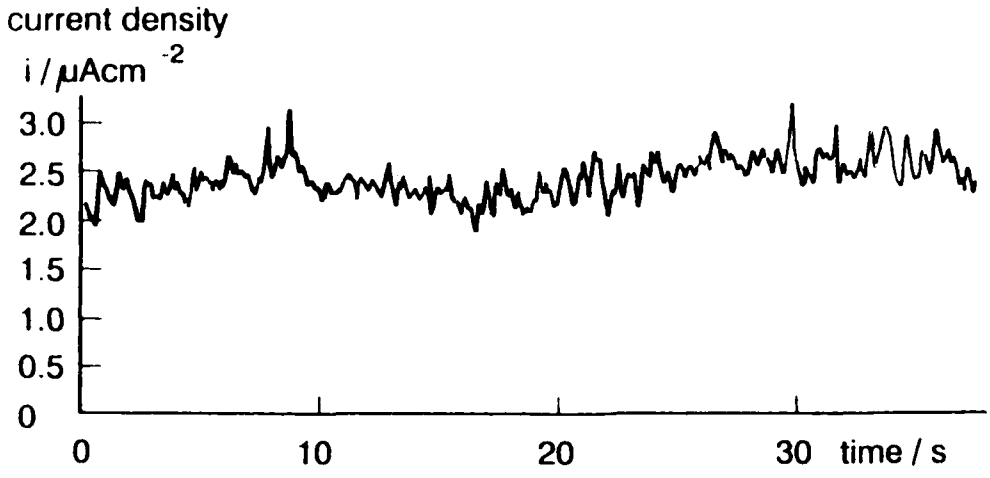

FIGURE 7
Current fluctuations on material G X40 CrNiMo 27 5, in seawater containing 0.03 vol. % quartz sand, U_H = +307 mV, particle diameter 0.31-0.4 mm, flow velocity 1.2 m/s

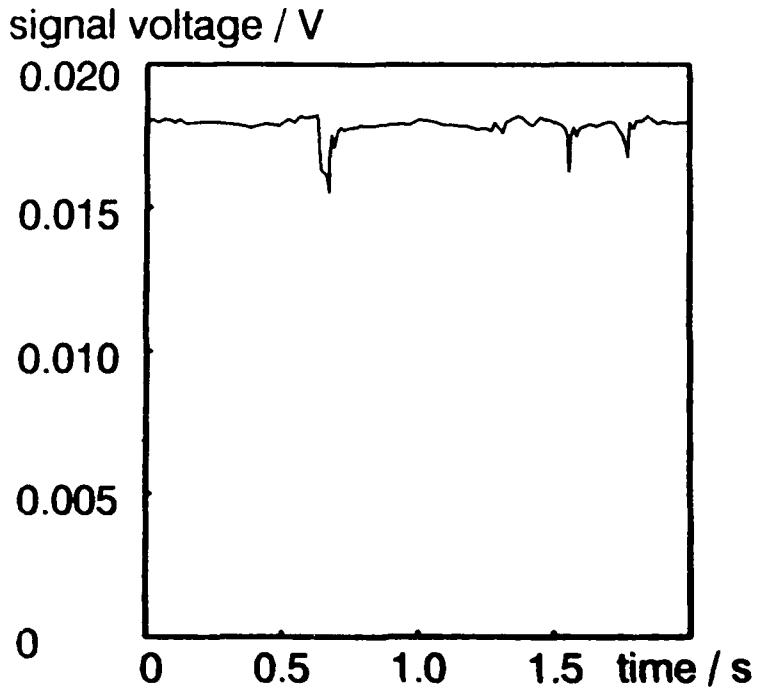

FIGURE 8
Signal of the particle rate sensor: current decrease caused by particles with a diameter of 0.8 mm in tap water at two stainless steel electrodes, voltage 1.9 V

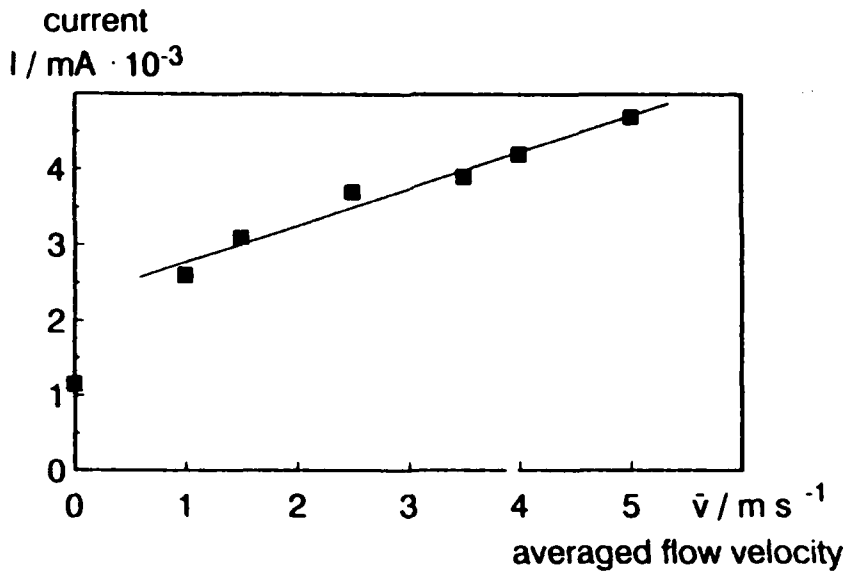

FIGURE 9
Current vs. mean value of flow velocity, U_H = -1200 mV, tap water with NaCl, measuring place of first ring after pipe expansion in Fig. 1

Monitoring and Prediction of Environmentally Assisted Crack Growth in Stainless Steel Piping

S. Ranganath
GE Nuclear Energy
175 Curtner Avenue
San Jose, California

Abstract

Stainless steel piping components used in nuclear power plants are exposed to the high temperature water environment and subjected to cyclic stresses as well as sustained stresses due to pressure, thermal and weld residual stresses. Crack initiation and subsequent growth due to corrosion fatigue and intergranular stress corrosion cracking (IGSCC) are the potential environmentally assisted cracking (EAC) mechanisms that should be considered in the piping design. For austenitic stainless steel piping in oxygenated water environment, IGSCC is the more probable damage mechanism since margin against fatigue initiation is already built into the ASME Code piping design. Margins on corrosion fatigue are also included, although there is some debate on whether the implicit margins are sufficient to account for environmental effects on fatigue.

One way of monitoring and protecting against EAC is to perform periodic inspections of piping to provide assurance of piping integrity. If crack indications are discovered as a result of the inspections, an immediate question that arises is what the expected crack growth rate is and whether continued operation can be justified on a short term basis. Determination of the crack growth rate requires some form of monitoring and analytical prediction. This paper describes several monitoring techniques for predicting crack growth in austenitic stainless steel piping in Boiling Water Reactors (BWR).

The three types of monitoring systems - the crack arrest verification system, the In-pipe electrochemical potential (ECP) Monitoring and the in-core stress corrosion monitor - provide plant specific environmental data. Prediction of plant component crack growth rate still requires extrapolation of the results of the monitoring system with crack growth predictive models. A major benefit of plant monitoring is that is enables measurement of the actual water chemistry parameters instead of relying on bounding values. This allows realistic crack growth predictions that can be used in planning and prioritizing inspections and in making operate 'as is' vs. repair decisions. The environmental monitoring systems also provide valuable water chemistry information which can be used to take corrective actions when operational problems such as condenser leaks, and resin intrusions arise. The environmental data are also important when mitigation measures such as hydrogen water chemistry are implemented. The monitoring techniques described in the report have been implemented in several operating boiling water reactors and thus successfully field tested.

Key terms: *monitoring*, intergranular stress corrosion cracking, environmentally assisted cracking, water chemistry

Introduction

Stainless steel piping used in nuclear power plants are exposed to high temperature water environment and are subjected to cyclic stresses as well as sustained stresses due to pressure, thermal and weld residual stresses. Crack initiation and subsequent growth due to corrosion fatigue and IGSCC are the potential environmentally assisted cracking (EAC) mechanisms that should be considered in the piping design. For austenitic stainless steel piping in an oxygenated water environment IGSCC is the more probable damage mechanism since margin against fatigue initiation is already built into the ASME Code piping design. Margins on corrosion fatigue are also included, although there is some debate on whether the implicit margins are sufficient to account for environmental effects on fatigue.

One way of monitoring and protecting against EAC is to perform periodic inspections of piping to provide assurance of piping integrity. The regulatory requirements for the inspections of austenitic piping are defined in Section XI, ASME Code[1] and in the U.S. Nuclear Regulatory Commission NUREG-0313[2]. If crack indications are discovered as a result of the inspections, an immediate question that arises is whether continued operation can be justified on a short term basis. The ability to continue to operate on an interim basis will allow repair or replacement measures to be implemented without expensive, unplanned plant outages. It will also allow time to procure material, fabricate replacement hardware, qualify the design and implement the repair. Since crack growth can continue during the period of interim operation, it is important to determine the expected crack growth rate and estimate the crack depth at the end of the evaluation period. Continued operation for this period is acceptable if the final crack depth is less than the allowable depth as specified in the ASME Code[1]. For austenitic piping components, where IGSCC is the principal environmental degradation mechanism. Several methods are available for monitoring and prediction of crack growth. This paper describes several monitoring techniques for predicting crack growth in austenitic stainless steel piping in Boiling Water Reactors (BWR).

Crack Growth Prediction Techniques

Crack growth due to IGSCC is time dependent and is a function of sustained stresses, material condition and water chemistry parameters. Crack growth predictions can be made to different levels of sophistication using a range of assumptions. Some of the commonly used techniques are briefly described here. Out of the five techniques, three (b, c and e below) are discussed in detail later.

a. Use of Bounding Crack Growth Rate Data.

   This involves use of a crack growth rate curve (da/dt vs. sustained stress intensity factor) that bounds laboratory data for a variety of environmental conditions. An example of such a curve taken from Reference 2 is shown in Figure 1. The only plant unique feature of the prediction is in the applied stress (including weld residual stress) used in the analysis. The prediction does not consider the actual water chemistry parameters such as conductivity and (ECP) and is inherently over conservative since the crack growth curve that is used is intended to bound available data for a variety of chemistry conditions. Although this approach is often used as a basis for regulatory submittals, because of its conservatism, it has little relevance to the actual plant conditions and cannot be used for planning or prioritizing in-service inspections.

b. Use of Crack Monitoring Systems

Crack Arrest or Advance Verification (CAV) systems have been used extensively in monitoring crack growth in austenitic piping components exposed to the recirculation system coolant in several operating BWR's[3-5]. The system, based on the reversing dc electrical potential technique, enables precision monitoring and detection of crack growth in fracture mechanics specimens exposed to recirculation system water. Since the crack growth rate data is for IGSCC precracked specimens in the reactor environment, the data are plant specific. By anchoring a typical IGSCC growth curve such as that in Reference 2, to the CAV data point (Figure 1), predictions can be made for crack growth in specific components. Thus, the CAV system provides an assessment of component behavior in terms of plant water quality performance.

c. Use of ECP Monitoring Systems

In the CAV system, crack growth is measured on an actively loaded fracture mechanics specimen that is exposed to the reactor environment in an autoclave. Thus, there is a direct measurement of crack growth on the specimen, which in turn, is extrapolated to determine crack growth in the component. In the ECP monitoring system, only the chemistry parameters (including conductivity, dissolved oxygen and ECP) are monitored. Crack growth rates are determined by the application of the film rupture model developed by Ford and Andresen[6].

d. Pipe Crack Monitoring

This technique involves use of the reversing DC electrical potential difference method to monitor the growth of a specific crack. Voltage probes are attached on both sides of the crack and the potential difference across the crack is monitored. The crack depth can be related to differential voltage and thus monitored over time.

e. In-Core Monitoring

In-core components are also susceptible to environmental cracking. However, monitoring the in-core crack growth requires separate characterization of the environmental conditions since the chemistry inside core is more oxidizing (because of radiolysis) than in external piping. Because this approach requires reactor penetrations, measurement of the ECP inside the core presents challenges. Crack growth predictions can be made once the ECP and the applied stresses are known. In-core monitoring has been successfully applied in three boiling water reactors. In all these applications a special precracked double cantilever beam (DCB) specimen has also been used to monitor crack growth.

The crack growth prediction and monitoring techniques described above (except the pipe crack monitor) have been successfully applied in several boiling water reactors. Of these, three methods have been selected for detailed discussion.

Crack Arrest Verification (CAV) System

The CAV system is designed to monitor crack growth in piping components exposed to the reactor water environment. It consists of three precracked fracture mechanics (compact tension) specimens that are actively loaded using a dead weight controlled load frame (Figure 2). The specimens are located in an autoclave connected to the recirculating system through a sample line. In general, three specimens - one made of furnace sensitized Type 304 stainless steel (this serves as a reference heat) and two other specimens e.g., Type 316 nuclear grade stainless steel or Alloy 182 weld material - are used. The autoclave has a volume of 1 1/2 gallons and the flow rate into the autoclave ranges from 2-5 gpm. The compact tension specimen is instrumented with probe wires that bridge the crack (Figure 3). A constant current is passed through the specimen and the potential difference across the crack is measured. As the crack grows, the resulting change in potential is measured via the probe wire using a high resolution voltmeter. A reference probe pair is also attached to each specimen so as to provide compensation for test temperature. The values of the potential field voltages are very small (typically on the order of 50 to 100 microvolts) and the changes for crack advance of less than 0.1 mil are even smaller. Therefore, extreme attention must be paid to minimizing system electrical noise.

In order to maximize chances of differentiating between genuine signal changes associated with crack growth and other sources of system drift, the reversing DC technique was developed. In this technique the current is allowed to flow through the specimen in one direction for 1/2 second and potential field measurements are made. Then the direction of the current flow is reversed and the potential field measurements repeated. The algebraic difference of these two measurements (i.e., the amplitude) is used in the algorithm for calculating changes in crack length. This amplitude based approach compensates for long term systematic drift. Reversing current also eliminates the potential for galvanic effects occurring at the crack tip. Crack length is calculated from the normalized potential drop (i.e., potential across the crack-reference probe potential) using crack length vs. potential correlation's developed using finite element analysis or test data.

In addition to the crack growth module, the CAV system also has an ECP module which consists of a smaller autoclave with is also exposed to the recirculation system water environment. In general, the ECP instrumentation includes a combination of silver/silver chloride, copper/copper oxide and platinum reference electrodes. Water temperature, dissolved oxygen, pH and conductivity are also monitored.

The instrumentation console contains the power supply to excite the test specimens. These signals are fed to a personal computer. A solid-state switch driven by this computer provides reversing dc voltage on a fixed-time base. A built-in digital voltmeter is provided in the console for calibration and maintenance. Temperature, flow and pressure displays for the test vessels are also provided. The computer equipment (for data acquisition/reduction) and test support equipment (amplifiers, power supply, etc.) are placed in either an air conditioned room enclosure or an air conditioned console.

Figure 4 shows typical results (crack length and conductivity) from a CAV system in an operating BWR over a period of 5000 hours of hot operation. An interesting result from the plot is the correlation between crack growth and water conductivity. For brief excursions in conductivity (shown in Figure 4), there is little change in crack growth rate. However, where

there are periods of high conductivity over hundreds of hours, there is a clear acceleration of crack growth. This suggests that a monitoring system such as the CAV system can be used to determine when plant shutdown is warranted in the event of a conductivity excursion.

It is also interesting to compare the crack growth rate measured in a CAV system with the NRC bounding crack growth curve recommended in[1] for sensitized stainless steel (Figure 1). It is seen that the measured growth rates are an order of magnitude lower than that predicted by the NRC curve. This highlights the importance of using crack growth rate data for the plant specific environment before decisions on inspection priority and operate 'as is' vs. repair choices are made.

One limitation of the CAV system is that in some cases the autoclave environment may not represent the actual conditions in the pipe itself. If the flow rate is too low and the transit time before the flow reaches the autoclave is too high, there is a possibility that short lived species such as peroxide would have dissipated before the sample reaches the autoclave. Thus, the measured ECP in the autoclave may not be the same as that in the pipe itself. This can be avoided by assuring adequate flow and minimizing the length of the line connecting the pipe to the autoclave. As a rough rule, the transit time between the pipe and the autoclave should be less than 30 seconds. Alternatively, if the ECP is monitored in the pipe itself instead of the autoclave, the uncertainty can also be avoided. This is explained in the next section.

In-Pipe ECP Monitoring

To address concerns on whether the CAV system water environment reflects the actual conditions inside the pipe, an in-pipe ECP monitoring system was developed. The system uses existing decontamination flanges in the recirculation system. Two approaches are feasible - the first involves just ECP monitoring while the second involves measuring crack growth with a wedge loaded DCB specimen. Figure 5 shows a schematic of the in-pipe ECP monitoring system. Two types of reference electrodes are used - silver/silver chloride and platinum. The ECP of the piping is measured directly. The use of the two reference electrodes provides verification of the system at high temperatures. The platinum and silver/silver chloride electrodes use a hardened leak proof design which is extremely important where accessibility to the electrodes is limited. One limitation of the in-pipe ECP monitor is that it provides chemistry information only. Crack growth prediction requires the application of modeling techniques such as that proposed by Ford and Andresen[6].

The analytical model relating the IGSCC growth rate to the applied stress intensity factor and the material and water chemistry parameters has been documented extensively[6-8]. Thus the slip dissolution/film rupture mechanism of crack propagation and the theoretical development will not be described here. The intent here is merely to summarize the equations used in the crack growth prediction.

The crack growth rate V_T is related to the crack tip strain rate ($\dot{\varepsilon}_{ct}$) as follows:

$$V_T = A(\dot{\varepsilon}_{ct})^n$$

The above equation represents the environmental component of crack growth which is additive to the mechanical component. The parameters A and n are complex functions of the material and water chemistry conditions and can be expressed in the following generic form:

$$n = \left(\frac{e^{f(k)}}{e^{f(k)} + e^{f(\phi)}} \right)^{f(EPR))}$$

where ϕ is the corrosion potential in V_{she}, k is the solution conductivity in $\mu S/cm$ and EPR is the electrochemical potentiokinetic repassivation value in C/cm^2 which is a (in some cases imperfect) measure of the grain boundary chromium content, a parameter of more direct importance than EPR. Three mathematical formulations for stainless steels of "low" (EPR = 0 C/cm^2), "average" (EPR = 15 C/cm^2) and "high" (EPR = 30 C/cm^2) degrees of sensitization, were developed. Between these three specific values of EPR, linear interpolation is used. A is given by the following expression:

$$A = 7.8 \times 10^{-3} n^{3.6}$$

Finally, the strain rate $\dot{\varepsilon}_{ct}$ for constant load condition is given by:

$$\dot{\varepsilon}_{ct} = 6 \times 10^{-14} K^4$$

$\dot{\varepsilon}$ is in S^{-1} and the stress intensity factor K is in ksi$\sqrt{in}$ units. Application of the model, therefore, requires monitoring of the ECP and conductivity as well as knowledge of the EPR and the applied K values.

Figure 6 shows typical results measured in the drain line of an operating BWR. The drain line was selected for detailed study since it provides environmental data for the bottom plenum. In particular, the drain line ECP monitor provides information on the amount of hydrogen injection needed (as part of Hydrogen Water Chemistry implementation) to achieve the protection level of -230mV SHE needed to assure IGSCC mitigation.

In-Core Monitoring System

The in-core monitoring (Figure 7) is focused on measuring the ECP and the crack growth rates inside the core where, because of radiolysis the water environment is more oxidizing. The other water chemistry information such as conductivity and dissolved oxygen are measured through external sampling lines. The ECP electrodes are located inside the housing of a local power range monitor (LPRM). Sensors are installed just below the active fuel and near the top of the fuel bundle. Two types of ECP electrodes are included in the LPRM. Both electrodes are the product of extensive testing and experience, and selected after a vigorous and extensive test program where the sensors are operated in simulated BWR environments. The reference electrodes are required to be within 0.030 V of their theoretical potential and pass impedance and visual tests before installation.

The silver and silver chloride electrode materials are contained within the sapphire crucible (an inert insulator), specially machined to form an internal hermetic seal (Figure 8). As long as the seal is intact, the electrode will provide the correct electrochemical potential. The

crucible is fitted with a tight fitting cover, which forms the liquid junction between the electrolyte in the crucible and the reactor environment. The tight fitting cover minimizes mass transport in and out of the crucible. A coaxial cable which passes out of the LPRM cover tube through the gland seal below the reactor vessel provides the electrical output. Finally, the cable is routed through the drywell and passes through an electrical penetration. From the electrical penetration the signal is routed to the data acquisition system.

Under hydrogen water chemistry conditions, the Pt electrode in a lower position is used to calibrate the Ag/AgCl electrode and can also be used as a reference electrode if the dissolved hydrogen and pH in its vicinity are known.

The Pt electrode shown (Figure 9) is manufactured by attaching a Pt cylinder to the end of an RS-200 seal which is welded to the end of a coaxial cable. The nickel tip of the seal is in electrical contact with the central wire of the cable and thus forms an electrical junction from the Pt sensor to the central wire in the coaxial cable. The arrangement for linking the platinum sensor to the data acquisition system is as described above for the silver/silver chloride electrode.

Wedge loaded DCB specimens (Figure 10) are also located within the LPRM to monitor crack growth. As in the CAV system, the specimens are precracked under IGSCC conditions to assure that the delay associated with initiation time for intergranular cracking is minimized. The crack driving force is provided by a ceramic wedge inserted into the crack mouth such that an appropriate stress-intensity factor (K) is applied to the crack tip. One of the DCB specimens is installed in the furnace sensitized condition to encourage crack growth early in the fuel cycle before appreciable neutron fluence accrues. The purpose of the sensitized specimen is to show that, in the core bypass water chemistry and in the presence of high local neutron and gamma flux, it is possible through sufficient hydrogen addition to arrest an actively growing intergranular crack. The second specimen is in the solution annealed condition with a fatigue precrack at the base of the specimen notch. The purpose of the annealed specimen is to determine if hydrogen addition will arrest actively growing irradiation assisted stress corrosion cracking (IASCC), after sufficient neutron exposure has accrued, in actual reactor internal materials. This assumes an actively growing crack will initiate after some extended period of operation (about 6-18 months). Crack growth is monitored in each of the sensors using the reversing dc/electrical potential crack growth technique. In this technique, voltage measurements made across the crack opening are converted to crack length by an algorithm contained in the computer software. Once per hour the computer calculates the crack length in each sensor from an average voltage obtained at each of four locations on each sensor. Behavior of the stress corrosion sensors can be evaluated rapidly using a graphics program (included with the computer software) that allows the user to produce plots of crack length, sensor temperature, and sensor current versus time.

Figure 11 shows typical ECP data from an in-core monitoring system. The in-core monitoring system is often used to determine the hydrogen injection (as part of a hydrogen water chemistry program) levels to bring the ECP down to the -230mV SHE level required to assure IGSCC mitigation. Figure 12 shows the dependence of the measured ECP on the feedwater hydrogen concentration. The in-core system has been used in three BWR's and is being currently installed in a fourth BWR. Future development of actively loaded crack growth sensors for in-core application will offer more realistic crack growth data. Efforts are

underway to develop pressure bellows or magnetic loading systems for use in the in-core crack growth sensors.

Summary

The three types of monitoring systems - the CAV system, the In-pipe ECP Monitoring and the In-core Stress Corrosion Monitor - provide plant specific environmental data. Prediction of plant component crack growth rate still requires extrapolation of the results of the monitoring system with crack growth predictive models. Monitoring systems of the type described here are for several benefits for the nuclear power plant industry. One advantage of plant monitoring is that is enables measurement of the actual water chemistry parameters instead of relying on bounding values. This allows realistic crack growth predictions that can be used in planning and prioritizing inspections and in making operate 'as is' vs. repair decisions. The environmental monitoring systems also provide valuable water chemistry information (e.g., conductivity, ECP, dissolved oxygen) which can be used to take corrective actions when operational problems - condenser leaks, resin intrusions arise. The environmental data are also important when mitigation measures such as hydrogen water chemistry are implemented. The monitoring techniques described in the report have been implemented in several operating boiling water reactors and thus successfully field tested.

Acknowledgments

Much of the work over the last ten years on the development of the monitoring techniques have been funded by the Electric Power Research Institute with several program managers including Joe Gilman, Robin Jones, Larry Nelson and Raj Pathania. At General Electric, major strides in monitoring were made with significant contributions from Peter Andresen, Lou Coffin, Peter Ford, Gerry Gordon, Don Hale, Maurice Indig, Willie Miller, Bob Nixon, Tom Prater and Dan Weinstein.

References

1. Section XI, Division I, "ASME Code Rules for Inservice Inspection of Nuclear Power Plant Component", 1989 Edition American Society of Mechanical Engineers.

2. W.S. Hazelton, "Technical Report on Material Selection and Processing Guidelines for BWR Coolant Pressure Boundary Piping", NUREG-0313, Rev. 2. U.S. Nuclear Regulatory Commission.

3. S. Ranganath and D.A. Hale, "Application of On-Line Crack Growth Monitoring to Evaluate Nuclear Power Plant Component Performance", "High Pressure Technology, Fracture Mechanics, and Service Experience in Operating Power Plants", ASME PVP Vol. 192. The 1990 Pressure Vessels and Piping Conference, Nashville, TN, June 17-21, 1990.

4. S. Ranganath et al, Prediction of "Environmentally Assisted Crack Growth in a Large Diameter Stainless Steel Pipe", Procedures of the 5th International Symposium on Environmental Degradation of Materials in Nuclear Power Systems - Water Reactors, Monterey, CA, August 1991.

5. D.A. Hale and C.G. Diehl, "Real Time Monitoring of Environmental Crack Growth in BWRs", CORROSION/ 88, (St. Louis, MI: National Association of Corrosion Engineers, 1988).

6. F.P. Ford and P.L. Andresen, "The Theoretical Prediction of The Effect of System Variables on the Cracking of Stainless Steel and Its Use in Design". CORROSION/87, (San Francisco CA: National Association of Corrosion Engineers, 1987).

7. P.L Andresen and F.P Ford, "Modeling and Life Prediction of Stress Corrosion Cracking in Sensitized Stainless Steel in High Temperature Water". Proceedings of ASME Piping and Pressure Vessel Conference, Miami, November 17-25, 1985.

8. P.L. Andresen, "Observation and Prediction of Environmentally-Assisted Crack Growth Variables on the Cracking of Stainless Steels in High Temperature Water", CORROSION/87, (San Francisco, CA: National Association of Corrosion Engineers, 1987

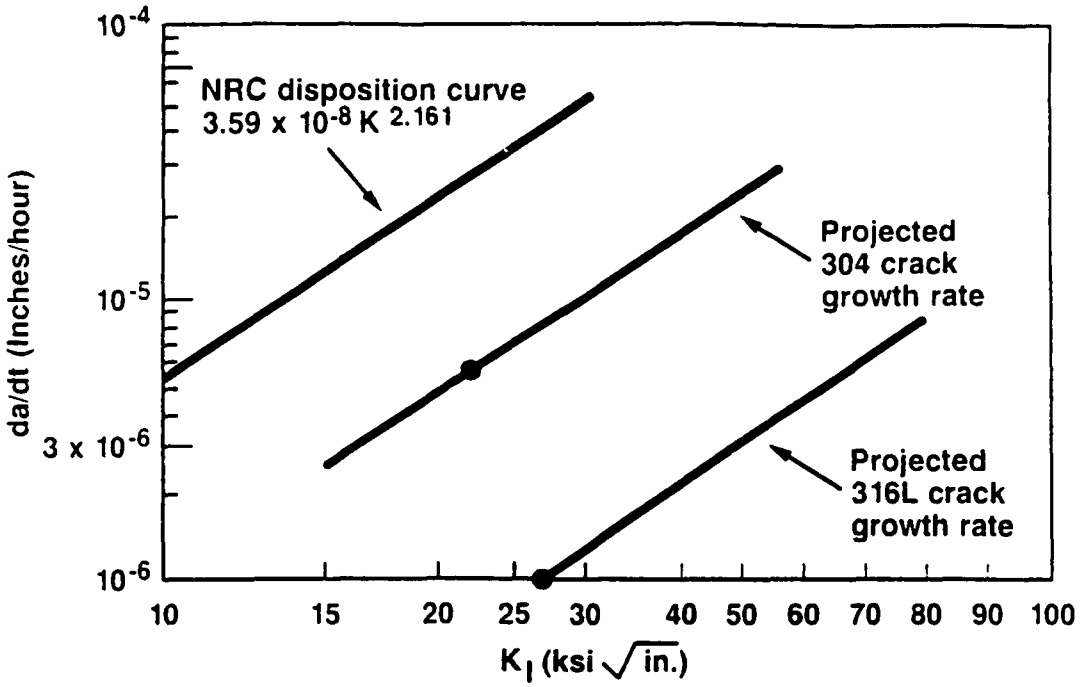

Figure 1 NRC Crack Growth Disposition Curve for IGSCC in Stainless Steel.

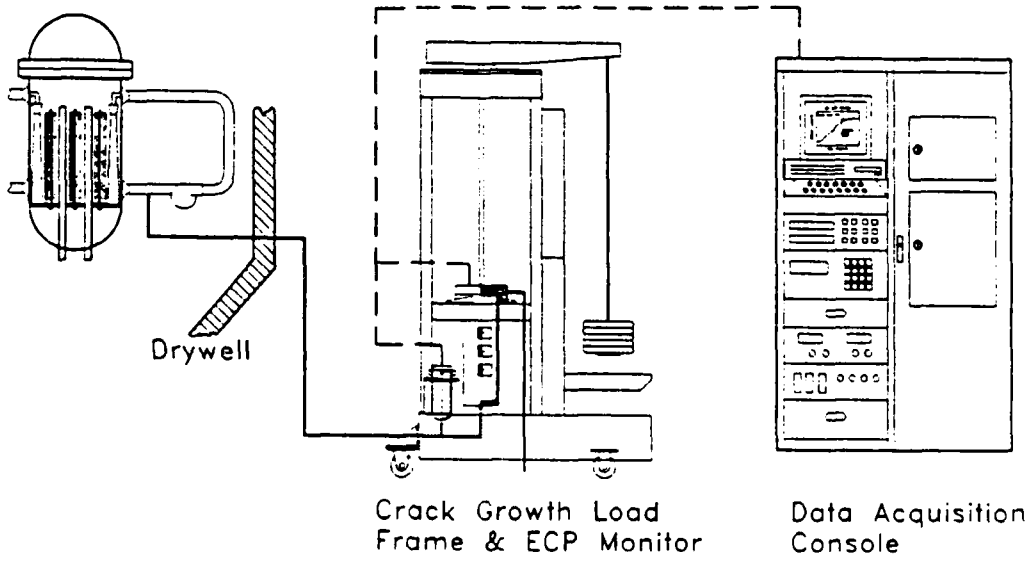

Figure 2 Schematic of the Crack Arrest Verification System.

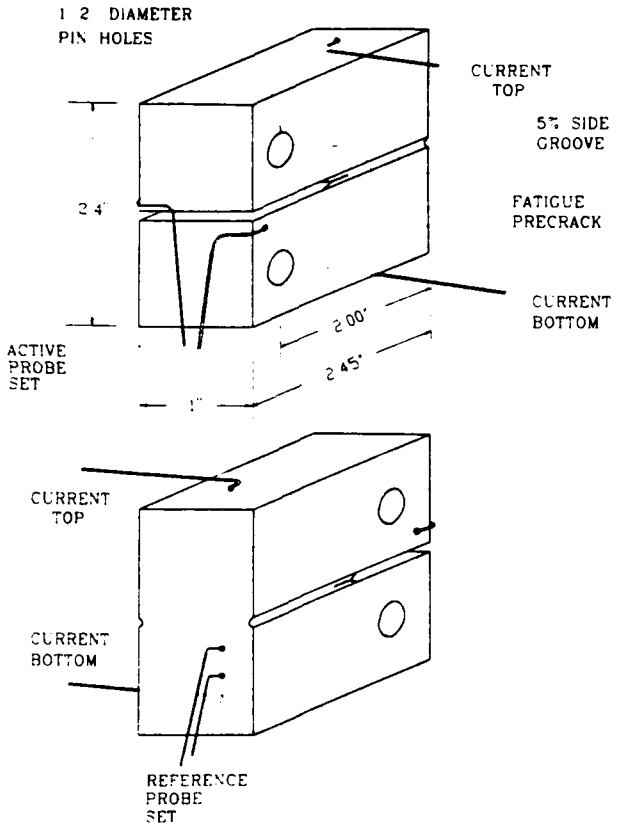

Figure 3 Compact Tension Specimen with Potential Probes.

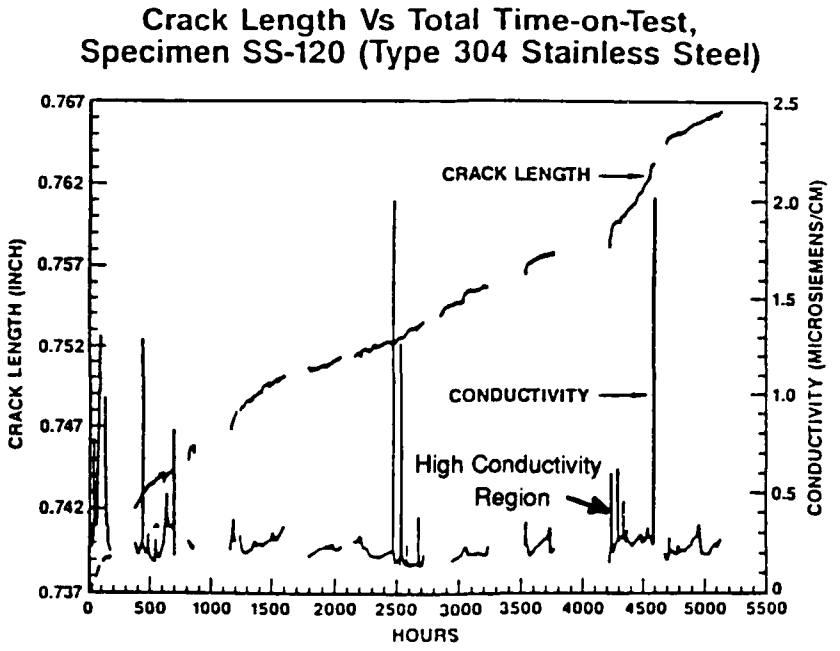

Figure 4 Typical results from a CAV System in an Operating BWR.

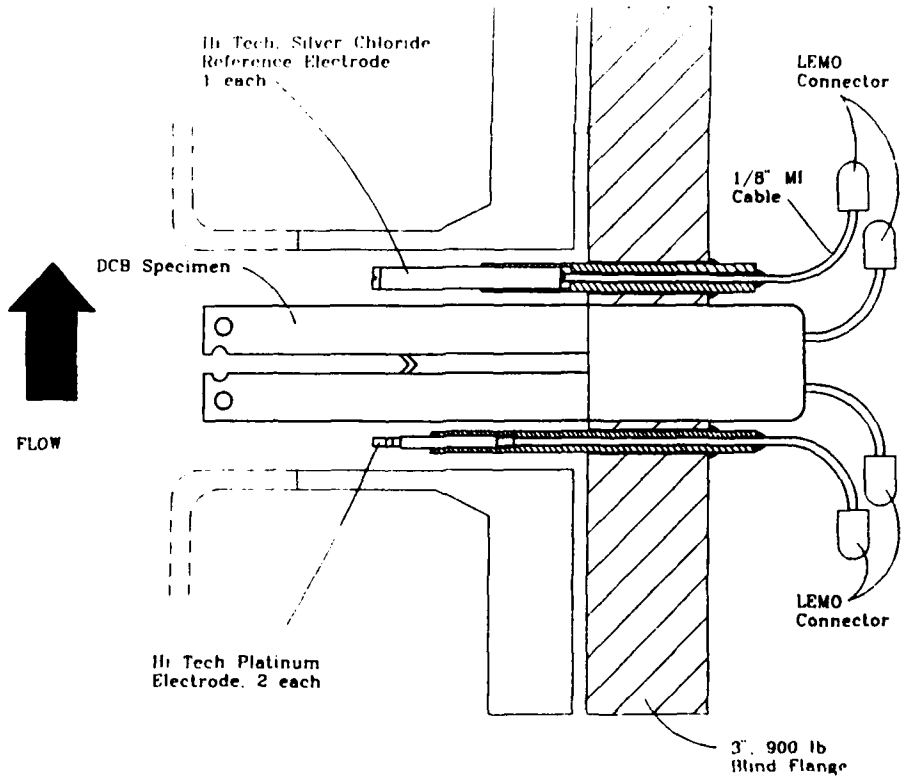

Figure 5 **In-Pipe ECP Monitor.**

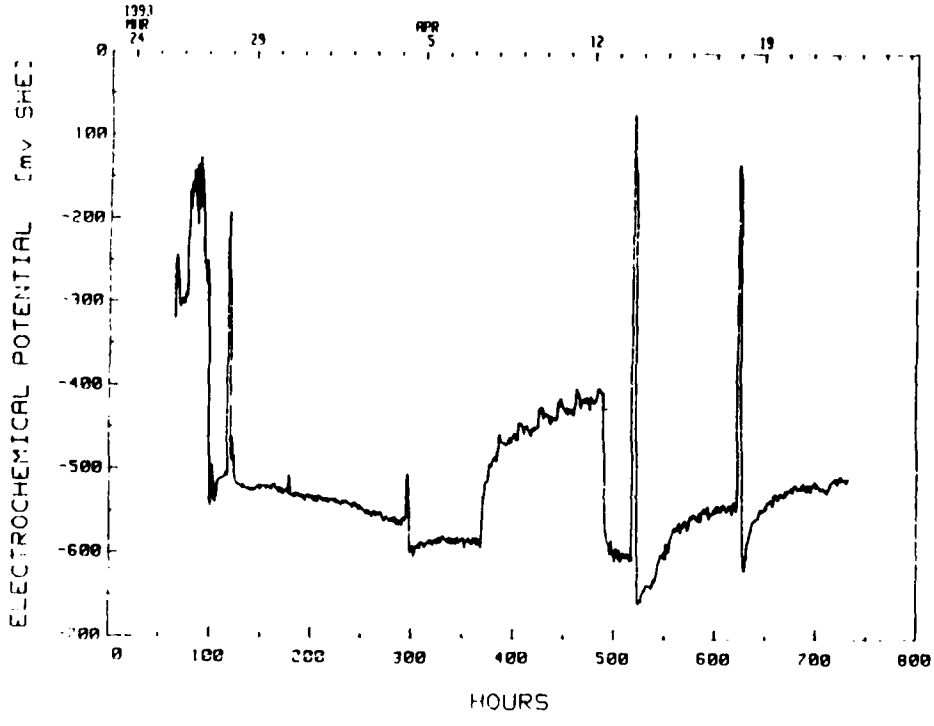

Figure 6 **Typical ECP Results from Drain ECP Monitor (Stainless Steel vs. Silver/Silver Chloride).**

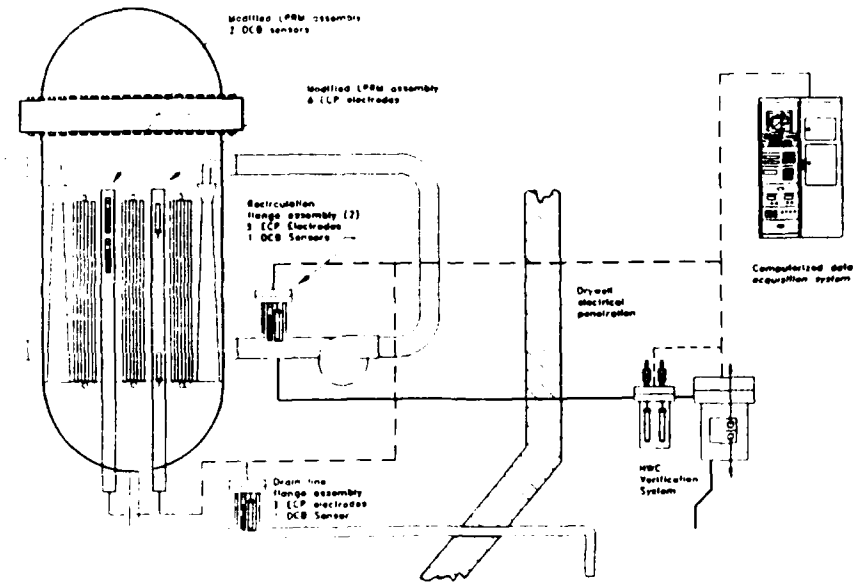

Figure 7 Schematic of In-Core Stress Corrosion Monitor.

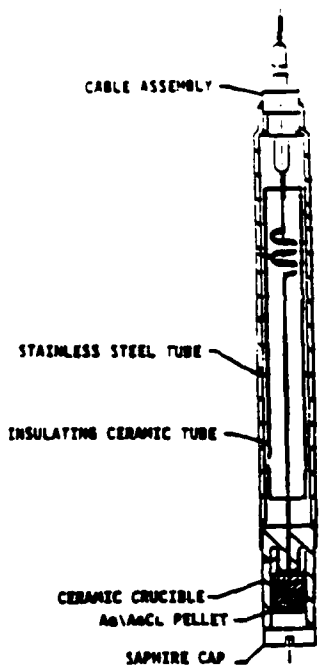

Figure 8 Silver/Silver Chloride Reference Electrode.

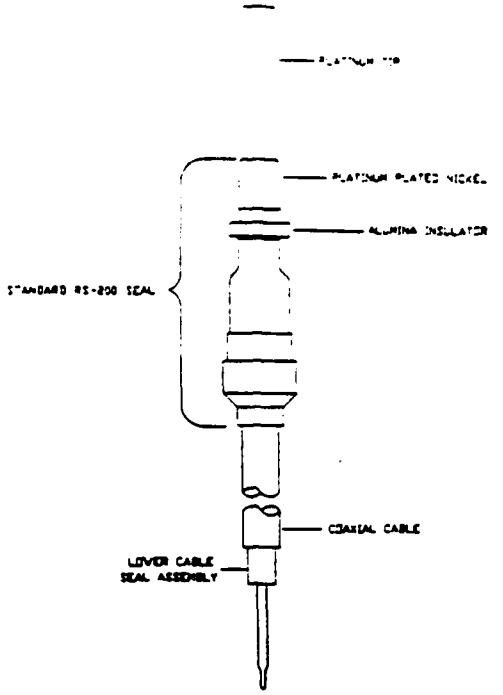

Figure 9 Platinum Reference Electrode.

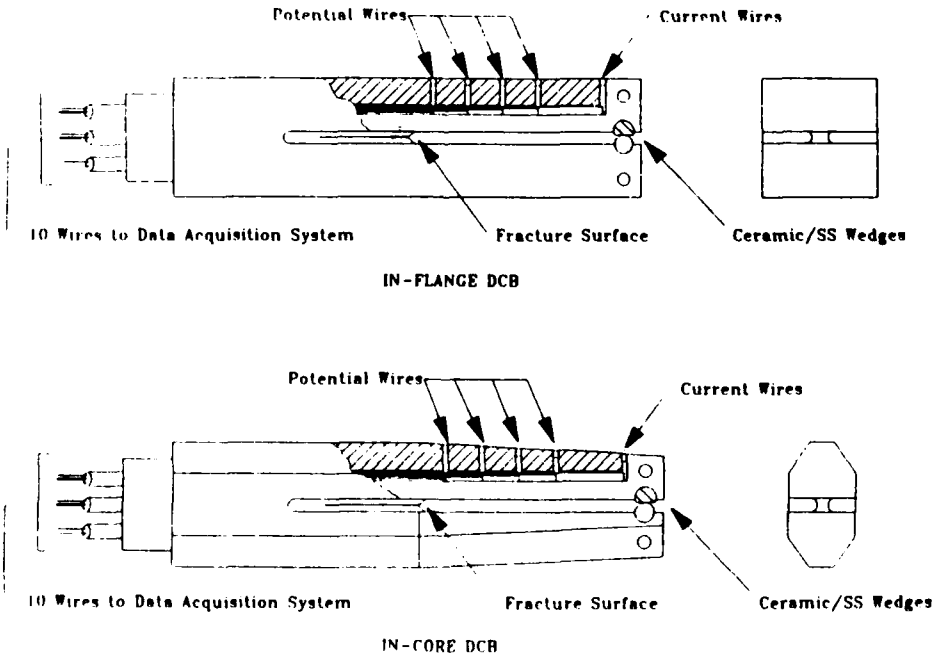

Figure 10 DCB Crack Growth Sensor for In-Core and In-Pipe Monitor.

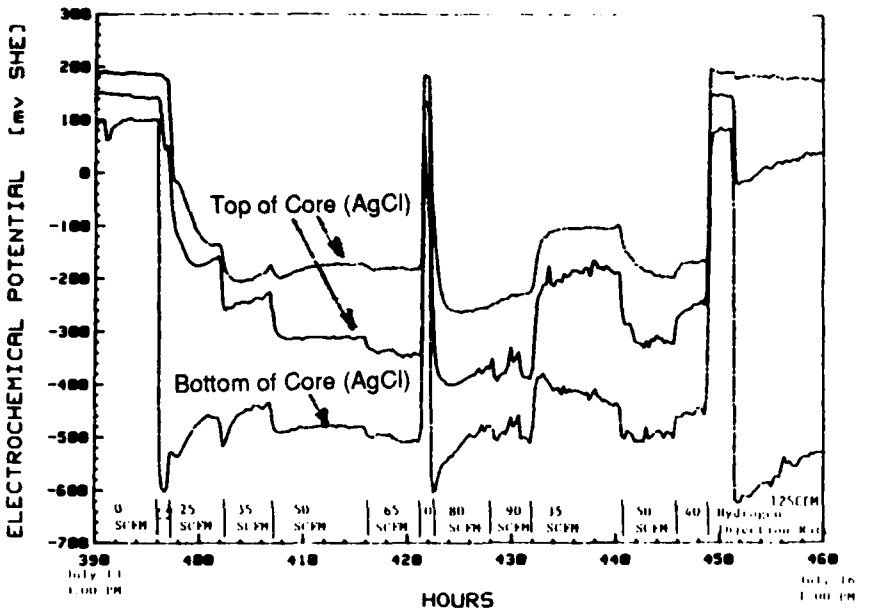

Figure 11 Typical ECP Results from In-Core Stress Corrosion Monitor.

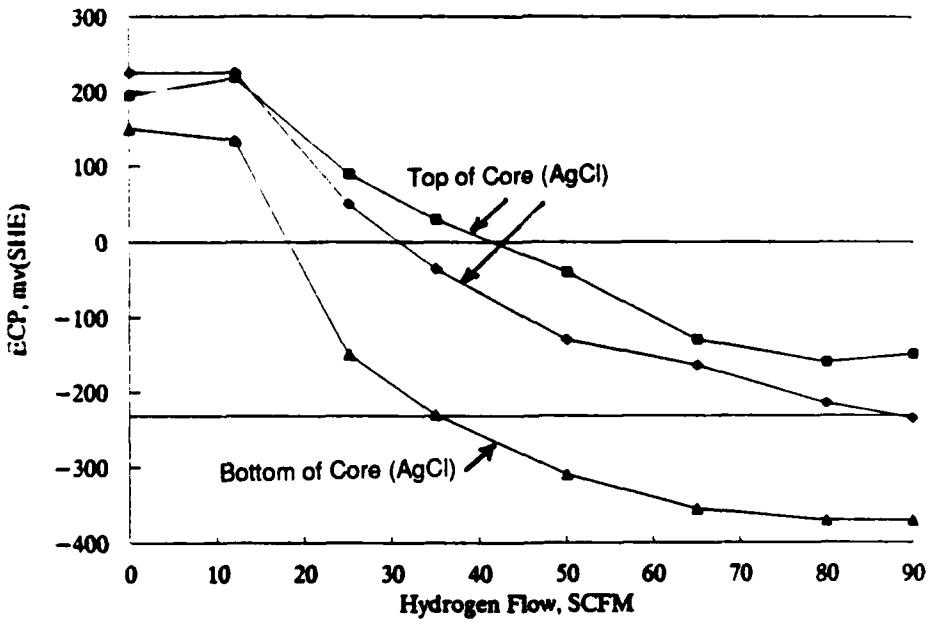

Figure 12 Dependence of In-Core ECP as a Function of Feedwater Hydrogen Concentration.

Corrosion Monitoring Using Harmonic Impedance Spectroscopy

Neil G. Thompson
Cortest Columbus Technologies, Inc.
2704 Sawbury Boulevard
Columbus, Ohio 43235

Barry C. Syrett
Electric Power Research Institute
3412 Hillview Avenue
Palo Alto, CA 94303

Abstract

Harmonic impedance spectroscopy (HIS) is a fairly recent development in corrosion monitoring. HIS is an electrochemical technique that uses the harmonic responses to a voltage perturbation to determine the corrosion rate. The primary difference between HIS and other electrochemical techniques is that it utilizes non-linear perturbations of the test specimen's electrochemical potential while all other techniques use linear perturbations. The primary advantage of HIS is that it is applicable to conditions where the metal surface is polarized away from its free-corrosion potential. For instance, it can be used to monitor corrosion of galvanic or macro-cell couples, and cathodically or anodically protected metals. No other electrochemical technique is applicable for polarized conditions. In this respect, HIS is a true breakthrough in corrosion monitoring. A recent application of HIS methodology to cathodically protected condenser water boxes in utility power plants is described.

Key terms: harmonic impedance spectroscopy, corrosion monitoring, corrosion rate, cathodic protection, condenser water box

Introduction

Corrosion monitoring methodologies have been recently reviewed by Thompson and Koch.[1] In this paper, corrosion monitoring methodologies were divided into two primary categories: periodic assessment and continuous monitoring. These categories were further divided into methodologies that provide a direct measure of corrosion and those that provide an indirect measure. Indirect measurements of corrosion often involve monitoring of environment chemistry (e.g. pH, temperature, specific ions), but also can include monitoring levels of hydrogen permeation through a metal and electrochemical potential measurement. Direct measurements of corrosion include weight-loss measurements and electrical resistance probes, but these methods provide only periodic assessment of the corrosion conditions.

Most continuous, direct corrosion measurement methodologies involve an electrochemical technique. These include linear polarization resistance (LPR), electrochemical impedance spectroscopy (EIS), electrochemical noise (EN), and harmonic impedance spectroscopy (HIS). LPR and EIS provide a direct measure of the polarization resistance for the metal surface being tested from which a corrosion rate can be calculated. The typical application of EN involves

monitoring either potential or current noise and inferring from this noise the localized corrosion condition of the metal coupon being monitored. Recently, the current and potential noise methods have been combined to calculate the resistance noise from which the polarization resistance can be calculated. The polarization resistance calculated for each of the electrochemical methods (EIS, LPR, and EN) should be the same assuming steady state behavior is obtained during the measurement. The common feature to each of these methods is that they rely on small voltage perturbations (plus or minus 20 mV), and resulting current responses to calculate a polarization resistance ($\Delta E/\Delta i$). The polarization resistance calculated by these methods is inversely related to the corrosion current by the Stern-Geary relationship given in Equation 1:

$$R_p = \Delta E/\Delta i = B_a B_c/[2.3\ (B_a+B_c)\ i_{cor}], \qquad (1)$$

where i_{cor} is the corrosion current density, B_a is the anodic Tafel slope, and B_c is the cathodic Tafel slope.[2] The Stern-Geary relationship is derived as a linear approximation of the Bulter-Volmer equation centered around the free-corrosion potential. If the voltage perturbation becomes too large, then the linear approximation for $\Delta E/\Delta i$ is not valid, and if the potential of the metal surface is polarized away from its free-corrosion potential, the Stern-Geary derivation is not applicable. Two common conditions that make methodologies based on the Stern-Geary relationship invalid are galvanic couples and cathodic protection. In addition to the linearity concerns, the constants B_a and B_c must be determined by a second set of measurements or values must be assumed based on experience. Because B_a and B_c can vary during a given exposure period, there are errors associated with measuring B_a and B_c for initial conditions and assuming that the measured values are constant for the entire exposure period. Periodic measurement of the Tafel constants by standard techniques is difficult because it is a destructive test requiring new test specimens for each measurement.

HIS is a technique with a similar methodology as EIS in that a sinusoidal voltage perturbation is applied to the test specimen and the resulting current response is measured. The difference is that a larger voltage perturbation is applied such that non-linear responses are measured. These non-linear responses show up as harmonics of the primary excitation voltage. Analyzing the primary frequency and the harmonics makes it possible to extract all the information (including Tafel constants) required to calculate corrosion rate.[3-8] Therefore, assumptions of the Tafel constants are not required. More importantly, the HIS relationships developed by McKubre are not confined to regions near the free-corrosion potential. The HIS methodology is applicable for polarized conditions including galvanic couples, stray currents, and cathodic protection. HIS is the first, and to date, the only electrochemical methodology capable of calculating corrosion rates for cathodically protected structures.

Principle Of Operation

The origin of the harmonic response is shown in Figures 1 and 2. In Figure 1, a sinusoidal input voltage at frequency f is superimposed on a current-voltage curve of the form,

$$I = I_{fc} \{\exp [B_a(V-V_{fc})] - \exp [-B_c(V-V_{fc})]\}, \quad (2)$$

where I_{fc} is the free-corrosion current defined at the free-corrosion potential (V_{fc}) as:

$$I_{fc} = I_a = -I_c. \quad (3)$$

Figure 1 shows that a sinusoidal voltage perturbation in the linear region about V_{fc} produces a linear current response. A voltage perturbation centered about a voltage away from V_{fc} within the non-linear region results in a non-linear current response which is composed of the primary frequency f and its harmonics 2f, 3f, etc. (Figure 2). These harmonic response terms contain sufficient information to completely specify the current-voltage curve at any DC voltage, and thus monitor the instantaneous corrosion rate even in the presence of an applied anodic or cathodic polarization.

General Application

HIS has been examined for various on-line monitoring applications including: cathodically protected condenser water box, crevice corrosion in a simulated nuclear tube/tubesheet crevice, condensed films, and the outlet duct of a pilot-scale wet SO_2 scrubber.[3] Although application of HIS may grow to include most conditions for which LPR and EIS are used, the most immediate applications are those involving cathodic protection for which no other corrosion rate monitor is available. These include condenser water boxes, underground piping and tanks, water tanks, etc. Of particular interest would be stray current situations for which even indirect potential measurements are not applicable.

Electric Power Research Institute (EPRI) is presently supporting a project in which HIS probes are installed in operating condenser water boxes for the purpose of monitoring the corrosion rates of the various materials of construction (water box, tubesheet, and tubes). Of primary concern is seawater or brine applications for which cathodic protection is applied. This application is described below and is typical of how HIS is applied for monitoring the corrosion performance of large structures.

HIS is typical of other electrochemical methodologies in that the surface area of the metal to be measured must be well defined. For a large structure, especially one in which the measurement probe should be non-intrusive such as a turbulent condenser water box application, monitoring is best accomplished through the use of relatively small test specimens (coupons). Therefore, HIS measurements are typically performed on specimens attached to the structure as opposed to being performed on the structure itself. In most applications, it is desired to position the HIS specimen flush with the structure surface. This will expose the HIS specimen surface to conditions as similar to the structure as possible. This is critical for flowing conditions, such as a condenser water box, and not as critical for stagnant conditions such as storage tank or buried pipeline conditions.

As for most other electrochemical techniques, a reference electrode is required to provide a reference for the magnitude of the potential perturbation. Because the electrochemical potential of the HIS specimen is not critical to the measurement, a metal reference electrode can be utilized. The primary requirement is that the reference electrode material is stable (will not corrode) in the environment of interest such that its potential is constant during the measurement period. Figure 3 shows a schematic diagram of an HIS probe assembly. The probe assembly consists of a center disc made out of the material of interest (the HIS test specimen) and a reference ring constructed from Alloy C-22 for seawater application. This geometry provides a good reference measurement of the entire test area and provides very little disturbance to the environment since there are no protruding parts.

The HIS methodology being employed in the condenser water box application utilizes the structure itself as the counter electrode. This is unique in electrochemical measurements. Because the structure is quite large compared to the small HIS specimen surface area, negligible voltage fluctuation of the structure is experienced during the test. Figure 4 shows a schematic diagram of the HIS test setup. The HIS test specimen and the structure must be shorted together for them to be at the same voltage and to experience the same corrosion behavior during non-measurement periods. During the HIS measurement, the instrumentation acts like a zero resistance ammeter and maintains the potential of the HIS specimen at the same value as that of the structure. While maintaining the average potential of the HIS specimen (working electrode) the same as the structure (counter electrode), the HIS instrumentation applies a sinusoidal voltage perturbation between the HIS test specimen and the structure. The magnitude of the perturbation is controlled by the potential difference between the reference ring and the HIS test specimen. In this fashion, the HIS measurement is made, and the harmonic responses measured by the HIS instrumentation. From this data, a corrosion rate for the HIS test specimen is calculated.

In the condenser water box applications, the HIS probes constructed of tube and tubesheet materials are flush mounted to the tube sheet as tube inserts. This provides realistic flow conditions for the tubesheet material but not for the tube materials. HIS probes constructed of the water box material are flush mounted in the box wall and experience similar conditions to the box wall. To monitor coated structures, the same (non-coated) HIS probe arrangement is used.

The assumption is that the HIS probe represents a void (holiday) in the coating of a similar size as the area of the HIS test specimen. This should be a reasonably conservative (worst case) corrosion condition for most coated structures.

With the above application, the effectiveness of a cathodic protection system can be monitored to provide adequate protection for the water box components, while limiting the amount of overprotection. The overprotection is a critical issue where titanium or ferritic stainless steel tubes are used. In these cases hydriding or hydrogen stress crack and eventual failure of the tubes can occur. Overprotection can also adversely affect coating performance causing more rapid degradation and disbonding of the coating.

Research is ongoing involving a full-scale test on two separate operating condenser water box systems. One has an impressed current cathodic protection system and the other has a sacrificial cathodic protection system. Materials of construction include carbon steel, cast iron, aluminum-bronze, copper-nickel, titanium, stainless steel, AL-6XN, and Muntz metal. This research is designed to provide proof of concept for operating condenser water box systems, by comparing corrosion rates based on weight-loss coupon data and HIS measurements. The project team is also designing and manufacturing field-worthy HIS monitoring instrumentation. This instrumentation will be a user friendly microprocessor based instrument that will quiz the user about his setup and particular application through a front end menu, make the HIS measurement, analyze the results, and display a corrosion rate. The instrument will be cost competitive with other marketed advanced corrosion rate devices (EIS and LPR). Both the instrumentation and the HIS probes will be marked by Cortest Instrument Systems, Inc. in Willoughby, Ohio.

Summary

Application

HIS is an electrochemical methodology and is applicable to any conditions for which electrochemical measurements are presently applied. In addition, HIS is applicable to conditions in which the metal surface of interest is polarized away from its free-corrosion potential. HIS is the first electrochemical technique to permit corrosion rate measurements on cathodically protected structures.

Advantages

HIS has two primary advantages over other electrochemical techniques: (1) it is applicable to polarized metal surfaces, and (2) it calculates the Tafel constants directly. Other electrochemical techniques may develop an error due to assumptions about the Tafel constants. For cathodically protected structures (e.g. condenser water boxes) the HIS techniques provides a direct measure of corrosion rate and can be used to optimize cathodic protection systems much more efficiently than conventional electrochemical potential measurements which provide only an indirect measure of the corrosion condition.

Future Work

The HIS technique has not been widely used to date and, therefore, remains to be proven for several applications. The ongoing EPRI project will prove its applicability for low resistivity, high flow conditions in fully operating condenser water boxes. As noted in this paper, laboratory proof of concept has been completed for several conditions, but its applicability for soil and other high resistivity applications is currently unknown.

References

1. N. G. Thompson, and G. H. Koch, Corrosion Monitoring and Process Control, "Solving Corrosion Problems in Air Pollution Control Equipment," Paper No. 28, Proceedings of the 1992 Air Pollution Seminar, Orlando, FL, (November, 1992).

2. J. Stern, A. J. Geary, Journal of the Electrochemical Society, 104, 56, (1957).

3. M. C. H. McKubre, and B. C. Syrett, "Harmonic Impedance Spectroscopy for the Determination of Corrosion Rates in Cathodically Protected Systems," ASTM Special Technical Publication 908, G. C. Moran and P. Labine, eds., "Proceedings of Symposium on Nondestructive Testing and Electrochemical Methods of Monitoring Corrosion in Industrial Plants," May, 1984, (Amer. Society for Testing and Materials, Philadelphia, PA, p. 433, 1986).

4. M. C. H. McKubre, "The Electrochemical Measurement of Corrosion Rates in Cathodically Protected Systems," EPRI Report CS-2858, Electric Power Research Institute, Palo Alto, CA, (February, 1983).

5. M. C. H. McKubre, C. M. Ablow, S. C. Leach, M. J. Madou, and H. B. Sierra-Alcazar, "On-Line Corrosion Monitoring in Cathodically Protected Systems," EPRI Report CS-5695, Electric Power Research Institute, Palo Alto, CA, (February, 1983).

6. B. C. Syrett and M. C. H. McKubre, "The HIS Corrosion Rate Monitor: A Technological Breakthrough," Proc. of the EPRI Condenser Technology Conference, held Sept. 1990 in Boston, MA, EPRI Report No. GS-7349, Electric Power Research Institute, Palo Alto, CA (July 1991).

7. B. C. Syrett and M. C. H. McKubre, "Device for In-Situ Monitoring of Corrosion Rate of Cathodically Polarized Metals," US Letters Patent No. 4,658,365 (April 14, 1987).

8. M. C. H. McKubre and B. C. Syrett, "Device for In-Situ Monitoring of Corrosion Rates of Polarized or Unpolarized Metals," US Letters Patent No. 5,006,786 (April 9, 1991).

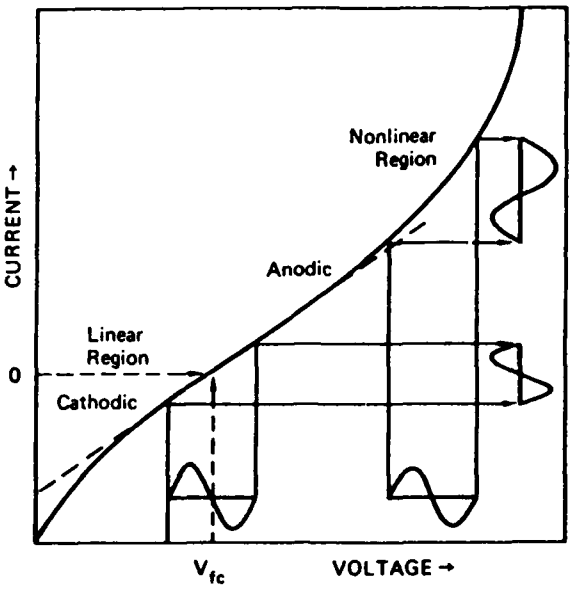

Figure 1. Source Of A Harmonic Response: Linear And Non-Linear Responses To An Input Potential Sine Wave.

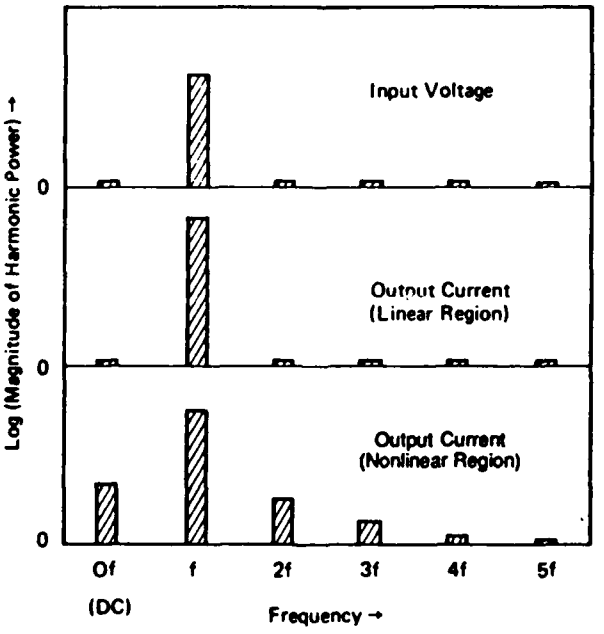

Figure 2. Source Of A Harmonic Response Shown As Frequency Domain Representation.

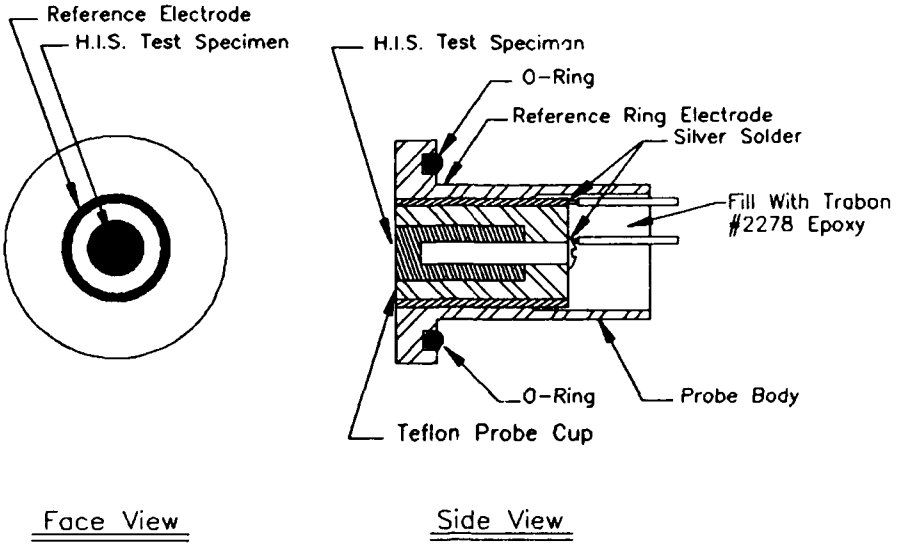

Figure 3. Schematic Of HIS Probe Design.

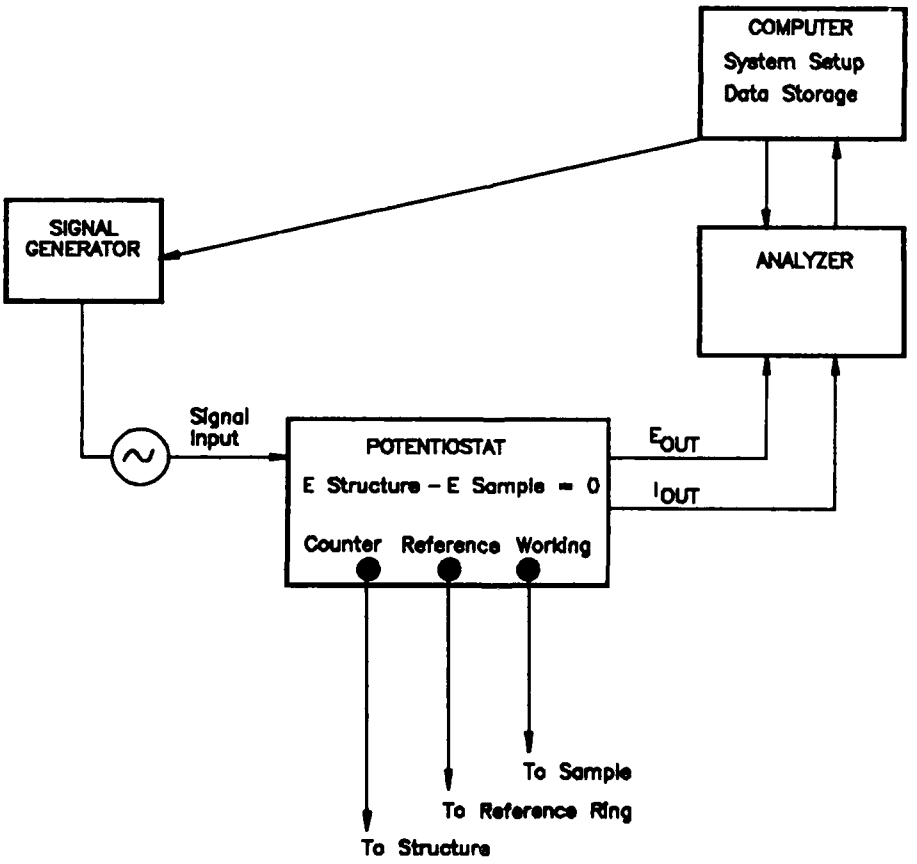

Figure 4. Schematic Diagram Of Measurement Circuit.

Extensions of Electrochemical Noise Methods As A Possible *In Situ* Corrosion Sensing Technique

Gordon Bierwagen*, Douglas Mills*& Dennis Tallman#

*Dept. of Polymers & Coatings
#Dept. of Chemistry
North Dakota State University
Fargo, ND 58105

Abstract

Electrochemical Noise (ECN) is the name given to the spontaneous fluctuations that continually occur in electrochemical systems that manifests itself either as potential noise or as current noise, depending on the mode of measurement. One can extract information concerning the spectral power distribution of the noise or the occurrence of specific corrosion events. Further, σ_{V_n} (standard deviation of the potential noise) divided by σ_{I_n} (std. dev. of current noise) can be identified with a polarization resistance R_n for corrosion for the coated metal system. If one can implant remotely accessible electrode configurations that allow ECN measurements, the possibility of *in situ* monitoring of corrosion processes follows directly, as the work of several programs sponsored initially by EPRI has demonstrated. Data from studies on several coating/ substrate systems using ECN methods are presented together with data obtained simultaneously on identical systems by other corrosion test methods. These data are acquired in an *ex situ* mode, but a discussion will be presented on our current thoughts on the modification of the experimental configuration to an *in situ* mode. Emphasis is on the equipment configuration, data acquisition system, sample preparation, and our proposals on possible modifications of our experimental system to allow *in situ* measurements. Possible modifications of software methods and data acquisition and data handling are presented. Data acquired are compared to past ECN studies as validation of the method. We then present our thoughts on possible extensions of the method emphasizing the development of *in situ* electrode configurations that could be utilized with this and other electrochemical techniques. Segmented electrode configurations are discussed, as well as the possible use of microelectrodes as implantable sensors for corrosion

Key Terms: Electrochemical Noise, Anti-corrosive Paints, Sensors, Microelectrodes

I. Introduction

Corrosion measurements that are of an electrochemical nature have been largely been performed in a laboratory with sensitive, non-robust instrumentation under carefully controlled conditions. This is especially true of electrochemical corrosion studies of coated (in the context of this paper, coated will refer to pigmented organic coatings- paints) metal systems. A review of such measurements has been given as of 1987 by Eden & Skerry[1] which discusses the typical evaluation methods that have been used to assess the performance and corrosion protective lifetimes of coatings. Significant information can be acquired by such investigations, and the state-of-the-art of corrosion protective coatings has been advanced considerably by such investigations. Those measurements of coated metal corrosion resistance that are acquired in the use

environment have to date consisted of exterior exposure of coated metal panels with ongoing subjective evaluation of appearance, and perhaps weight loss measurements. To our knowledge, little has been done (and published) of using *in situ* electrochemical methods of corrosion assessment for coated metal systems. However, there are many reasons for seeking the development of such methods, and recent developments in the electrochemical assessment of corrosion in coated metal systems need to be examined in this context.

The entire field of sensor development is heading toward miniaturized, implantable sensors coupled to on-line signal analysis and response methods. "Smart sensors" is the current buzz-word, especially for expensive, large objects, such as a power station. "Electrochemical corrosion sensors" that can be easily installed, that are non-obtrusive, and that can be remotely interrogated both either continuously or discontinuously would seem be an important contribution to extending the developments of corrosion science to practical use. ECN techniques coupled to an insertable electrode configuration offers the possibility of such a sensor,"and this has direct implication to power station corrosion monitoring.

There has been some work done on *in situ* electrochemical measurements of corrosion in power plants. Capcis March Limited (CML) of Manchester, UK has done considerable work in this area, some sponsored by EPRI, and ECN techniques are a key method in these studies[2,3,4,5]. These references do not describe all of the work done in this area but they give a good indication of what has already been done. However, this past work has not been in any way optimized with respect to data acquisition methods, the design of the electrodes used for monitoring, the software for control of the data acquisition, or the data interpretation methods. We are currently using CML equipment for laboratory studies of corrosion in coated systems, and many possible improvements for its use in this mode and also for remote sensing are apparent to us from our experiences with the equipment.

The detailed information provided by ECN measurements varies as a function of data acquisition rate. Using a computer controlled data acquisition system that enables the experimenter to choose the time interval at which data is acquired, an examination of the various features of the corroding system that appear in the electrochemical noise record vs. the rate of data acquisition will be discussed. We are currently examining the rate of data acquisition in our ECN studies, and will include in our discussions early results from such studies. Long term data acquisition is still in progress.

In the measurement of corrosion by electrochemical means, the measurement techniques can be separated into intrusive and non-intrusive methods, with the intrusive methods defined in the context of this paper as those that impose an external field of some sort on the measurement system. By this definition, all DC measurements will be intrusive and, thus, most electrochemical methods such as DC resistance, cyclic and square wave voltammetry, are intrusive. AC impedance is another technique which in its most common configurations is also intrusive. Electrochemical noise measurements are by the above definition non-intrusive, and can be performed even in marginally conductive environments (see ref. 2-5) with pseudo-reference electrodes[6]. The measurements may not demand the immersion in electrolyte that has been used for coated systems in lab studies[1,7,8,9]. Studies to verify this conjecture are in progress in our laboratories.

II. Experimental Procedures and Results

A. Experimental Studies

Electrochemical noise methods of corrosion characterization in coated metal systems are currently underway in our laboratories and they are proving valuable in providing a continuous monitoring method for following the progress of corrosion in coated panels. We are comparing these results with those from more conventional assessment techniques. Here we present some initial results from ECN data. We use the measurement circuitry of Figure 1 and the test geometry of Figure 2. 256 data points were gathered from one probe at a rate of one point every two seconds. Data was acquired for ten minutes in every 100 for each probe (ten probes in total being monitored). The coatings were alkyd primers and the area exposed was 50 cm^2.

Figure 3 shows the mean electrode potential (V_m) from noise data for two different primers over a steel panel as recorded when immersed in dilute Harrison's solution (0.35% ammonium sulphate, 0.05% sodium chloride) for five days. Probe 9 (paint with no inhibitive pigment) settles rapidly to a steady state potential, while probe 7 (paint with phosphate inhibitive pigment) initially fluctuates. Figure 4 shows the variation in mean electrochemical current (I_m) from noise data over the same time period. The mean current for probe 9 fluctuates during the first two days, then begins to steadily increase to 4×10^{-7} amps. For probe 7, coated with the same coating except that it contained phosphate as inhibitor, the current settles early on to a lower value of 1×10^{-7} amps reducing to 2×10^{-8} by the end of the experimental period. Figure 5, the "coating resistance" calculated from statistical parameters of the voltage and current noise data shows both probes behaving similarly. Within five or six hours, the "resistance" drops from a high value to a fairly steady value of around 4×10^6 ohms-cm^2. The time for this initial drop we have tentatively identified as the time for complete penetration of the film by the immersion electrolyte. For the coating with no inhibitive pigment, we visually observed considerable blistering but no corrosion products while virtually no blistering was observed for the coating with phosphate inhibitive pigment.

These data are typical of what can be generated *in situ* using ECN methods, with the *caveat* that the data portrayed here is for primer coat only; hence, the systems are much poorer in performance than one might normally encounter. In a complete, high performance coating system, these large changes in ECN data may take months to years to develop.

B. Discussion

The aim of this paper is not to discuss the results given above in detail. However we give some suggestions for improvements in the equipment that become apparent from this present work. Our experience suggests that the CML equipment is very much a prototype instrument for this application. There are a number of improvements which could be made and additional options which could be incorporated both to the hardware and to the software. These could greatly improve its usefulness, flexibility, ease of application and the precision of the results obtained for routine, *in situ* sensing of corrosion of coated metal. At present the equipment is designed to be run in just one way and the data has to be treated in just one way. There is very little flexibility in-built into either the software or the hardware to enable the experiment to be modified or to change important parameters in the way the data is acquired and treated. Also, a major loss of data occurred without warning either from the software or from the equipment manuals when we unwittingly overloaded a data storage file. Further, the inability to treat data

separately on another computer while still gathering data or the data acquisition computer is a major disadvantage.

Some suggestions for improvement we have are as follows:

1) There should be the facility to treat and inspect data gathered without needing to terminate data acquisition, *e.g.* this could take the form of running data acquisition in the background while previous data is being examined in the foreground, or automatic dumping of data from the open file to a backup file which could be accessed seperately.

2) More information should be included about file handling, file creation and file storage limitations . Also there should be automatic visual and sound warning of file overload,as loss of data on a system designed specifically to acquire data unattended is a severe problem.

3) The user needs to have separate control over data acquisition from individual probes or at least batches of three. At present whichever parameters are set for one probe apply to all probes . With twelve probes running simultaneously, there will often be a need to gather data more slowly or more frequently on some probes than on others. This is not true multiplexing as described in the system description.

There is one other possible major problem which could arise with application of this ECN method *in situ* to coated metal systems. The high resistance and low current which are the inevitable result of making measurements on paint systems, make the likelihood of recording extraneous and adventitious noise data very high. This was shown by Hardon, *et al.*[10] who used the ECN method to monitor the corrosion of reinforcement bars in concrete. Despite being conducted in a laboratory and with extensive shielding , all measurements had to be made in the evening and at night. We have also observed this in our work, with electrical equipment switching in and out elsewhere in the building causes the trace recorded by our equipment to "spike". This has affected the absolute value of R_n. We suggest that an electronic solution be sought to this problem . For example by incorporation of a control circuit which was monitored in parallel with the electrochemical circuit, any spikes in the control circuit could be subtracted automatically from the data record.

These suggestions for improvement in no way suggest that there is no value of the system. The present system has allowed us to very rapidly get "up and running " on our researches on corrosion under coatings, and has provided a very sensitive and robust research tool for monitoring multiple sample experiments. It must be taken into account that the ECN system which we are using was developed for monitoring similar locations within one site and has to be robust for use in a power station environment. However there do appear to be deficiencies in its use for coated metal systems. If the changes suggested above were incorporated it would make it a very much more flexible and useful measuring tool for both laboratory work and for on-site investigations.

IV. Future Work on Sensors

A. Introduction

To use the method *in situ* which is discussed above for obtaining ECN data, requires coated sections whose metal substrates are not in electrical contact with one another . There must also be a liquid electrolyte of some sort connecting the coated faces. If the coating is not immersed then in theory the surface conductivity provided by adsorbed species (water and ions) may enable measurements to be made. However with the present configuration the size of the electrode surfaces, and the difficulty of isolating the electrodes electrically while maintaining

them close together would prevent the acquisition of useful data under non-immersed conditions. This may be handled by either using segmented electrodes or micro-electrodes.

B. Segmented Electrodes

Techniques involving segmented electrodes are potentially a very powerful methods for *in situ* monitoring of corrosion under coatings. By segmented electrodes, we mean 8 x 2 mm steel plates separated by 50 μm Melinex film) which seem eminently suitable for various areas of power plants[11]. The use of such electrodes for corrosion sensing has been reported.[12] A specific advantage of segmented electrodes is that they do not require an external conducting environment, *i.e.*, they work under atmospheric conditions. A type of multielectrode/microelectrode/ segmented electrode approach was used in laboratory studies by McIntyre and Leidheiser[13]. It involved applying a very thin layer of metal onto a non-conducting substrate etching a grid to separate out areas , putting a p ·ot on top and connecting wires (perhaps 5 on one side, 10 on another) to the metal layer. By monitoring (DC) the resistance of each of the wires as a function of time the amount of corrosion and the *location* of the corrosion could be identified. Such an array perhaps could have application in a modified form in some specific areas of Power Station Plant.

C. Microelectrodes

1. Definitions. We also intend to explore the application of microelectrodes for sensing corrosion at the interface between a corroding metal substrate and an organic coating or in otherwise hidden or inaccessible locations. The placement of micrometer-dimensioned sensing electrodes at the substrate-coating interface or in otherwise inaccessible locations is an attractive approach for developing sensors for *in-situ* corrosion detection. The development of ECN measurement methods using micro-electrodes as the test/sensing electrode are in the planning stage in our laboratories. There are a considerable number of reasons for considering microelectrode methods for corrosion monitoring, including the problems in electrically isolating whole sections of the system under examination, less intrusive data acquisition, and various electrochemical factors.

In contrast to conventional *macro*electrodes of millimeter or greater dimensions, a *micro*electrode has at least one characteristic dimension on the order of a micrometer. Applications of microelectrodes to electrochemical measurement have increased dramatically during the last decade, a consequence of the several advantages that microelectrodes provide. The advantages of importance to future work include a) the ability to make measurements with high spatial resolution, permitting the mapping of corrosion events and the elucidation of corrosion mechanisms; b) the small current flow which minimizes the resistive (IR) drop within the measurement cell, even for highly resistive environments; c) the enhanced flux due to convergent diffusion, which leads to highly sensitive detection capability; and d) the small RC time constant of the measurement cell, which should permit access to data at higher frequencies and/or shorter times than is possible using conventional approaches. In spite of the increasing number of microelectrode applications in general electrochemical studies, there has been only very limited application of microelectrodes to the study of corrosion.

Microelectrodes have at least one characteristic dimension on the order of a micrometer or smaller and can be fabricated in a variety of geometries, including cylinder, disk, band, ring, and sphere, as well as in arrays and ensembles of such geometries.[14,15] The electrochemical behavior of such microelectrodes can differ strikingly from their macroelectrode counterparts (of millimeter dimension), depending on the size of the electrode and the time scale of the

measurement. With proper care in data acquisition and interpretation, the use of microelectrodes provides information that is of the same validity as macroelectrodes. As a matter of fact, under most experimental conditions, microelectrodes exhibit a number of measurement advantages compared to macroelectrodes. Their small size permits them to sense and sample micro-environments with a high degree of spatial resolution. This advantage has led to measurements in single biological cells[14] and to such techniques as scanning electrochemical microscopy.[16] Microelectrodes will, on time scales as short as milliseconds, exhibit voltammetric current influenced by convergent (or multidimensional) diffusion, leading to significantly enhanced current **density** compared to macroelectrodes employed under identical conditions, and some geometries give rise to steady-state current similar to that observed at macroelectrodes under hydrodynamic conditions.[13] The enhanced current density leads to lower detection limits, while steady-state behavior permits time-independent measurement. The small physical size of microelectrodes leads to two additional advantages. Firstly, the small interfacial area results in small double layer capacitance and a concomitant small RC cell time constant, permitting electrochemical measurements to be made on shorter time scales and at higher frequencies.[14] Secondly, the very small current typically observed at a microelectrode (nanoamperes to picoamperes) reduces the IR drop within a cell to negligible values, even for rather resistive cell electrolytes.[14] This small IR drop even makes possible 2-electrode measurements in resistive environments.

2. Potential Applications We intend to employ microelectrode arrays (of varying electrode sizes, numbers, and spacing) in combination with polymer electrolytes to build arrays of microelectrochemical cells on the substrate surface (eventual implantation into the substrate surface may be possible). Various organic coatings will be applied to the substrates, sandwiching the microelectrochemical cells which then become sensors of processes occurring at the substrate-coating interface. These assemblies will then be subjected to corrosion environments appropriate to the individual problem areas of hidden corrosion within large, expensive objects. The influences of the various coatings on the corrosion process will be assessed. Measurements will consist of electrochemical noise (both potential and current noise), AC impedance, and cyclic and square wave voltammetries. Such measurements at the arrays of microelectrochemical cells will provide both spatial and temporal information about corrosion mechanisms, enhancing our understanding of corrosion, and may provide the basis for eventual development of *in-situ* detection devices.

To achieve this, the following are needed:

a) The development of the strategies and methods necessary for creating arrays of disk, ring, and/or band microelectrodes (each electrode within the array being individually addressable) which can be placed beneath the organic coating of a coated substrate, the array being separated from the substrate by a thin film of a conducting polymer electrolyte. Fundamental issues to be addressed during this phase of the research include i) the optimum electrode geometry and array geometry; ii) the optimum electrode size and spacing within an array; and iii) the optimum materials used for constructing the electrodes and the polymer electrolyte. To address these issues, use will be made of the results of corrosion measurements described below, and optimization will be performed in the sense of obtaining the maximum useful information.

b) The deployment of the assemblies developed above for the study of corrosion beneath organic coatings. Electrochemical noise and impedance measurements at the individual microelectrodes will be analyzed over the entire accessible frequency range and as a function of time as corrosion

proceeds. The premise here is that each microelectrode will act as a local sensor of its immediate electrochemical environment, the corroding substrate itself serving as the counter/quasi-reference electrode. By interrogating each microelectrode and analyzing its temporal noise and impedance behavior, a two dimensional profile of the corrosion process should emerge. Particular attention will be given to features which may signal the onset of corrosion, permitting an early detection strategy to be developed. Concomitant with the noise and impedance measurements, voltammetric measurements employing cyclic and square wave techniques will be used to further characterize corrosion events and corrosion products. Products of substrate corrosion will diffuse through the polymer electrolyte and be detected by the microelectrode. Each microelectrode will detect products from its own local environment with a spatial resolution on the order of micrometers, providing geometric information about the distribution of corrosion anode/cathode pairs. Furthermore, the diffusion of external species through the organic coating may be studied, using the microelectrode array to monitor the time-dependent arrival of the species at the coating/ substrate interface and any subsequent movement of the species along the interface. The influence of such external species on corrosion processes can then be assessed.

V. Summary and Conclusions

We feel that there is significant potential in the extension of *in situ* electrochemical corrosion monitoring methods using already developed measurement techniques coupled to new electrode configurations including segmented electrodes and microelectrodes. As shown in the preliminary work described above, electrochemical noise measurement is the electrochemcical corrosion monitoring method that provides the most potential as an *in situ* measurement method. Coupling it and and the others mentioned above with microelectrode methods and other electrode designs has considerable to offer for corrosion sensor deveolopment, but will require considerable development studies to bring to practical usefulness. This is has extensive implications as shown in Fig. 6.

Acknowledgements

The authors wish to acknowledge the Office of Naval Research Grant Number N00014-93-1-0013, Dr. John Sedriks, program manager, for support of the experimental work described in this paper. We also wish to acknowledge the helpful advice and criticsm of Dr. Brian Skerry and Dr. Barry Syrett in the preparation of this paper.

Bibliography

1. B.S.Skerry, D.A.Eden, "Electrochemical Testing to Assess Corrosion Protective Coatings", **Prog. Organic Coatings, 15**, 269-285 (1987).

2. G.P. Quirk, P.E. Doherty, D.A.Eden, & W..M. Cox, "Corrosion Monitoring Developments for Steam Generators in Ontario Hydro," *Conf. on Steam Generators & Heat Exchangers*, Toronto, 1990

3. P.E. Doherty, D.C.A. Moore, W..M. Cox & J.J. Dawson, "An Application of Advanced Electrochemical Monitoring to Corrosion of Heat exchanger Tubing," *4th Int. Symp. Environmental Degradation of Materials in Nuclear Power Systems-Water Reactors*, Jekyll Island, GA August 1989

4. W.Y. Mok, D.C.A.Moore, W.M.Cox & B.C.Syrett, "On-Line Electrochemical Corrosion Assessment of Materials for FGD Outlet Ducts," *Proc. of the 1992 Air Pollution Seminar*, Orlando, FA, Nov. 1992

5. D.M. Farrell & W.M.Cox,"Multisystem Corrosion amonitoring in a Condensing Flue gate: Phase 2," **EPRI Report GS-7540**, Oct. 1991

6. Private Communication, D.A. Eden, Jan. 1993

7. Eden, D.A, M.Hoffman, and B.S.Skerry, "Application of Electrochemical Noise Measurements ro Coated Systems," **ACS Symposium Series, No.322,** *Polymeric Materials for Corrosion Control,* R.A.Dicke & F.L.Floyd, eds.,ACS (1986)

8. Chen, C.T., & B.S.Skerry, " Assessing the Corrosion Resistance of Painted Steel by AC Impedance and Electrochemical Noise Techniques,"**Corrosion, 47** (1991) 598-611

9. Skerry, B.S.; Eden, D.A., "Characterisation of coatings performance using electrochemical noise analysis", **Prog. Organic Coatings, 19**, 379-396 (1991).

10. Hardon, R.G., Lambert, R., and Page, S.L., "Relationship Between Electrochemical Noise and Corrosion Rate of Steel in Salt Contaminated Concrete," **Br. Corros. J.,23** (1988) 225-228

11. M. Camina, M. Chauhan, C. Florence, H. Mendoza, D.J.Mills, A. Sherwood, T. Shuker, J. Sykes,and S. Turgoose, Paint Research Association Technical Report, TR/2/91 (1991), PRA, Teddington, UK

12. S. Feliu, J.M.Bastidas & M. Morcillo, "Corrosion Monitoring of Coated Steel Using A 'Multi-layer Sandwich' Cell," **J.Oil Colour Chem. Assoc., 1985, 133-36**

13. J.F.McIntyre & H. Leidheiser, "Resistance Measurements on Thin-Film Substrates as a Technique for Studying the Deterioration of Coated Metals," **I&EC Prod. Res. & Dev., 24** (1985) 348-53

14. M. Fleischmann, S. Pons, D.R. Rolison and P.P. Schmidt (Eds.), *Ultramicro-electrodes*, Datatech Systems, Morganton, NC, 1987.

15. R.M. Wightman and D.O. Wipf, *Electroanalytical Chemistry*; A.J. Bard, Ed.; Marcel Dekker, Inc.; New york, 1989 Vol. 15, 268.

16. A.J. I ard, F.-R. Fan, D.T. Pierce, P.R. Unwin, D.O. Wipf, and F. Zhou, **Science, 254** (1991) 68.

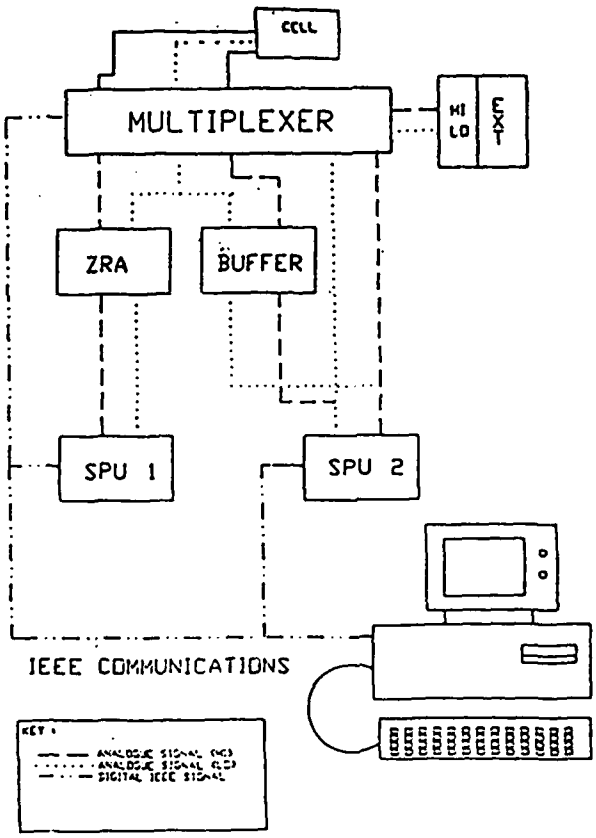

Figure 1: Block Diagram of the Electrochemical Noise Monitoring Instrumentation

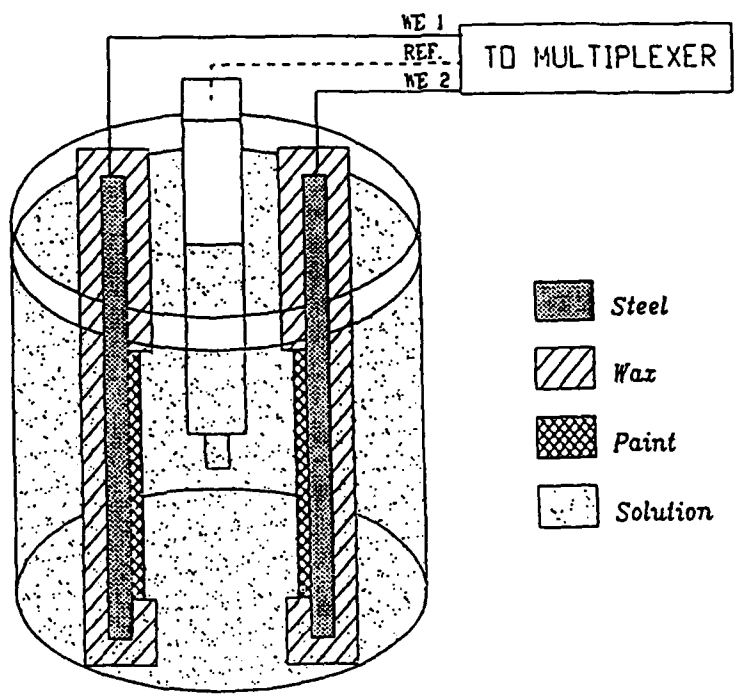

Figure 2: Cell Arrangement for Measuring Electrochemical Noise

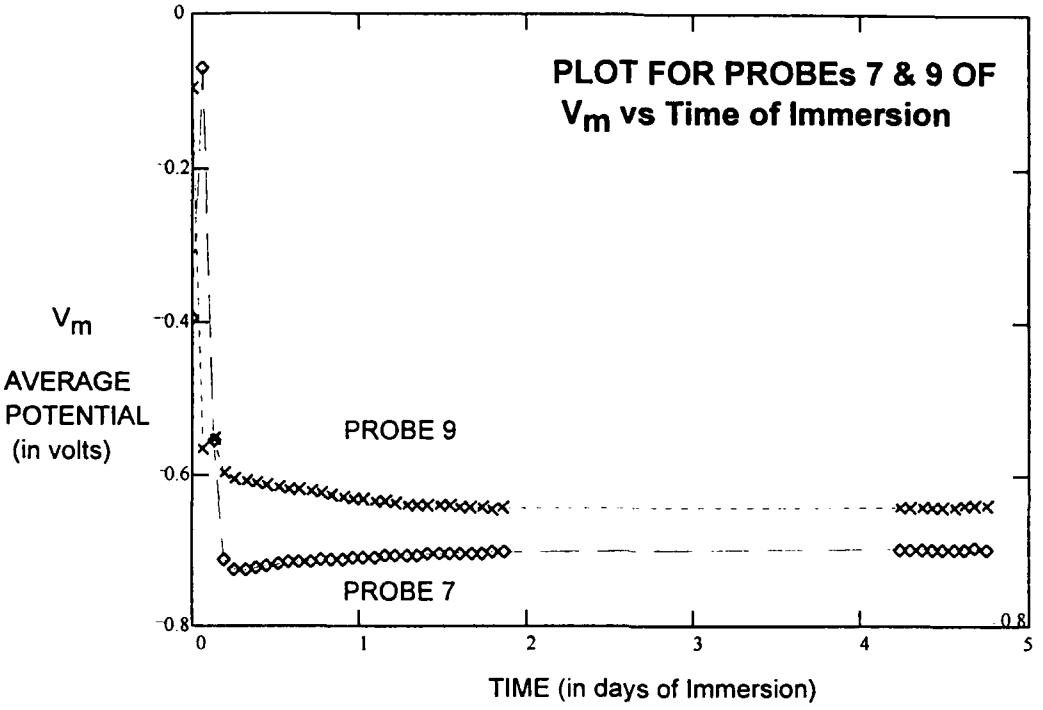

Figure 3. Plot for Probes 7 and 9 of V_m against time of immersion

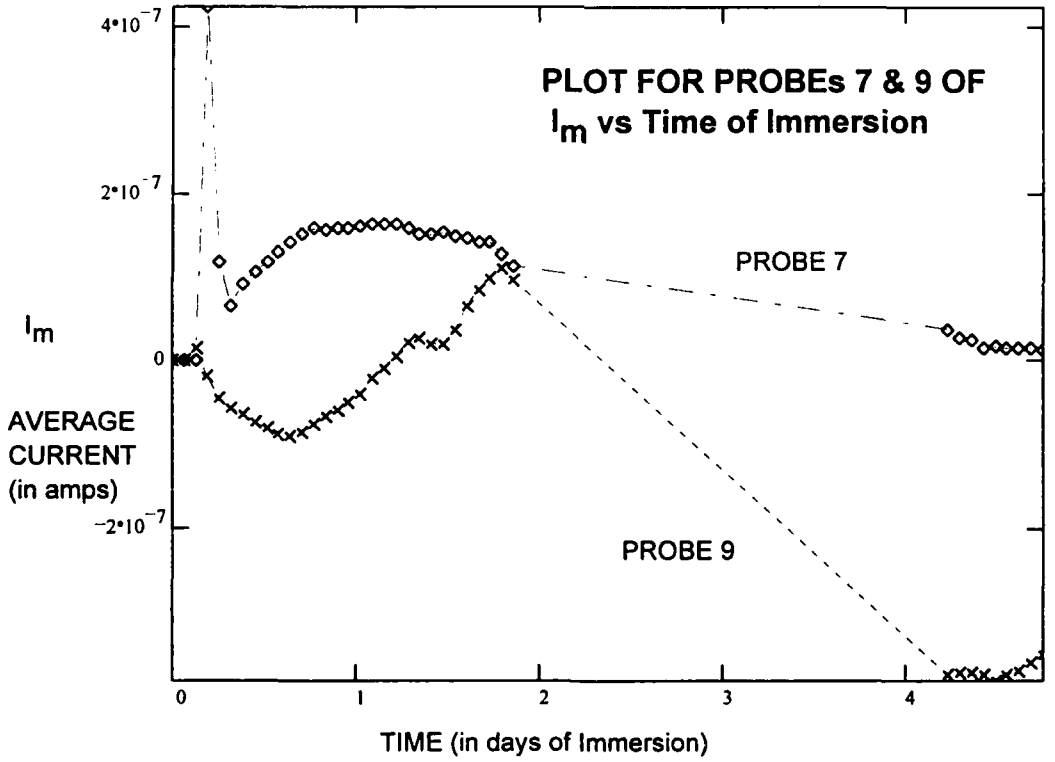

Figure 4. Plot for Probes 7 and 9 of I_m against time of immersion

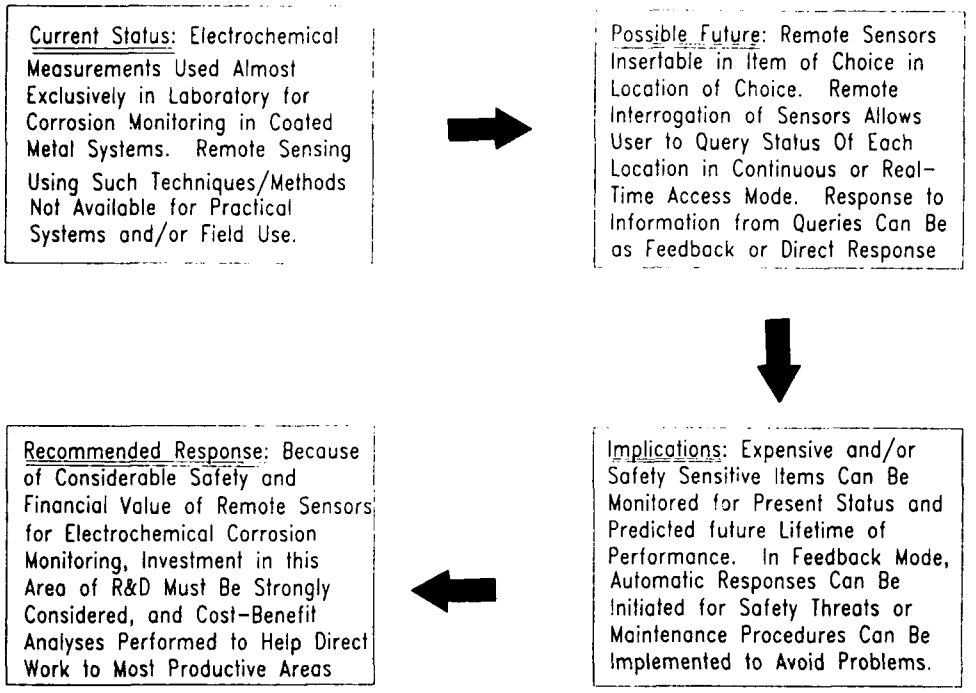

Figure 6. Pertinent Considerations for Electrochemical Corrosion Sensors

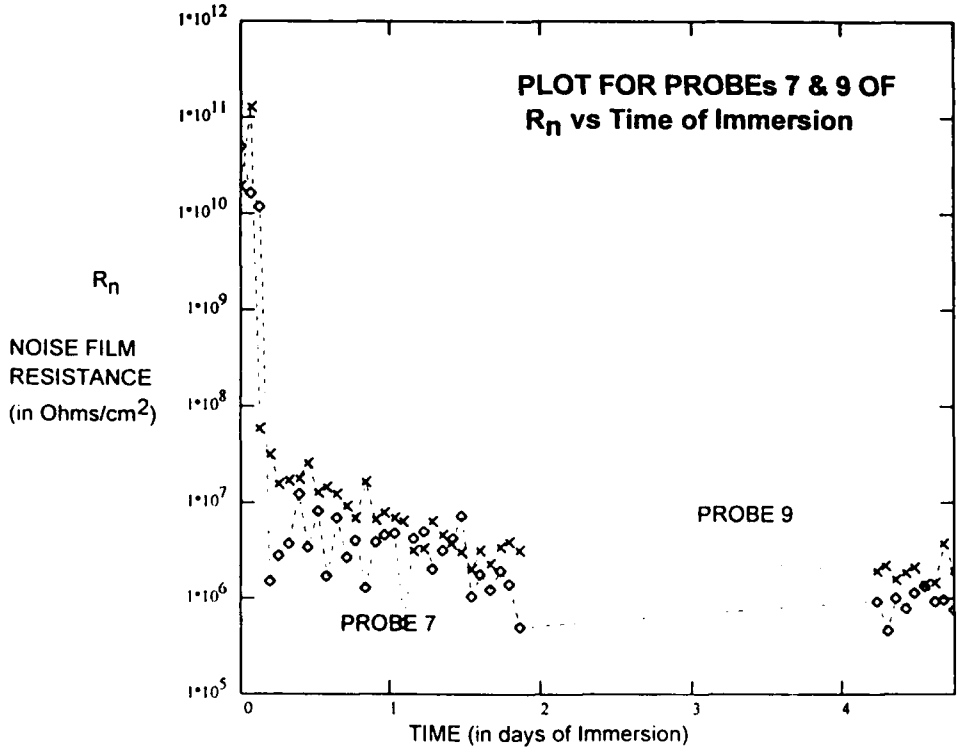

Figure 5. Plot for Probes 7 and 9 of R_n against time of immersion

Simultaneous Rig Investigations of Electrochemical and Chemical Corrosion of Low Carbon Steel in Feedwater with Oxygen and Ammonia

Anatoly M. Sirota
All-Russia Heat Engineering Institute
14/23 Avtozavodskaya Str.
1Ø928Ø Moscow Russia

Vyacheslav I. Latunin
All-Russia Heat Engineering Institute
14/23 Avtozavodskaya Str.
1Ø928Ø Moscow Russia

Vladimir E. Donnikow
All-Russia Heat Engineering Institute
14/23 Avtozavodskaya Str.
1Ø928Ø Moscow Russia

Abstract

Most on-line corrosion rate monitores are designed for electrochemical applications and their readings are trustful if the corrosion process is of the electrochemical nature. In order to indentify corrosion mechanism systematic rig investigations of low carbon steel corrosion in the stream of demineralised water with oxygen and ammonia at 15Ø C were undertaken. The electrochemical and weight loss corrosion rates were measured simultaneously on the same specimen exposed for 1Ø hours.The specially developed equipment for obtaining galvanostatic polarisation curves for deionised water flow in the earthed pipes is based on the known method of short-term interruption of the polarisation current. In contrast to widely spread opinion, the chemical mechanism of corrosion has been shown to be predominant both for neutral and ammoniated feedwater. The rate of electrochemical mild steel corrosion as defined from the polarisation curves at 3Ø ppb oxygen is two orders of magnitude lower those determined by the weight loss measurements for the same specimen.

It is widely recognized that the power plant equipment made of carbon steel undergoes in an aqueous medium electrochemical corrosion. In contrast to this opinion the VTI investigations have shown that the chemical mechanism of corrosion is predominant in deionized water flow. For chemical corrosion there is no relationship between the electrode overpotential and polarizing current supplied from an external source. As a result, on-line corrosion rate monitors based on all kinds of polarization techniques are useless for chemical corrosion detection. In order to compare electrochemical and chemical corrosion, the polarization and weight-loss corrosion rates, K_e and K , were measured in the same rig experiments using the same specimens.

The water is supplied from the VTI Experimental plant where ammonia - hydrazine water chemistry regime is applied. The plant's feedwater is additionally passed through the ion-exchangers at the rig whereupon gaseous oxygen and/or ammonia are dosed. The electric conductivity past the rig's ion-exchangers q at 25 C is Ø.Ø65 - Ø.11 μS/cm, the flow velocity near the specimen - Ø,7 m/s, the exposure time - 1Ø hrs, the temperature in the most of measurements - 15Ø C (the temperature of the maximum corrosion-product release for carbon steel). The cylindrical specimens made of carbon steel (the main elements, %: Ø,2ØC, Ø,38Mn, Ø,24Si, Ø,Ø4S, o,14P) are used. Before the test the specimens are degreased, polished by three types of emery paper on a lathe and stored for a day in a desiccator over silica gel. Corrosion behavior is established in two ways: from initial, scaled and descaled weights and from the polarization curves. The known method of short-term interruption of the polarization current was applied to eliminate ohmic voltage drop in the electrolyte - the main constraint for electrochemical measurements in weakly conducting media,such as deionized water. Upon

breaking the circuit,ohmic voltage drop disappeares practically instantaneously, while the electrode potential changes rather slowly and can be measured. The VTI-developed equipment for obtaining galvanostatic polarization curves for weakly conducting media flow in the earthed pipes is based on the "storage condenser" concept. The specimen is one of the electrodes of the electrochemical cell (the studied electrode, SE, Figure 1). It is installed axially with auxiliary electrode, AE. The variation in the electrode potential under current (polarization) is measured with reference to an intermediate electrode, IE - a small thin ring. The AE and IE electrodes are made from stainless steel. Before the start of polarization and at the end of the experiment the potential of IE is measured with reference to a glass electrode RE. The difference in potentials between SE and IE is measured by the storage condenser. It is connected with SE for 2Ø mS upon breaking the external current circuit, then the command unit switches on the polarization circuit and the voltage of the storage condenser is measured.The unsteady polarization curves (each value of E being held for 5 min.) were used for evalution of corrosion current by extrapolation in semilogarithmic coordinates.

In Figure 2 the corrosion current calculated from weight measurements K is compared with anodic polarization curves. It is obvious that $K >> K_e$. The discrepancy is the largest at 2Ø ppb oxygen: K and K_e are about 6ØØ and 5 $mg/m^2 h$, respectively, with up to 9Ø % K being the corrosion-product release. This result is uncommon: from the literature it is known (1) that an excellent correspondence was achieved between K_e and K for carbon steel exposured for 5ØØ hrs at 29Ø C in stagnant water (q at 25 C and 29Ø C are Ø.5 and 2Ø $\mu S/cm$). For verifying the possible K(q)-dependence we conducted the tests in plant's feedwater with cation q 1$\mu S/cm$ (2) and deionised water with ammonia dosed in it. Ammonia

increases the K in both cases, especially in feedwater,while K_e does not change considerably. The K-oxygen concentration curve shows a maximum, with the oxygen concentration at maximum being water electrical conductivity dependent.

These new findings should be taken into account when on-line corrosion rate electrochemical monitores are used.

References

1.B.E. Wilde,Corrosion - NACE, 53 (1967): p.379.

2.A.M. Sirota,V.I. Latunin,Teploenergetica, 39 (1992): p. 51.

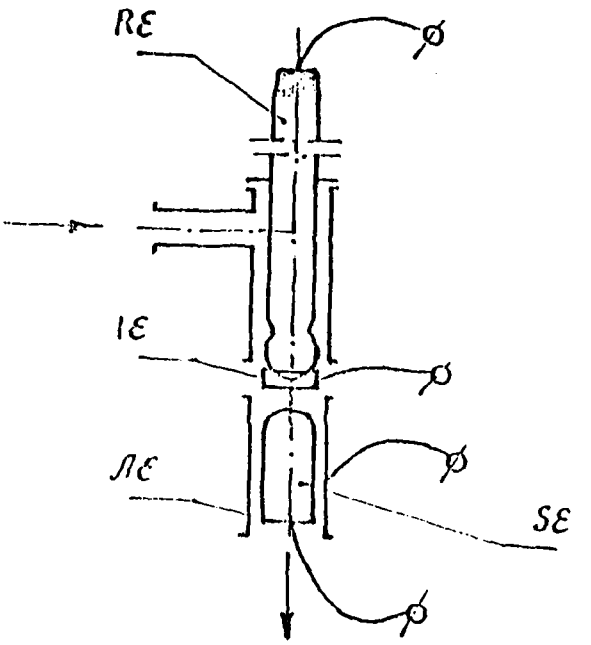

Fig. 1. Electrochemical cell: SE - studied electrode, AE - auxiliary electrode, IE - intermediate electrode, RE - reference glass electrode.

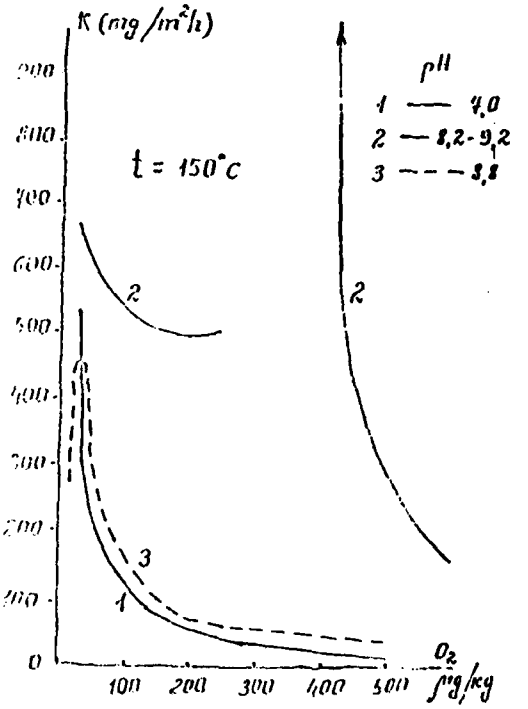

Fig. 2. Corrosion rate of carbon steel in deionised (1,3) and feedwater (2).

Electrochemical Sensors For Application to Boiling Water Reactors

ME Indig
GE Nuclear Energy
Vallecitos Nuclear Center
P. O. Box 460
Pleasanton, CA 94566

Abstract

An effective measure in combating the intergranular cracking of stainless steel in Boiling Water Reactors (BWRs) is the control of the electrochemical corrosion potential (ECP). It has been found that when the ECP of austenitic stainless steel alloys susceptible to cracking is decreased below -0.230 V(SHE) cracks will not initiate. Similarly, the decrease in potential decreases crack growth rate of existing cracks. Decrease of the potential to acceptable values is accomplished by addition of hydrogen to the reactor feedwater. The amount of hydrogen required is determined by the ECP measured at high temperature either in-situ or from a water sample delivered to an external monitoring station.

Both reference and metal sensor electrodes are required to determine the ECP. A multiplicity of reference electrodes are used to verify the validity of the measurements. The reference electrodes, Ag/AgCl, the yttria-stabilized ZrO_2 sensor and the platinum electrode are designed for either remote, high radiation environments or accessible monitoring installation at plant operating temperatures. In the former application the support structure for the electrochemical sensor is fabricated from ceramics, usually sapphire, and ceramic-to-metal brazes are used for seals. Metal-to-metal seals are welds. For accessible installations high temperature elastomeric seals are used as long as some periodic maintenance is possible. Just as the reference electrodes are designed for remote or accessible installation, the metal sensor electrodes, principally stainless steel, can be manufactured with ceramic-to-metal brazes or elastomeric seals. The complete electro-chemical package, with data acquisition system, is then used by plant personnel to control the feedwater H_2 injection rate for environmental crack mitigation.

Key terms: High temperature electrochemical measurements, reference electrodes, stress corrosion cracking

Introduction

The normal chemical constituent in Boiling Water Reactors (BWRs) is high purity water at temperatures from 275°C to 290°C. Due to radiolysis reactions in the reactor core, the water contains dissolved O_2, H_2, H_2O_2, and other oxidizing and reducing radicals. Depending on the specific location within the reactor vessel or the recirculation piping system, the concentration of the above species will vary, as well the resultant electrochemical corrosion potential. Because of the low concentration and short half life of the free radicals, it is considered that the main contributors to the electrochemical potential are the O_2, H_2O_2 and H_2.

If the materials in the BWR are in a susceptible metallurgical condition, and in the presence of a tensile stress, the normal BWR environment is sufficiently oxidizing to initiate intergranular stress corrosion cracking (IGSCC) or irradiation assisted stress corrosion cracking (IASCC) of BWR components. The metallurgical condition responsible for IGSCC is classical sensitization (chromium depleted grain boundaries). IASCC can occur after sufficient neutron radiation exposure has accumulated, $>5x10^{20}$ n/cm^2.

Over the years improved power plant practices have resulted in a decrease in reactor water conductivity from about 1.0 to <0.3 μS/cm in today's operating BWRs, as shown in Figure 1. While this improvement has undoubtedly decreased crack growth rates of austenitic stainless steel, the improvement has not been sufficient to eliminate the cracking. However, if the benefits of improved conductivity can be combined with control of the electrochemical potential, it is possible to mitigate both IGSCC and IASCC.

It has been found in laboratory and in reactor tests that at potentials <-0.230 V(SHE) intergranular cracks in austenitic stainless steel do not initiate, and existing cracks have extremely low propagation rates. The application of electrochemical control in BWRs involves injecting hydrogen into the reactor feedwater system. Just as radiation can produce oxidizing conditions, hydrogen addition with high radiation levels can decrease the concentrations of O_2 and H_2O_2, and thus lower the electrochemical potential of reactor components. However, if we are to control the electrochemical potential as a crack mitigation technique, we must have a method of measuring this parameter.

Electrochemical Measurements in BWRs

The simplest method of measuring the electrochemical potential is the routing of aqueous samples via sampling lines to a test vessel (autoclave) located outside the reactor vessel. This approach has been used in determining hydrogen injection rates required to protect the recirculation piping. Generally, a family of different reference electrodes are

installed in the autoclave. These include silver/silver chloride, $Cu/Cu_2O/ZrO_2(Y_2O_3)$ and platinum reference electrodes. Each reference electrode responds to a different electrochemical reaction (potential determining species) and their electrochemical potential can be calculated on the standard H_2 electrode (SHE) scale. These calculated values compared to the SHE at temperature are shown in Figure 2. By measuring the difference between any pair of reference electrodes and comparing the measured value to the theoretical potential difference from Figure 2, a high temperature verification of the validity of the reference electrodes is obtained. It should be pointed out that the zirconia and platinum electrodes are pH sensitive. For each unit change in pH at 275°C the potential will change by 0.108V according to the Nernst equation. However, in high temperature, high purity water, such as in a BWR, the increased dissociation of water results in only a small pH variance of 5.65 to 5.68 in the range of interest (250°C to 290°C). The platinum electrode potential also shifts with hydrogen concentration; thus the dissolved hydrogen in the reactor water should be known or measured. However, in the dissolved hydrogen concentration ranges of interest for BWR applications, Table 1, shows that errors in measuring or estimating the hydrogen concentration are not a significant contributor to platinum electrode potential uncertainty. Hence, both the stabilized zirconia electrode and platinum electrode can be used as reference electrodes for electrochemical measurements in BWR circuits as long as the pH remains moderately constant.

Typical standard reference electrodes for autoclaves are shown in Figures 3, 4, and 5. Each electrode is joined to a standard Conax insulating and sealing gland, which allows the electrode lead wire to pass from the high pressure internal autoclave location to the ambient and provides the pressure barrier seal for the electrode.

The corrosion potential is determined by the potential difference between a stainless steel surface and one of the reference electrodes. The measured potential is then converted to the potential on the SHE scale by adding (with the proper sign) the specific potential of the reference electrode on the SHE scale, shown in Figure 2, to the measured potential. For example, consider that the measured potential between stainless steel and the Ag/AgCl reference is -0.100 V at 275°C. Figure 2 indicates that the Ag/AgCl potential on the SHE is 0.192V. Then the potential of stainless steel on the SHE scale is -0.100+ 0.192=0.092 V(SHE). In the example, the stainless steel surface could be a stainless steel electrode or the autoclave. Since the autoclave is grounded, any conventional electrical ground can serve as the electrical connector. If a stainless steel electrode is used, then the electrode is of the same design as the platinum sensor shown in Figure 3, except that the metal sensing tip is now fabricated from stainless steel. The stainless steel electrode should be prefilmed in the laboratory for at least two weeks in normal BWR water chemistry, or in the field until the measured potential is 0.0 V(SHE) or higher. If prefilming is not performed, one may expect the corrosion potential of the stainless steel to rise by about 0.4V over a two week period as the film is formed in the field. This will create significant uncertainties on the stainless steel potential.

In-situ Measurements

The best way to eliminate possible sample line effects in measuring electrochemical potential is to perform the measurements in-situ. However, for this approach the design and manufacture of reference and metal sensor electrode had to be mechanical and radiation hardened. In high radiation regions Teflon is unstable. Thus the application of Teflon for compression seals, electrode bodies, or insulation had to be eliminated. The replacement insulator material chosen was sapphire. In place of the elastomer compression seals, ceramic-to-metal braze seals and metal-to-metal welds were used. The materials, including the ceramic-to-metal brazes had to be resistant to corrosion or dissolutions in high temperature water, both in the recirculation piping system and in the high radiation core region.

In an analogous fashion to the autoclave application, the Ag/AgCl, platinum and the $Cu/Cu_2O/ZrO_2$ sensors have been adapted to the more severe service environments. Figure 6 showed the Ag/AgCl sensor. The potential determining reaction occurs inside the sapphire container. The electrolytic contact to the environment is maintained by the circumferential aqueous path around the sapphire crucible cover. It is important to maintain close tolerance between the cover and the crucible to minimize mass transport in and out of the crucible. In order to fix the cap to the crucible, metal straps (not shown) are fitted to slots at the top of the cover, and are then spot welded to the stainless transition piece described below.

The wire lead in the crucible must make electrical contact to the Ag/AgCl element and must be sealed so that no water leak path exists to the compartment below. This compartment is made up of the bottom of the sapphire crucible and a Kovar tube braze to the O.D. of the sapphire. Kovar was chosen because of the compatability of thermal expansion properties to sapphire and its corrosion resistance. The Kovar tube is welded to a stainless steel transition piece, which is then welded to the collar of the Al_2O_3 insulated coaxial cable. The Al_2O_3 insulated cables are the usual signal carriers used for neutron detectors in the reactor core region.

The platinum reference electrode is shown in Figure 7. The platinum sensing cap is brazed to one end of the sapphire insulator and the Kovar skirt to the opposite end. A stainless steel transition tube is welded on one end of the skirt and on the other end to the collar on the insulated coaxial cable. The nickel conductor wire is electrically joined by brazing to the underside of the platinum sensing cap and passes through a hole in the sapphire insulator. The wire then passes through the Kovar skirt and stainless steel transition tube and is joined to the central conductor wire in the Al_2O_3 insulated coaxial cable. In place of the platinum, a stainless steel cap could also be brazed to a sapphire insulator to form a stainless steel electrode.

The zirconia sensor is shown in Figure 8. A number of dry oxide/metal mixtures can be used to develop a stable electrochemical potential. In the present example, the mixture is Cu/Cu_2O and the potential is determined by the reaction: $Cu_2O+2H^++2e \Leftrightarrow Cu+H_2O$. Electrochemical potentials of the reaction have been calculated as a function of temperature for the pH appropriate to BWR operation.

The zirconia tube is packed with the proper dry mixture of about 50% oxide and 50% metal by weight. The conductor wire is buried in the mix and a Kovar tube is brazed to the open end of the zirconia tube. The general construction is quite similar to construction of the Ag/AgCl and Pt sensors discussed above.

In the present in-situ installations, just the Ag/AgCl and platinum reference electrode have been used as reference electrodes. In most cases the stainless steel potential is obtained from the voltage between electrical ground and the appropriate reference electrode. The concept for this measurement is that the ground connection functions as a lead wire connected to the grounded region that is in close proximity to the reference electrode. Just as the ground connection was used to measure the autoclave potential in the external sampling system, in this case, the ground measures the stainless steel housing in the immediate vicinity of the reference electrode.

In-Situ Testing Arrangements

A typical arrangement of reference electrodes in the reactor core region is shown in Figure 9. The sensors are placed inside a stainless steel tube that usually contains just the neutron detector for monitoring reactor power. The housing is referred to as a local power range monitor (LPRM) housing. Holes at the bottom and top of the housing allow reactor water to flow through the length of the LPRM at a velocity of about 1.0 m/s. In most of the recent installations there is room for just five electrochemical sensors. The split of sensors is either three in the bottom and two near the top of the LPRM, or the reverse. In some of the earlier tests there were questions concerning whether platinum could be used as a reversible hydrogen reference electrode, especially for the upper LPRM location. It was thought that even with excess hydrogen concentration, radiolysis reaction might result in excess oxidizing species, which could polarize the platinum positively. However recent results given in a subsequent section indicate that platinum can function as a reversible hydrogen reference electrode in BWR in-situ applications.

Results

It is not the purpose of this paper to present detailed experimental results. Instead, the highlights of the most recent studies in the core region of a BWR will be reported, where the electrochemical sensors described in this paper were applied.

Figures 10 and 11 show some of the in-core electrochemical results obtained from an LPRM installed in the J.A. FitzPatrick BWR in New York State. These measurements were obtained during a hydrogen ramping test in July 1991, and are for two elevations in the LPRM. The location of the upper two sensors was just below the top fuel guide and the lower location was below the active fuel. The Gnd notation indicates the stainless steel LPRM in the immediate vicinity of a specific Ag/AgCl reference electrode, noted by either **T**Ag or **B**Ag. The letter **T** indicates one of the two top Ag/AgCl sensors. The letter **B** indicates one of the two bottom Ag/AgCl sensors. Clearly the stainless steel ground positions in the vicinity of the reference electrode in both measuring positions responded to the hydrogen injection by indicating a decrease of electrochemical potential. Also, it was evident that when the hydrogen injection was interrupted, the potentials returned to the steady state normal BWR water chemistry values.

As expected, the decrease of electrochemical potential with hydrogen injection was greater at the lowest locations. Thus, it required about 35 and 90 SCFM hydrogen injection in the feedwater to achieve -0.230 V(SHE) for the lower and upper locations respectively. This is shown in Figure 12. To relate injection rate to the feedwater hydrogen concentration, it is necessary to know that 1 ppm dissolved H_2 = 33 SCFM H_2. However, this conversion factor varies for each BWR, depending on the feedwater flow rate.

The question concerning the validity of the platinum as a reversible hydrogen reference and the validity of the high temperature electrochemical measurements in general was answered early in the FitzPatrick test program. Figure 13 shows the behavior of platinum and stainless steel in the lower and upper LPRM locations during a brief hydrogen injection shortly before the main hydrogen ramping program. The platinum ECP measured with the bottom Ag/AgCl sensor is shown as BPt(BAg1). The platinum potential is seen to drop dramatically, and its potential measured against the Ag/AgCl, is close to the theoretical potential, which provided confidence in the behavior of both reference electrodes . Much smaller, but understandable potential decreases occurred at the stainless steel ground locations.

During February and March 1992, a hydrogen water chemistry (HWC) demonstration was conducted at an overseas BWR. In this program, both platinum and Ag/AgCl sensors were installed in the upper and lower LPRM positions. Figure 14 shows the behavior of the two platinum sensors with hydrogen injection. When these measured values are compared with the calculated voltages of reversible hydrogen electrodes under the specific operating parameters of partial pressure of H_2, pH and temperature, the agreement was excellent. These in-reactor measurements provided confidence on the use of both platinum and Ag/AgCl reference electrodes in BWRs for HWC applications. In addition, these measurements provide a critical criteria for environmental cracking prevention of reactor components.

Future Directions

One purpose of performing electrochemical measurements in the BWR circuit is to provide operating and predictive criteria for crack growth control. Figure 15 shows a possible arrangement of ECP sensors in various accessible sections in the BWR circuit. Measurements obtained from these sensors would permit the quantification of hydrogen injection requirements throughout the system. While the feedwater hydrogen requirements will vary, at least the requirements for non-easily replaceable components could be determined.

Finally, to obtain ECP measurements for at least a fuel cycle (18 months), reference electrodes are being life tested that have improved metal-to-ceramic seals and more corrosion resistant materials. Moreover, electrodes are also being designed and developed based on newer concepts and newer materials in an attempt to continually improve the ECP electrode product line.

The Effect of H_2 Concentration on the Potential of the Platinum-H_2 Reference

271°C, Neutral Water

	H_2 ppb	H_2 atm
1)	200	0.0311
2)	150	0.0233
3)	100	0.0156
4)	50	0.0078

1)	-0.529 for 200 ppb
2)	-0.522 for 150 ppb
3)	-0.513 for 100 ppb
4)	-0.496 for 50 ppb

$E = E_O - (.108)(5.65) - 0.054 \log H2 (atm)$

Table 1

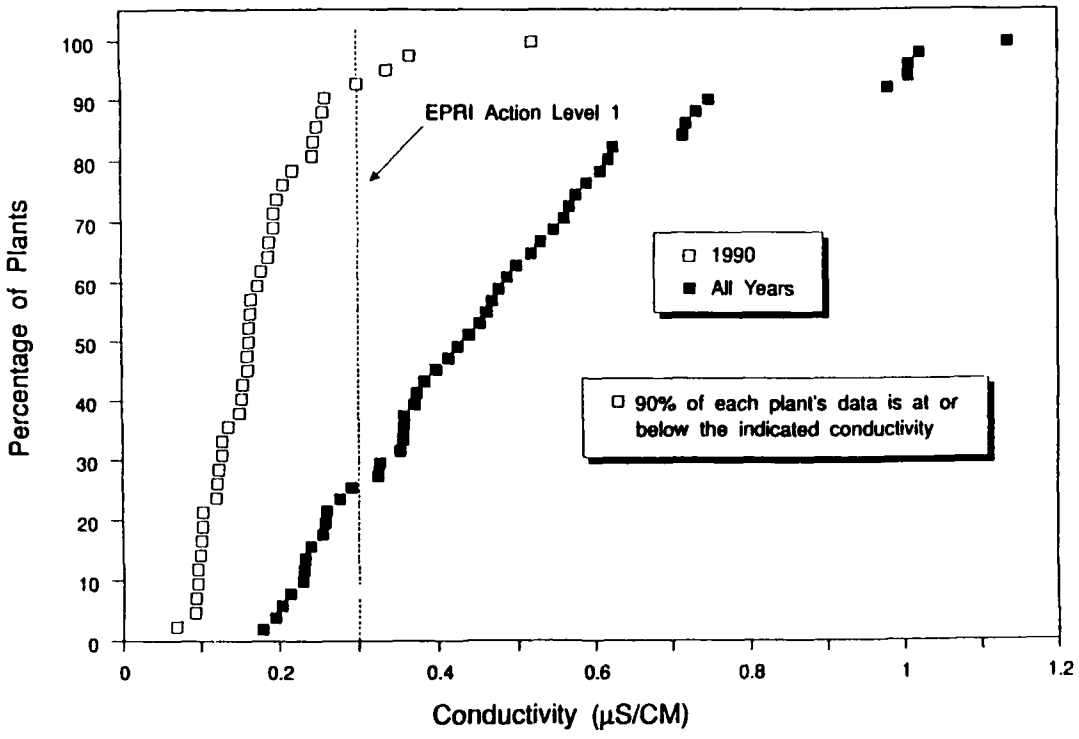

Figure 1 GE BWRs
Reactor Water Conductivity

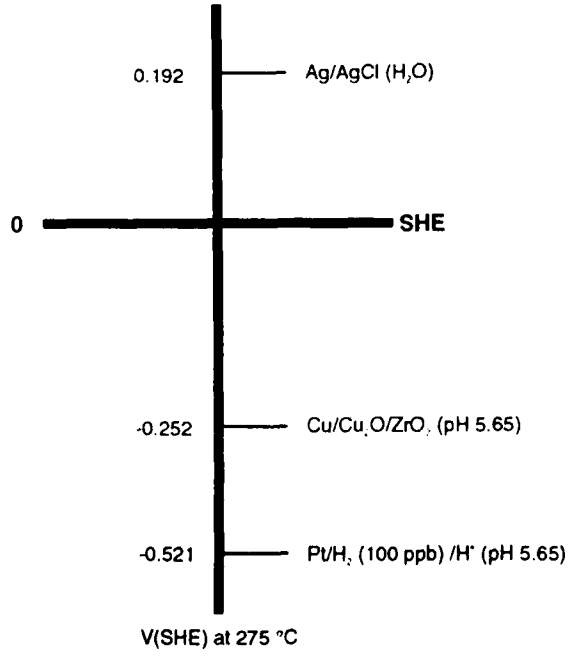

Figure 2 ECP of Reference Electrodes

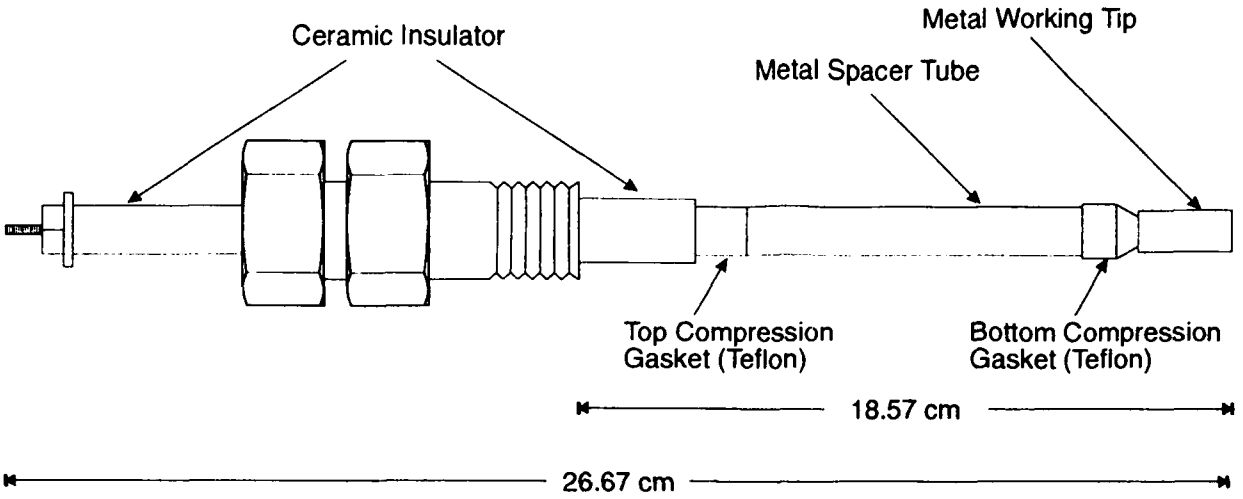

Figure 3 Pt Sensor

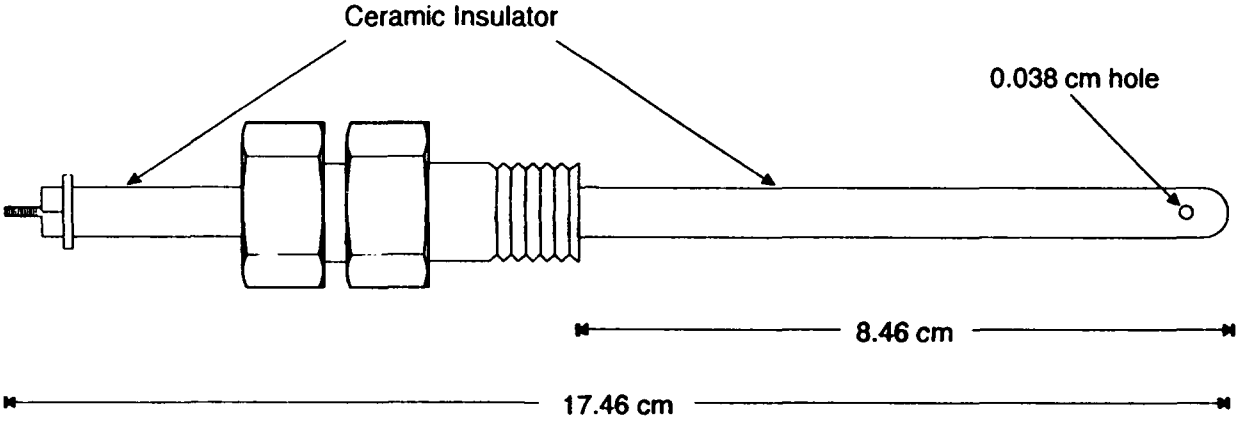

Figure 4 Ag/AgCl Sensor

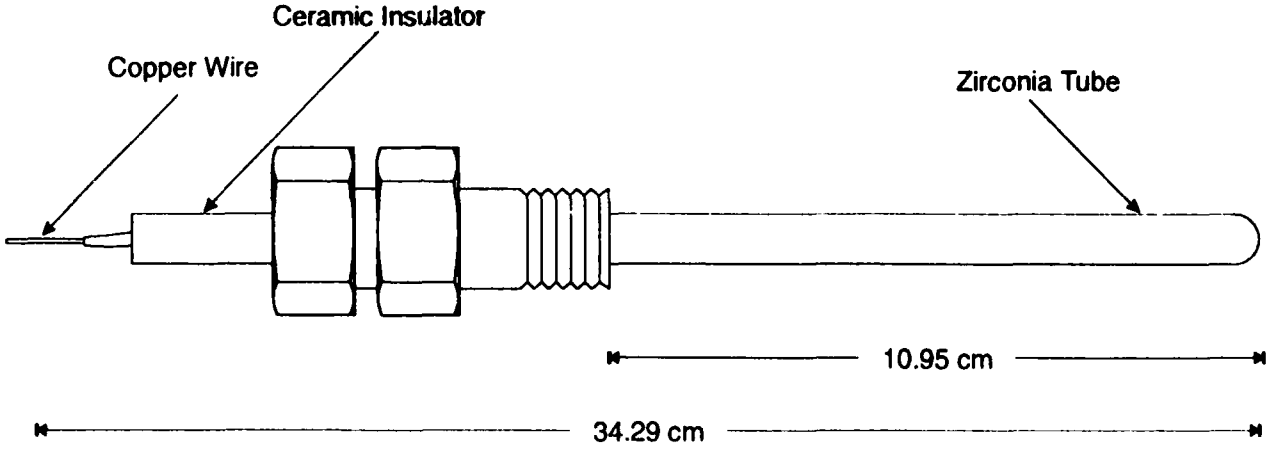

Figure 5 $Cu/Cu_2O/ZrO_2$ Sensor

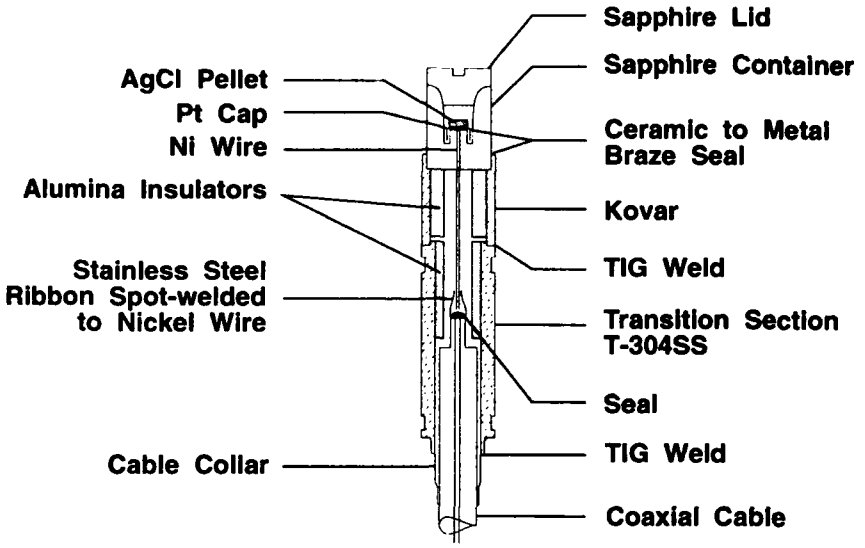

Figure 6 Ag/AgCl Reference Electrode

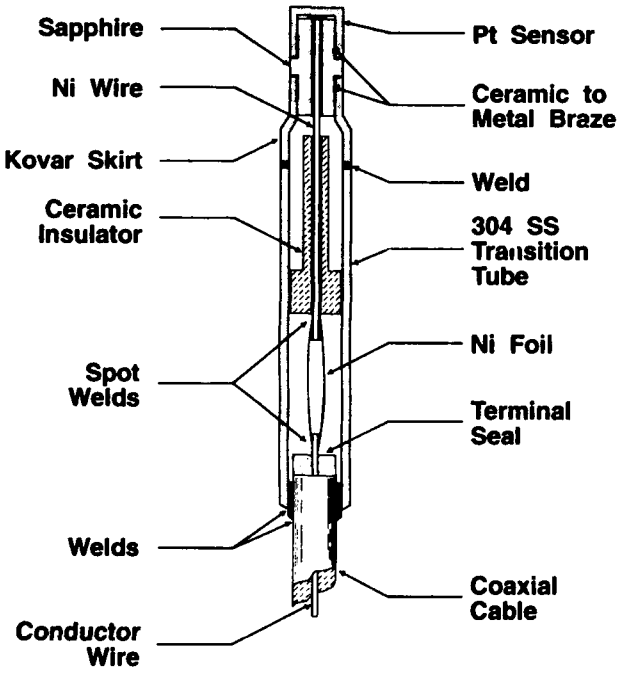

Figure 7 Micro-Cap Sensor (Pt,SS)

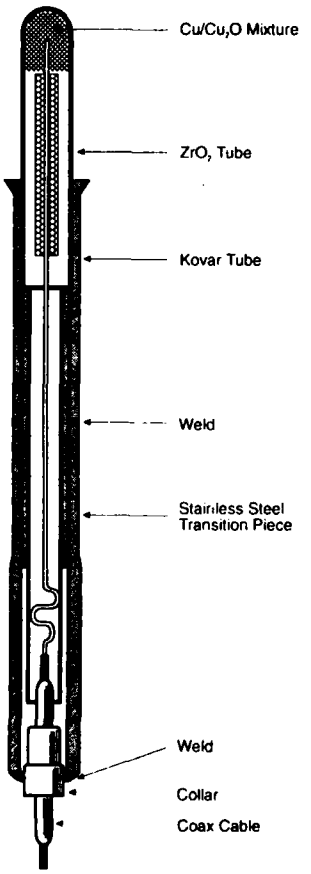

Figure 8 Cu/Cu_2O Sensor
Brazed Construction

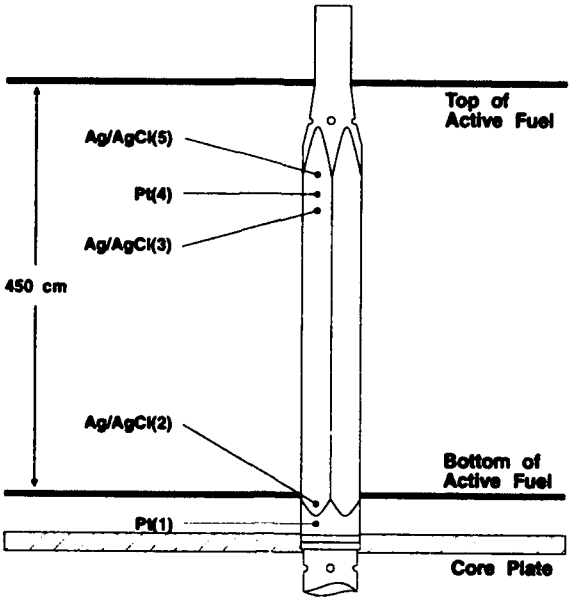

Figure 9 Location of ECP Sensors

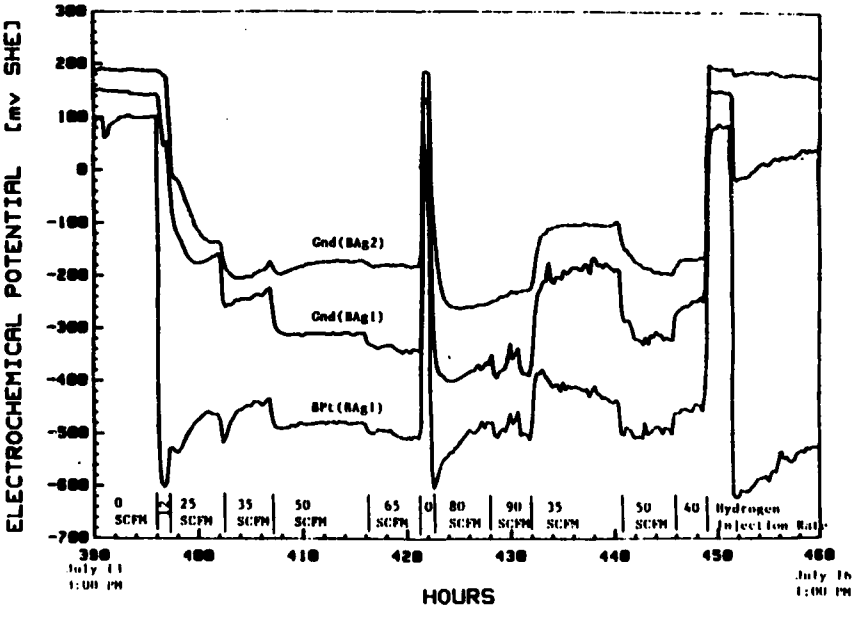

Figure 10
Corrosion Potentials from Lower In-Core Position

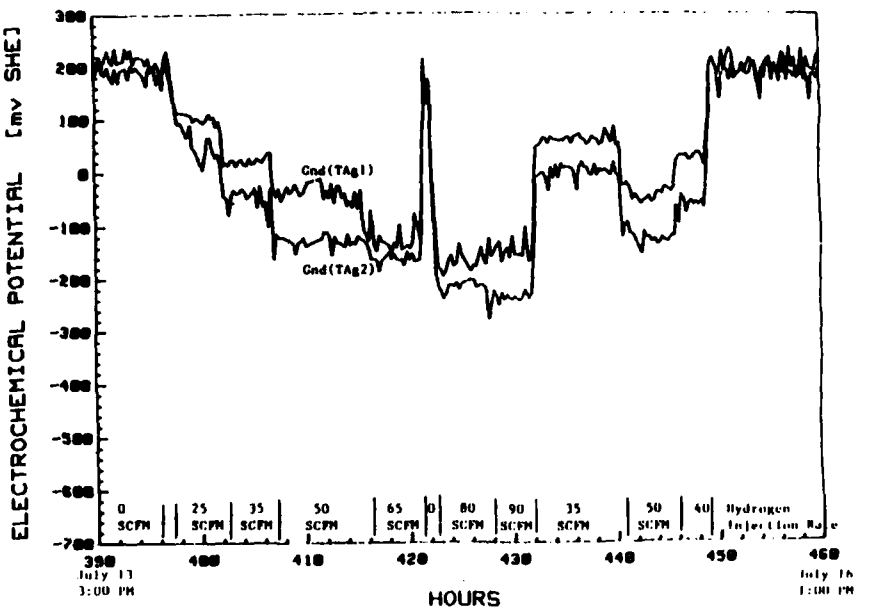

Figure 11
Corrosion Potentials from Upper In-Core Location

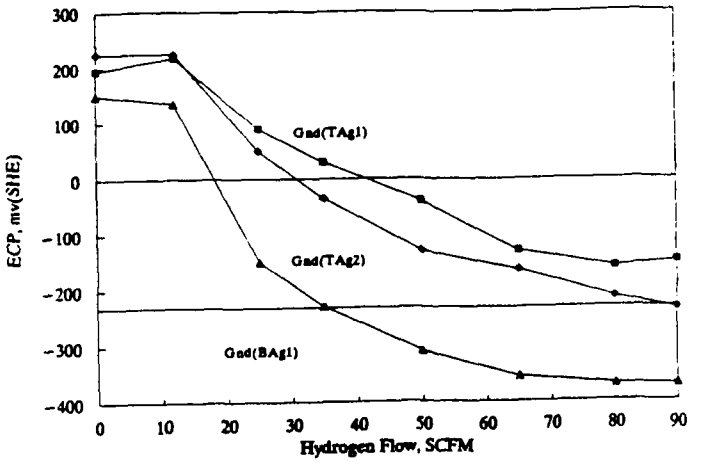

Figure 12
In-Core 304 SS Potential vs Feedwater Hydrogen

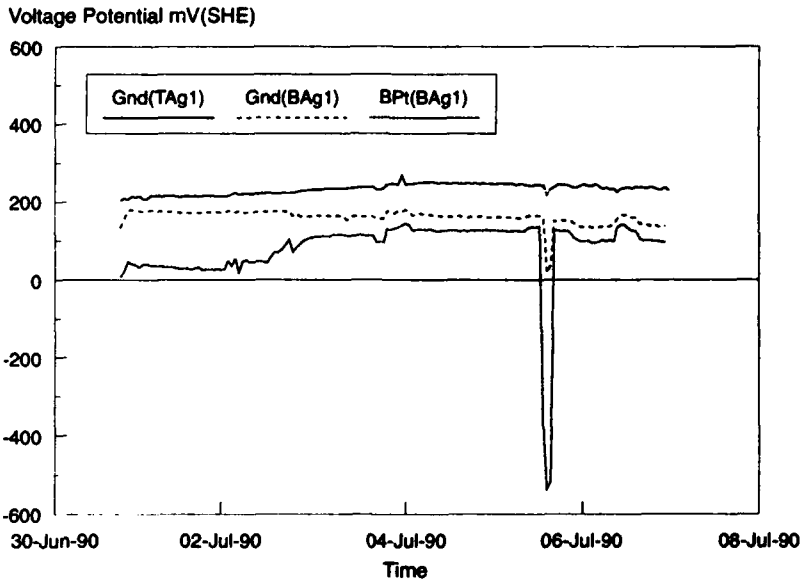

Figure 13 ECP Data During Normal Water Chemistry Prior to H_2 Ramping

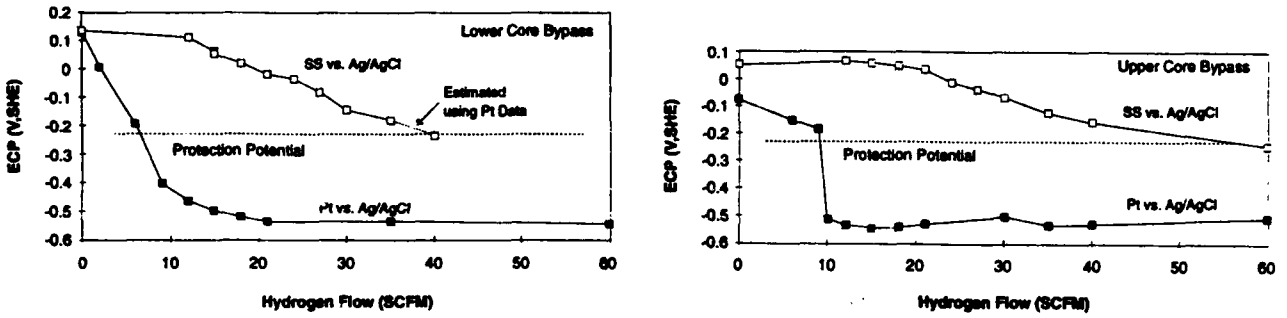

Figure 14 ECP Results from Overseas BWR

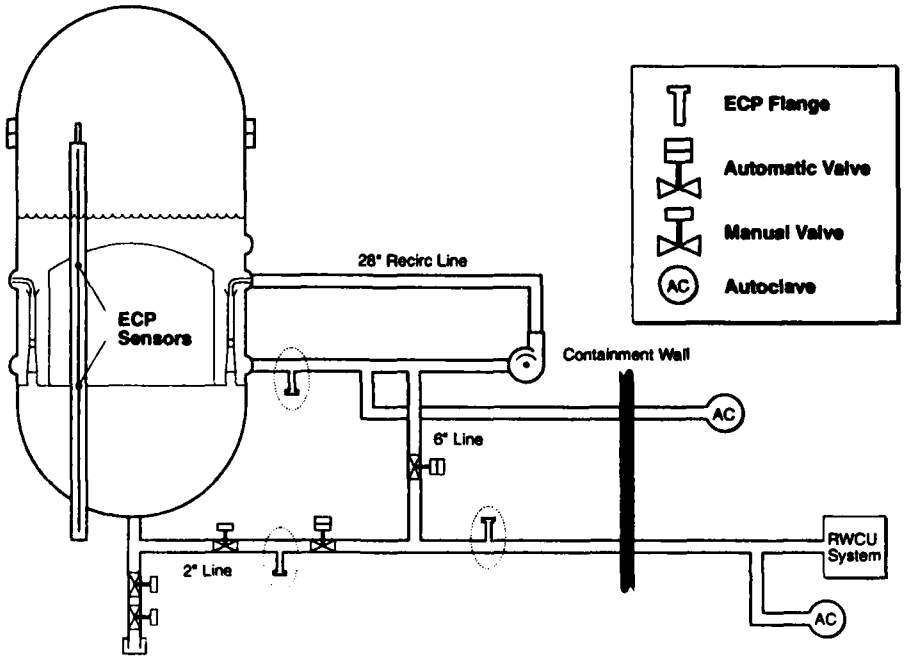

Figure 15 ECP Measurement Arrangement
For Upper & Lower Plenum, Reactor Water Clean-up Inlet & Recirculation Piping

Electrochemical Potential Monitoring in the Feedwater at the St. Lucie 2 PWR

W. R. Kassen
NWT Corporation
7015 Realm Drive
San Jose, CA 95119

J. S. Seager
Florida Power & Light Company
700 Universe Blvd.
Juno Beach, FL 33408

K. E. Beichel
Florida Power & Light Company
St. Lucie Power Plant
6501 South A1A
Jensen Beach, FL 34957

Abstract

Reducing conditions are necessary in nuclear steam generators to minimize local corrosion phenomena, e.g., stress corrosion cracking. To achieve this goal, the electrochemical potential (ECP) should be maintained below the threshold at which these corrosion mechanisms occur. Ideally, in-situ ECP measurements in the steam generator would allow for monitoring and controlling oxidant ingress to maintain the desired reducing conditions. Unfortunately such measurements are difficult to implement. However, oxidant ingress can be monitored and controlled via ECP measurements in the high pressure feedwater. A feedwater ECP monitoring system was installed at the St. Lucie 2 PWR of Florida Power and Light Company to assess this approach.

Variations in feedwater ECP and corrosion product transport were monitored. As chemistry was varied, Alloy 600 ECP was shown to depend on the feedwater hydrazine/condensate dissolved oxygen ratio. Operation at hydrazine/oxygen ratio above 6 was necessary to maintain a low ECP.

Introduction

Oxidant ingress to PWR steam generators can lead to an increase in electrochemical potential (ECP) of Alloy 600 and 690 tubing materials and thereby increase the tendency of IGA/SCC in acidic or basic crevices[1]. Thus, minimization of oxidant transport by the feedwater, i.e., oxygen and cupric, cuprous and ferric species, should be a general goal of a well managed secondary system chemistry control program. Obviously, it would be desirable to monitor the oxidation state of feedwater borne species on a real time basis and also directly monitor steam generator tubing ECP in crevice regions where corrosion occurs to assure that the tubing ECP remains very low. Unfortunately, neither of these measurements can be easily made. Specifically, no on-line corrosion product oxidation state monitor is available, and monitoring ECP in a PWR steam generator crevice presents significant problems.

In-plant ECP measurements in the feedwater and the steam generator sludge pile have been reported[2,3]. Results from Biblis A have shown that the ECP of Alloy 800 continues to decrease as the feedwater hydrazine concentration is increased to 100 ppb with a diminishing effect above this level. It also was shown that Alloy 800 ECP in the sludge pile and the feedwater were very similar and responded similarly to changes in oxidant and reductant concentrations. Thus, it was concluded that an Alloy 800 specimen in the feedwater could be used as a surrogate of the steam generator tubing.

On this basis, an evaluation of the dependence of Alloy 600, carbon steel and stainless steel ECP on secondary system chemistry was performed at the 830 MWe St. Lucie 2 PWR. Emphasis was placed on the impact of hydrazine and oxygen concentrations[4].

Monitoring System

Reference and Measuring Electrodes

The reactor proven external reference electrode shown in Figure 1[5] was selected for the evaluation. This electrode meets the four key performance criteria for reference electrodes, specifically, 1) they must have well defined and known potentials in the test environment, 2) they must not be affected by the working environment, 3) they must not

adversely affect that environment, and 4) they must have a reasonable service life.

Two reference electrodes (both filled with $5(10^{-5})$ N potassium chloride solution) were installed. This practice is employed in most BWRs based on numerous years of experience because of the difficulty of eliminating reference electrode failure as a factor to be considered if ECP variations are observed during normal operation.

The measuring electrode is shown in Figure 2 and has also been reactor proven[6,7]. Three electrodes of this configuration were employed, one with an Alloy 600 measuring billet, another with a carbon steel billet and the third with a platinum billet. The electrodes were installed in the flange of a 1-liter, Type 316 stainless steel autoclave. A schematic is shown in Figure 3. The autoclave also was used as a stainless steel (Type 316) measuring electrode.

ECP Measurement

At St. Lucie 2, potentials of Alloy 600, carbon steel, platinum, and the Type 316 stainless steel autoclave were measured versus the two reference electrodes. The autoclave was electrically connected to ground via its connecting piping. This configuration has been shown to be acceptable in both theory and practice[8,9]. A schematic of the ECP measuring system is given in Figure 4. As shown the output of each electrode is processed by a unity gain or "buffer" amplifier that has a nominal input impedance of 10^{12} ohms. Amplifier output signals are sent to a multichannel, programmable remote transmitting unit where the signals are digitized and transferred to a 386 PC. ECP data are stored at 5 minute intervals with the autoclave temperature, system flowrate, and feedwater dissolved oxygen concentration. ECP trends are displayed on the PC monitor and are continuously updated.

Potential readings via a 0.1 N KCl filled reference electrode can be converted to the standard hydrogen electrode (SHE) scale and expressed in volts as follows[10]:

$$E_{SHE} = E_{Reading} + 0.286637 - 1.003217(10^{-3})\,\Delta T + 1.7447(10^{-7})\,\Delta T^2 - 3.03004(10^{-9})\,\Delta T^3 \qquad (1)$$

where ΔT (°C) = Process fluid temperature minus 25±°C

This expression was used to develop the results presented below. However, recent experiments at 280°C have shown that 0.115 V must be added to the Equation 1 value to correct for the use of the $5(10^{-5})$ N KCl electrolyte[11]:

Calibration of the $5(10^{-5})$ N fill solution electrode to SHE for the 220°C feedwater temperature at St. Lucie is planned.

Monitoring System

Installation at St. Lucie 2

The ECP monitoring system at St. Lucie 2 is shown in Figure 5. High pressure feedwater is taken from the B feedwater train immediately upstream of the feedwater flow control valve. The system is connected via 0.5 inch x 0.049 inch wall stainless steel tubing that is connected to the feedwater system via a former pressure tap. Since reactions of hydrazine and oxygen occur in the sample line, the measuring equipment was located in close proximity to the sample point. Approximately 12 feet of 1/2 inch tubing was used to connect the sample point to the ECP autoclave. At the system flowrate of 4 gpm, the velocity through the sample line is 23 ft/sec and the residence time is approximately 1/2 second.

Previously reported data[8,12] have indicated that the potential of a Type 304 stainless steel specimen is highly dependent on the mass transfer coefficient from the bulk water to the specimen surface particularly at very low concentrations of oxidants. Based on such considerations, it has been recommended[8] that the ECP measuring electrode be exposed to yield a mass transfer coefficient similar to that in the piping system of interest. To address this issue, the ECP autoclave was fitted with flow guides to establish a 5 ft/sec past the electrode surfaces at the system flowrate of 4 gpm. Transit time from the autoclave inlet to the electrodes was approximately 0.05 seconds.

On exiting the autoclave, the monitoring system flow is cooled by plant service water. The temperature and flowrate of the cooled water are measured prior to the water being dumped to drain through an air operated isolation valve followed by a fixed flow restrictor and two manual throttle valves connected in series (Figure 5).

This flow control/pressure reduction scheme was mandated by the fact that the monitoring system inlet is located upstream of the feedwater flow control valve. As such, system pressure can vary from approximately 830 psig to approximately 1350 psig depending on plant power. The system provides rangeable and tractable flow control at the two backpressure extremes with one throttle valve full open during normal operation and half throttled at reduced power and the other approximately half throttled at either condition (Figure 5).

The air operated isolation valve closes on receipt of a high temperature signal from the monitoring stream subsequent to passing through the system coolers. Such isolation was mandated by safety considerations relative to flashing 220°C fluid in a low pressure drain line subsequent to cooling water failure. The valve is designed to fail closed on loss of electrical power or compressed air, and its control logic will not allow system restart until an operator executes a reset procedure.

The throttle valves provide excellent control of the thermal gradient encountered when the monitoring system is started up. To avoid thermal shock to the monitoring system, a small flow is allowed while observing the system temperature increase. Full flow is established once the monitoring system temperature approximates that of the inlet fluid.

The corrosion product sampler and oxygen analyzer module are close coupled to the ECP autoclave. Delay times to the inlet of the corrosion product sampler and the oxygen analyzer module are <0.2 seconds and approximately 0.8 seconds, respectively. The corrosion product sampler is shown schematically in Figure 6. The sampler provides for collecting filterable and nonfilterable corrosion products on membranes. A 0.45 micron membrane is used to collect filterable species from a continuous flow of approximately 100 ml/min over one to three days. A Toray cation exchange membrane is inserted beneath the filter to collect non-filterable species. The oxygen analyzer module is shown in Figure 7.

The scheme of cooling and dumping the monitoring system flow to an open drain was an expedient with regard to schedule and manpower considerations since the installation was considered temporary. In a permanent installation, the monitoring system effluent preferably would be returned to the feedpump suction without cooling.

At St. Lucie 2, the autoclave, corrosion product sampler, oxygen analyzer module, and electronic data acquisition modules were located on the outdoor turbine deck. For weather protection of the electrical/electronic components, this equipment was installed in a converted Conax box with doors, windows, and a window mounted air conditioner. In a permanent installation, the plumbing and electronic modules could be separated by significant distances to take advantage of existing environmentally controlled areas.

For an outdoor turbine deck installation of the ECP autoclave, a removable rain cover would be required.

System Performance

The monitoring system performed satisfactorily through shutdowns, restarts, normal power operation and even an episode where the water in the autoclave flashed.

However, feedwater oxygen data are limited due to analyzer drift that occurred within days of sensor rejuvenation and calibration. This problem occurred with several different sensors, both new and old, while similar sensors performed very well in condensate service. Thus, differences in feedwater and condensate chemistry may have caused the failures. Specifically, hydrazine concentrations are significantly greater in the feedwater. According to plant personnel, sensor failure also occurs frequently on a plant power change when a crud burst is experienced. This is attributed to membrane fouling by a loosely adhered layer of feedwater corrosion products. This behavior has not been observed for sensors employed for condensate measurements[13]. The analyzer manufacturer indicates that the difficulty may be in the sensor membrane, and an alternate membrane designed to better handle these conditions is available on new analyzers[14]. Unfortunately, the membrane is not available for the analyzers in service at St. Lucie.

ECP Results

Variations in feedwater ECP and corrosion product transport to the steam generators were assessed as secondary system chemistry, i.e., condensate dissolved oxygen, feedwater hydrazine and hydrazine/oxygen ratios, was varied. Variations of Alloy 600, platinum, carbon steel and stainless steel ECP are given in Figure 8 along with a corresponding condensate dissolved oxygen and feedwater hydrazine variations for the test interval.

The ECP monitoring system was placed in service August 9, 1992 and performed flawlessly through 3½ months of operation and during a plant trip and restart (August 10 through August 15) and two ECP system isolations and restarts during plant operation (August 23 through 25, and September 28 through 29) (Figure 8). Operational events are summarized in Table 1. Throughout the test interval, the reference electrodes in the system were in agreement within ±10 mV.

The plant was shut down for maintenance on November 24 at 0330 hours and the ECP system was shut down approximately 12 hours later. Subsequent to the depressurization and plant restart after the outage, the ECP system was returned to service. At identical feedwater hydrazine and condensate dissolved oxygen concentrations, ECP measurements before and after depressurization were identical within ±20 mV.

The variations in ECP were shown to depend on variations in feedwater hydrazine and condensate dissolved oxygen concentrations and to correlate very well with the ratio of these concentrations. Depending on the hydrazine to oxygen ratio, the changes in ECP with changes in a single parameter ranged from significant to negligible. In the instance of significant changes, the rate of response was nearly instantaneous. The rate and magnitude of ECP response to changes in hydrazine concentration have assisted plant personnel in early detection of problems with the hydrazine injection system and the hydrazine analyzer[15].

On September 23, the condensate dissolved oxygen concentration was increased via an induced air leak to the condenser. Prior to this increase, feedwater hydrazine and condensate dissolved oxygen were 30 and 7 ppb, respectively. Feedwater hydrazine concentration was maintained at 30 ppb while the oxygen was allowed to increase. The ECP response was very rapid. At 30 ppb hydrazine and 12 ppb dissolved oxygen in the condensate, the Alloy 600 potential increased approximately 220 mV while the platinum, carbon steel and stainless steel ECPs increased approximately 100 mV, 170 mV and 230 mV, respectively (Figure 9).

On November 2, the hydrazine concentration in the feedwater was increased from 32 to 100 ppb at a condensate dissolved oxygen concentration of 11 ppb. As a result, the Alloy 600 ECP decreased by approximately 260 mV (Figure 10). The ECPs of platinum, carbon steel and the stainless steel autoclave behaved similarly. Again, the magnitude of the response to the change was different for each material, i.e., the

platinum, carbon steel and stainless steel autoclave ECPs decreased 130, 165 and 220 mV, respectively, compared to the Alloy 600 decrease of 260 mV.

Feedwater Corrosion Products

Feedwater iron concentrations during the evaluation are given in Figure 11. A significant reduction in iron concentration was observed during the three week interval at 100 ppb feedwater hydrazine and approximately 10 ppb condensate dissolved oxygen. Specifically, the feedwater iron concentration averaged 7 ppb at 30 ppb hydrazine and 3 ppb at 100 ppb hydrazine. This decrease is attributed primarily to the increase in feedwater and condensate pH from averages of 9.45 and 9.65 before the increase to 9.9 and 10, respectively, after the increase. However, a synergistic effect of hydrazine may also be present. Note that studies at Genkai[16] indicated a reduction in iron transport at an increased hydrazine concentration and constant pH. However, experiments by others[17] have shown that the tendency for flow assisted corrosion increases at decreased ECP, and a decrease in ECP was observed with the hydrazine increase.

To determine the nature of the iron corrosion products transported by the feedwater, Mossbauer analyses were performed on filter samples taken over a three day period at a feedwater hydrazine of 70 to 130 ppb and condensate dissolved oxygen at 10 to 14 ppb and also at a hydrazine concentration of 30 to 90 ppb and an oxygen concentration of 5.5 to 6.0 ppb. Note that the hydrazine to oxygen ratios remained similar. Magnetite and hematite concentrations on the filters were similar (Table 2).

ECP Response to System Changes

The relation of stainless steel ECP to dissolved oxygen content in high purity water at 275°C based on BWR experience is given in Figure 12. As shown, very small changes in oxygen concentration can result in large changes in ECP. In addition, the specific characteristic of the ECP/oxygen relation are dependent on the system history. For example, in the Forsmark 2 BWR recirculating system which operated for about three years in a fully deoxygenated hydrogen water chemistry environment, the stainless steel ECP increased significantly with an increase in dissolved oxygen from 0 to approximately 0.4 ppb[12].

A similar relation may be derived from the St. Lucie data. Specifically, the relation of Alloy 600 ECP to the ratio of the feedwater hydrazine concentration to the condensate dissolved oxygen concentration is shown in Figure 13. On decreasing the feedwater hydrazine/condensate dissolved oxygen ratio from approximately 10 to 2, the Alloy 600 ECP increases gradually until a ratio of approximately 6 is reached at which time a sharp transition occurs to a region of relatively high potential.

Hydrazine/oxygen ratio changes on either end of the curve yield relatively small changes in Alloy 600 ECP. Conversely, small hydrazine/oxygen ratio changes result in large ECP changes in the transition region. It should be noted that the location of the transition region is expected to vary depending on system chemistry and operational history. This phenomenon coupled with the relatively narrow band of hydrazine/oxygen ratio that defines the observed transition region in the St. Lucie 2 feedwater underscores the importance of the sample representativeness and mass transfer considerations discussed earlier.

In an attempt to assess the impact of these factors, plant personnel reduced autoclave flow from 4 gpm to approximately 0.17 gpm on November 9. As a result, the residence time between the feedwater line and the autoclave was increased from approximately 0.5 second to 12.5 seconds. At that time, the feedwater hydrazine and condensate oxygen concentrations were 100 and 10 ppb, respectively.

Based on feedwater dissolved oxygen analyses when the analyzer was performing satisfactorily, the dissolved oxygen concentration entering the autoclave at a 4 gpm flow was on the order of 2 ppb. At the reduced flowrate, the oxygen concentration is predicted[19] to be approximately 1 ppb at the autoclave inlet. The hydrazine concentration is assumed to be 100 ppb at the inlet at 4 gpm. At the reduced flowrate, the hydrazine concentration is predicted[20] to decrease to approximately 95 ppb. The change in temperature from full flow to the reduced flowrate condition was 3°C.

Based on the above, the 25 to 1 decrease in flowrate only resulted in changing the hydrazine to oxygen ratio at the autoclave inlet from approximately 50 to 95. Thus, it was not surprising that during the 6 hour experiment, the potential decrease was very small, i.e., approximately 5 mV.

If this experiment had been conducted at a feedwater hydrazine/condensate dissolved oxygen ratio in the transition region (Figure 13), a significant reduction in ECP would have been observed with the flowrate reduction. Since this effect would lead to a false indication of satisfactory ECP control at low flowrates, maintenance of high flowrates to the autoclave is necessary.

Comparison of the St. Lucie 2 ECP results to those obtained for the feedwater at the Ringhals 3 PWR[21-23] indicates that the results are not totally consistent. This could be a result of plant-to-plant and/or measurement methodology differences. For example, during a test at zero hydrazine and 40 ppb condensate dissolved oxygen, the platinum ECP at the high pressure feedwater monitoring location at Ringhals 3 increased very slowly by only 70 mV[23]. By deduction from the St. Lucie data, the ECP would rapidly increase by several hundred millivolts if a similar experiment were performed at St. Lucie 2.

Differences in mass transfer rates to the measuring electrodes at St. Lucie 2 and Ringhals 3 may be partially responsible for the observed differences since the fluid velocities past the electrodes (St. Lucie 2, 5 ft/sec; Ringhals 3, 0.08 to 0.32 ft/sec) are significantly different. However, the differences appear too great to be accounted for by mass transfer considerations alone and thus other differences appear to exist between the secondary systems at these plants.

Summary

The ECP monitoring system performed satisfactorily for approximately four months on St. Lucie 2 high pressure feedwater. The measurement program has demonstrated that valid ECP data are a reliable indicator of the success of approaches for reducing oxidant ingress to PWR steam generators. A strong dependence of Alloy 600 ECP on the feedwater hydrazine/condensate dissolved oxygen ratio was shown to be present. These data give reasonable justification for controlling this ratio at a value above 6. Since plant to plant differences which can significantly impact on ECP appear present, measurements are considered advisable at each plant.

At a feedwater hydrazine concentration of 100 ppb and a condensate dissolved oxygen concentration of 10 ppb, corrosion product transport to the steam generators was reduced significantly. This is attributed primarily to the increase in system pH at the higher hydrazine concentration.

Future Work

Additional testing is planned to determine the effect of a broadened range of feedwater hydrazine and condensate dissolved oxygen concentrations and their ratios on the feedwater ECP of Alloy 600 and the corrosion product transport to the steam generators.

Acknowledgment

The authors gratefully acknowledge the cooperation of the St. Lucie Plant management and staff throughout the equipment installation and the monitoring effort. Funding and permission to publish by Florida Power and Light Company (FP&L) and the Electric Power Research Institute (EPRI) is also gratefully acknowledged. The authors are indebted to Mr. R. J. Frechette (FP&L, St. Lucie) and Dr. P. J. Millett (EPRI) for their continued technical support.

References

1. "Interim PWR Secondary Water Chemistry Recommendations for IGA/SCC Control," prepared by Secondary Water Chemistry Guidelines Revision Committee, September 1992 (TR-101230).

2. W. Beyer, B. Stellwag, and N. Wieling, "On-Line Monitoring of Electrode Potentials in the Steam Generator of a PWR," 3rd International Symposium on the Environmental Degradation of Materials in Nuclear Power Systems - Water Reactors, Traverse City, Michigan, 1987.

3. B. Stellwag and R. Killian, "Influence of O_2 and N_2H_4 on the ECP in High Temperature Water," 5th International Symposium on the Environmental Degradation of Materials in Nuclear Power Systems - Water Reactors, Monterey, Calif, 1991.

4. W. R. Kassen, "Electrochemical Potential Monitoring in the PWR Secondary Cycle," Electric Power Research Institute, to be published.

5. W. R. Kassen, "Reference Electrode for PWRs," Electric Power Research Institute, May 1987 (NP-5155).

6. J. Leibovitz, W. R. Kassen, W. L. Pearl, and S. G. Sawochka, "Improved Electrodes for BWR In-Plant ECP Monitoring," Electric Power Research Institute, August 1982 (NP-2524).

7. J. Leibovitz, W. R. Kassen, W. L. Pearl, and S. G. Sawochka, "In-Plant Measurements of Electrochemical Potentials in BWR Water," Electric Power Research Institute, May 1984 (NP-3521).

8. "Corrosion Potential (ECP) Measurement Sourcebook," Electric Power Research Institute, January 1991 (NP-7142).

9. W. R. Kassen, J. L. Tollefson, R. P. Jones, "The Impact of Hydrogen Water Chemistry at the Monticello BWR," Corrosion 92, April 1992 (Paper 112).

10. D. D. Macdonald, A. C. Scott, and P. Wentrcek, "External Reference Electrode for use in High Temperature Aqueous Systems," J. Electrochem. Soc., 126, No. 6, p. 908, 1979.

11. W. R. Kassen, "Insitu ECP Monitoring in PWR Model Boilers", Electric Power Research Institute, February 1993, to be published.

12. M. Ullberg, "On Corrosion Potential Measurements in BWRs," 4th Intl. Symposium on Environmental Degradation of Materials in Nuclear Power Systems - Water Reactors, Jekyll Island, Georgia, August 1989.

13. K. E. Beichel, Florida Power & Light, Personal Communication, September 23, 1992.

14. W. Miller, Orbisphere Laboratories, Personal Communication, April 2, 1993.

15. K. E. Beichel, Florida Power & Light, Personal Communication, September 25, 1992.

16. S. G. Sawochka, "Secondary Water Chemistry Control at Genkai No. 1 - Design and Operating Considerations," Electric Power Research Institute, May 1981 (NP-1863).

17. I. S. Woolsey, G. J. Bignold, C. H. De Whalley, K. Garbett, "The Influence of Oxygen and Hydrazine in the Erosion/Corrosion Behaviors of Carbon Steel under Boiler Feedwater Conditions, presented at 4th BNES Meeting, London, 1986 (Paper 96).

18. M. E. Indig, A. R. McIlree, J. Weber, "Electrochemical Measurements," Task 3 of "Evaluation of Near-Term BWR Piping Remedies Third Semiannual Progress Report," General Electric, pp. 5-8, 5-9, April-September 1977 (NEDC-21463-3).

19. S. B. Dalgaard and M. O. Sanford, "Review of the Hydrazine/Oxygen Reaction Kinetics," Materials Performance, p. 32, 1992.

20. N. L. Dickinson, D. N. Felgar, and E. A. Pirsh, "An Experimental Investigation of Hydrazine-Oxygen Reaction Rates in Boiler Feedwater," Proc. Amer. Power Conf., Volume XIX, p. 692, 1957.

21. L. Bjornkvist, and A. Molander, "Potential Measurements in Side-Stream Autoclaves on PWR Feedwater," Proc. of EPRI Workshop on ECP Monitoring and Detection of Crack Initiation and Growth, Washington, D.C., 1991.

22. A. Molander, et al., "Electrochemical Measurements in the Secondary System of the Ringhals 2 PWR," BNES International Conference on Water Chemistry of Nuclear Reactor Systems 6, Bournemouth, 1992.

23. A. Molander, B. Rosborg, P. Andersson, L. Bjornkvist, "ECP Measurements in the Secondary System at Ringhals 3," EPRI PWR Plant Chemists' Meeting, San Diego, CA, November 1992.

Table 1
OPERATION EVENT LEGEND
RE: Figure 8[4]

1 - Plant shutdown August 10, 1992

2 - Plant restart and operation at reduced power

3 - Operation at full power

4 - ECP system isolated for hurricane watch

5 - ECP system restarted

6 - Condenser air inleakage induced

7 - ECP system shutdown for cooling water problem

8 - ECP system restarted

9 - Terminated induced air inleakage

10 - Commence hydrazine increase from 30 to 100 ppb

11 - Commence hydrazine reduction

12 - Plant shutdown, ECP system depressurization episode begins

Table 2
RESULTS OF THE MOSSBAUER SPECTROSCOPY ANALYSIS
OF ST. LUCIE 2 HIGH PRESSURE FEEDWATER SAMPLES
(PERCENTAGE OF Fe IN DIFFERENT PHASES)[4]

	Sampling Interval	
	9/30/92-10/2/92	10/2/92-10/5/92
Feedwater Hydrazine, ppb	70-130	30-90
Condensate Oxygen, ppb	10-14	5.5-6.0
Feedwater Hydrazine/ Condensate Oxygen, ppb	5.4-13	5.0-15
Alloy 600 ECP, SHE, mV	-450 to -635	-565 to -625
Corrosion Product Composition		
Fe_3O_4, %	64.9 ± 1.7	71.9 ± 4.2
Alpha-Fe_2O_3, %	26.3 ± 2.3	18.6 ± 3.4
Gamma-FeOOH, %	2.9 ± 0.2	4.1 ± 0.3
Alpha-FeOOH, %	5.9 ± 0.4	5.4 ± 0.5
Feedwater Total Iron, ppb	5.4	--

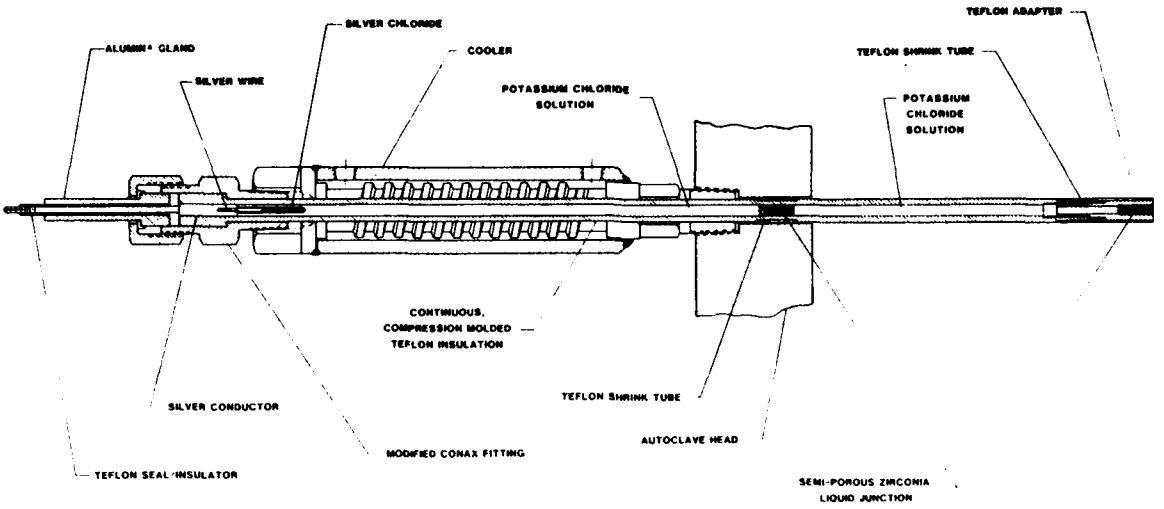

Figure 1 Cooled-Seal, Double-Junction, External Reference Electrode Assembly[5]

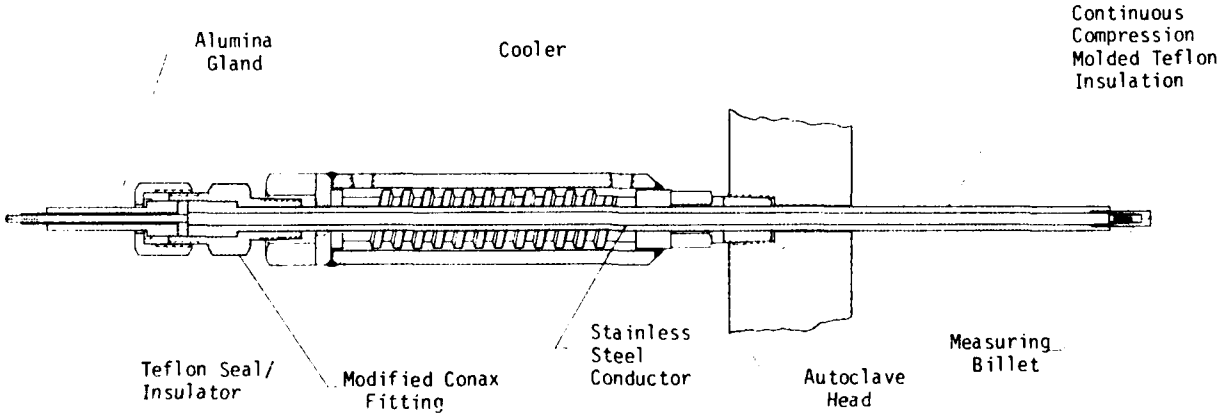

Figure 2 Cooled-Seal Measuring Electrode Assembly[6,7]

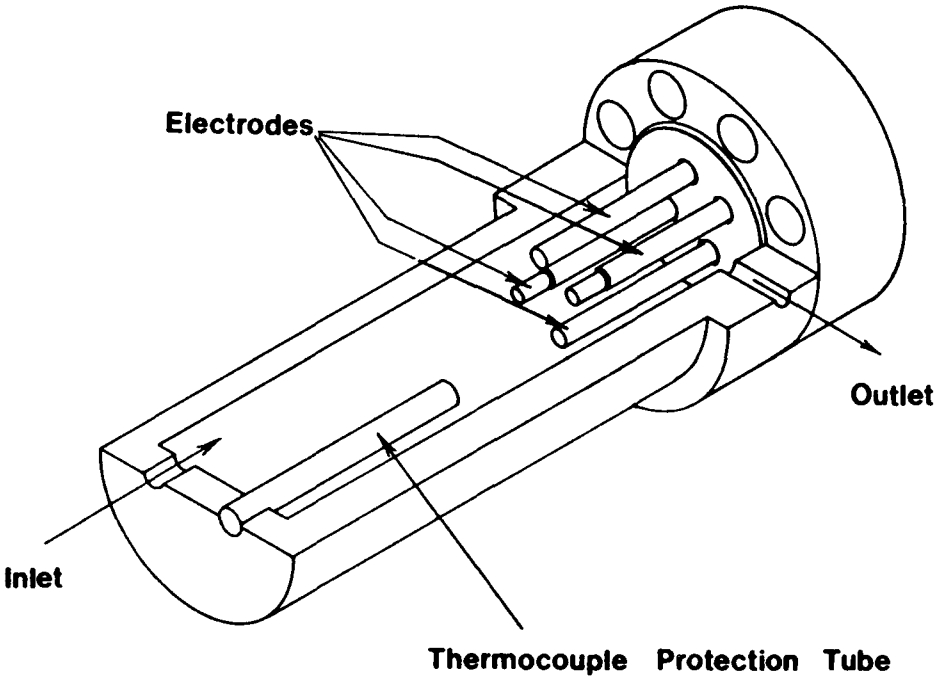

Figure 3 ECP Autoclave

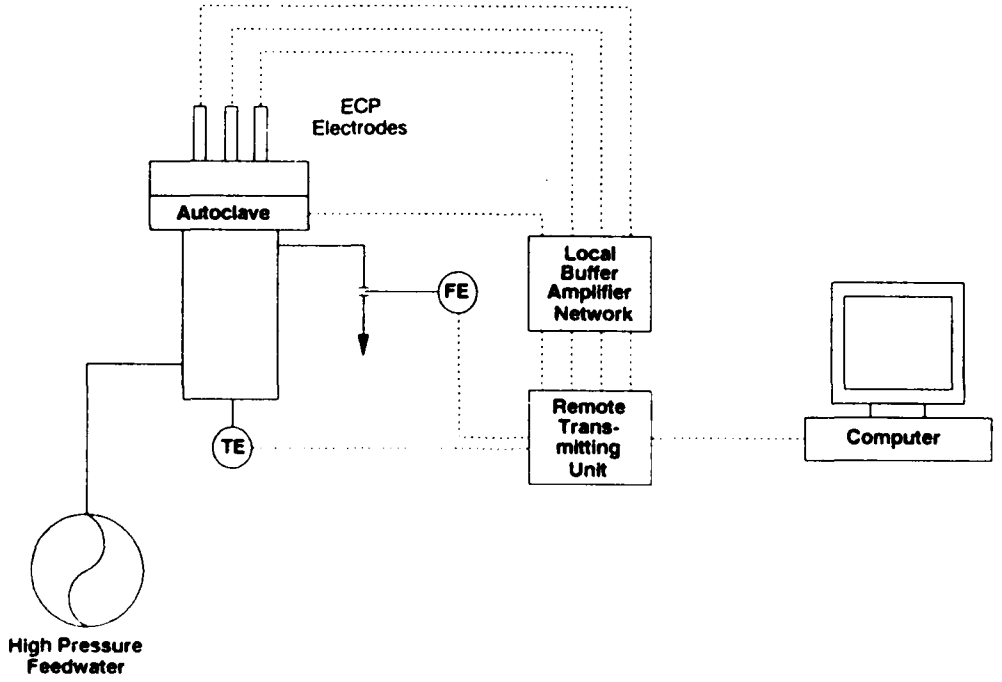

Figure 4 Feedwater ECP Monitoring Scheme

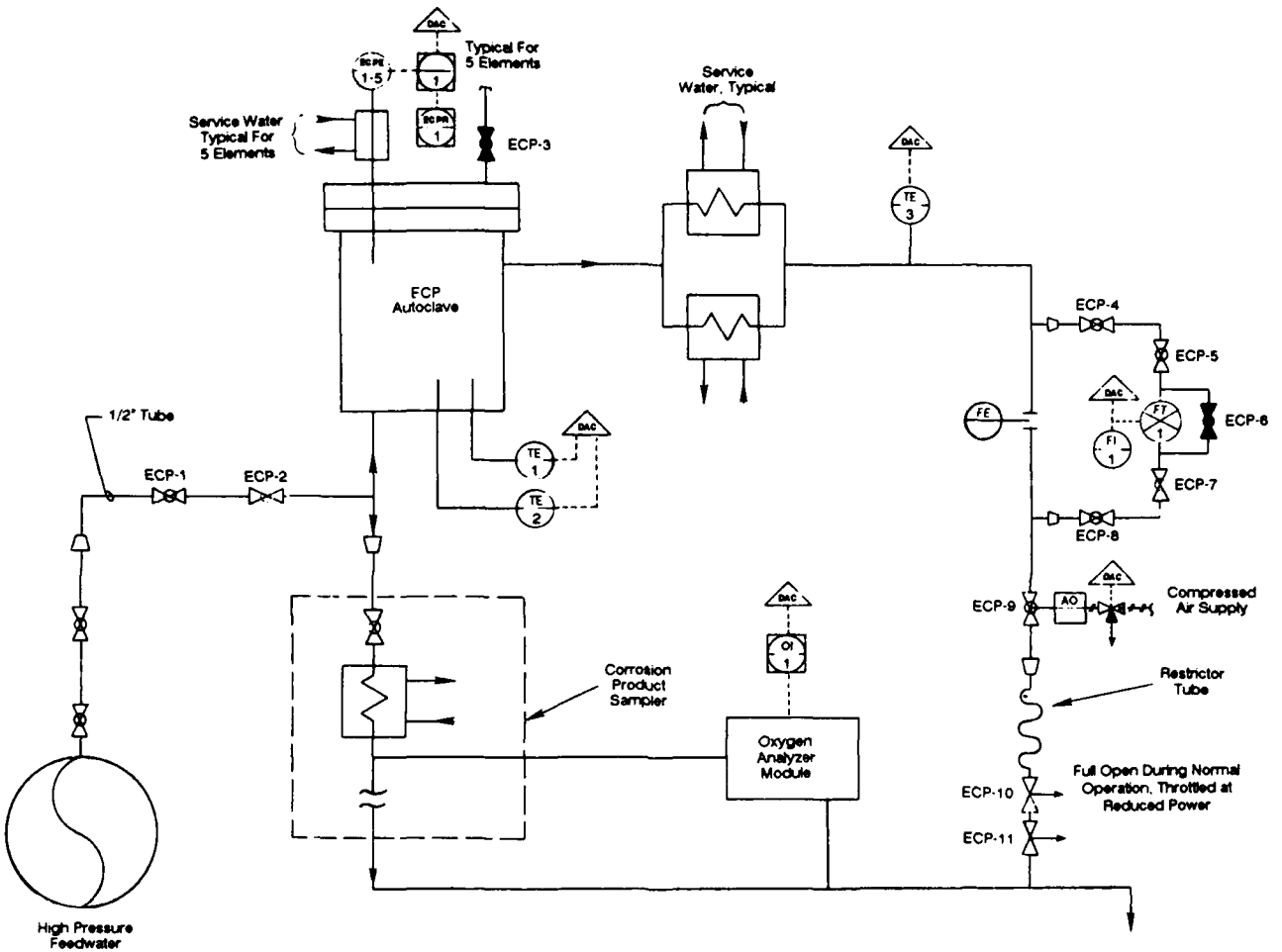

Figure 5 Piping and Instrument Diagram - ECP Monitoring System at St. Lucie 2[4]

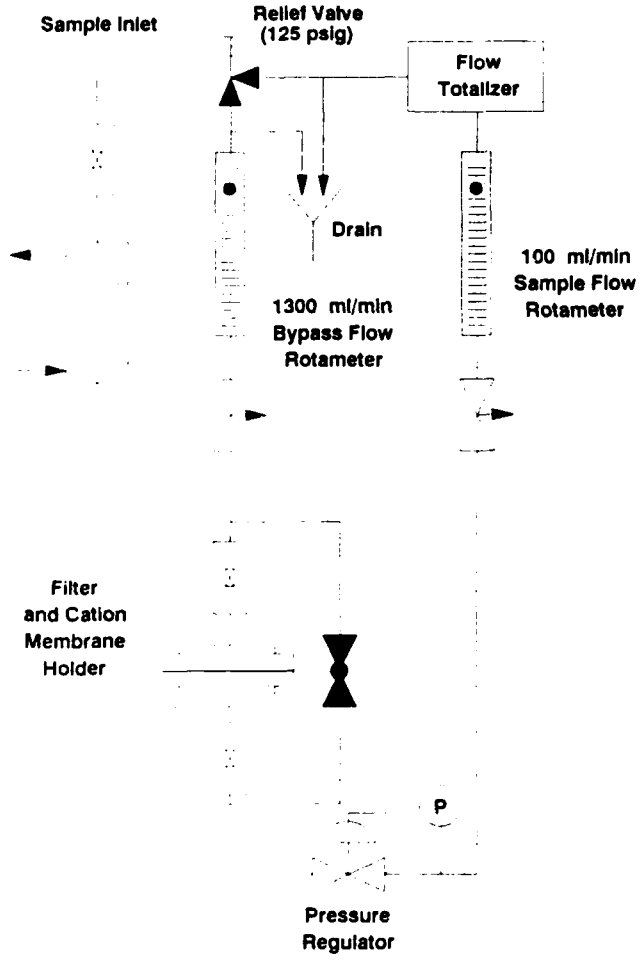

Figure 6 Corrosion Product Sampler

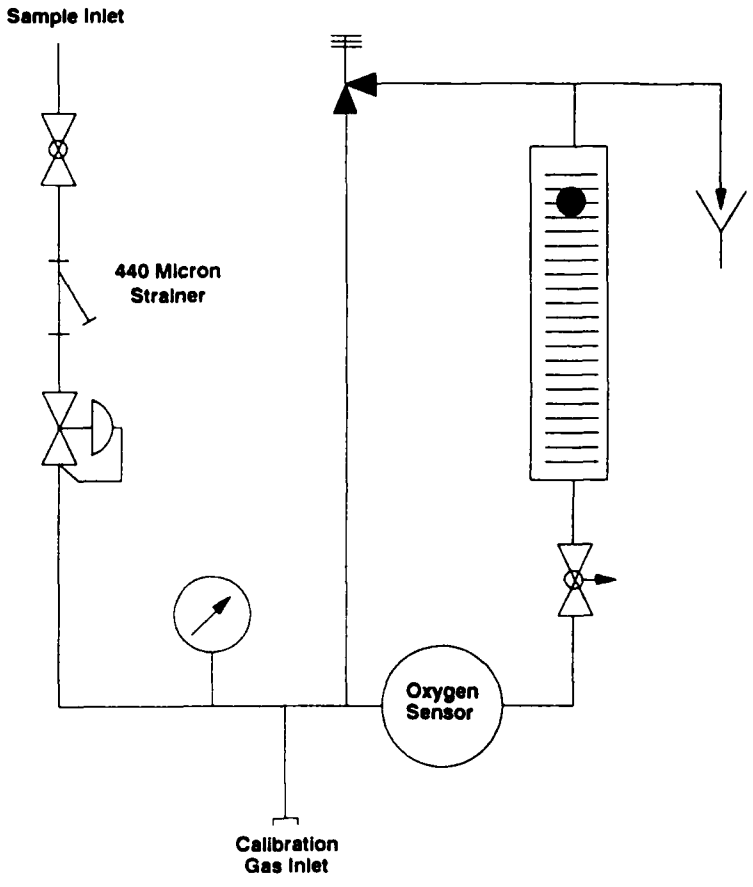

Figure 7 Oxygen Analyzer Module

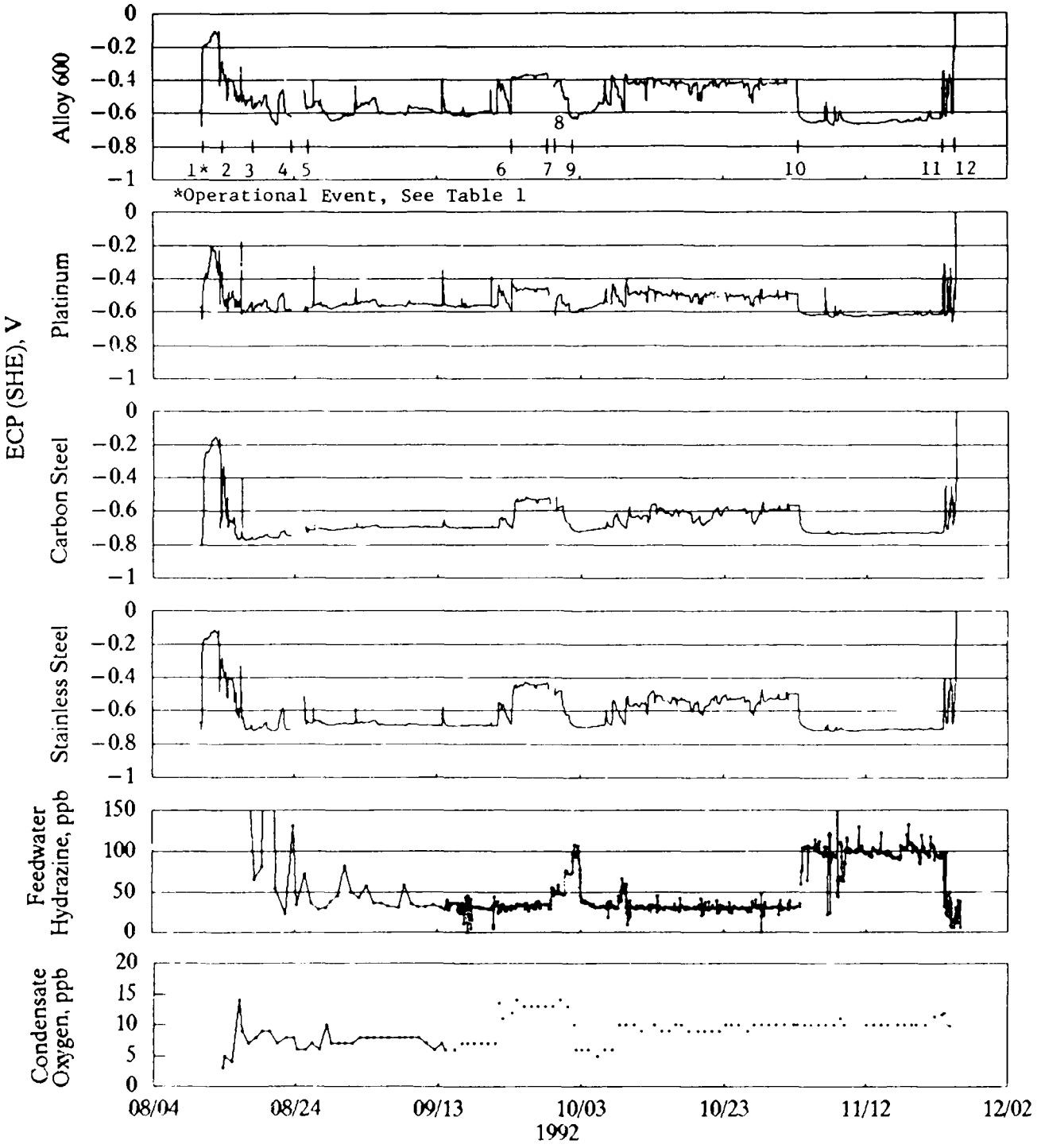

Figure 8 Alloy 600, Platinum, Carbon Steel and 316 Stainless Steel ECP Variations in St. Lucie 2 Feedwater at 220°C, Feedwater Hydrazine and Condensate Dissolved Oxygen Variations[4]

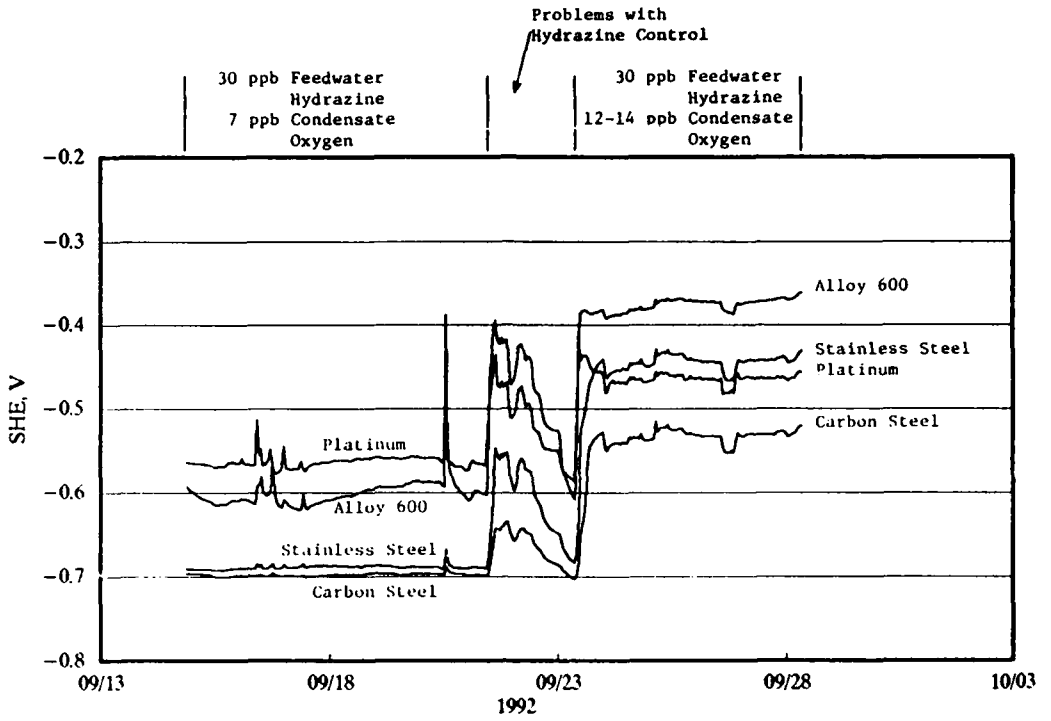

Figure 9 Comparison of ECP Variations in St. Lucie 2 Feedwater at 220°C on Increase of Condensate Dissolved Oxygen Concentration[4]

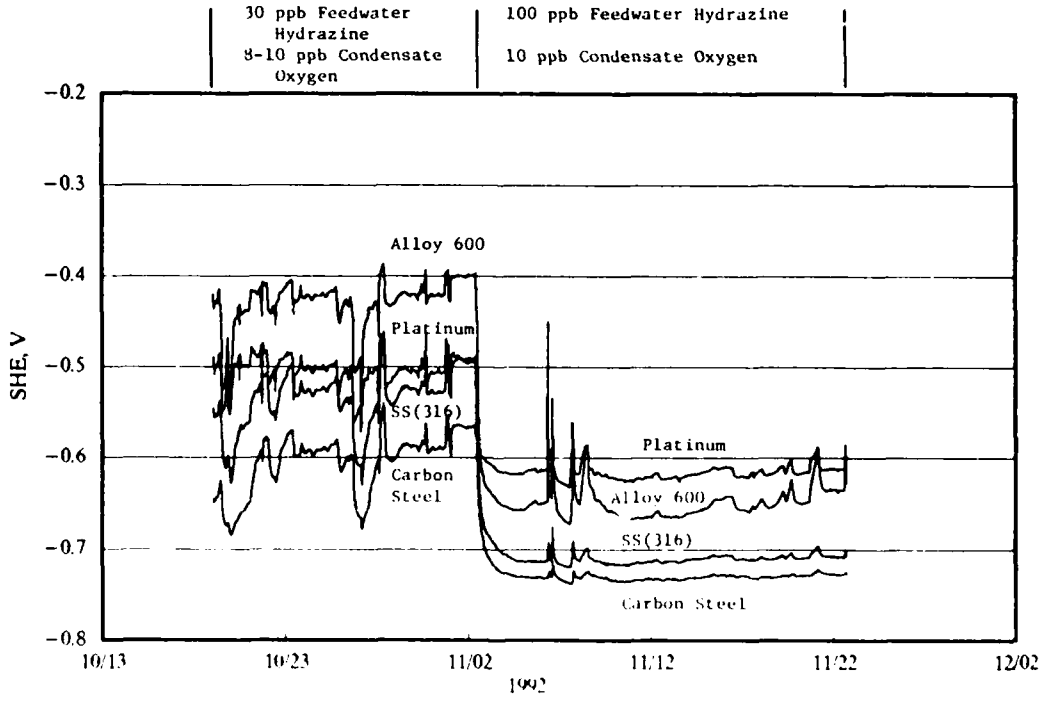

Figure 10 Comparison of ECP Variations in St. Lucie 2 Feedwater at 220°C on Increase of Feedwater Hydrazine Concentration[4]

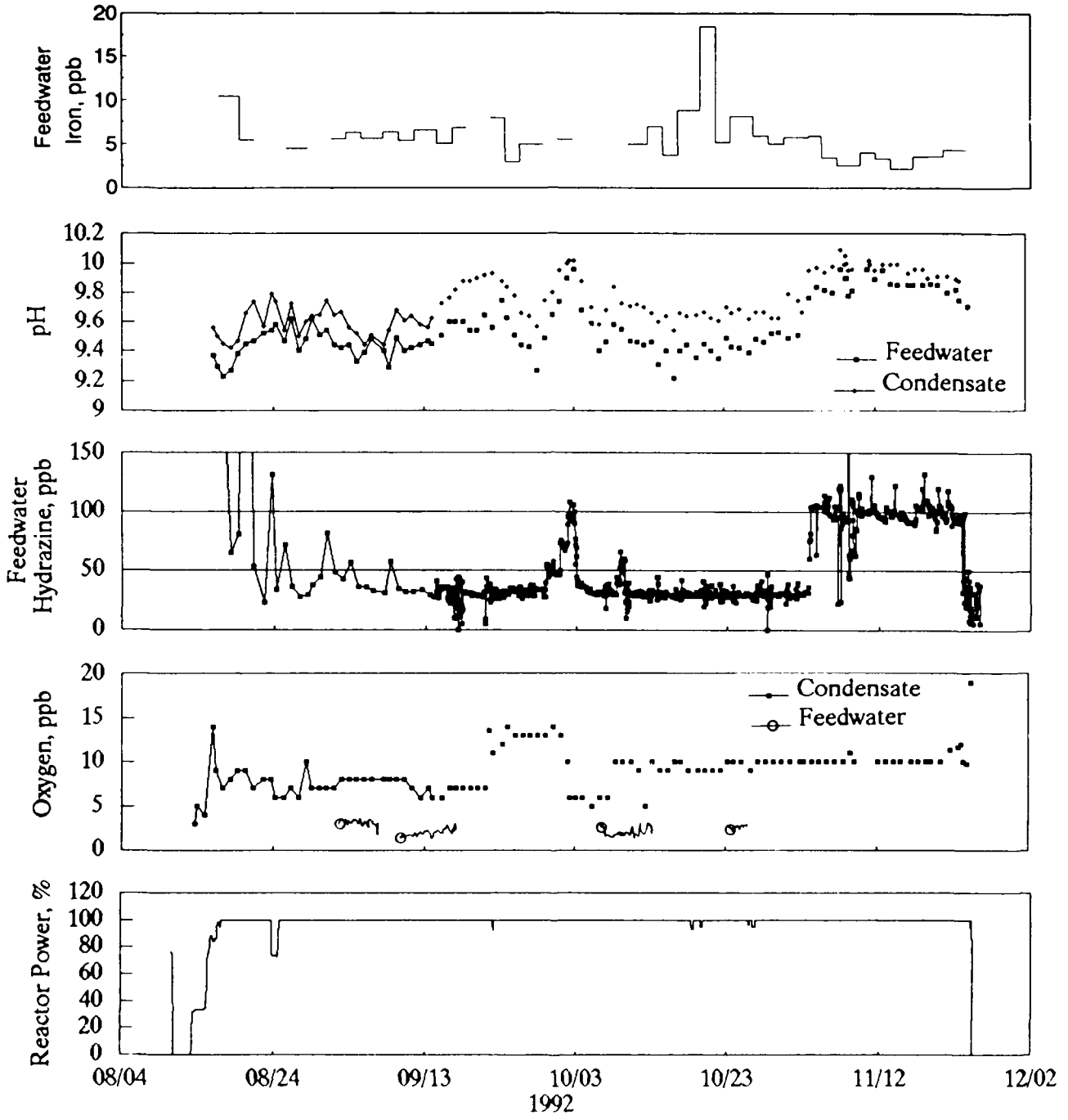

Figure 11 St. Lucie 2 Feedwater Iron, pH, Hydrazine, Dissolved Oxygen and Reactor Power Variations[4]

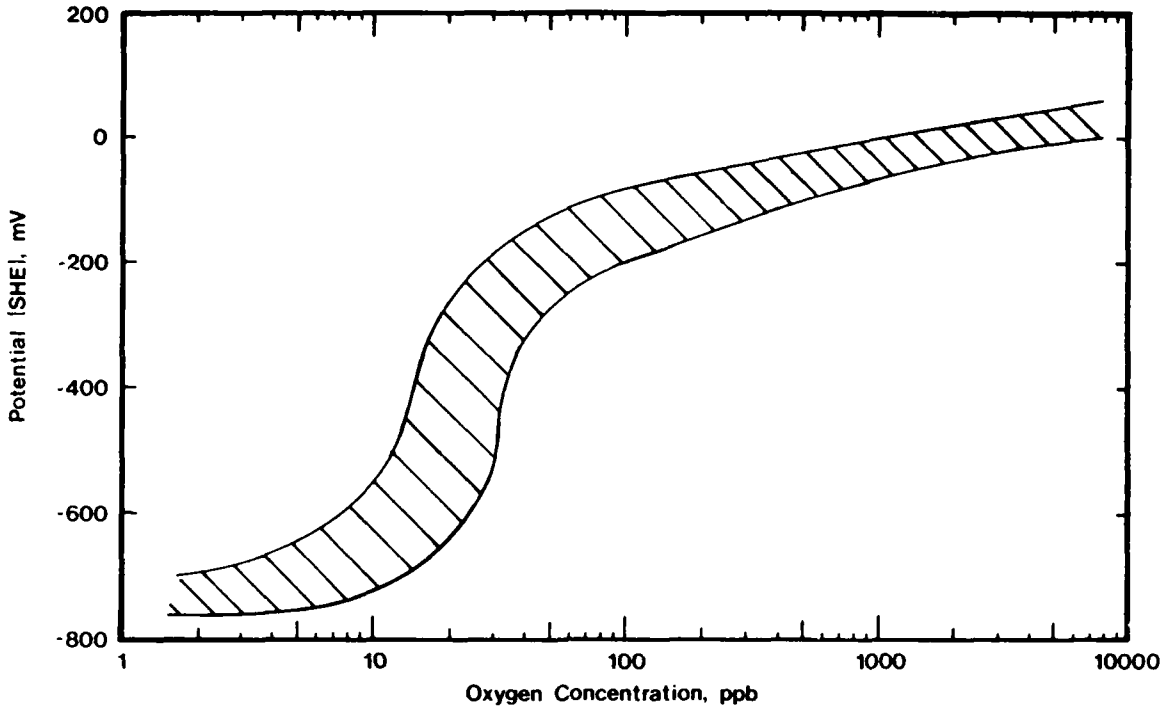

Figure 12 Oxygen-ECP Relationship at Typical BWR Temperature and Conductivity for Type 304 Stainless Steel at 274°C[18]

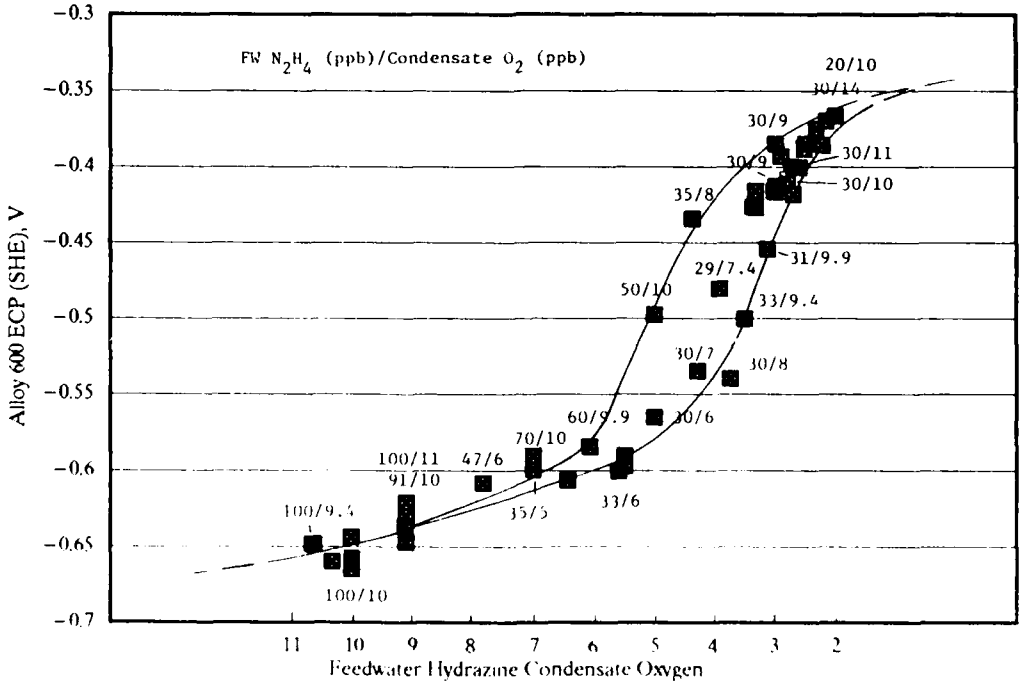

Figure 13 Alloy 600 ECP Variations in St. Lucie 2 Feedwater at 220°C as a Function of Feedwater Hydrazine/Condensate Dissolved Oxygen Concentration Ratio Variations[4]

On-Line Chemistry Control in EDF Nuclear Power Plants

Jacques Doyen
Electricité de France - Groupe des Laboratoires
21, Allée Privée - Carrefour Pleyel
93206 Saint-Denis Cedex 1 - France

Abstract

The document describes Electricité De France (EDF) policy concerning chemistry control in Nuclear Power Plants (NPP).

Due to the great importance of some parameters, and high risks of pollution of grab samples, the main parameters are continuously measured by reliable chemical on-line monitors. EDF has consequently developed a large program of tests to select the best instrument, in a specific facility installed in a NPP. In addition, a guideline document describes all the operations necessary for the correct use of all chemical monitors.

Periodic evaluations are organized to ensure the good quality of in-plant measurements: they consist of a complete inspection of all the monitors implemented in the unit, and comparative measurements between the unit monitors and those of Groupe des Laboratoires (GDL), the central laboratories of EDF.

EDF is presently designing chemical expert systems, making it possible to improve reliability and to shorten response time for all operation phases. The main advantage expected is an improvement of chemistry quality in the plants, resulting from quicker operator reaction in case of abnormal situations.

Key terms:

Introduction

Most corrosion that occurs in the circuits of a NPP is due:

- either to bad conditioning; ammonia or morpholine levels are too low, sometimes too high, hydrazine level is too low compared to the air ingress levels, or
- to the pollution of the water; for instance, sodium coming from the make-up water demineralization system or cooling water ingress, and oxygen coming from the air ingress to the condenser.

At EDF, chemistry is mainly ensured by automatic on-line monitors (pH, conductivity, sodium, oxygen) rather than by extensive sampling and manual analyses.

The majority of the monitors are equipped with alarm systems, with different activation levels depending on the chemical specifications locally available. Generally, the most important parameters are provided with redundant monitors and/or alarms (e.g.: 2 sodium-meters in condensate water, for sea water cooled plants, for more reliable and thus quicker detection of cooling water inlets).

On-Line Monitors at EDF

A. The Monitors of a Nuclear Unit

The equipment depends on the circuit itself on which measurements are performed and also on the chemical specifications available. Of course, on-line monitors operate on sample lines, at room temperature and after depressurization, and not in situ, at operating temperature and pressure.

The different monitors used, and the corresponding circuits in the nuclear plants, are listed hereafter versus the intended purpose of the instrument: [1], [2]

1. Quality of the steam generators water

- Na-meters and conductivity monitors (cation conductivity) at the steam generator (SG) blowdown.

From 4 to 8 monitors, depending on the type of unit.

2. Pollutants detection and diagnosis

- pH-meters at the SG blowdown
- conductivity monitors (cation conductivity) at the main steam and Moisture Separator-Reheaters (MSR) drains
- conductivity monitors (cation conductivity) at condensate water and each condenser fraction
- oxygen-meters at condensate water and feedwater
- sodium-meter at condensate water
- conductivity monitors (cation conductivity) at SG blowdown treatment.

From 20 to 25 instruments, depending on the type of unit.

3. Conditioning conformity

- pH-meter and hydrazine-meter on feedwater.

2 instruments on each unit.

In addition, the demineralization system for make-up water is controlled by chemical monitors:

- 1 sodium-meter and 1 conductivity monitor on each production line
- 1 conductivity monitor and 1 silica-meter common to the system
- several conductivity monitors to control resin regeneration.

For all the systems, each unit is equipped with more than 35 on-line monitors. Figure 1 shows the different chemical monitors installed and their function.

The total number of monitors for all these parameters at EDF is over 1,800, not including the primary circuit. They are distributed for the different parameters as follows:

Type of monitor	Total number	Samples
Oxygen-meter	> 120	Condensate and feedwater
Hydrazine-meter	> 100	Condensate and feedwater
Sodium-meter	> 120	Condensate water - SG blowdown makeup water
pH-meter	> 250	Condensate or feedwater SG blowdown - makeup water
Conductivity monitor	> 1,250	Condensate water - condenser fractions main steam - MSR drains SG blowdown and treatment

Periodic surveys gather the opinion of the users on all the monitors implemented in their plant, stimulating the after-sale service by the supplier and building a database on the quality of a particular part of the instrument: e.g. the electrodes. This feedback also identifies deterioration in the quality of some chemical monitors; consequently the operators now install other types.

B. Monitor Tests

Due to the importance of chemical monitors, EDF has developed a comprehensive program of tests to select the best instrument. A specific facility has been implemented in a nuclear power plant. The main advantage is to analyze representative water from the units instead of "artificial" water.

The main parameters evaluated during the tests are:

- output signal and alarms
- calibration
- accuracy and repeatability
- response time, for increasing and decreasing values
- sensor flow-cell quality.

Depending on the parameter studied, the reference value is measured by a specific method; the main cases are:

- O_2: gas chromatography
- N_2H_4: colorimetric method (benzaldehyde para-dimethyl amino)
- Na: the reference value is calculated from the concentration of the solution injected in the sample line and the dilution factor
- λ: same as Na, using the reference conductivity of KCl injected for the different levels studied
- pH: same as Na, using ammonia and morpholine for the different pH studied.

The monitors are finally operated in accordance with the supplier specifications; this endurance test is performed to evaluate the quality of the whole instrument: flow-cell and electronic parts, and more specially the drift of the monitor.

Throughout the tests, frequency and importance of all maintenance are evaluated to estimate their cost for normal in-plant operation.

At the end of the tests, the monitor is declared:

- either **AUTHORIZED** for the equipment of the units
- or **FORBIDDEN**.

C. Guideline for use

A guideline document has been written to describe all the operations necessary for the correct use of all the chemical on-line monitors in a plant. [3]

The different operational checks included in the document can be summarized as follows:

- electrical signal transmission
- sample line
- sensor flow-cell (including calibration)
- maintenance of the monitor when running and when stopped.

For each of these parameters, the maximum deviation from the reference value is indicated, as well as the operations necessary to restore to a normal situation. The guide was written to be applied to all types of monitors in all the EDF units. After a test period in all the units, the guide was officially applied at the beginning of 1992.

The guide headings are as follows:

1. Electrical signal relay to the control room
2. Sample lines check
3. Internal conditions of the monitor operation check
4. Electronic parts check
5. Electronic calibration
6. Sensor flow-cell check
7. Physical calibration
8. Cross comparisons between monitors at the same sample point
9. Maintenance during operation

Figure 2 is an example of typical forms included in the guide.

D. In-plant evaluations

Periodic evaluations are organized every year, to ensure good quality of in-plant measurements. About three plants a year are generally involved. These evaluations consist of:

- a complete inspection of all the monitors installed in the unit (except for primary circuit)
- comparative measurements between the unit monitors and those of Groupe des Laboratoires to evaluate the validity of the results obtained by the plant.

The parameters involved in these comparative evaluations are sodium and cation conductivity at SG blowdown, and oxygen in condensate water; sodium in makeup water is also verified. In case of a difference between the plant values and those of GDL, a reference method is used to resolve the discrepancy. For instance, gas chromatography is the reference method for oxygen measurements, while for sodium, standard additions made to the sample line are measured at the same time with both monitors.

Until now, all these operations have confirmed the validity of the measurements performed in EDF plants. The only problems, previously pointed out, were related to measurements of:

- oxygen in condensate water
- sodium in demineralized water.

Corrective solutions were proposed and applied shortly thereafter.

E. Expert system

Expert systems are beginning to have an influence on units in operation and will also become influential in the chemistry field in the near future. At the present time, EDF is testing a chemical expert system for the secondary system. [4]

The values of the measurements obtained by the on-line chemical monitors will be continuously taken into account, making it possible to improve reliability and to shorten response time for all operating phases.

The main advantage expected is an improvement in the chemistry of the plants, resulting from quicker operator reaction in the case of abnormal situations concerning either conditioning or pollution in the circuits.

Depending on the parameter out of specification, the operators' reaction will be facilitated by the system:

- pH of the feedwater - modification of the ammonia/morpholine injection
- Na in the SG blowdown - diagnosis of cooling water in-leakage, or trisodium phosphate from the auxiliary cooling circuits, or sodium hydroxide leakage at the outlet of the demineralization system
- O_2 in the condensate - increase the hydrazine injection rate; check for air ingress.

To ensure total efficiency of such a system, operational monitors, capable of indicating the right value at any time, must be available.

Conclusion

EDF applies ALARA concept (**A**s **L**ow **A**s **R**easonably **A**chievable) to chemistry in NPP, and on-line chemical monitors are one of the means used to reach the challenge and thus to fight against corrosion of the materials of NPP circuits.

Avoiding grab sampling and manual analysis, the quality of measurements are consequently:

- more reliable
  human error is avoided; pollution of the samples is minimized
- continuous
  transient phenomena are taken into account

parameter trends are analyzed and interpreted.

In order to ensure the best possible monitor reliability, EDF controls the following:

- selection
  instruments are tested in a specific laboratory before being selected for plant use
- utilisation and maintenance
  a guideline describes all that must be done for good operation of the monitors, from the sample line up to and including the control room
- in-situ evaluations
  to ensure the perfect quality of the measurements in all the plants.

Expert systems are starting to be developed more and more, necessitating the use of reliable on-line monitors, but on the other hand making possible better operation of the nuclear units, especially because of the rapidity and high dependability of diagnosis in the case of abnormal situation.

Finally, it must be mentioned that on-line ion chromatography tends to appear to be a good alternative solution for future, the advantages being:

- a more precise analysis
  anionic and cationic species are evaluated continuously
- a more accurate diagnosis
  the levels of measurements performed are much lower than those of traditional methods, 0.01 ppb being nowadays a current sensitivity for most ions measured with on-line chromatography.

This technique should be used increasingly in the future.

References

1. Ph. Berge, F. Nordmann, PWR Secondary Water - Chemistry and Corrosion (1988 - JAIF International Conference on Water Chemistry in Nuclear Power Plants)

2. F. Nordmann, B. Liquette, Spécifications chimiques - Centrales du type R.E.P. (Janvier 1988)

3. A. Stutzmann, C. Guillon, Doctrine d'utilisation des automates chimiques en centrales (Avril 1992)

4. P. Eon Duval, J.-M. Fiquet, P. Hannedouche, O. Menet, SODEXPERT - Prediction and Diagnosis of PWR Secondary Side Chemical Pollution (1991 - JAIF International Conference on Water Chemistry in Nuclear Power Plants)

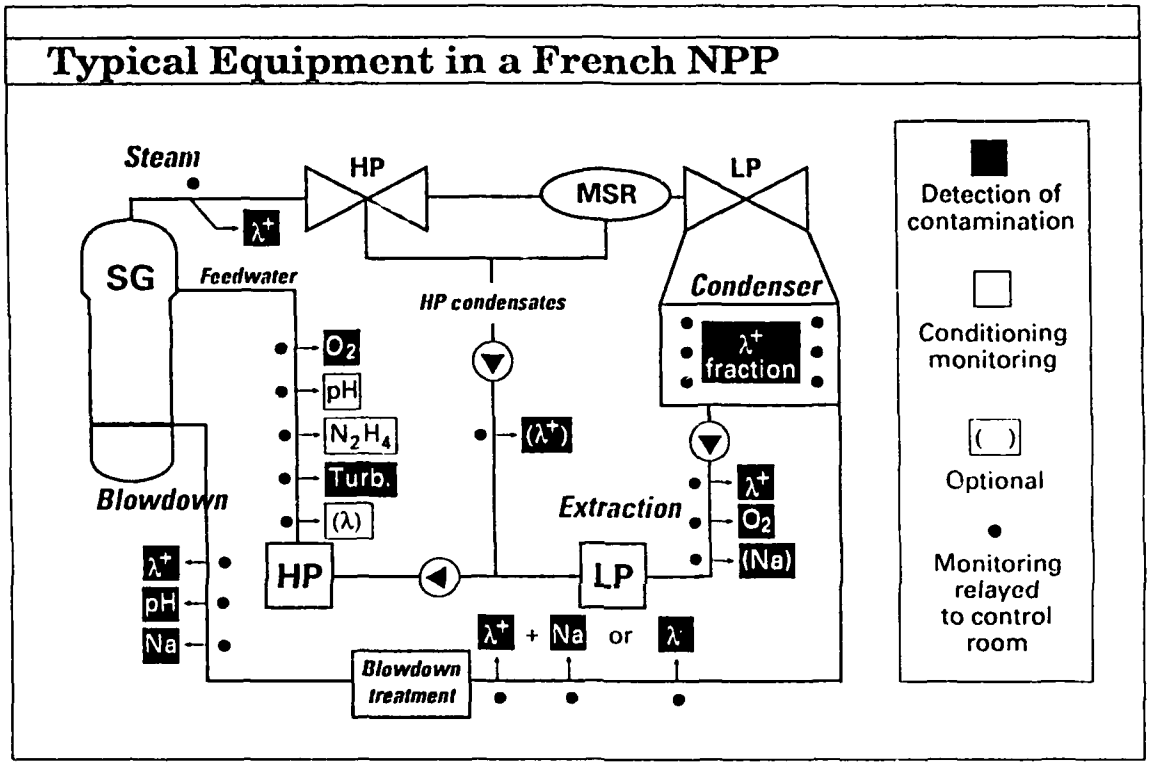

Figure 1: typical equipment in a French nuclear power plant

(a) Sensor Flow-Cell Check — FORM A 3.5

Na

Method	Frequency	Deviation
a) Atomic Absorption Spectrometry - furnace for Na < 5 $\mu g.kg^{-1}$ - flame for Na > 5 $\mu g.kg^{-1}$ OR b) Use of a standard	WEEKLY	1 $\mu g.kg^{-1}$ (AAS) 2 $\mu g.kg^{-1}$ (standard)
Action		
Physical calibration of the monitor: FORM A 3.6		

(b) Cross comparison — FORM A 3.7

Na

Method	Frequency	Deviation
Cross comparison between the monitor data at the SG blowdown	DAILY	2 $\mu g.kg^{-1}$ (AAS)
Action		
Check of the environmental conditions: FORMS A 3.2 and A 3.3		

Figure 2: typical forms of EDF guideline document for correct use of on-line monitors
(a) specification for sensor flow-cells (Na-meters) and corrective action
(b) cross comparison between Na-meters in the SG blowdown

Potential Transients, Transmission and Electrochemical Corrosion Detection

Hugh S. Isaacs
Brookhaven National Laboratory
Upton, NY 11973

Jeong-Hwan Cho
Department of Chemistry
Yonsei University
Seo-Dae-Moon Gu, Shinchon Dong 143
Seoul 120-749
Korea

Abstract

The transmission of potential along a passive metal/electrolyte interface is important in open circuit corrosion monitoring when the containment system rather than an insulated metal specimen is monitored. Potential variations have been considered for transitory and sustained corrosion processes. The observed signals are modified and delayed by the passive surface. Using a transmission line as the equivalent circuit of a pipe and incorporating the impedance characteristics of the passive-metal/solution interface, enabled a quantitative analysis of the effectiveness of corrosion monitoring methods to be carried out.

Introduction

The corrosion or open circuit potential of a metal has long been considered as a method for monitoring changes in corrosion [1,2]. The technique is inherently simple to implement requiring only a reference electrode immersed in the same environment. More recently transients or "noise" associated with the open circuit potential have also been proposed for corrosion monitoring [3].

Various changes in the corroding environment or the metal surface take place that initiate localized corrosion or alter corrosion rates. In many applications a metal sample, insulated from but having the same composition as the metal containment, is used to monitor changes in the environment chemistry. The initiation of many forms of localized corrosion depend on the interaction of mechanical or metallurgical heterogeneities in the containment metal as well as changes in the environment. Here a simple insulated insert cannot be used to monitor the onset of corrosion. The system itself must be monitored but in general, the site at which corrosion will imitate is not known. The question then arise as to the ability of a reference probe to sense changes in potential associated with the onset of corrosion and what form the potential changes may take at some distance from this site.

This paper offers a possible approach for the analysis of these issues and identifies some of the factor requiring further investigation.

Analysis of Open Circuit Potentials

(a) Small areas

The influence of changes in steady-state polarization behavior of anodic or cathodic processes on the open circuit potential have been clearly elucidated [2]. The analysis is directly applicable when there are slow changes in the potential. When the potential changes rapidly complications arise because of the important role played by the capacitance of the passive surface during non-steady state measurements. For example, following pit initiation,the open circuit potential decreases rapidly as the pit grows. The current from the pit flows to the passive surface which supplies the necessary cathodic current. The cathodic current is generally too large to be accounted for by the faradaic, oxygen reduction process. It arises from the discharge of the capacitance of the passive surface/solution interface [4,5]. Following pit repassivation, the capacitance is recharged as the potential increases. The recharging of the capacitance requires a compensating cathodic current. This cathodic current is from the slow electrochemical reduction of oxygen on the passive surface which only now becomes the significant cathodic process. The rate of this slow reaction dominates the recharging of the capacitance and thus the slow rate at which the open circuit potential increases. Based on the these processes, a quantification of the characteristic pitting transients with its rapid potential drop and slow potential increase can be made. It has also been shown that more complex transients can also be quantitatively predicted based on the impedance of the passive surface [4].

When pits do not repassivate, the rate at which the potential drops, decreases and eventually the potential becomes steady. As the rate decreases, the capacitative current contributes less and less to the required cathodic current. Here, too, the slow oxygen reduction process supplies an increasing fraction of the required cathodic current and eventually supplies all the cathodic current when the steady potential is reached.

(b) Large areas

A large area may be considered to be one where the solution resistance plays a significant role in determining the flow of current to areas supplying the required cathodic current, be it faradaic or non-faradaic. In order to simplify the analysis of potential variations detected by a reference electrode, the geometry of the large area is consider to be the inner surface of a pipe carrying water. The geometry can be represented by a one-dimensional equivalent circuit, analogous to a transmission line as shown in Fig 1. Rebars in concrete [6], pores in electrodes [7], and wires in solution [8] are also examples with analogous circuit diagrams. More complex geometries can be analyzed using finite element or other computer aided techniques.

Two positions in this semi-infinite pipe-line are important: the point where corrosion takes place and the point where the potential is monitored. The potentials and currents are

symmetrical about the point of corrosion. A transmission line terminating at this point can be substituted with appropriately halved currents flowing from the corrosion site.

The analogous electrical components of the transmission line depend on the impedance of the passive surface and the solution resistivity. They are calculated per unit length of the pipeline. The values of the impedance of the passive surface per unit length is Z, and R is the solution resistance per unit length along the axis of the pipe.

Two oversimplified potential responses are now introduced for further analysis, a simple potential step due to the start of sustained corrosion and, a single rectangular corrosion transient pulse, caused by a pitting-repassivation event. It is possible to consider more representative potential changes associated with the corrosion process. The transient is analyzed in terms of its component sine waves and summing their modified contribution at the site of detection [9].

Sustained corrosion

If sustained corrosion initiates as a step at time $t=0$ (seconds) and the impedance of the interface is considered to be a purely capacitative with a value C in units of F/cm, then a step change in potential from V_o to V_f (volts) produces a potential change along the pipe at a distance x cm from the corrosion site given by [8,10]

$$V = V_o + (V_f - V_o)\,erfc\left\{\frac{x}{2}\sqrt{\frac{RC}{t}}\right\} \qquad (1)$$

Eq 1 shows that the potential changes with time and distance has a similar form to a diffusion controlled process with a diffusion coefficient of $1/RC$. In this case the potential of the entire pipe would eventually change from V_o to V_f. Eqs 1 and 2 can be used to determine the potential changes for specific situations. For example, the rate of potential change depends on the interfacial capacity ,c (F/cm^2), water resistivity, ρ (ohm-cm), radius of the pipe r (cm) and the distance from the site of corrosion. Then

$$RC = \frac{\rho}{\pi r^2}\,2\pi r\,c = 2\frac{\rho\,c}{r} \qquad (2)$$

Taking a solution resistivity of 10000 ohm-cm, a 50 $\mu F/cm^2$ interfacial capacitance and a radius of 5 cm for the pipe, then the potential would reach a value midway between V_o and V_f within a minute at a distance of 5 cm and at 1000 cm in 2 days.

In contrast to a capacitative interface, the potential changes for a purely resistive interface are immediately transmitted along the pipe. However, the distance over which a significant potential change is seen is limited. Taking the interfacial resistance as R_i ohm/cm in series with an emf equal to the prior open circuit value V_o, and a potential of the corrosion site V_f, then the potential at a distance x from the corrosion site is given by

$$V = V_o - (V_o - V_f) \exp\left(- x \sqrt{\frac{R}{R_i}} \right) \tag{3}$$

If the interfacial resistivity is given by Ω, then

$$\frac{R}{R_i} = \frac{2\rho}{r\Omega} \tag{4}$$

Hence, from Eq. 3 the potential change at a particular distance x, increases with decreasing solution resistance, decreasing pipe diameter and increasing interfacial resistivity. Taking the interfacial resistivity of the passive surface as 10^7 ohm-cm^2 and the same solution resistivity and pipe diameter as above, a significant potential change of >10% due to the corrosion will be observed up to about 120 cm.

Transitory Corrosion

Potential transients, associated with the onset and repassivation of localized corrosion, have been considered as noise [3,10] and their frequency spectrum, a method of corrosion monitoring. In a pipe a representative transient would not be observed, as its shape has a strong dependence on the distance of the reference electrode from the site of corrosion.

Eq.1 can be expanded to analyze the changes in response of a rectangular corrosion transient in a pipe with capacitive passive interface [8,9]. In Fig. 2 a series of responses at increasing distances from the source are shown. The magnitudes of the potentials and the sharpness of the response decrease rapidly with distance. The transmission line acts as a

filter, removing the high frequency components of the originating transient, and the amplitude of all the lower frequency components decrease exponentially with distance from the source [12,13]. If such breakdown sites take place along a pipe any noise analysis will be a conglomerate of the component frequencies of these curves and the low frequency components are most important as they propagate the greatest distances.

In the case of a purely resistive interface the magnitude of the potential change again varies with distance from the corrosion site according to Eq. 2. The shape of the signal would, however, remain the same as that at the corrosion site. This assumption will be a poor approximation when rapid changes or short times are involved as the capacitative components of the interface then determines the impedance of the interface.

Discussion

The analysis shows that the potentials measured at a distance from the site of corrosion are markedly changed down a pipe. A means for calculating these effects is also given. In the examples provided, only purely resistive or capacitative interfaces were considered. With true surfaces, the impedance is a complex function of the frequency and more accurately predicted responses require Fourier analysis of the potential at the corrosion site and the summation of the modulated components for each frequency at the required distance from the source. This has been done for a passive steel surface which has a constant phase angle impedance character over a wide range of frequency [13].

The examples given do indicate that under certain circumstances, where the interface shows a high impedance, open circuit potential measurements may monitor over relatively long distances. Impedance measurement can be used to detect the location of a corrosion site (1). However, where the impedances are low and not capacitative, the range of influence of a corrosion site is restricted. The low surface impedance may arise because of rapid electrochemical reactions. These may involve general corrosion or a reversible redox reaction. In high temperature water above 200°C, stainless steel surfaces show low resistivities and high resistivities at lower temperature . No electrochemical detection of stress corrosion cracking is made at and above 200°C but transients at low temperatures due to cracking are clearly observed [14]. This example demonstrates that an understanding of the electrochemistry of a system is required both because of its effects on determining the impedance characteristics of the metal interface and the choice of corrosion monitors as well as on the possible modes and causes of corrosion.

Acknowledgments

Part of this work was performed under the auspices of the U. S. Department of Energy, Division of Material Sciences, Office of Basic Energy Sciences under Contract No. DE-AC02-76CH00016.

References

1) O. Gatty, E. C. R. Spooner, The Electrode Potential Behavior of Corroding Metals in

Aqueous Solutions, (Oxford University Press, 1938).

2. U. R. Evans, The Corrosion and Oxidation of Metals, (Edward Arnold Ltd., 1960), p. 874.

3. U. Bertocci, J. Kruger, Surf.Sci, 101 (1980): p. 608.

4. H. S. Isaacs, Y. Ishikawa J. Electrochem Soc. 132, (1985): p. 1288.

5. H. S. Isaacs, Corrosion Sci., 29, (1989): p. 313.

6. D. D. Macdonald, M. C. McKubre, M. Urquidi-Macdonald, Corrosion, 44 (1988): p. 2.

7. R. deLevie, Advances in Electrochemistry and Electrochemical Engineering, Edt P. Delahay, Vol. 6, (Interscience Publishers, 1967), p. 329.

8. H. S. Isaacs, A. J. Davenport, J. Electrochem Soc., 137,(1990): p. 2196.

9) J. H. Cho, H. S. Isaacs, A. J. Davenport, to be published.

10. H. S. Carslaw, J. C. Jaeger, Conduction of Heat in Solids, (Oxford University Press 1959), p. 69.

11. C. Gabrielli, M. Keddam. M. Krarti, C. Pallotta, Computer Acquisition and Analysis of Corrosion Data, Proceedings Vol. 85-3, M. W. Kendig, U. Bertocci, J. E. Strutts, Eds. (Pennington, NJ: The Electrochemical Society Inc., 1985), p. 210.

12. C. Fiaud, M. Keddam, A. Kadri, H. Takenouti, Electrochimica Acta, 32 (1987): p. 445.

13. J. H. Cho, H. S. Isaacs A. J. Davenport, (Pennington NJ: The Electrochemical Soc. Inc.) Meeting Vol 89-2, Hollywood, Florida, Oct.,1989, Extended Abstract 147.

14. H. S. Isaacs, Surfaces, Inhibition, and Passivation, (Pennington, NJ: The Electrochemical Society Inc., 1985), Proceedings Vol. 86-7, E. McCafferty, R. J. Brodd, Eds., p. 440.

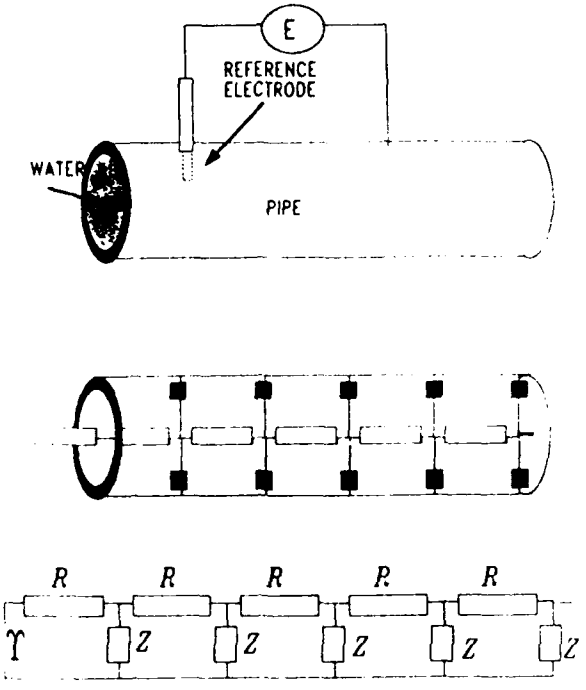

Figure 1. Transmission line equivalent circuit of a site of corrosion in a pipe. Z is the impedance of the passive surface per unit length of pipe and R is the resistance of the solution per unit length of pipe. Υ is the site of corrosion.

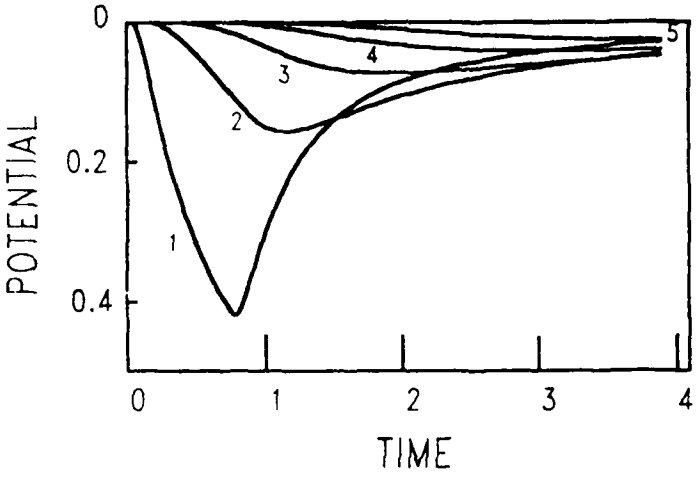

Figure 2. Simulated potential transients at distances of 1 to 5 in units of magnitude $2\sqrt{(1/RC)}$. The initiating transient was a negative rectangular potential pulse of unit magnitude lasting for 0.7 time units.

Development of Sensors for In-Situ Monitoring of Corrosion and Water Chemistry Parameters for the Electric Power Utility Industry

Digby D. Macdonald, Jing Pang, and Chun Liu
Center for Advanced Materials
The Pennsylvania State University
University Park, PA 16802, USA

Enrique Medina, José Villa, and José Bueno
Investigacion y Nuevas Tecnologias
Union Electrica Fenosa, S.A.
Capitan Haya 53, 28020 Madrid, Spain

Abstract

The in situ monitoring of the chemistry and electrochemistry of aqueous heat transport fluids in thermal (nuclear and fossil) power plants is now considered essential if adequate assessment and close control of corrosion and mass transfer phenomena are to be achieved. Because of the elevated temperatures and pressures involved, new sensor technologies are required that are able to measure key parameters under plant operating conditions for extended periods of time. In this paper, we outline a research and development program that is designed to develop practical sensors for use in thermal power plants. Our current emphasis is on sensors for measuring corrosion potential, pH, the concentrations of oxygen and hydrogen, and the electrochemical noise generated by corrosion processes at temperatures ranging from ~250°C to 500°C. The program is currently at the laboratory stage, but testing of prototype sensors in a coal-fired supercritical power plant in Spain will begin shortly.

Introduction

The effective control of corrosion and of mass transport and deposition in thermal power plants requires the continuous monitoring of key water chemistry and system parameters, most notably the pH, concentrations of oxygen and hydrogen, corrosion potential, conductivity, and corrosion activity. Normally, only a few of these parameters are monitored, and then only at ambient temperature and pressure. Consequently, only a partial picture of the development of damaging conditions in an operating plant can be obtained because the parameters under the actual operating conditions are not determined. This problem has been recognized for many years, but the lack of viable sensors for monitoring key parameters at elevated temperatures and pressures has impeded the introduction of more accurate monitoring systems.

In this paper, we outline an ongoing program to develop in situ sensors that are designed to provide more accurate monitoring of the chemistry and corrosion conditions that exist in the heat transport circuits of thermal power plants. In particular, we describe reference electrodes, pH sensors, probes for measuring hydrogen and oxygen, and electrochemical noise sensors, all of which operate at elevated temperatures and pressures and in some cases at temperatures above the supercritical temperature of water.

Chemical and Electrochemical Sensors

Reference Electrodes

From an electrochemical thermodynamic viewpoint, two of the most important parameters that should be monitored in thermal power plant heat transport circuits are the corrosion potential and pH. This is also because these two parameters define what corrosion processes are thermodynamically possible and hence provide a basis for interpreting the development of damage in terms of electrochemical reactions. To be fully effective, the reference electrode must provide a potential that is independent of the composition of the environment and which can be

placed on a viable thermodynamic scale. Thus, the electrode needs to be sufficiently rugged to withstand the high temperatures and pressures, and to survive the large changes in temperature and pressure associated with heat-up and cool-down of the system. The electroactive element of the reference electrode must be thermally and chemically stable. Furthermore, the internal solution in contact with the electroactive element must be well-defined thermodynamically, in that the activity of the potential-determining ion must be known at the temperature, pressure, and concentration of interest. The transport properties and concentration of the internal solution should be such that the liquid junction potential between the internal and external environments is reduced to as low a value as possible or can be estimated reliably. As noted above, one of the most important characteristics of any reference electrode is that its potential must be related to a rational thermodynamic scale (e.g., the standard hydrogen electrode (SHE) scale), either by calculation or by direct calibration.

The reference electrodes that have been used in high temperature aqueous systems can be divided into two classes: (i) external reference electrodes, of which the External Pressure Balanced Reference Electrode (EPBRE) is the most prominent member; and (ii) internal reference electrodes (IREs). We will discuss these two types of reference electrodes separately.

(i). External Pressure Balanced Reference Electrode. The EPBRE was introduced by Macdonald, Scott, and Wentreek[1] in 1981 in an attempt to produce a highly stable reference electrode for monitoring potentials in high temperature aqueous systems over extended periods of time. The principal problem that this design attempted to address was the thermal hydrolysis of AgCl, which was observed to occur in some internal Ag/AgCl reference electrodes at temperatures above 275°C. The calibration procedures are described elsewhere[2]. A typical design is shown in Figure 1. In the assembly shown in Figure 1, some parts fabricated from PTFE (polytetrafluoroethylene) are exposed to the high temperature aqueous environment. In our experience, once the temperature is higher than about 340°C, PTFE cannot be used because of rapid deformation under load. However, by employing alternate materials, reference electrodes have been developed that can operate under supercritical conditions (T > 374 °C). Figure 2 shows the design of an EPBRE electrode for use in supercritical aqueous systems. In this modified design, a small hole was drilled in the bottom of a zirconia tube using a laser or ultrasound. With proper care, the size of the hole can be made in the range of several micrometers. It should be emphasized here that a yttria stabilized zirconia tube must be used rather than pure ZrO_2, because of its ability to withstand the thermal shock that results from laser drilling and its high chemical resistance in high temperature aqueous solutions.

Compared with an Ag/AgCl (KCl solution) IRE of the type originally used by Greeley et al.[3], the EPBRE is less accurate due to the uncertainty in the thermal liquid junction potentials. However, EPBREs offer considerable advantages in terms of long term stability and serviceability. They are ideally suited for measuring potentials in the systems where moderate accuracy is acceptable (e.g., in corrosion and solubility studies).

(ii). Internal Reference Electrodes. For highly accurate pH measurements, internal reference electrodes (IREs) are preferred. The principal drawback of IREs based on the Ag/AgCl (KCl solution) electroactive element is thermal hydrolysis of AgCl, which generates a mixed potential rather than an equilibrium potential as well as changing the chloride activity. Nevertheless, the Ag/AgCl element is one of the most accurate and serviceable in electrochemistry, so that considerable incentive exists for retaining its use in the study of high temperature aqueous systems. The IRE used in our laboratory for pH measurements at elevated temperatures (275 - 325 °C) is shown in Figure 3. As shown, the electrode is of conventional design except for the liquid junction. The porosity of the porous zirconia plug is critical in determining the lifetime of the reference electrode. A suitable plug technology has been developed in our laboratory using yttria stabilized zirconia powder (0.1-0.3 mm, TOYOSODA). Furthermore, finely-divided AgCl powder is also contained in the reference compartment, in order to prevent the loss of silver chloride from the Ag/AgCl reference element via diffusion of $AgCl_2^-$ (for example) across the junction. No matter how well the porous junction is made, loss of chloride ions through the plug junction is the principle factor limiting the operational life of the electrode.

In some instances, it is possible to periodically calibrate a reference electrode if a second (indicating) electrode is available in the same system. For example, we routinely measure the potential of the reference electrode against that of a pH sensor in a solution of known pH at the elevated temperature of interest. Since the pH of the

"standard" solution is known, the activity of chloride ion in the reference electrode, a_{Cl^-}, can be calculated using the following equation:

$$\log a_{Cl^-} = pH - \frac{F}{2.303\,RT}(E^\circ_{Hg/HgO} - E^\circ_{Ag/AgCl,Cl^-} - E_{meas} + E_J) + \frac{1}{2}\log a_{H2O} \quad (1)$$

where $E^\circ_{Hg/HgO}$ is the standard potential (vs SHE) of the internal Hg/HgO couple in the pH sensor, $E^\circ_{Ag/AgCl}$ is the standard potential (vs SHE) of the Ag/AgCl couple, E_{meas} is the measured potential, E_J is the liquid junction potential, and a_{H_2O} is the activity of water. We have found that this technique can help not only to increase the operational life of an IRE, but also to increase the accuracy of the measurements.

In an attempt to immobilize the chloride in the reference electrode, Hettiarachchi and Macdonald[4] explored the use of polymer electrolytes based on high temperature epoxy matrices containing aqueous KCl.. The design is shown in Figure 4. The electrolyte sets as a rubber, with the result that the electrode within the pressure vessel is easily manipulated to produce the optimum configuration. The performance of this electrode is discussed elsewhere[2]. Because the thermodynamic properties of KCl in the electrolyte are ill-defined, it is not possible to calculate the potential a priori from theory. Nevertheless, the electrode is readily calibrated and has provided stable performance over many hours at temperatures as high as 275°C. In one instance, the polymer electrolyte reference electrode was inadvertently taken to ~340°C for a short time with no apparent ill-effects.

Yttria-Stabilized Zirconia pH Sensor

Over the past decade, considerable interest has arisen in using oxide ion-conducting ceramic membrane electrodes based on yttria stabilized zirconia to measure pH in high temperature aqueous systems[4-8]. The most popular of these devices employs a metal/metal oxide internal reference element to fix the activity of oxygen vacancies on the inside surface of the ceramic membrane. Details of the thermodynamic analysis of this type of electrode can be found in References 7 and 8. The design of the Hg/HgO/$ZrO_2(Y_2O_3)$ sensor currently being used in our laboratory is shown in Figure 5. In the assembly shown in Figure 5, the zirconia powder and ceramic cement serve to prevent the Hg/HgO mixture from leaking from the electrode at high operating temperatures. We also found great variability in the response time of the sensors, which we attribute to differences in the electrical properties of the membranes. If the response time of the sensor to a change in pH was excessively long (several hours), the sensor was discarded. The pH can be calculated from the potential (E_{meas}) measured between the pH sensor and the reference electrode (IRE) according to the following equation.

$$pH = \frac{F}{2.303\,RT}(E^\circ_{Hg/HgO} - E^\circ_{Ag/AgCl,Cl^-} - E_{meas} + E_J) - \frac{1}{2}\log a_{H2O} + \log a_{Cl^-} \quad (2)$$

The symbols in the above equation are defined as in Equation 1. The standard potentials of Hg/HgO and Ag/AgCl were calculated from thermodynamic data given by Naumov et al[9]. The calculation of the liquid junction potential can be found in Reference 2, although a more accurate procedure is currently being employed in our laboratory at The Pennsylvania State University. We emphasize that the liquid junction potential can be a significant correction and, under certain conditions, a discrepancy as large as 1 unit of pH can result from this source.

Both internal and external reference electrodes can be employed with the pH sensor to make pH measurements. Figure 6 presents typical measured variation of pH as a function of temperature for 0.01 M KOH solution[2]. The EPBRE reference electrode and a YSZ sensor were used for these measurements. This work, which was carried out by one of the authors while at SRI International[2], is the first attempt to extend pH measurements to temperatures above the critical temperature of water. Figure 7 presents measured titration curves for $NaOH/H_2SO_4$ solutions at temperatures of 275, 300 and 325°C. In this set of measurements, an internal reference electrode (as described in Figure 3) and YSZ sensor were used. The reference electrode was calibrated with a "standard" solution prior to each measurement.

Electrochemical Noise Monitor

We have developed a technique for monitoring various corrosion processes by analyzing the noise in the coupling current between two identical carbon steel specimens. Because specific corrosion processes can be associated with more-or-less unique conditions that exist in the heat transport circuit, it is important that the electrochemical noise monitor be used in conjunction with the other monitors, such as those for measuring oxygen, hydrogen, pH, and corrosion potential.

All general and localized corrosion processes, such as general attack, pitting, crevice corrosion, or stress corrosion cracking, result in fluctuations in the free corrosion potential and in the anodic and cathodic currents. These fluctuations are observed as electrochemical "noise" that is thought to contain significant information about both the rate and mechanisms of attack. Some researchers believe that the electrochemical noise is principally due to the formation of hydrogen bubbles[10] at least in the case of general corrosion. Extensive work has been reported on analyzing electrochemical noise from pitting and crevice corrosion[11-15], stress corrosion cracking[16-18], and inhibited systems[19]. In many cases the experiments are primitive in nature, and viable theories for the origin of the noise have yet to be developed[20]. After reviewing the literature, we selected a bi-electrode design for the electrochemical noise analyzer, because of its simplicity and readiness for on-site application. This approach differs from many other designs found in literature[21]. The two electrodes are identical and the electrochemical noise at the free corrosion potential is measured without applying an external perturbation.

The apparatus consisted of a high temperature/high pressure autoclave, in which the bi-electrode is placed through an electrically-insulated fitting. An electrolyte solution reservoir and a recirculation loop provided the simulated heat transport fluid of an operating power plant conditions. A magnetic driver was used to agitate the fluid inside the autoclave to simulate the flow of the heat transport fluid in power plant circuits. The bi-electrode was fabricated from carbon steel, in the form of a pair of rods of ϕ1.5 mm x 40 mm. The electrodes were identical in dimensions to a precision of 0.01 mm. The electronic circuit is shielded so that electrical noise from the environment are adequently avoided (see Figure 8). The electrochemical noise analyzer processes only the noise signal, because any DC component (defined here as $f < 1.6$ Hz) of the noise signal is filtered. Note that if the electrodes were truly identical, then the DC component should be zero. The noise is first amplified using an analog amplifier, then filtered using a band-pass filter. The signals are finally processed by a RMS (Root Mean Square) module in order to provide a DC output that is a measure of the amplitude of the signal. Theoretically, a time-invariant component would only be obtained if the noise was a sinusoid of constant amplitude. In practice, the noise has a very complex structure so that the output from the RMS module is itself a time-varying signal.

Below, we describe the use of this device to study the electrochemical noise associated with the corrosion of carbon steel in the high temperature/high pressure water saturated with oxygen. Figure 9 shows the electrochemical noise as a function of time and corresponding temperature. The corrosion noise level is found to increase with temperature. This is expected because the high temperature increases the activity of the corrosion process. It is also found that the relation between the corrosion noise level and the temperature is reversible; in another words, the noise level increases when the temperature increases, and decreases when the temperature decreases with little apparent hysteresis. This phenomenon indicates that, under the present conditions (constant oxygen concentration in the autoclave), only the temperature determines the level of the corrosion-induced noise. Stirring is also found to greatly increase the noise level (Figure 10). This is also expected, because stirring enhances the mass transfer to the metal surface. Finally, the noise level is found to depend on the bandwidth of the filter. In one set of experiments, the lower roll-off frequency was fixed at 1.6 Hz while the upper roll-off frequency was set at 100 Hz, 1 kHz, or 10 kHz. No significant difference was detected in the noise signal when the upper roll-off frequency was changed from 1 kHz to 10 kHz, indicating that components of frequency greater than 1 kHz are not present to any significant extent in the noise. On the other hand, a significant increase is observed in the noise signal as the upper roll-off frequency was changed from 10 Hz to 100 Hz, which indicates that significant noise components with frequency in the 1.6-100 Hz range are generated at the interface during the corrosion of carbon steel in oxygenated water at 237^{o}C (see Figure 11).

Hydrogen Monitor

A technique, that is both rugged and sensitive, for measuring low concentrations of hydrogen in high temperature aqueous systems, was developed a number of years ago[22]. The sensor itself consists of two wires, one palladium and the other platinum, wound around an insulated mandrel (Figure 12). An external box of electronics automatically compares the resistance of the Pd wire with that of the Pt wire (not shown in the figure). The resistance of the Pd wire is determined by both the hydrogen content of the medium (and hence of the metal due to absorption of H) and the temperature, whereas that of the Pt depends only on temperature, because platinum does not absorb significant amounts of hydrogen from aqueous solutions. However, the temperature coefficients of the resistances of Pt and Pd are sufficiently different that compensation is necessary in order to isolate the change in resistance due to hydrogen absorption alone. One function of the electronic package is to correct for this difference, so that the relative changes in the resistances of the two wires, as indicated by a voltage output (Vc), reflect only the changes due to hydrogen. The sensitivity of this monitor was explored[23] by measuring the concentration of hydrogen in 0.1 M $B(OH)_3$ solution at 275°C, as shown in Figure 13. The sensitivity of this first-generation monitor was such that 10 ppb of dissolved hydrogen could be detected. The sensitivity has been improved to 1 ppb, and its operating temperature has been extended to 350°C. We see no fundamental reason why the sensitivity cannot be increased to the sub-ppb level, and the temperature range extended to at least 400°C. Indeed, a hydrogen sensor of this type has been tested recently at 350°C in an in-reactor loop at an experimental nuclear reactor in Canada[23].

In the solutions that had previously contained oxygen, the response to the addition of hydrogen was found to be much slower owing to the presence of adsorbed oxygen on the palladium surface[23]. Apparently, the sensor does not respond to the addition of hydrogen until the adsorbed oxygen is desorbed from the palladium surface, but, once this has happened, the sensor responds rapidly. We do not see this as a major problem for fossil power plants, because oxygen and hydrogen are unlikely to coexist for a significant time, particularly in the presence of hydrazine, whereas they do so in a BWR because of the radiolysis of water in the reactor core.

Oxygen Monitor

In situ measurement of oxygen in steam cycle environments has proven to be very difficult, particularly in the elevated temperature regions where corrosion damage is most likely to occur. No commercial instrument that we know of is capable of measuring oxygen directly in the steam phase, at either high subcritical or supercritical temperatures. However, we have tested a sensor that can be used to determine the oxygen concentration in both steam and liquid phases or in supercritical fluids. Although this technique is strictly ex situ in nature, because of the need to sample the fluid through a sampling line, it provides a continuous output with minimum transit time from the steam cycle environment, and it does not involve condensing the steam. Accordingly, the method avoids the concomitant problem of oxygen partitioning between the vapor phase and the condensate.

The technique used to measure oxygen in high temperature aqueous fluid is an adaptation of the solid electrolyte method commonly employed to measure oxygen in gases. The sensor makes use of a potentiometric cell of the type

$$\text{Air(Pt)/}ZrO_2(Y_2O_3)\text{/(Pt)Steam} + O_2 \qquad (3)$$

where the electrolyte is an oxygen ion conducting yttria-stabilized zirconia of the same type as used for our pH sensors. Both sides of the zirconia sensor are coated with porous platinum, and one side is exposed to ambient air as a reference (P_{O_2} = 0.21 atm) while the other side is exposed to the steam. The equilibria that occur at the interfaces can be written as

$$1/2\ O_2 + V_O^{\cdot\cdot} + 2\ e'(Pt) = O_O \qquad (4)$$

where $V_O^{\cdot\cdot}$ and O_O are an oxygen vacancy and an oxygen ion in a normal oxygen lattice site, respectively, and e' represents an electron in the porous platinum. The activity of O_O is unity (by definition), and the potential across the ceramic/environmental interface is given by the Nernst equation

$$E = E^{\circ}_{O2/O_o} - \frac{2.303RT}{2F}\log\left[\frac{1}{P_{O2}^{1/2}a_{V_o}}\right] \quad (5)$$

where E°_{O2/O_o} is the standard potential for the O_2/O_O couple, P_{O_2} is the partial pressure of oxygen, and a_{V_o} is the activity of oxygen vacancies at the interface. Provided that the ceramic electrolyte is in equilibrium with respect to the oxygen vacancies, the potential difference between the two platinum electrodes is given by

$$\Delta E = \frac{2.303RT}{4F}\log\left[\frac{P_{O2}}{P^{r}_{O2}}\right] \quad (6)$$

where $P^{r}_{O_2}$ is the reference partial pressure of oxygen (0.21 atm). Thus, by rearranging Equation 6, we obtain

$$P_{O2} = P^{r}_{O2}\exp\left[\frac{4F\Delta E}{RT}\right] \quad (7)$$

so that by measuring ΔE and knowing $P^{r}_{O_2}$ and T, we can determine the partial pressure of oxygen in the steam. The sensitivity of this technique is such that oxygen levels in the sub-ppb range are easily measured. Figure 14 shows a calibration curve of this type of oxygen sensor against oxygen in steam/air mixtures[24]. In this particular experiment known amounts of air were metered into steam from a boiler from a building central heating system. Although the temperature of the steam was not monitored, the sensor operated at ~700°C which is the temperature (T = 973 K) that is substituted into Equation (7) when determining P_{O_2}.

Summary and Conclusions

In this paper, we describe the use of EPBRE and IRE reference electrodes, the YSZ pH sensor, a noise monitor, a hydrogen monitor, and an oxygen monitor for the in situ monitoring of corrosion and water chemistry parameters in subcritical and supercritical aqueous systems. The construction and operation of these sensors are described. In our laboratories, we are working on an ongoing program to develop these in situ monitors, which will be placed in a by-pass loop connected to the heat transport circuit of a coal-fired power plant in Spain. The working temperature is in the range of about 250-500°C, and the working pressure is approximately 2000 psi. The sensors (besides those described above, a fracture monitor and a conductivity sensor are also being developed in this program) are currently being tested in our laboratory and at SRI International in Menlo Park, CA. To our knowledge, this is the first attempt to simultaneously monitor these chemical and electrochemical parameters in situ under high temperature/high pressure conditions. Based on our current data, we draw the following conclusions:

1. EPBREs are serviceable in both subcritical and supercritical aqueous systems. If an accurate calibration can be performed, external pressure balanced electrodes are convenient devices for monitoring electrochemical potentials over a wide range of temperature and pressure.

2. IREs are capable of yielding accurate potential measurements because they do not involve a thermal liquid junction potential. However, for long term studies, it is necessary to calibrate IRE on-line to maintain the accuracy of the potential measurement.

3. The YSZ pH sensor is a convenient and reliable device for measuring pH in both subcritical and supercritical aqueous systems.

4. Corrosion of carbon steel in oxygenated water at elevated temperatures and pressures can be monitored by analyzing the electrochemical noise.

5. The hydrogen monitor is sensitive to sub-ppb levels of hydrogen, and it can be used to measure the concentration of hydrogen in subcritical and possibly in supercritical aqueous systems.

6. Although the oxygen sensor is an ex situ monitor, it can be used to measure oxygen concentrations accurately and rapidly in steam environments at subcritical and supercritical environments.

Acknowledgments

The authors acknowledge support of this work by the Union Electrica-Fenosa in Madrid, Spain, through a number of contracts over several years. The authors are also grateful to Dr. Rosa Crovetto for her contributions in the early stage of this project.

References

1. D.D.Macdonald, A.C.Scott, and P.R.Wentrcek, J.Electrochem. Soc. 126 (1979): p. 908.

2. D.D.Macdonald, S.Hettiarachchi, H.Song, K.Makela, R.Emerson, and M.Ben-Haim, J. Solution Chemistry, 21 8 (1992): p. 849.

3. R.S.Greeley, W.T.Smith, R.W.Stoughton, and M.H.Lietzke, J. Phys. Chem. 64 (1960): p. 652, p. 1445, and p. 1861.

4. S.Hettiarachchi, D.D.Macdonald, J. Electrochem. Soc. 131 (1985): p. 2206.

5. Z.Nagy, and R.M.Yonco, J. Electrochem. Soc. 133 (1986): p. 2232.

6. S.Hettiarachchi, P.Kedzierzawski, and D.D.Macdonald, J. Electrochem. Soc. 132 (1985): p. 1866.

7. D.D.Macdonald, S.Hettiarachchi, and S.J.Lenhart, J. Solution Chem. 17 (1988): p. 719.

8. D.D.Macdonald, H.Song, and S.Hettiarachchi,, Acidity Studies on High Temperature Solutions Simulating PWR Crevice Environments. Final Report for Research Project RPS407-27 from Electric Power Research Institute, August 1991.

9. G.B.Naumov, B.N.Ryzhenko, and I.L.Khodakovsky, Handbook of Thermodynamic Data (Translated by G.J.Soleimani, U.S.Geological Survey), Moscow, Atomizdat (1971).

10. C. Gabrielli, F. Huet, M. Keddam and M. Macias, Corrosion 86 (NACE) (1986): p. 507.

11. K. Hladky and J. L. Dawson, Corros. Sci., 21 4 (1981): p. 317.

12. J. L. Dawson, D. M. Farrell, P. J. Aylott and K. Hladky, Corrosion 89 (NACE) (April 17-21, 1989): Paper No. 31.

13. M. Kendig and D. Anderson, Corrosion, 48 3 (1992): p. 178.

14. U. Bertocci, J. L. Mullen and Y- X. Ye, Proceedings of the Fifth International Symposium on Passivity of Metals and Semiconductors, ed. M. Froment, Elsevier Science Publishers B. V., Amsterdam, New York, Elsevier (1983): p. 229.

15. J. Flis, J. L. Dawson, J. Gill and G. C. Wood, Corros. Sci. 32 8 (1991): p. 877.

16. D. A. Eden, and A. N. Rothwell, Corrosion/92, The NACE Annual Conference and Corrosion Show (1992): Paper No. 292.

17. D. A. Eden, A. N. Rothwell and J. L. Dawson, Corrosion 91, The NACE Annual Conference and Corrosion Show (1991): Paper No. 444.

18. J. Stewart, D. B. Wells, P. M. Scott and D. E. Williams, Corros. Sci. 33 (1991): p. 73.

19. C. Monticelli, G. Brunoro, A. Frignani and G. Trabanelli, J. Electrochem. Soc., 139 3 (1992): p. 706.

20. C. Gabrielli, F. Huet and M. Keddam, in Electrochemical and Optical Techniques for the Study and Monitoring of Metallic Corrosion, ed. M. G. S. Ferreira and C. A. Melendres, pb. Kluwer Academic Publishers (1991): p. 135.

21. C. Gabrielli, F. Huet and M. Keddam "Real time measurement of electrolyte resistance fluctuations", J. Electrochem. Soc., 138.12 (1991): p. L82.

22. D.D.Macdonald, M.C.H.McKubre, A.C.Scott, and P.R.Wentrcek, I&CE Fundamentals, 20 (1981): p. 290.

23 D. McCraken, and M.C.H. McKubre, private communication (1990).

24. D.D.Macdonald, and M. Urquid-Macdonald, Development of Corrosion and Chemistry Monitors for Fossil-Fueled Power Stations. Proposal for Research PYC 90-310 (1990) for Union Electrica-Fenosa (UEF), Spain.

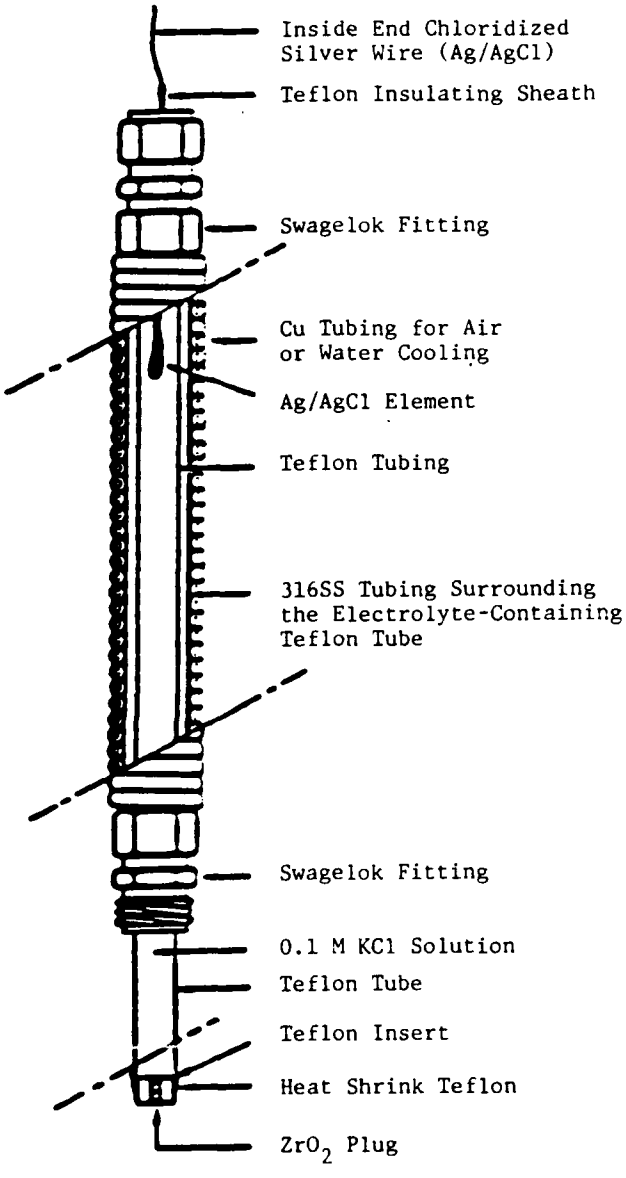

Figure 1. External Pressure Balanced Reference Electrode assembly.

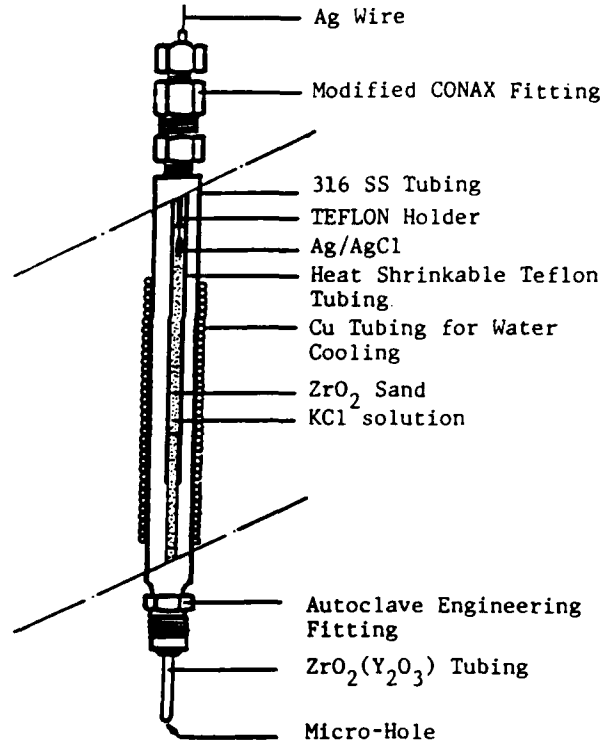

Figure 2. The EPBREs used for supercritical aqueous systems.

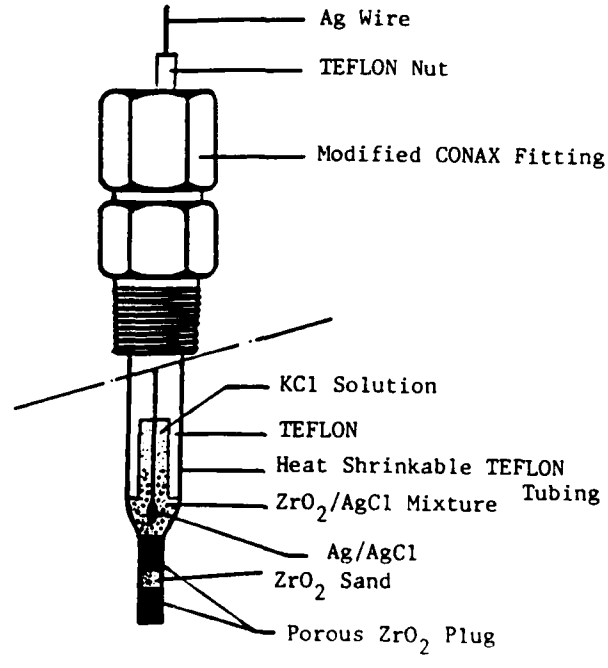

Figure 3. The Ag/AgCl internal reference electrode assembly.

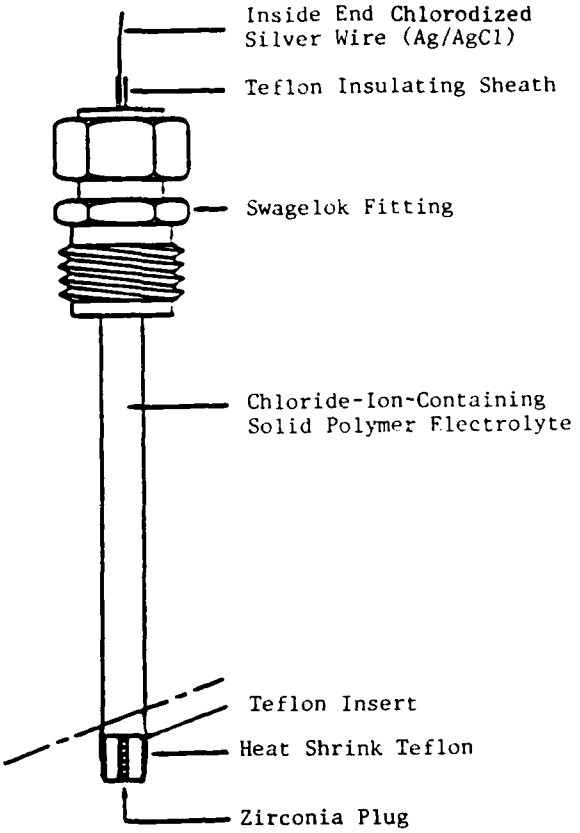

Figure 4. Solid polymer electrolyte-based internal reference electrode.

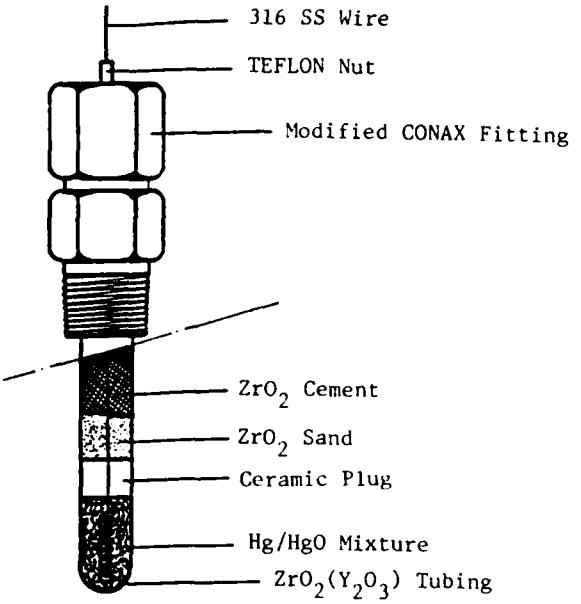

Figure 5. The $Hg/HgO/ZrO_2(Y_2O_3)$ ceramic membrane pH electrode.

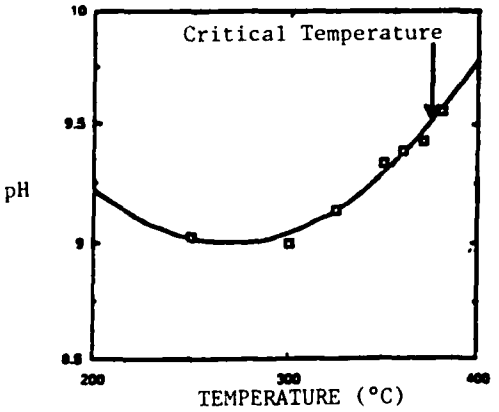

Figure 6. Variation of pH as a function of temperature for 0.01 M KOH solution. Note that the highest temperature is just above the critical point.

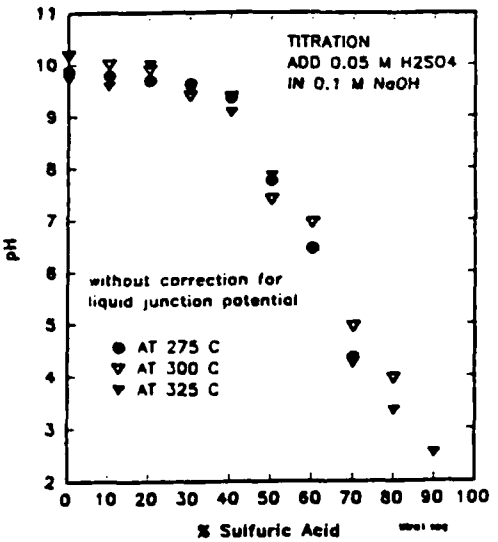

Figure 7. Titration data for $NaOH/H_2SO_4$ solutions at 275, 300 and 325°C. The 0.05 mol/l (25°C) H_2SO_4 solution was added into the 0.1 mol/l NaOH solution by certain weight percentage as indicated in X-axis.

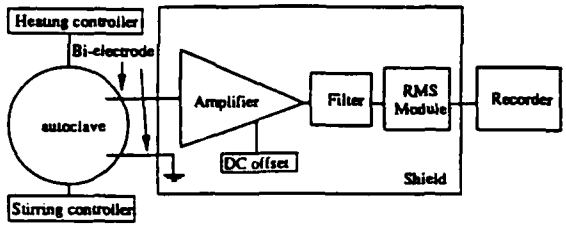

Figure 8. Schematic of the apparatus for electrochemical noise analysis.

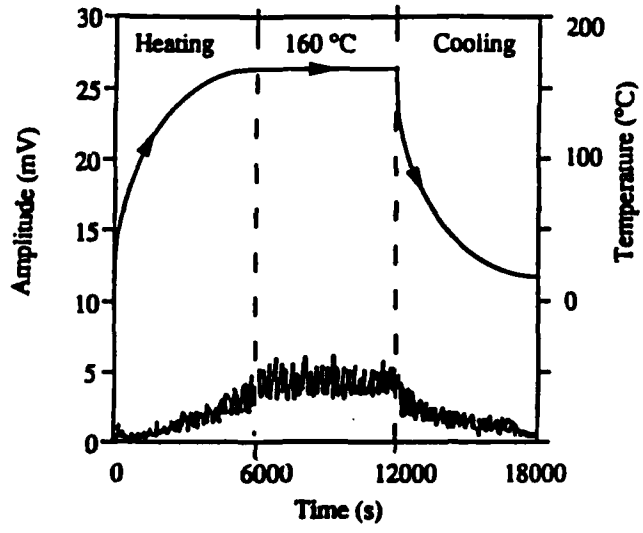

Figure 9. Evolution of electrochemical noise induced by corrosion of carbon steel during a heating-cooling cycle (oxygen pressure = 40 psi, in-vessel pressure = 1200 psi, gain = 1000, upper roll-off frequency = 10 Hz).

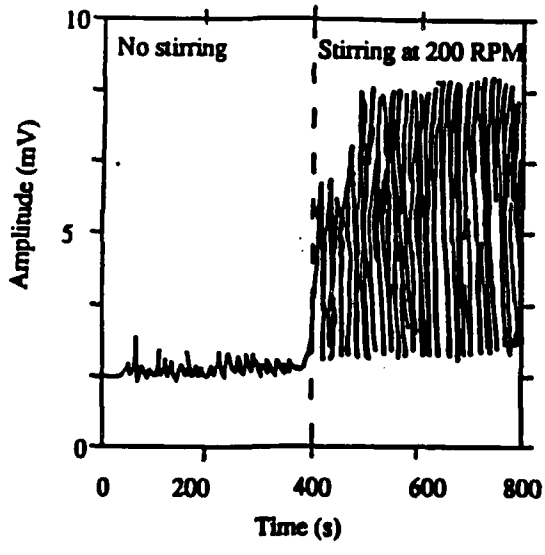

Figure 10. Effect of stirring on the electrochemical noise induced by corrosion of carbon steel in water at 244°C (oxygen pressure = 40 psi, in-vessel pressure = 1200 psi, gain = 1000, upper roll-off frequency = 10 Hz).

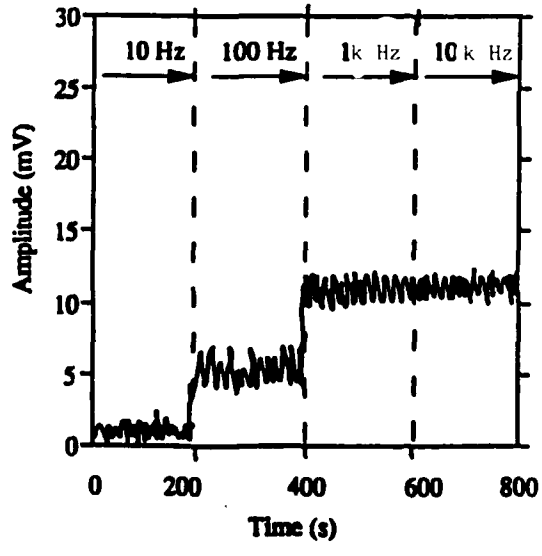

Figure 11. Dependence of RMS noise amplitude on the lower roll-off frequency for the corrosion of carbon steel in water at 237°C (oxygen pressure = 40 psi, in-vessel pressure = 1200 psi, gain = 1000, upper roll-off frequency = 10 Hz).

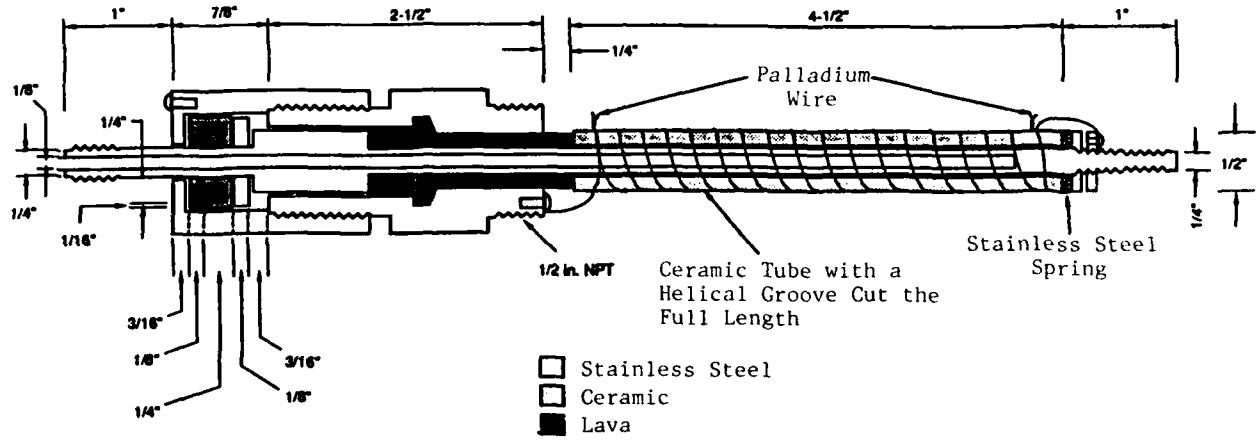

Figure 12. Temperature-compensated palladium resistance probe for monitoring hydrogen in high temperature aqueous systems.

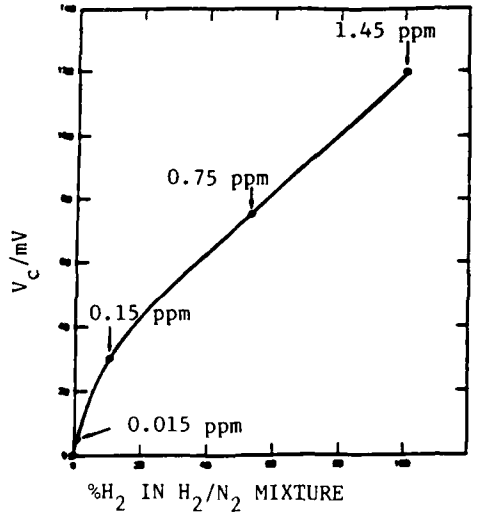

Figure 13. Calibration curve for the hydrogen monitor in 0.1 M boric acid solution at 275 °C (The hydrogen concentrations are calculated using Henry's law).

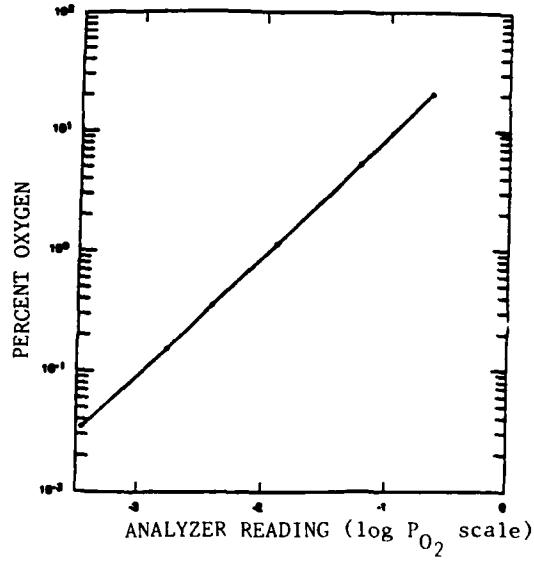

Figure 14. Calibration of oxygen analyzer against oxygen in steam/air mixtures (initial analyzer setting at 0.035% oxygen).

An Electrochemical Sensor for Oxygen and pH in Aqueous Systems

Charles B. Alcock, Li Wang, Baozhen Li and Nikesh Bakshi
Center for Sensor Materials
University of Notre Dame
Notre Dame, IN 46556

Abstract

A new electrochemical sensor which is based on the use of a highly conductive solid electrolyte, lanthanum fluoride containing a small amount of strontium or barium fluoride in solid solution, is described. The electrochemical cell consists of a one-end closed tubular electrolyte with a thin layer of noble metal electrode on its outer surface, and a condensed phase internal reference electrode sealed inside. The combination has been shown to undergo negligible corrosion during exposure in water up to 523 K and 54 atmosphere pressure. The testing cell for the sensor is constructed with pyrex glass for temperatures below 373 K and with stainless steel for temperatures above 373 K, so that the device is capable of on-line use up to these temperatures and pressures.

The determination of the oxygen chemical potential and pH in aqueous solutions employing the following cells

$$\text{Pt, Ag/Ag}_2\text{O} \mid 5\%\ \text{La}_2\text{O}_3 + \text{La}_{0.95}\text{Ba}_{0.05}\text{F}_{2.95} \mid \text{H}_2\text{O}\ (\text{O}_2/\text{Ar}), \text{Pt}$$

and

$$\text{Pt, Zr/ZrH}_{1+x} \mid \text{La}_{0.95}\text{Sr}_{0.05}\text{F}_{2.95} \mid \text{H}_2\text{O (pH buffer), Pt}$$

has been conducted over the temperature range 310-464 K. The results demonstrate a linear response of cell emf to pH and to oxygen chemical potential (RT Log(p_{O2})) at each given temperature, but there is a cross interaction between these two variables.

Key terms: electrochemical sensor, oxygen, pH, lanthanum fluoride, water.

Introduction

Corrosion-related phenomena in the cooling systems of power plants are closely related to the oxygen electrochemical potential and pH of the solution. In plant environments, oxygen and pH are usually monitored at ambient temperature on a "grab" sample basis (1,2). In this procedure, it is difficult to ensure that the sample thus analyzed is representative of the solution in the high temperature environment, so it is desirable to develop probes for in-situ oxygen and pH measurements. The widely used oxygen sensors with stabilized zirconia as the solid electrolyte are not suitable for use at temperatures below 623 K due to insufficient electrical conductance of the stabilized zirconia, which causes slow response and even unstable emf readings of the sensor. Great efforts have been made to lower the operating temperature of such oxygen sensors by increasing the electrical conductance of the electrolyte or by developing new electrolytes. The pH measurement of aqueous systems has long been investigated for monitoring and controlling the quality of water and steam in power plants (3-5). However, a suitable, well-defined solid state oxygen or pH sensor has not been established for these requirements. In this paper, a new electrochemical oxygen and pH sensor based on LaF_3-SrF_2 or LaF_3-BaF_2 solid solutions as an electrolyte is reported for the on-line monitoring of the cooling system in power plants. This type of electrolyte is a fluorine ion conductor and its conductivity is much higher than that of stabilized zirconia at temperatures below 523 K (6, 8, 9).

A typical electrochemical sensor arrangement used in this work can be described as:

$$Pt, Ag/Ag_2O \mid La_{0.95}Ba_{0.05}F_{2.95} + 5\%\ La_2O_3 \mid H_2O\ (O_2+Ar), pH, Pt \qquad (I)$$

In this sensor, the internal reference electrode, the mixture of Ag/Ag_2O, defines the oxygen chemical potential of the reference electrode at each given temperature through the chemical equilibration between Ag and Ag_2O:

$$Ag_2O = 2Ag + 1/2O_2 \qquad K = p_{O2}^{-1/2} = \exp(-\frac{\Delta G^o}{RT}) \qquad (1)$$

For a given content of dissolved oxygen and pH level in the aqueous solution, i. e. in the working electrode, there is a corresponding oxygen chemical potential. The difference between the two oxygen chemical potentials in the two electrodes will establish a corresponding emf across the electrolyte tube.

The use of a fluorine-ion conducting electrolyte for oxygen determination is based on the principle of converting a fluorine potential difference into an oxygen potential difference by including an appropriately dispersed oxide in the electrolyte. In cell (I) the chemical potential conversion is realized through the reaction

$$2/3\ LaF_3 + 1/2\ O_2(g) = 1/3\ La_2O_3 + F_2\ (g) \qquad (2)$$

which has an equilibrium constant

$$K = \frac{(a_{La_2O_3})^{1/3}\ (p_{F_2})}{(a_{LaF_3})^{2/3}\ (p_{O_2})^{1/2}} \qquad (3)$$

Since the activities of La_2O_3 and LaF_3 are constant in the electrolyte, the partial pressures of oxygen and fluorine at the electrode/electrolyte interfaces are related according to

$$p_{F_2} = K'\ p_{O_2}^{1/2} \qquad (4)$$

According to the Nernst equation, the cell emf generated by the fluorine potential difference across electrolyte is given by

$$E = \frac{RT}{2F}\ \ln(\frac{p''_{F_2}}{p'_{F_2}}) = \frac{RT}{2F}\ \ln(\frac{((p_{O_2})_{aq})^{1/2}}{((p_{O_2})_{Ag/Ag_2O})^{1/2}}) = \frac{RT}{4F}\ \ln(\frac{(p_{O_2})_{aq}}{(p_{O_2})_{Ag/Ag_2O}}) \qquad (5)$$

where $(p_{O_2})_{aq}$ represents the oxygen partial pressure equilibrated with the aqueous solution, and $(p_{O_2})_{Ag/Ag_2O}$, the equilibrium oxygen partial pressure of Ag and Ag_2O. Therefore, cell (I) is a true oxygen concentration cell, and the fluoride electrolyte can be used for oxygen chemical potential determination with the incorporation of an appropriate oxide.

Experimental

The tubular electrolytes were prepared by a slip-casting technique (10). To fabricate these electrolyte tubes, finely ground oxide-doped fluoride powders in a liquid suspension, or slip, were poured into a porous mold which absorbed the liquid and left a layer of electrolyte deposited on the wall. When a desired thickness of electrolyte had been obtained, the excess liquid was poured out. The deposited casting was dried and removed from the mold and then sintered at about 1470 K in purified argon for 12 hours. After sintering, the tubular fluoride solid solution was examined by

X-ray diffraction to confirm the presence of the expected phases.

To prepare a solid internal reference electrode, a mixture of metal/metal oxide or metal/metal hydride powders was tightly packed in the electrolyte tube. A layer of porous platinum was deposited by pasting a layer of platinum paint and then heating it at 1200 K for one hour, or a Pd/Au thin film was sputtered on the outside surface of the electrolyte tube as sensing electrode to achieve a proper electrical contact between electrolyte and working electrode. Platinum wire was used for the electrical leads of the emf measurement. Figure 1 is a schematic drawing of the testing cell which was mainly operated at temperatures below 373 K. The testing cell is mainly constructed with pyrex glass, and the electrolyte tube was connected to the glass testing cell using Swagelok. The reference electrode was sealed in the electrolyte tube with epoxy cement. The pyrex parts of the testing cell were replaced by stainless steel for measurements at higher temperatures and higher pressures.

The oxygen chemical potential in water was controlled by purging O_2/Ar gas mixtures through the water, the composition of the gas phase being controlled by MKS mass flow meters and controllers. Standard commercial pH buffer solutions were used to control the pH values of water. Cell emfs were recorded at 10 minute intervals until a stable value was obtained. The reproducibility of the cell emf was checked by randomly changing the temperature and comparing the original emf value to the new one obtained when the system was returned to the original temperature and by comparing the results from two identical sensors under the same condition but separately prepared and the results were found to be reproducible within ± 3% of the absolute value of the sensor output.

Experimental Results

Stability of Electrolytes in Water

The solid state electrochemical sensors which have been developed are expected to operate at high temperature and in pressurized water for an extended period of time, and hence the chemical and physical long-term stability of the electrolyte in water is a major concern. The corrosion tests have been performed through monitoring the changes of weight, electrical conductivity, X-ray diffraction pattern, and surface morphology of the selected electrolytes in water from 373 K to 523 K.

The LaF_3-rich solid solutions were found to be very stable in water at temperatures up to 523 K. No substantial dissolution, corrosion and electrical property changes were observed after being exposed to pressurized water for up to two weeks, which is believed adequate for the preliminary sensor development in the laboratory scale. Among these fluoride electrolytes tested, $La_{0.95}Sr_{0.05}F_{2.95}$ and $La_{0.95}Ba_{0.05}F_{2.95}$ have the highest stability and higher electrical conductivity than other solutions in the LaF_3-SrF_2 or LaF_3-BaF_2 system. Hence they were selected as the electrolyte for electrochemical oxygen and pH sensors for the aqueous system.

Development of Oxygen Sensors

With the design as shown in Figure 1, the electrochemical oxygen sensor responded to the change of oxygen partial pressure in water quite rapidly (it took about 10 to 15 minutes to achieve a stable emf) and the measured emf showed a logarithmic dependence on oxygen partial pressure at 366 K and 333 K (Figure 2). The reproducibility of the sensors prepared separately was within 10 mV, which is about 3% of the absolute value of the sensor output.

The investigation was mainly focused on the low temperature region (below 373 K). However, a few measurements were carried out at high temperatures above 373 K. Figure 3 gives two

examples of the response of cell emf to the change of oxygen partial pressure equilibrated with water at two temperatures. The cell emf followed the oxygen partial pressure change in water closely. With the variation of the oxygen partial pressure from one value to another, the emf changed accordingly from one stable value to another.

Development of pH Sensors with Oxide Electrodes

In the previous section, using oxide-doped $La_{0.95}Ba_{0.05}F_{2.95}$ fluoride electrolyte for oxygen determination in water has been described. A sensor identical to that used for oxygen determination was assembled to check the response of emf to the pH level in solutions. Figure 4 shows the rapid response of emf to a sudden change of the pH in solution at 360 K for cell (I). The sensor therefore responds to the change of both oxygen and pH level. In order to clarify this interaction between oxygen and pH determination, the variations of cell emf with oxygen partial pressure at different pH levels (pH = 7, 8, and 9) and the variations of cell emf with pH at different oxygen partial pressures were investigated at a fixed temperature (339 K) for cell (I). The results are shown in Figure 5 and 6. The contributions to the cell emf from oxygen chemical potential and pH of the solution were derived as equation (6) through mathematical treatment

$$\text{Emf (mV)} = 39.37 + 52.62 \log p_{O_2} - 47.4\ \text{pH} \quad (p_{O_2} = 0.09 - 0.91, \text{pH} = 7 - 9) \qquad (6)$$

This clearly shows the interaction between the oxygen partial pressure and pH in the solution. Further research is needed to build models to interpret the exact physical meanings of these coefficients of the equation.

pH Sensors with Hydride Electrodes

Cell (I) has shown rapid response to both oxygen chemical potential and pH of the aqueous solutions. This character of the sensor may result from the effect of the oxide dispersant in the electrolyte and the use of a metal/metal oxide internal reference electrode. In order to attempt to distinguish between the contributions to the emf from oxygen and pH, a new pH sensor was developed based on the basic structure of cell (I). The metal/metal oxide internal reference electrode was replaced by a metal/metal hydride mixture, and the oxide dispersant was eliminated from the electrolyte. In our previous studies, the $La_{0.95}Sr_{0.05}F_{2.95}$ electrolyte had been used in hydrogen sensing in gas sensors, and significant protonic conduction at elevated temperatures was observed (7). Therefore, a true hydrogen concentration cell might be developed using this electrolyte and the metal/metal hydride internal reference electrode. Since Zr and ZrH_{1+x} coexist over the temperature range required by the power plant (from room temperature to 523 K), this metal/metal hydride mixture was chosen as internal solid hydrogen reference electrode for pH determination. The cell emf was measured in solutions at various pH values as a function of temperature. Some experimental results are presented in Figure 7 for the following cell:

$$\text{Pt, } Zr/ZrH_{1+x} \mid La_{0.95}Sr_{0.05}F_{2.95} \mid \text{pH Buffer, Pt} \qquad \text{(II)}$$

In comparison measurements, some commercial buffer solutions were utilized to replace metal/metal hydride as internal reference electrode in cell (II), and some typical experimental results are also shown in Figure 7. The expected linear response of emf to temperature was achieved for cell (II) with both metal/metal hydride and pH buffer solution internal reference electrodes.

Discussion

Charge Transfer at Electrode/Electrolyte Interfaces

It has been shown that cell (I) functions as an oxygen concentration cell, and the Nernst equation may be directly used to calculate the oxygen chemical potential in water through the measured cell emf. However, at low temperatures (usually below 570 K), the calculation based on the simple Nernst equation assuming n = 4 for the formation of O^{2-} ions does not conform with the experimental results in many cases. The present experimental results with cell (I) for an aqueous system can be shown as an example. The n values was found varying with temperature. Several possible explanations have been proposed for this phenomenon, one assumption being that there is an incomplete electron transfer on the electrode/electrolyte interface at low temperatures. For a high temperature galvanic oxygen sensor with the cell structure like cell (I), the electrode process can be described as equation (7)

$$O_2\,(\text{gas}) + 4e^-\,(\text{metal}) = 2\,O^{2-}\,(\text{electrolyte}) \qquad (7)$$

A complete oxygen ionization occurs at the triple gas-electrolyte-metal contact. But the mechanism of the oxygen ionization may be modified when the working temperature of the cell is below 500 K. Kleitz and Siebert (11) suggested the succession of a number of oxygen electrode process as:

$$O_2 \xrightarrow{1} O_2^- \xrightarrow{2} O_2^{2-} \xrightarrow{3} 2\,O^- \xrightarrow{4} 2\,O^{2-} \qquad (8)$$

as the temperature is raised from room temperature to about 700 K.

To generate a well-defined emf, a redox reaction does not have to reach the end of this chain. At high temperatures, the reaction always goes to the end of the chain to complete the ionization of oxygen, so showing a four-electron-transference electrode reaction. However, at low temperatures, some steps may be difficult to achieve (e.g. the rupture of the O-O bond in the oxygen molecule does not occur easily at low temperatures, so step 3 is blocked), and the electrode reaction can be reduced to 2 or 1 electron transfer.

Our experimental results indicated that the n value in the Nernst equation is close to 2 for cell (I) (derived from $dE/d(\ln P_{O_2})$) for oxygen determination at 339 K.

Interaction between Oxygen Chemical Potential and pH

In an aqueous system, the mechanism of the electrode reaction may be further modified by solvent water through reaction (9) in acidic solutions or (10) in alkaline solution

$$O_{2,\,aq} + 4H^+ + 4e = 2H_2O \qquad (9)$$

$$O_{2,\,aq} + 2H_2O + 4e = 4OH^- \qquad (10)$$

These two reactions clearly show the dependence of pH and oxygen chemical potential in the aqueous solution. The variation of one variable, such as pH, will cause the variation of the other, i. e. oxygen chemical potential in this example, through the chemical equilibration in the solution. Therefore, cell (I), an oxygen concentration cell, responded not only to the variation of the oxygen chemical potential in solution, but also to the pH levels. Similarly, cell (II), a hydrogen concentration cell, responded both to pH level and to oxygen chemical potential in the solution.

In the view point of industrial application, the cross interaction between pH and oxygen chemical potential in solution may cause some difficulty due to the introduction of one extra variable of the sensor parameter. To determine unambiguously the oxygen chemical potential (or pH) in solution, the pH value (or oxygen chemical potential) must be known. It must be noted that this complication does not originate from the sensor design, but from the reaction involved in the internal equilibration in the solution. A new approach to develop a sensor array is being investigated by the authors to solve this problem.

Summary

A series of experiments have been conducted on the development of a solid state oxygen sensor for use in cycle chemistry control and a solid state pH measuring device for aqueous systems in fossil fueled plants. The results show that:

1) $La_{0.95}Sr_{0.05}F_{2.95}$ and $La_{0.95}Ba_{0.05}F_{2.95}$ are chemically stable in water up to 523 K.

2) A mixture of Ag/Ag_2O has been found a very suitable, convenient internal reference electrode at temperatures below 460 K. Using this reference electrode and fluoride-based composite electrolyte forming an electrochemical probe, stable emfs could be quickly established at fixed temperatures and they responded to the oxygen chemical potential in water in Nernstian behavior .

3) The same sensor as developed for oxygen determination (using oxide-doped fluoride electrolyte and Ag/Ag_2O reference electrode) also responded to the pH change in the solution, through the equilibration of OH^-, H_2O, and O_2 in the aqueous systems. This cross interaction between oxygen potential and pH may cause some difficulty for industrial application of the sensor since one variable must be known before a relation between the cell emf and another variable can be defined.

(4) The sensor using Zr/ZrH_{1+x} as the internal reference electrode and fluoride electrolyte has shown some promising results for pH determination over a wide temperature and pH range.

Further experiments are underway to study the long term stabilities of solid electrolyte tubes in industrial application environments, to understand the cause and to solve the confusion of the cross interaction between the oxygen potential and pH in the aqueous solution.

Acknowledgment

The authors gratefully acknowledge the financial support from Electric Power Research Institute for this work.

References

1. D. D. Macdonald, A. C. Scott, P. Wentrcek, M. C. H. McKubre, EPRI Report NP-2806, (Palo Alto, CA: Electric Power Research Institute, 1983).

2. S. Hettiarachchi, S. J. Lenhart, D. D. Mcdonald, EPRI Report NP-5193, (Palo Alto, CA: Electric Power Research Institute, 1987).

3. M. J. Danielson and O. H. Koski, J. Electrochem. Soc., 132 8 (1985): p. 2037.

4. S. Hettiarachchi, D. D. Macdonald, H. Song and K. Makela, AIChE Symposium Series, 278 86 (1990): p. 54.

5. L. W. Niedrach, J. Electrochem. Soc., 133 7 (1986): p. 1521.

6. C. B. Alcock and B. Li, Solid State Ionics, 39 (1990): p. 245.

7. C. B. Alcock and N. Bakshi, to be published.

8 C. B. Alcock, L. Wang, High Temperatures-High Pressures, 22 (1990): p. 449.

9. C. B. Alcock, B. Li, J. W. Fergus and L. Wang, Solid State Ionics, 53-56 (1992): p. 39.

10. A. D. Pelton and M. Rivier, U.S. Pat. No 4 338 272 July 6, 1982.

11. M. Kleitz and E. Siebert, in T. Seiyama (ed.), Chemical Sensor Technology, Vol. 2, Elsevier, Amsterdam, 1989, p.151.

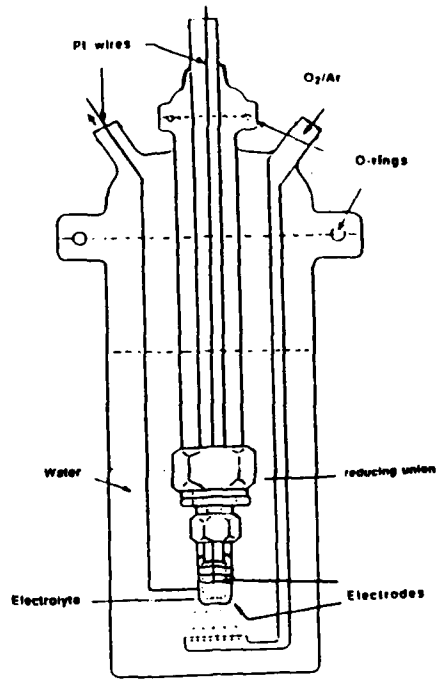

Figure 1 Cell Configuration for Oxygen Determination in Water below 373 K and at 1 atm.

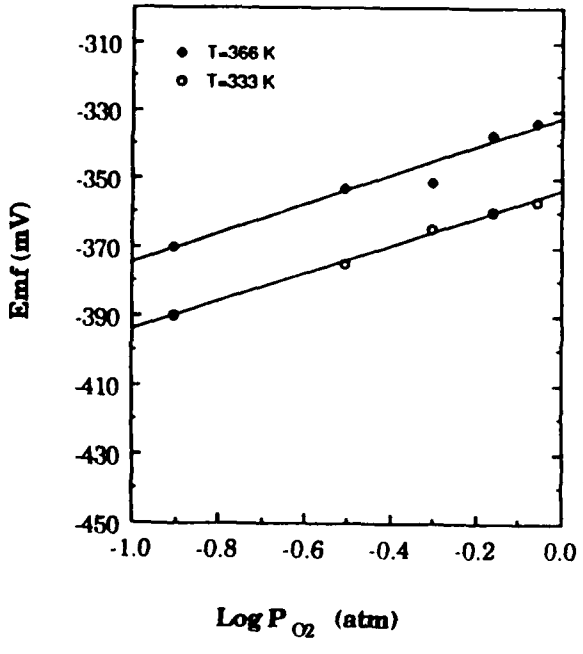

Figure 2 Emf Change with Oxygen Partial Pressure for Cell (I)

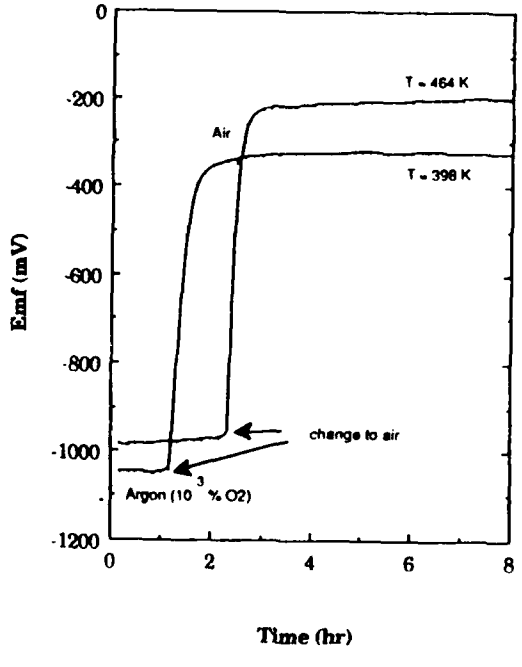

Figure 3 Emf Response to Oxygen Partial Pressure at Two Temperatures for Cell (I)

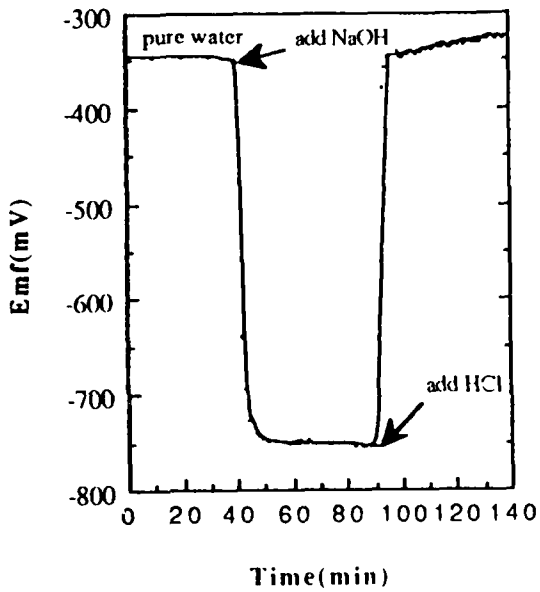

Figure 4 Emf Response to pH Change at 360 K for Cell (I)

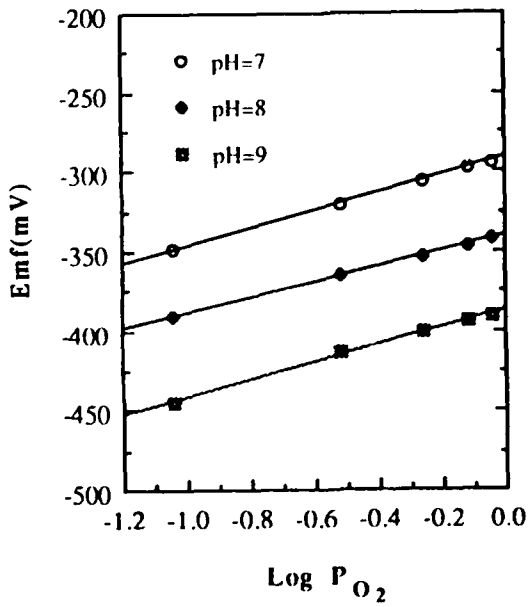

Figure 5 Influence of Oxygen Pressure on Emf at 339 K for Cell (I)

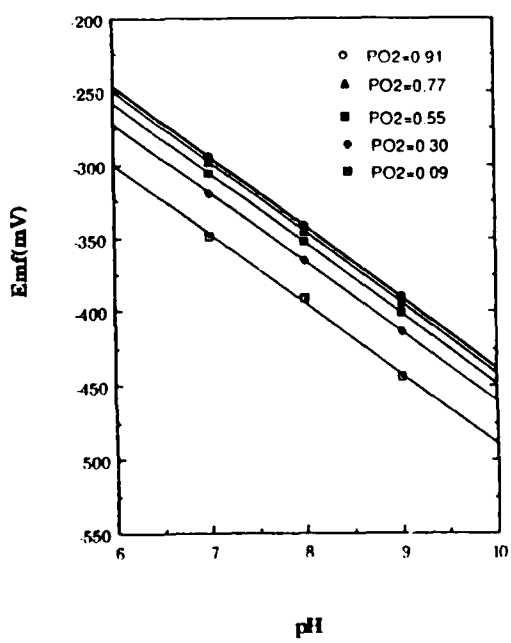

Figure 6 Influence of pH on E... at 339 K for Cell (I)

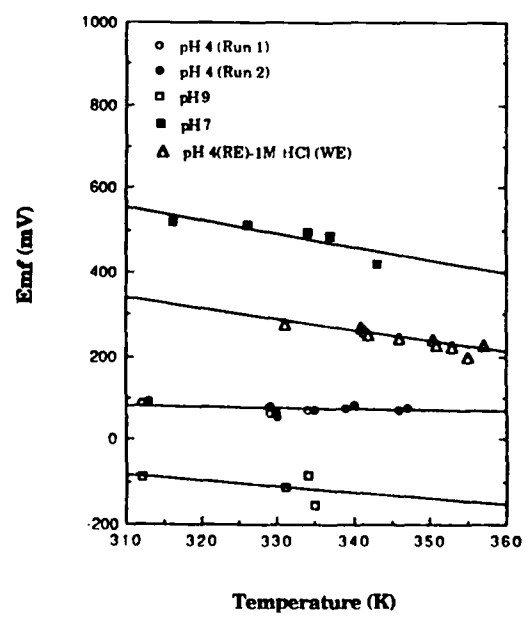

Figure 7 Emf vs. Temperature Plot for Cell (II) A cell with reference electrode pH 4 buffer and 1M HCl as working electrode is also shown

On-line Particulate Iron and Sulfur X-ray Monitor

Dennis Connolly
Babcock & Wilcox
Alliance Research Center
1562 Beeson Street
Alliance, Ohio 44601

Abstract

Corrosion product levels in the water circuits of power plants provide insight to the effectiveness of a water treatment program. By monitoring corrosion products at selected sampling points throughout the plant, transport patterns are determined. Typically, studies of particulate corrosion products consist of two separate activities: sampling and analysis. Two main problems with this scheme are:

a) the collection of corrosion products (sampling) usually takes place over the course of hours or days so that the analysis can only yield average values for these "integrated" samples

b) there is usually a time lag between collection and analysis of corrosion product samples (often the samples need to be taken off site for analysis).

This project was undertaken to develop a method for on-line analysis of particulate corrosion products. The sampling system has been automated and incorporated into the sample chamber of an X-ray fluorescence spectrometer. Using a specially designed flow cell, accumulated waterborne particulates are continuously irradiated by the analytical X-ray beam. Under a computer controlled schedule, water is periodically evacuated from the sample chamber to enhance the X-ray measurement and fluorescence data are collected. The monitor continues to cycle between these modes of sample collection and X-ray analysis until particulate loading in the sample chamber signals time for a filter change. In this way, each filter sample may be retained along with the analytical data record of its time in service.

By this method, the frequency of analytical reporting has been increased from hours or days to minutes and lag time between collection and analysis has been eliminated to provide a real time monitor. The instrument was designed to operate with a minimum of attendance by power plant personnel. The monitor was initially configured as a two channel instrument to measure iron and sulfur. However, simultaneous multi-element capability is possible for future work.

I. Introduction

Knowledge of the extent of corrosion and the migration of corrosion products in the steam/water circuits of electric generating station components is used diagnostically to gauge the success of a water treatment program. The presence of iron at key locations throughout the plant reminds us of the basic incompatibility of metals and water. Corrosion product monitoring strategies reflect the continual effort by plant operators to mediate the interaction between the two substances.

Techniques for monitoring and analysis of corrosion products have gone through several evolutionary stages in recent years. Sample collection by filtration of corrosion products is now supplemented by backup ion exchange membranes to capture both filterable as well as dissolved material. Analytical methods have progressed from quick and rough estimation using comparison charts, through element specific instrumental analysis (via AA or ICP), to the rapid, multi-element methods of X-ray fluorescence spectroscopy.

Despite these refinements, corrosion product monitoring techniques have retained the significant limitation that each individual analysis represents an integrated sample which can, at best, give only average concentration values for any particular sample collection period which may range from hours to days. The final analytical result lacks a distinction between a case of a steady rate of corrosion product transport and one by which transient instances of high corrosion product concentration account for the majority of the collected sample. This latter information, were it available, might be usefully correlated in time with controllable operational parameters of the plant. For example, the two graphs shown in Figures 1a and 1b represent hypothetical 24 hour accumulation of corrosion products on a filter. The two samples would give identical results by traditional collection and analysis since only the final amount at 24 hours is measured. However, the real time details of the corrosion product buildup shown in Figure 1b allows the operator to investigate potential causes of the discreet step increases at 9 and 16 hours into the test period.

This paper describes a new, on-line particulate monitor developed at the Babcock & Wilcox Alliance Research Center under contract with the Electric Power Research Institute (EPRI contract 3173-03). This monitor increases the sampling rate of corrosion products from hours or days to minutes to give a more complete time profile of the behavior of waterborne particulates.

II. X-ray Fluorescence

The new monitor is based on the X-ray fluorescence (XRF) technique of elemental analysis. In XRF, a sample is irradiated with X-rays of an appropriate energy to excite,

through ionization, the elements of interest in the sample. Upon spontaneous de-excitation, sample elements emit fluorescent radiation the component energies of which are characteristic for each element and the intensities of which may be correlated with the elemental concentrations in the sample. The XRF analysis, then, comprises a plot, or spectrum, of fluorescent intensity (counts per second) as a function of the energy of emission (kilo-electron volts, KeV). An example of an XRF spectrum is shown in Figure 2. Measurement of peak placement along the horizontal axis identifies the fluorescing element and vertical measurement (peak integration) indicates, through calibration, the amount of an element in the sample. The excitation X-rays may be obtained from an electronic X-ray tube or from a radioactive isotope source. XRF analysis is rapid and non-destructive. The spectrum shown in Figure 2 was obtained in two minutes.

III. The Monitor

Presently, the main target element of the monitor is iron. Since iron levels in most sample streams of interest are typically below the detection limit of direct XRF analysis, a concentration mechanism is required. The new monitor utilizes an XRF probe with a specially designed sample collection cell to continuously measure the buildup of particulate iron on a membrane filter. The initial version of the monitor contains a second parallel system (separate collection cell and separate X-ray probe) to similarly monitor sulfur containing particulates in the sample stream. The iron and sulfur channels may be operated simultaneously or separately. A diagram of the components of the monitor is shown in Figure 3. The main components of the monitor are:

a. X-ray probe

b. sample flow cell

c. valve switching system

d. flow totalizer

e. control and data acquisition system

A. The X-ray Probe

The X-ray probes for iron and sulfur measurement are made by Outokumpu Electronics. Each probe consists of a sealed radioisotope excitation source and a proportional counter type fluorescence detector. The radioisotope for the iron probe contains 60 millicuries of curium-244 and the sulfur probe contains 80 millicuries of iron-55. The probes are designed such that the radioisotope is shielded with a shutter mechanism which is open only when the probe body is properly set into a measurement position over the sample cell. In this way,

samples are continuously irradiated; however, data acquisition from the detector is initiated either manually or via a computer program when a measurement is desired.

The two probes are electrically connected through a multiplexer to a single electronics unit which can support up to six separate probes. The electronics unit can store all required calibration data so that for each measurement cycle, fluorescent intentensities are directly converted to elemental mass which is then transmitted to the computer for storage, trending or other uses. Alternatively, the complete XRF spectrum may be transmitted and stored. However, at the monitor's rate of sampling, this would tend to quickly deplete computer memory unless the operator chose to periodically download (for example, on a weekly basis) to storable media.

The X-ray unit may be taken off line at any time and used for individual measurements via manual keypad control.

B. The Sample Flow Cell

The sample flow cell is shown schematically in Figure 4. The cell body is constructed from delrin, an acetal type polymer. The cell contains a sample chamber sandwiched between an 0.45 micron sample filter and a kapton X-ray window. The sample inlet is on the side and sample flow is directed approximately parallel to the surface of the filter. The sample inlet channel is oriented at a slightly upward angle to the filter plane and slightly off-center to the filter chamber. This arrangement induces a swirling effect in the incoming liquid which promotes a uniform deposition of particulates on the filter surface. The sample drain is directly below the filter support.

The X-ray probe fits over the top of the flow cell such that the radioisotope source and detector are aligned with the kapton window and less than one inch from the surface of the filter. Both the X-ray probe and the flow cell are contained in a closed cell box during operation.

C. The Valve Switching System

Since water, even small thicknesses of it, severely attenuates the X-ray signals, a method was developed to enhance the sensitivity of the monitor by periodically evacuating the sample chamber and flushing with helium. Thus, the monitor will alternate between two modes during operation:

a. sample collection mode during which the sample is flowing and particulates are depositing on the filter;

b. sample measurement mode during which the sample is temporarily diverted from the flow cell, water is evacuated from the sample chamber, and a helium flush

proceeds while the measurement takes place.

Electrically actuated solenoid valves set the operating mode, and software control of the valves automatically switches between modes on a predetermined schedule.

D. Flow Totalizer

In the sample collection mode, a flow totalizer (Engineering Measurements) continuously monitors the flow through the filter. This is a positive displacement piston-type flowmeter which utilizes four pistons driven by the liquid being measured. The pistons drive a crankshaft which rotates at a velocity directly proportional to the volumetric flow through the meter. A magnetically coupled transmitter sends an output signal for each rotation of the shaft. These "counts" are monitored by the controlling computer and related through calibration to the volume through the filter chamber during any portion of a sampling period. This measurement is then used in conjunction with the subsequent X-ray analysis to determine the analyte concentration (micrograms/liter or ppb) of the sample stream. The flow totalizer is installed on the outlet drain of the filter chamber.

E. The Control and Data Acquisition System

Control of and data acquisition from the monitor are handled by a 486 type PC using a LAB-PC (National Instruments) data acquisition card for interface and LabVIEWS for Windows (National Instruments) software. This package distributes the necessary electronic signals to control the sequencing of valve settings and maintains the scheduling between the two modes of operation. Triggering signals are provided to initiate acquisition of X-ray and flow data at appropriate times through a monitoring period. Input includes X-ray analytical data and flow totals. Data processing includes conversion of raw X-ray data (counts) to elemental mass, combining mass and flow values to concentrations, displaying current and historical measurements, as well as a variety of graphing and other data formatting activities. The monitor also provides sensing and control capability for protection against overpressurization and leaks, diverting sample flow and alerting the user in these eventualities.

The initial version of the monitor utilizes a standard desktop PC. Since the monitor is relatively compact, a laptop or notebook type computer may be substituted (with appropriate interfacing) to minimize the overall size.

IV. Operational Considerations

Delivering a representative sample to the monitor is the responsibility of the user. Although the X-ray measurement is temperature independent, the kapton X-ray window imposes sample

pressure and temperature limitations (<35 psig, <60C). A sample line is connected to the flow cell via 1/4 inch tubing using common Swagelok fittings.

There is no functional limit on the flow rate through the sample chamber. In fact, higher flow rates enhance the sensitivity of the process due to the faster deposition of measurable material. During laboratory testing of the monitor, flow rates of 0.5 liters per minute were routinely achieved at 30 psig. However, once deposition begins to occur on the filter, the flow rate will steadily decrease. One of two situations will warrant a change of filters: the amount of deposition will either plug the filter sufficiently to lower the flow rate below a useful range, or the amount of iron in the deposited material will produce a fluorescent signal beyond the linear response curve of the detector. Which will occur first will likely depend on the characteristics of the particulates in the sample. Fine particles (possibly silica) will tend to plug the filter, while more coarse particles (iron oxides) will tend to build up to the point that the X-ray linear response limit is exceeded with good flow still possible. In either case, the user will be advised of the condition and that a filter change is in order. Flow rates, then, should be determined by the sample stream characteristics. For particularly clean streams, the highest achievable flow (within the pressure limitation) should be used to enhance the sensitivity of the monitor for very low concentration levels. For dirtier streams, a lower flow rate would be more advisable to extend the service life of an individual filter.

When a filter is changed, the used filter should be labelled and stored. In this way, both a filter sample and the corresponding X-ray data record while in service are retained.

From the time a new filter is in place to the time it is removed from service, there is no required user interaction once a monitoring procedure is initiated from the computer terminal. However, a user should periodically ensure that flows and helium levels are in good order. Also, the computer monitor should be checked for messages.

A full multi-point calibration should be performed monthly. A single point re-normalization should be performed weekly or upon a change of the kapton X-ray window. This re-normalization will correct for variances in the kapton thickness and for natural decay of the radioactive source strength. Procedures for calibration and re-normalization are outlined in the user's manual.

V. Potential Extended Capabilities

A. Additional Elemental Analyses

Since the XRF spectrometer used in the monitor is of the

energy dispersive type, elements in addition to the two presently being targeted (iron and sulfur) are also amenable to simultaneous detection and measurement. For the iron probe, the range of elements within about 50% of the sensitivity for iron is chromium to strontium on the periodic table (lead and some other heavy metals may also be included). For the sulfur probe, the range of elements within about 50% of the sensitivity for sulfur is phosphorus to vanadium. Some elements outside these ranges may also be possible though at lower sensitivities. Testing for sensitivities and potential inter-element interferences, and preparation of calibration procedures will be required before additional elements can be included.

B. Additional Instrumentation

The software package controlling the X-ray monitor is capable of handling additional monitoring tasks. With appropriate interfacing, the package may be extended to include pH, conductivity or other parameters of interest.

acknowledgement: this work was funded by the Electric Power Research Institute (EPRI 3173-03); EPRI project manager: Dr. Thomas O. Passell

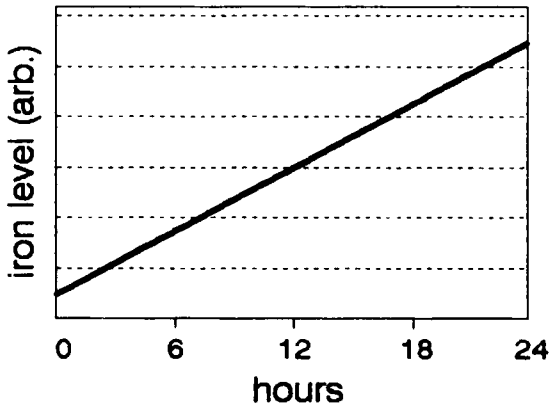

Figure 1a: steady deposition

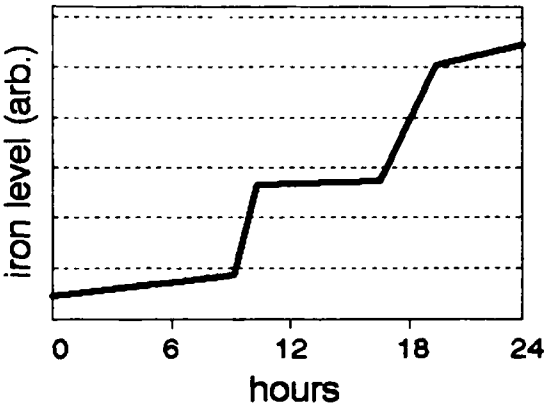

Figure 1b: erratic deposition

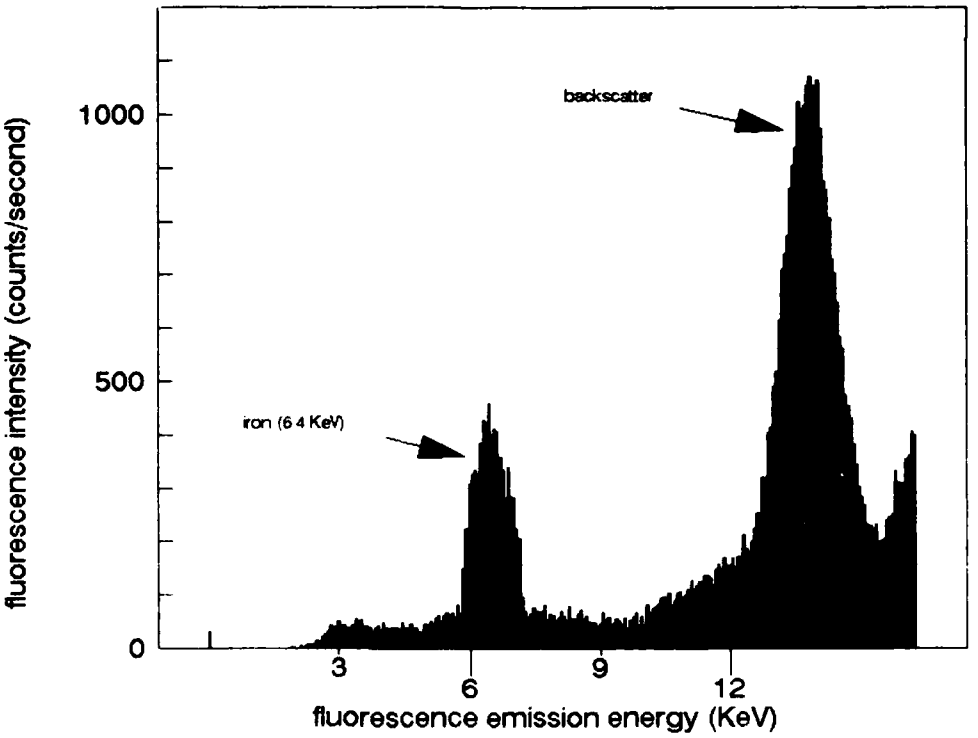

Figure 2: X-ray Fluorescence Spectrum of Filtered Iron

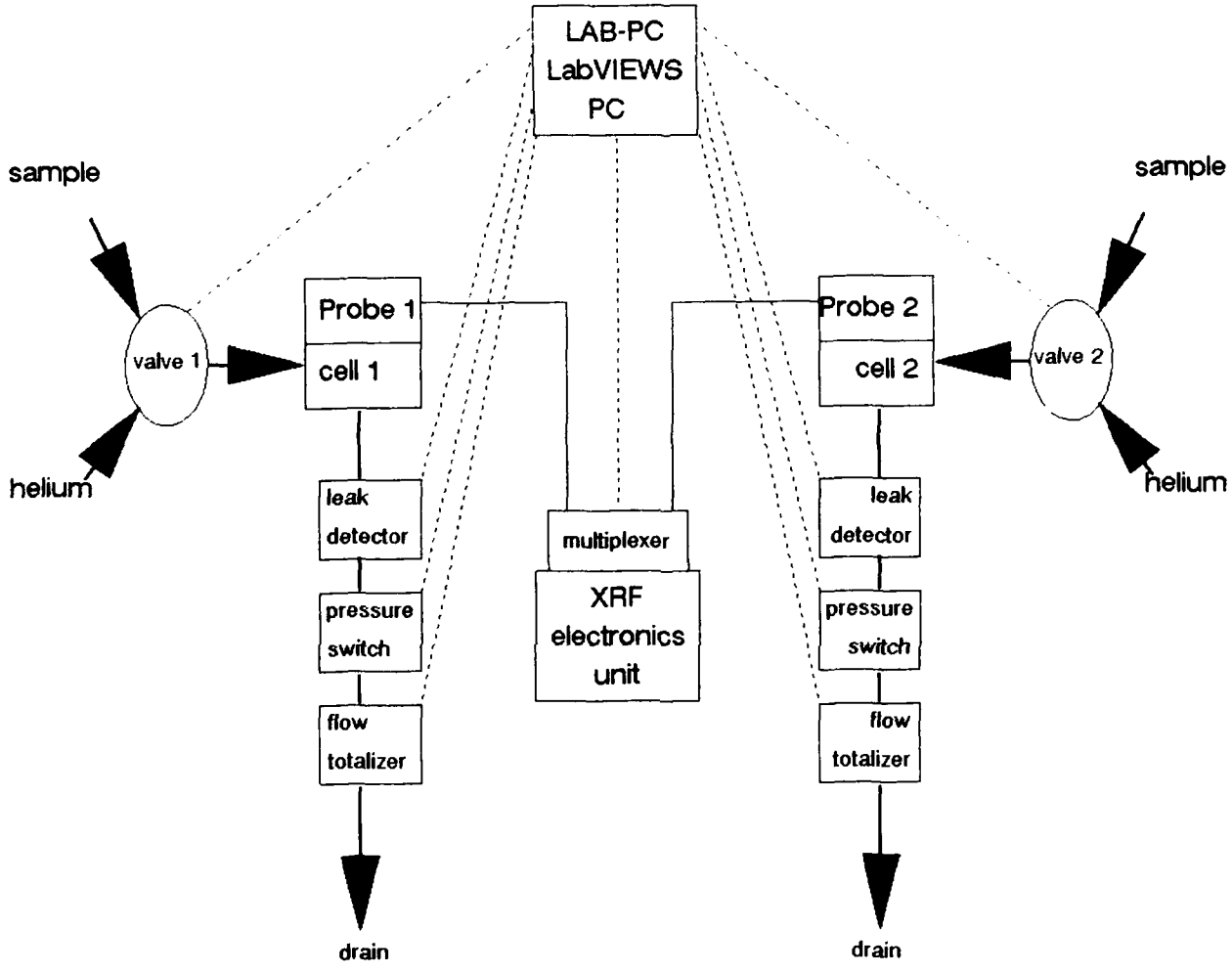

Figure 3: components of the on-line X-ray monitor

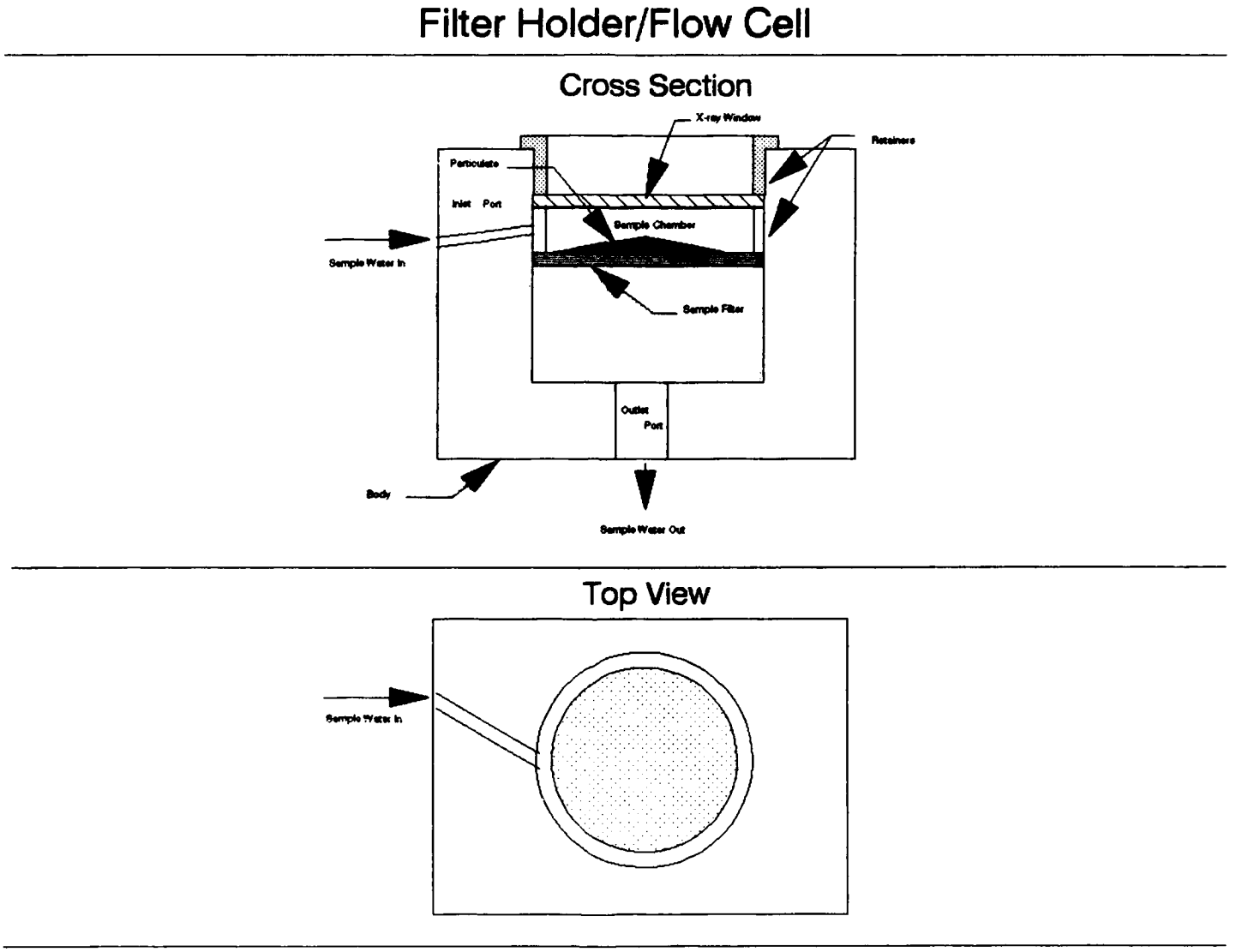

Figure 4: concentrating flow cell for on-line X-ray monitor

On-Line Dissolution and Analysis of Corrosion Products

Michel N. Robles
GE Nuclear Energy
Vallecitos Nuclear Center
PO Box 460, MC: V19
Pleasanton, CA 94566-0806
USA

Abstract

A technique is being developed for the on-line dissolution and analysis of iron in corrosion products using flow injection, microwave heating and ion chromatography. Alternate analytical techniques such as flow injection analysis with a colorimetric finish has also been used. This development effort was funded under EPRI contract RP 1447-1 and included the testing of several acid solutions for the dissolution of corrosion products. Dissolution rates, parameters and the impact of these reagents on the analytical systems are discussed.

Key Terms: analysis of corrosion products, on-line dissolution

Introduction

The input of corrosion product iron to the Boiling Water Reactor (BWR) via the feedwater system presents numerous operational problems. The "crud" that forms, deposits on fuel clad surfaces in the core. This can lead to poor heat transfer, fuel failures and increased radiation levels throughout the plant.

Specifically, deposits on fuel clad have resulted in fuel clad failure through "crud induced localized corrosion". These deposits also contain low concentration levels of impurities such as, cobalt, nickel, zinc and chromium. These impurities are activated by the neutron flux and, when dislodged due to power or flow transients, they deposit in low flow areas of the recirculation piping resulting in "hot spots". Hot spots increase personnel exposure rates and increase the time it takes to perform maintenance functions due to increased shielding installation, planning, etc.

The sources for iron in the feedwater are carbon steel surfaces of the steam extraction piping, turbine structures and condenser shell-side support structures.

In the neutral water chemistry of a BWR, carbon steel will corrode, releasing iron and other impurities as soluble and insoluble corrosion products into the feedwater prior to entering the reactor core. Testing by GE Nuclear Energy (GE) has shown that plant operation can have a significant impact on the corrosion rates of these carbon steel systems. For example, in normal water chemistry conditions, high purity feedwater corrosion rates will be very high if dissolved oxygen levels are allowed to drop too low.

GE is working under an Electric Power Research Institute (EPRI) contract to develop and commercialize an analytical system that will provide near real-time measurements of corrosion product levels in nuclear reactor feedwater. Specifically, this device will measure iron particulates in feedwater with a detection limit of ≤1 ppb (ng/ml). An instrument of this type allows timely remedial action when process parameters such as oxygen are out-of-specification.

Potentially, a system of this type could provide an analytical basis for improving crud removal systems, such as, hollow-fiber filters or could monitor the effects of chemistry changes on corrosion particulates. This paper describes the development of an instrument system, how it is configured, operates and some of the problems encountered.

Technical Approach

Two parallel development efforts are being funded by EPRI. One is based on filtration and measurement of the accumulated corrosion product particulate by X-ray fluorescence. The other is the GE approach, which involves dissolution prior to analysis by an on-line technique. A number of commercially available analytical systems have the potential of achieving the objectives of this program. What GE did was to survey available systems and after procuring one, either modify it or work with the manufacturer to modify the system to successfully operate in a power plant environment. The selection criteria used stressed the following points:

- Simplicity - The system had to be uncomplicated, so that, with minimal training a technician could operate it;
- Reliability - System components had to be rugged to minimize downtime and survive in a power plant environment;
- Automation - Operation had to be automated to minimize chemistry staff requirements and radiation exposure;
- Size - Compactness is an issue. At many power plants space for large analytical systems is not available close to sample sinks and
- Cost - The lower the cost of implementation, the easier the system will be to commercialize.

The technique selected was Flow Injection Dissolution and Analysis. The analysis portion is accomplished with on-line ion chromatography (IC). An alternate to IC is a colorimetric determination.

From the literature search conducted, it became apparent that devices capable of dissolving and measuring iron corrosion products have been around for many years[1-4], but for one reason or another were not successful. The most common problem seemed to be incomplete dissolution of the corrosion product particulates. Once complete dissolution is achieved a number of analytical techniques can be applied. This is where most of the testing was directed.

Experimental

Instrumentation

It was felt that rapid heating to a higher temperature and pressure than previously used would solve the incomplete dissolution problem. Microwave heating provides the ability to rapidly heat water and at least one vendor provides ports into and out of the microwave field. With the selection of microwave heating, the material for constructing a dissolution loop had to be non-metallic. A continuously flowing "loop" constructed of a plastic capable of withstanding high temperature (>150 °C) and high pressure (≤1.4 MPa) had to be developed.
A simple and easily controllable method of injecting the dissolution reagent into the sample stream was the next item to select. This mixture then had to be continuously pumped through the dissolution loop against a large enough back pressure to prevent boiling within the loop. This was accomplished by using an HPLC (high pressure liquid chromatography) pump. Selecting an HPLC pump that was capable of low pressure gradient operation, also solved the dissolution reagent injection problem. Pressure within the loop is maintained through the use of back pressure regulators. These are essentially, spring-loaded check valves which seal both ends of the Loop. These regulators are constructed so that only PEEK (polyether ether ketone) and Teflon are in contact with liquid.

Dissolution Module - The HPLC pump selected is a Shimadzu LC-10AD Solvent Delivery Unit (Shimadzu Scientific Instruments, Inc., Columbia MD). This pump is capable of producing low pressure quaternary gradient solutions through the use of an automatic flow control valve (FCV-10AL Low Pressure Gradient Valve) also available from Shimadzu. This pump is equipped with high and low pressure limits that can be set to stop operation when exceeded.
The microwave oven selected is a CEM MDS-2000 (CEM Corporation, Matthews, NC). The MDS-2000 is equipped with four ports, allowing easy introduction of reagents and solutions into the microwave field. It is also equipped with a pressure sensor, which can be used to shutdown the microwave field if the dissolution vessel pressure exceeds 1.4 MPa (200 psig). If the pressure drops suddenly, more than 20 % (catastrophic leakage), the microwave system is shutdown, aborting the dissolution process. The safety features of these components reduce the chances of uncontrolled sample leaks.

Analytical Systems - Two analytical techniques were selected to provide an analysis of the corrosion product solution obtained from the dissolution module. The first, is an IonTrac-401 (GE Nuclear Energy, San Jose, CA) on-line ion chromatograph (IC). The second, is a Flow Injection Analysis (FIA) system that combines an iron-specific chromophore, TPTZ (2,4,6 tris(2-pyridyl)-s-triazine) with the dissolved corrosion products and pumps this solution to a spectrophotometric detector. A Wiz® peristaltic pump (Isco, Inc., Lincoln, NE) is used to combine these two streams and pump them through the detector. Data acquisition and control for both analytical systems is provided by an Intel '486 compatible computer (Advantech, San Jose, CA) using Windows® ver. 3.1 as the operating system. EZChrom® (Scientific Software Inc., San Ramon, CA) chromatography workstation software is used in the IonTrac-401 system and

LabVIEW® (National Instruments®, Austin, TX) is used to acquire and display data for the FIA system.

Reagents

The dissolution reagent selected is thioglycolic acid (Sigma Chemical Co., St. Louis, MO). It was long ago identified as a very effective acid for solublizing iron oxides.
There are two IC reagents: 1) eluent, 3 mM pyridine-2,6-dicarboxylic acid (J.T.Baker Inc., Phillipsburg, NJ), 4.8 mM lithium hydroxide (J.T.Baker Inc.), 2 mM sodium sulfate, 25 mM sodium chloride and 1 mM ascorbic acid and 2) Post Column Reagent, 0.2 mM PAR (4-(2-pyridylazo)resorcinol monosodium salt), 0.5 mM ammonium hydroxide, 0.3 M sodium bicarbonate, 0.5 M dimethylaminoethanol (Aldrich Chemical Co., Milwaukee, WI).
The FIA reagent is 0.5 mM TPTZ (Eastman Kodak Co., Rochester, NY), 3 M ammonium hydroxide and 1 M glacial acetic acid.
The corrosion product sample stream was simulated by suspending α-Fe_2O_3 (Kroma Red Oxide, paint pigment obtained from Chas. Pfizer & Co., New York) in deionized water. This oxide has a particle size range of 0.5 - 3 microns.
Dilutions of commercially prepared iron standard solutions were used to calibrate both analytical systems. All reagents were prepared using deionized water purified in a Milli-Q® UV Plus water system (Millipore Corporation, Bedford, MA).

Results and Discussion

The first tests conducted defined conditions needed to dissolve iron oxide. Closed Teflon® vessels containing 20 mg of oxide and 20 ml of 1% thioglycolic acid (TGA) were microwaved at various power levels for increasingly longer time periods. As each container was removed from the microwave oven, it was immediately cooled in an ice bath and a filtered aliquot was taken for analysis. Figure 1, shows the results of this dissolution study. From these curves it is apparent that 30 % microwave power was sufficient to dissolve all of the oxide within five minutes.

The next step tested the dissolution process using a continuous set up (see Figure 2). In this configuration a coil of 3 mm OD (outside diameter) and 1.5 mm ID (inside diameter) Teflon® tubing 10 m long was wound around a Teflon mandrel and placed inside a Teflon beaker in the microwave oven. Teflon tubing, 1.5 mm OD and 0.25 mm ID , connected to the coil with PEEK® fittings. The other end was connected, outside the microwave oven to the gradient pump. The loop was sealed at both ends with back pressure regulators (spring-loaded check valves) which set the internal pressure of the loop at 1.1 MPa (150 psig). The effluent from the dissolution process is routed to a transition metals IC channel where iron and other metals are measured (see Figure 3). A number of tests were done with the coiled dissolution loop set up, but it proved not to be reliable. The coil blew out several times when the combination of temperature and pressure became too great. It was also discovered that PEEK fittings on Teflon tubing failed regularly due to heat deformation of the tubing. To improve reliability alternate materials had to be used. PEEK tubing is much harder than Teflon and has a higher tolerance for pressure and heat.

The next dissolution loop fabricated consisted of a series of six empty PEEK chromatography columns connected with 1.5 mm OD PEEK tubing. This dissolution loop is shown in Figure 4. Preliminary testing with this loop began in December, 1992. More testing must be done to determine its effectiveness.

During the testing of the coiled Loop it was noticed that recoveries were lower than expected. They also exhibited a downward trend with time. This appears to be due to iron oxide "plate-out" on the walls of the standard reservoir and on tubing walls before it reaches the dissolution loop. This drop-out problem occurred even though vigorous stirring was being used to keep the oxide suspended. To overcome this problem we have increased the linear velocity of the iron oxide suspension through the tubing feeding the gradient pump. This was done by increasing flowrate and reducing the inner diameter of the connecting tubing. How effective these changes have been, remain to be tested. All other components in the dissolution module seem to be working very well.

Future Work

By the time this paper is orally presented, the following tasks will be completed or in process:

Complete the testing of the on-line dissolution module.

We need to solve the oxide plate out problem. Higher linear velocity rates through the tubing and the use of ultrasonic agitation may reduce or eliminate this problem. Continue search for an alternate acid to dissolve corrosion products. If possible, thioglycolic acid must be replaced with a less noxious acid.

Investigate ways to reduce waste generated by the dissolution and analytical systems. Mixed waste disposal is a severe problem for the plants and it is getting worse. For example, micro-bore columns could be used in the IC analytical finish. This would cut analytical waste by almost 70%. With the Flow Injection Dissolution and Analysis system flow rates could be cut from the expected rate of 1.5 ml/min. to 0.5 ml/minute. This would result in a 67 % cut in waste generated.

Complete the testing of the Flow Injection Dissolution and Analysis configuration, procure and test software for displaying iron corrosion product trends (see Figure 5).

Fabricate the Plant Prototype On-Line Dissolution Module for use in the field.

Complete Preparation of IonTrac-401 for use in the field.

Complete the above tasks by August 1, 1993.

Complete two field test campaigns of the on-line corrosion product analyzer using ion chromatography as the measurement technique by the end of 1993.

Conclusion

A lot of the preliminary work for developing a successful on-line corrosion product analyzer has been completed, but much still needs to be done.

References

1. C. C. Hach, "Iron Analysis Reagent Formulation", U. S. Patent 3,709,662, Jan. 9, 1973

2. Suda Masataka, "Automation of Total Iron Concentration Monitoring on Start-up of Fossil Power Plants", 51st International Water Conference, Pittsburgh, Pennsylvania October, 1990.

3. E. Baumgartner, M. A. Blesa, and A. J. G. Maroto, "Kinetics of the Dissolution of Magnetite in Thioglycolic Acid Solutions", J. Chem. Soc. , Dalton Trans., pp. 1649 - 1654; 1982.

4. S. G. Sawochka, D. T. Snyder, " Feedwater Corrosion Product Monitoring System", NEDE 13102, GE Nuclear Energy; April, 1970.

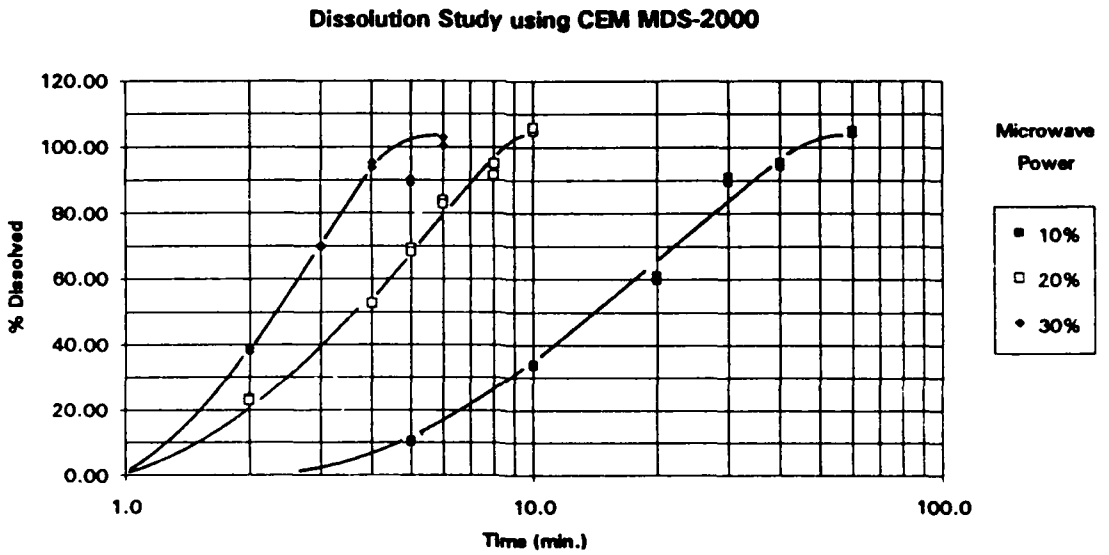

Figure 1. Dissolution Rate versus Microwave Power

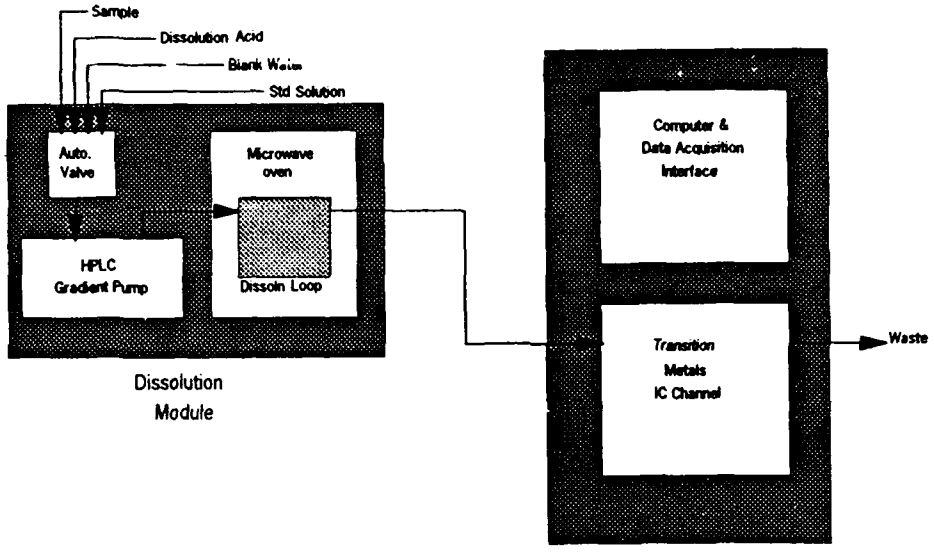

Figure 2. On-Line Dissolution Module Connected to an On-Line Ion Chromatograph

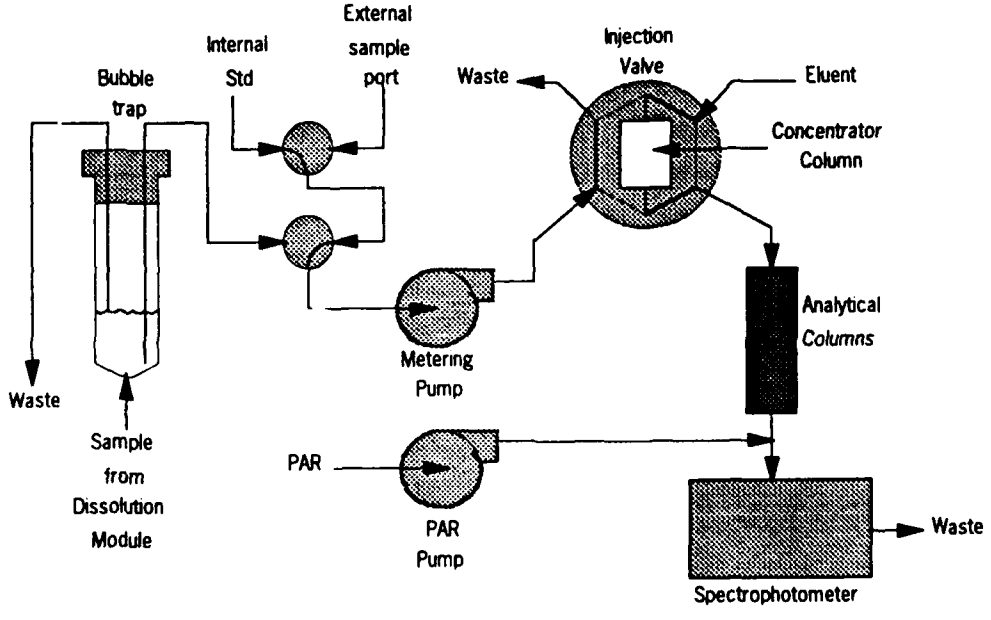

Figure 3. Transition Metals IC Flow Diagram

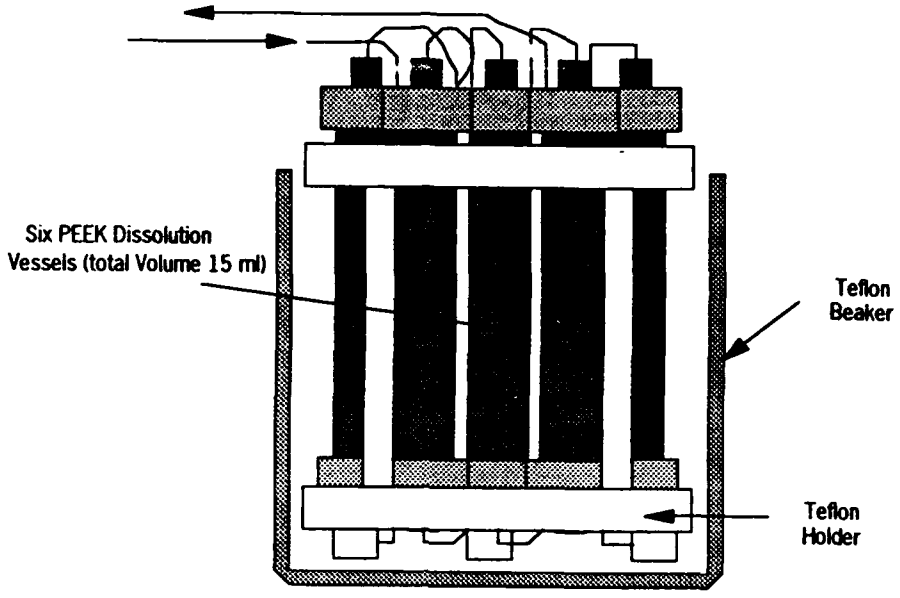

Figure 4. Column Type Dissolution Loop

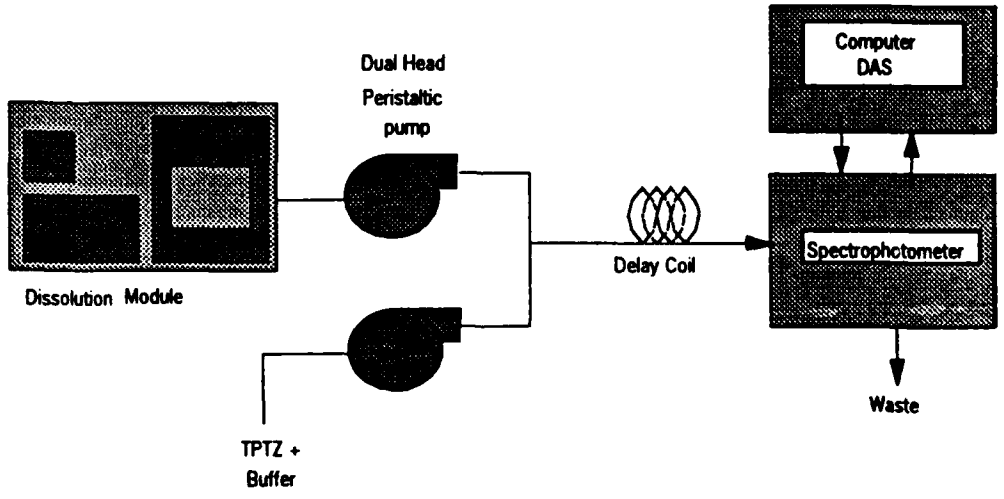

Figure 5. Flow Injection Dissolution Analyzer

Remote Monitoring of Corrosion Chemicals Via Fiber Optic Raman Spectroscopy

L. A. Jeffers
Babcock & Wilcox
Research and Development Division
1562 Beeson Street
Alliance, Ohio 44601

J. W. Berthold
Babcock & Wilcox
Research and Development Division
1562 Beeson Street
Alliance, Ohio 44601

Abstract

Remote Raman spectroscopy through optical fibers has potential for use in a wide variety of corrosion monitoring applications including: steam generator inspection, corrosion contaminant identification in cervices, and characterization of new corrosion inhibitors in autoclaves.

We report on a series of experiments aimed at demonstrating the feasibility/applicability of fiber optic Raman spectroscopy for in-situ monitoring of corrosion products and other chemicals.

Raman spectra were recorded through 20 meters of fiber using an Argon ion laser as the source and an intensified photodiode array detector coupled to a 1/4 meter polychromator. Spectra were recorded of solid phase Fe_2O_3, and Fe_3O_4, as well as disodium and trisodium phosphates in both the liquid and solid phase.

Introduction

B&W has had a longstanding interest in the development of fiber optic based Raman spectroscopy[1,2] because of potential applications that include:

- on-line monitoring of water chemistry
- on-line monitoring of corrosion and deposits
- in-situ inspection of steam generators during outages
- autoclave studies of high-temperature corrosion chemistry.

The work reported here was a feasibility study, conducted using an on-hand system that was developed for fluorescence spectroscopy. Although far from an optimum system for Raman work, it nevertheless served the purpose of:

Key terms: Raman spectroscopy, corrosion monitoring

- establishing the feasibility of remotely (through an optical fiber) obtaining Raman spectra of several compounds of interest
- identifying problems that must be addressed in the implementation of the technique
- provide the background for planning the next phase of the development.

Raman spectra are the result of inelastic collisions between incident photons and molecules in the sample. As in the more familiar infrared spectroscopy, the analytic capability is based on the fact that the spectral distribution of the Raman light is characteristic of the molecular species involved.

Some of the advantages of Raman over conventional infrared are:

- measurements can be made in the visible region of the spectrum which opens the possibility of remote measurement through optical fibers.
- measurements can be made on solid, liquid, or gaseous samples.
- the signal is directly proportional to the concentration.

The main disadvantages of Raman are related to the fact that the effect is so weak. Raman cross sections are typically 10 orders of magnitude smaller than cross-sections for absorption. Furthermore, the low signal level is subject to being swamped by sample or impurity fluorescence.

The use of optical fiber probes provides several advantages, including:

- ability to make measurements in otherwise inaccessible regions such as the interiors of steam generators.
- ability to make measurements across a pressure boundary (autoclave for example).
- remote measurement capability which includes the possibility of multiplexing a large number of distributed measurement points to a single centrally located analyzer.

The extreme weakness of the Raman effect poses special problems when using fibers. Most important of these is the generation of fluorescence and Raman lines in the optical fiber material. Nevertheless, several successful applications of fiber optic Raman spectroscopy have been reported[3,4].

Apparatus

Figure 1 is a block diagram showing the major components of the apparatus. Excitation was provided by an argon ion laser operating at 488 nm. The average power delivered to the sample by the fiber was 100 mW. A small 1/8 meter focal length monochromator was used between the excitation laser and the fiber. The purpose of this monochromator pre-filter was to keep the nonlasing plasma lines

from the laser discharge from entering the fiber and being ultimately transmitted to the detector as noise.

The excitation fiber was a 20 meter long, 600 µm core silica fiber with silicate cladding, 3M Part #FG-600-UAT. This fiber is designed for optimum transmission in the blue and ultraviolet end of the spectrum. Typical attenuation at 400 nm is given by the manufacturer as .04 dB/m so the loss in the fiber was minimal.

The pick-up fiber was a bundle of seven silica core fibers with core diameter of 365 µm arranged in a circular pattern at the pick-up end and in a linear array at the monochromator end. The arrangement in a linear array was to match the rectangular geometry of the monochromator slit. This fiber bundle was designed for use in the study of fluorescence and was not very efficient for use in the Raman work. In the fluorescence work, spectral resolution is relatively unimportant and the monochromator slits can be opened to a width of 350 µm to pass nearly all of the light delivered by the fiber bundle. To get the desired resolution for the Raman spectra, the slits were narrowed to 40 µm which resulted in about 14% delivery efficiency.

The detector was a 1024 element, intensified, diode array (Princeton Instruments IRY 690C) that provides simultaneous detection of all wavelengths. The integration/exposure time of the detection is controlled by the detector controller through the computer which acts as the operator interface and data storage device.

Figure 2 shows the details of the delivery/pick-up optics assembly. The excitation light emerges from the delivery fiber and illuminates a small area on the surface of the sample. Lens 1 is spaced by its focal length from the sample surface so that the reflected/scattered light collected by lens 1 is collimated and passed through the holographic notch filter. The filter has an optical density >4 at the excitation wavelength, and the transmission rises very rapidly on either side of the excitation wavelength. This allows a very high degree of discrimination against the elastically scattered light while passing the inelastically scattered Raman light even at quite low frequencies. The light that passes through the filter is focused by lens 2 onto the circular end of the 7 fiber pick-up bundle.

Results

Raman spectra were obtained on the following samples:

- Na_2HPO_4 (DSP) both 1% and saturated solutions
- Na_3PO_4 (TSP) both 1% and saturated solutions
- CCl_4 100%
- Fe_2O_3 as powder
- Fe_3O_4 as powder

Figure 3 shows the raw spectra obtained for the 1% solution of DSP. The plot is in terms of the measured intensity as a function of the difference in frequency between the measured light and the excitation light.

The measured intensity can be written as

$$M = D + \{R+F+\rho[I_o+R_f+F_f]\}T \qquad (1)$$

where

- D is the electronic "dark" noise
- R is the Raman signal from the sample
- F is the fluorescent signal from the sample
- ρ is the reflectivity of the sample
- I_o is the intensity of the excitation light
- R_f is the Raman signal generated in the fibers and other optical components
- F_f is the fluorescent signal generated in the fibers and other optical components
- T is the transmission of the pick-up optical system.

It should be remembered that each of the terms in Equation 4 is dependent on the frequency shift $\Delta\nu$.

Typically, I_o is many orders of magnitude greater than any of the other terms in Equation 1. The holographic notch filter, however, has a transmission that is extremely low at the excitation wavelength and high everywhere else. As a result, the product I_oT is comparable or less than all of the other terms except at wavelengths very close to the excitation wavelength, i.e., at small values of $\Delta\nu$.

All of the spectra (with the exception of the CCl_4 which is a very strong Raman scatterer) look much the same as shown in Figure 3 because the sample independent terms R_f and F_f in Equation 1 are about two orders of magnitude larger than the Raman signal from the sample.

Figure 4 shows the measured CCl_4 spectrum. The general features of the fiber background seen in Figure 3 appear in Figure 4 with the lines of the CCL_4 spectrum superimposed.

Figure 5 shows the result of subtracting Figure 3 from Figure 4 to essentially remove the fiber related background "noise". The result is the classic Raman spectrum of CCl_4. The measured frequencies are indicated above the individual peaks. The values in parentheses are the known values reported in the literature.[5]

The curve plotted in Figure 5 shows nothing but the spectrum of CCl_4. This is because CCl_4 is a much stronger Raman scatterer than is the 1% DSP solution. If the DSP had any lines comparable in intensity to the CCl_4 they would have shown up as negatively going peaks.

Although all of the spectra, with the exception of that from CCL_4, look superficially the same due to the dominance of the fiber generated terms, there are differences that can be revealed by eliminating the "common mode" fiber contribution. Figure 6 shows the result of subtracting the measured spectrum for TSP from that of DSP. The two positive peaks are Raman lines from the DSP while the negative peak is from TSP. The values of frequency given in parentheses are published values.[6]

This background subtraction technique provides a very powerful tool for dealing with the fiber background problem and is why the array detector and digital signal processing are vital to the fiber-based Raman. The limitations of the technique can be appreciated by reference to Equation 1. If there were no difference in the spectral reflection of the two samples, the fiber related terms would cancel completely. In the case of the DSP and TSP samples, the cancellation was close enough to clearly reveal the Raman lines of both.

The spectral reflectivity difference between DSP and the powdered iron oxides, however, were too great to get useable results. The two oxides, however, were close enough together that they could be used for correcting each other, as shown in Figure 7, where several Raman lines were observed. The values in parentheses are those reported in the literature.[7,8] Values shown above the curve are for Fe_2O_3 lines while those shown below the curve are for Fe_3O_4.

Conclusions

We have demonstrated the feasibility of measuring Raman spectra of various compounds through 20 meters of optical fiber using a non-optimized system. A prototype system could be built and evaluated for steam generator inspection during planned outages. The prototype could be made compatible with fiber optic borescope probes currently used for visual inspection in steam generators. With the demonstrated detection capability for hematite, magnetite, and phosphates, such an inspection system would be useful for identification of localized corrosion problem areas.

Measurements can be made in the presence of severe background noise due to fluorescence and Raman generation within the fibers, using a previously stored reference spectrum.

Use of digital data acquisition and an array type detector that allows simultaneous detection of the signal at all wavelengths is vital to the implementation of background correction.

Even with background subtraction, the magnitude of the fiber background sets the limits of detectability.

Fiber fluorescence and attenuation loss are strongly wavelength dependent -- both increasing with decreasing wavelength. This would suggest that a longer wavelength excitation source might be preferred. However, the intensity of the desired Raman signal is

inversely proportional to the 4th power of the wavelength. The optimum wavelength will therefore be determined by a trade-off between these two factors. For very short delivery-fiber applications such as autoclave corrosion studies, the 488 nm Argon line is ideal. At intermediate fiber lengths (20 meters or so) it may be advantageous to use the 514.5 nm Argon line. For applications requiring delivery through 100 m or more, a near-infrared diode-laser would be preferable.

References

1) W.E. Allmon, J.W. Berthold, and N.J. Mravich, "Role of Chemical Additives in Transporting and Depositing Corrosive Impurities in Steam," Phase II Final Report to Electric Power Research Institute, NP3487 (1984).

2) W.E. Allmon and J.W. Berthold, "High-Temperature Laser Induced Spectroscopy in Nuclear Steam Generators," U.S. Patent #4,907,883.

3) M.A. Leugers, and R.D. McLachland, "Remote Analysis by Fiber Optic Raman Spectroscopy," SPIE Publication *Chemical, Biochemical, and Environmental Applications of Fibers, Vol. 990*, (1988) pp 88-95.

4) K.P.J. Williams and S.M. Mason, "Fourier Transform Raman Spectroscopy in an Industrial Environment," *Trends In Analytical Chemistry*, vol. 9, no. 4, (1990) pp 119-127.

5) D.A. Long, "Raman Spectroscopy," McGraw Hill, New York, (1977).

6) K. Nakamoto, "Infrared Spectra of Inorganic and Coordination Compounds," 2nd Edition, Wiley-Interscience, London. (1970).

7) D. Thierry, D. Persson, and C. Leygraf, "In-Situ Raman Spectroscopy Combined with X-Ray Photoelectron Spectroscopy and Nuclear Microanalysis for Studies of Anodic Corrosion Film Formation on Fe-Cr Single Crystals," J. Electrochem Soc., 135, No. 2, Feb. 1988, pp 305-310.

8) T. Ohtsuka, K. Kubo, and N. Sato, "Raman Spectroscopy of Thin Corrosion Films on Iron at 100 to 150 C in Air," Corrosion - NACE 42, No. 8, August 1986, pp 476-481.

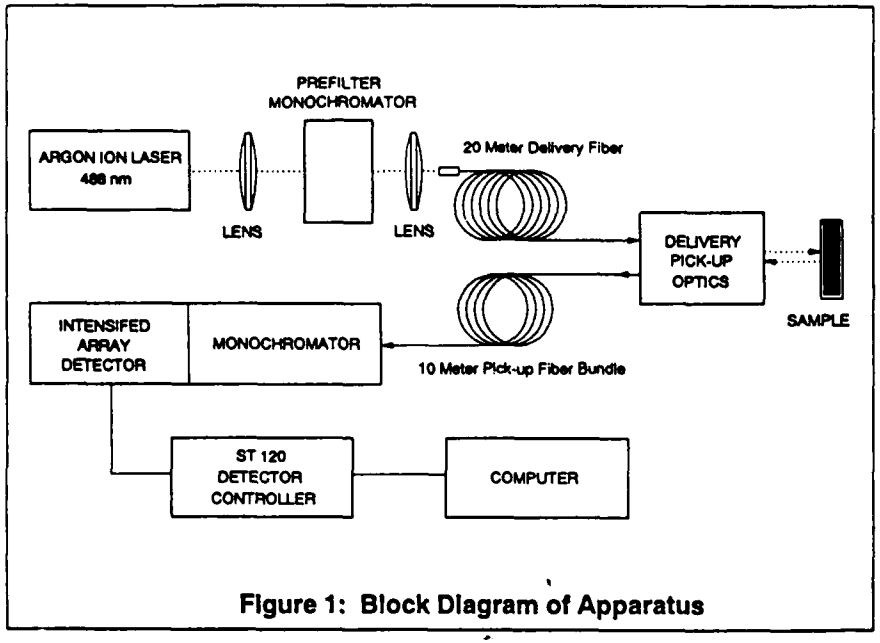

Figure 1: Block Diagram of Apparatus

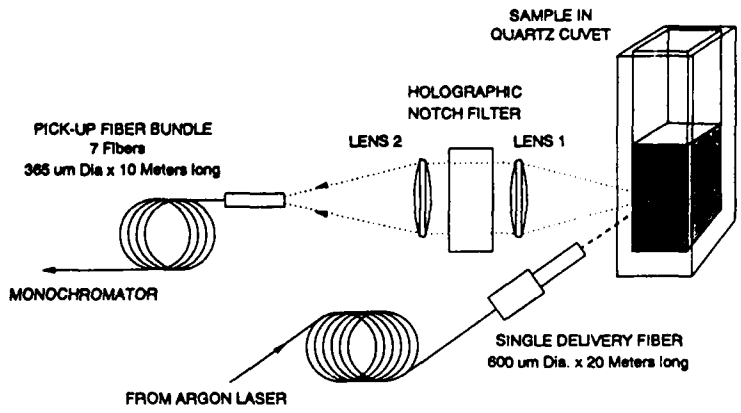

Figure 2: Delivery and Pick-up Optics

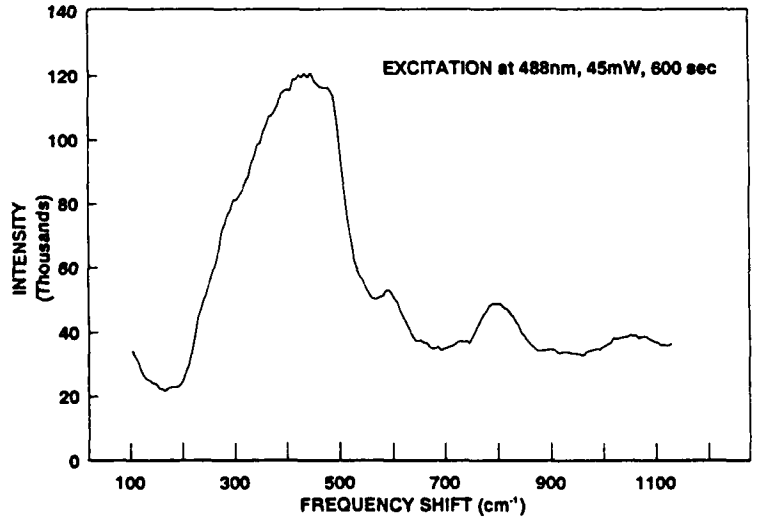

Figure 3: Uncorrected Raman Spectrum of 1% Disodium Phosphate Solution

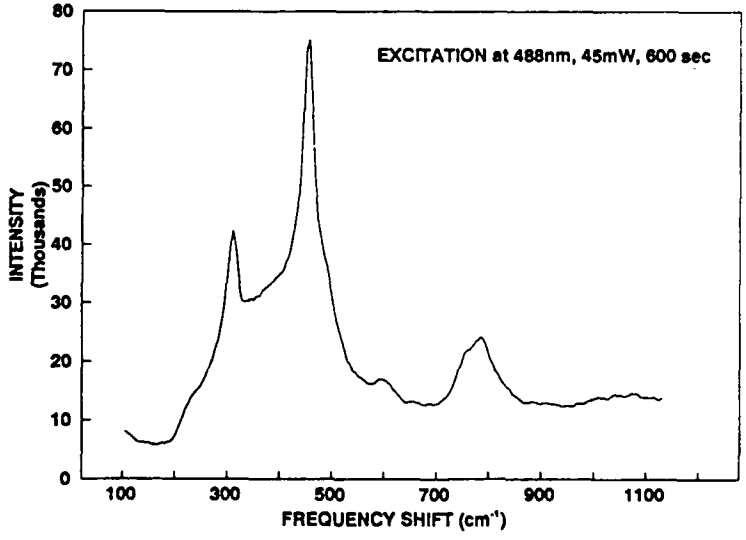

Figure 4: Uncorrected Raman Spectrum of CCl_4

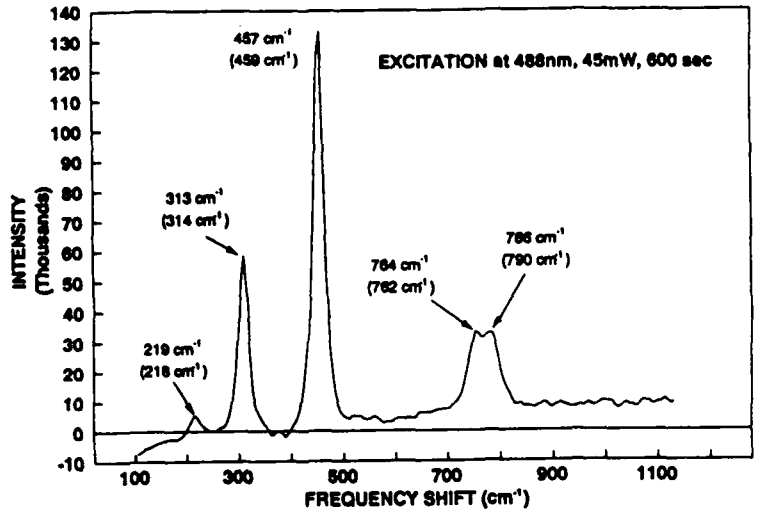

Figure 5: Raman Spectrum of CCl_4 After Subtraction of Fiber Background

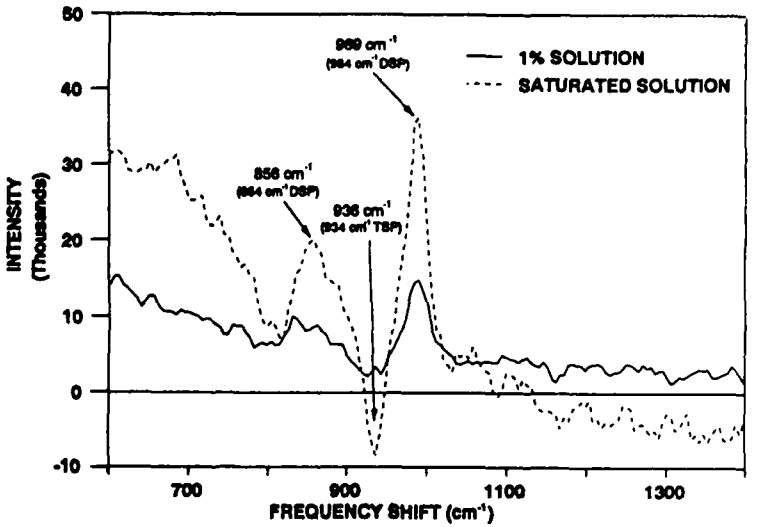

Figure 6: Difference Spectrum, Disodium Phosphate - Trisodium Phosphate

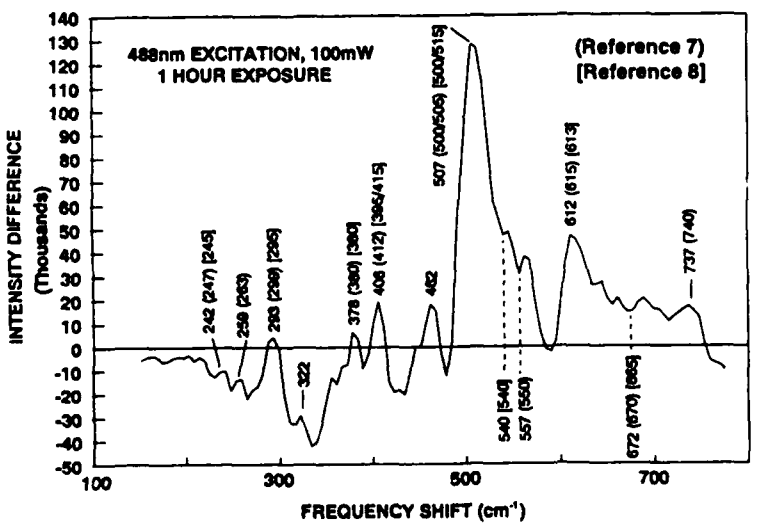

Figure 7: Difference Spectra, Fe_2O_3 - Fe_3O_4

Surface Enhanced Raman Scattering as an In-Reactor Monitor of Phenomena of Interest to the Nuclear Power Industry.

T.M. Devine
Department of Materials Science and Mineral Engineering
University of California
Berkeley

Overview

Surface enhanced Raman spectroscopy (SERS) is proposed as a technique for monitoring *in situ* the passive films and corrosion products that form on the surfaces of alloys of interest in nuclear power plants. The technique is a highly sensitive procedure for detecting even very small quantities of species present on surfaces, in particular the surfaces of metallic alloys. The data could, for example, identify the constitutents in passive films that are less than a monolayer in average thickness. Processes such as ^{60}Co pick-up could be monitored in real time. In fact, if it is known that incorporation of ^{60}Co occurs when a particular oxide film forms on the surface of the alloy, then measurement of the SER spectra could indicate when such films are beginning to form and thereby provide an early indication that conditions inside the reactor are now suitable for ^{60}Co pick-up in the passive films.

Raman Spectroscopy

Raman scattering is an inelastic light scattering process. When a monochromatic beam of light, such as that provided by an optical laser, is made incident on a transparent material the frequency of a small fraction of the scattered light is shifted as a result of interaction with a molecule whose polarizability is changing with time on account of molecular vibrations. The change in frequency of the light is numerically equal to the vibrational frequency of the scattering substance. If it has more than one vibrational mode, then there will be more than one peak in the Raman spectrum (which plots intensity of the scatterd light as a function of its difference in frequency with respect to the incident light). Thus, the Raman spectrum can act as a "fingerprint" in identifying an unknown substance. Not every vibrational mode is Raman active, however, there are well-known selection rules obtained by Group Theory. If the symmetry (space group for crystals and point group for individual molecules) of the material is known then the number of Raman active modes and their symmetries are readily determined. In fact, for most common species, including various oxides, hydroxides and oxyhydroxides of metals such as iron, chromium, nickel, etc., the Raman spectra have already been determined and are compiled in various atlas'.

One of the more attractive features of Raman spectroscopy is that it utilizes optical radiation which is, of course, transmitted by most aqueous solutions. Consequently, it is possible to obtain the Raman spectrum of a passive film or corrosion product as the sample sits in the solution. It is thus possible to use Raman spectroscopy to continuously monitor the films that form on metals and alloys immersed in aqueous solutions. The major shortcoming of Raman spectroscopy is that it is an extremely weak phenomenon. The Raman scattering cross-section of a typical material is approximately 10^{-10} smaller than its infrared absorption cross-section. This makes it extremely difficult and, in the absence of sophisticated optical equipment, practically impossible to obtain the Raman spectrum of very small quantities of material such as a thin passive film immersed in an aqueous solution. This obstacle has been overcome through the use of surface enhanced Raman scattering (SERS).

When certian metals are illuminated by an optical laser, collective electron surface oscillations called surface plasmons are excited. The only metals that are capable of this and which are relatively stable in an aqueous solution are silver, copper and gold. The usefullness of surface plasmons lies in the intense electric field that accompanies these charge density waves. The strength of the electric field falls exponentially with distance from the metal surface with a characteristic distance ≈ the wavelength of the incident radiation. The net result is that the optical field of the incident laser close to the metal surface is magnified by many orders of magnitude. As a result, the intensity (which is proportional to the square of the electric field strength) of the Raman scattered radiation from species close to the metal surface is greatly enhanced. This has enabled the measurement of the vibrational Raman spectra of species adsorbed on surfaces of silver, copper and gold. It is also important to note that surface plasmons on smooth surfaces of silver, copper and gold can not couple with photons incident through air or water because it is not possible to simultaneously satisfy momentum and energy conservation. If, however, the metal surface is suitably rough, then the momentum of the photons is lowered through the grating effect and the incident light will excite the surface plasmon. The use of SERS to obtain the vibrational spectra from species present on the surfaces of metals, other than roughened surfaces of silver, copper and gold, while they are immersed in aqueous solutions and corroding or forming passive films or reaction products has been achieved by a relatively simple idea. Small particles (≈ 50 nm diameter) of silver are deposited onto the surface of interest, for example, stainless steel, and are spaced a distance apart ≈ 600 nm. These particles then act as Raman antennae and enhance the optical field on the surface of the metal of interest. This technique, for example, was able to provide detailed information of the ≈2 nm thick passive film formed on iron in aqueous borate buffer (pH 8.4). Of course, it is necesary that the presence of the silver particles *not interact galvanically with the alloy under investigation.* This has been ensured by performing the experiments while controlling the potential of the alloy (and, of course, the silver particles) with a potentiostat. Since the potential of the composite surface is fixed there is no galvanic effect between the alloy and silver. In addition, the tests are performed at potentials below the local equilibrium potential for oxidation of the silver so that the silver itself is not oxidized during the experiments. Thus the silver particles act as electrochemically inert, Raman antennae and enhance the Raman spectra of species close to the surface of the alloy under study without affecting the corrosion or film-forming processes.

Uufortunately, the aqueous solution of interest in nuclear power plants is very high purity water which has a high resistivity that prevents the use of a potentiostat to control the potential. Thus, silver particles would galvanically couple with the alloy and thereby alter its corrosion behavior. To circumvent this difficulty and to produce a sample that could be used in high temperature, high purity water, a different approach has bee taken. The new sample consists of a roughened surface of silver that is coated with a thin layer of the alloy of interest. The layer must be thin enough to permit sufficient intensity of laser light to reach the silver interface. The layer must also be thick enough to have surface properties (such as corrosion rate, passivation characteristics, etc.) that simulate those of macroscopically thick quantities of the alloy. Results suggest that layer thicknesses on the order of 10 nm satisfy these requirements. In order to assure that the thin layer has the same chemistry as macroscopic quantities of the alloy, the layers were deposited onto the silver surface by laser ablation. The composition of these layers (Fe, Ni and Cr contents) were then measured by Auger Spectroscopy and shown to be identical to the composition of the bulk material from which they were formed. In this study layers of 304 stainless steel were evaluated.To verify the ability to measure the Raman spectra of thin quantities of material present on the surface of the stainless steel, the samples were immersed in an aqueous solution of 0.1M KCl + 0.05M pyridine. The

surface enhanced Raman spectrum of pyridine adsorbed on the surface of stainless steel was then measured.

Thus, in reactor studies samples of any alloy of interest will be laser ablated onto roughened substrates of silver. These will then be inserted into an autoclave which is connected to the reactor via a bypass line and their Raman spectra can either be measured continuously or intermittantly.

Description of Apparatus

In brief, samples are produced by laser ablating 10 nm thick coatings of the alloys on roughened surfaces of silver. In principle the size of a sample does not need to be limited to within a narrow range. Then samples must be at least 1 mm in diameter in order to present a reasonable size area for measurement. The maximum size of the sample is primarily limited by the size of the autoclave. In practice, flat samples that are $\approx$ 1 cm in diameter have been found to provide a large enough surface area to accurately represent the behavior of the alloy and to easily be illuminated by the laser while, at the same time, being small enough to fit inside a small and relatively inexpensive autoclave. The samples are positioned inside an autoclave that is connected via a bypass line to a particular region of interest inside the power plant. Practically speaking, the autoclave can be as small as one with a 100 ml internal volume or larger. It is fitted with 2 optically transparent windows. Preliminary results suggest that saphire windows will have sufficient corrosion resistance to enable their use. In the event that the corrosion rate of saphire in 288°C water is too high to permit their use over longer periods of time than have been used to date, then their inner surface would be coated with a 10 nm thick deposit of gold.

During operation of the surface enhanced Raman facility the samples positioned inside the autoclave are irradiated with an optical laser such as a krypton- or argon-ion laser. As discussed below in the description of Raman scattering a very small fraction of the incident laser beam will be inelastically i.e., Raman, scattered. Most of the Raman scattered light comes off the sample as a cone whose axis is perpendicular to the surface of the sample and which has an included angle of $\approx 60°$. This radiation then passes through the water that lies between it and the saphire window (perhaps ~1 cm of water), then through the saphire window where it is collected by a series of lenses and focussed into the entrance slits of a single monochromator where it is dispersed. Prior to entering the monochromator, the light passes through a notch filter that is centered at the wavelength of the incident laser radiation. The notch filter excludes light from entering the monochromator that is within ≈ 50 cm^{-1} on either side of the laser line. This protects the light-sensitive photon-counting device located at the exit slit of the monochromator from overexposure as well as improving stray-light rejection and signal-to-noise ratio. Either a photomultiplier or a charged diode array may be used to measure the intensity of the dispersed, Raman scattered light that exits from the monochromator. The charged diode array is able to provide a measured spectrum much faster than is possible with the use of a photomultiplier tube and is the device of choice for this application. Complete spectra of passive films and corrosion product layers on a given sample can be generated in the order of minutes.

Equipment Costs

Depending on the power required, optical lasers can be purchased for under $15,000. A single monochromator with gratings and optical multi-channel analyzer can be obtained for approximately $25,000. The cost of the notch filter is approximately $500. Additional lenses and mirrors for focusing the laser on the sample and for collecting the scattered light would cost approximately $500. The cost of a saphire

window (2 required per autoclave) is ≈ $200. The cost of the autoclave depends, of course, on its size and material of construction. A 250 ml, 304 stainless steel autocalve with 2 saphire windows and feed throughs for solution inlet and outlet, measuring thermocouple, reference electrode, counter electrode as well as a sample feed-through would cost ≈ $5,000. For a Hastalloy C autoclave the cost is approximately double. Hence, the total cost of the system, excluding the cost of installing the by-pass line and the relatively inexpensive costs associated with the fabrication of samples is $46,000.

A New Contact Electric Resistance Technique for In-Situ Measurement of the Electric Resistance of Surface Films on Metals in Electrolytes at High Temperatures and Pressures

T. Saario and V. A. Marichev
Technical Research Centre of Finland
Metals Laboratory, P. O. Box 26
SF-02151 Espoo, Finland

Abstract

Surface films play a major role in corrosion assisted cracking. A new Contact Electric Resistance (CER) method has been recently developed for in situ measurement of the electric resistance of surface films. The method has been upgraded for high temperature high pressure application. The technique can be used for any electrically conductive material in any environment including liquid, gas or vacuum. The technique has been used to determine in situ the electric resistance of films on metals during adsorption of water and anions, formation and destruction of oxides and hydrides, electroplating of metals and to study the electric resistance of films on semiconductors. The resolution of the CER technique is 10^{-9} Ω, which corresponds to about 0.03 monolayers of deposited copper during electrochemical deposition Cu/Cu^{2+}.

Electric resistance data can be measured with a frequency of the order of one hertz, which enables one to follow in situ the kinetics of surface film related processes. The kinetics of these processes and their dependence on the environment, temperature, pH and electrochemical potential can be investigated.

Introduction

Environmentally assisted cracking, e.g. stress corrosion cracking and hydrogen embrittlement, continues to be a significant issue to the power generation industry. In many cases it has been found that electrochemical potential and pH play the key role in determining the degradation of structural materials. This has resulted in increasing demand for sensitive and reliable in situ monitoring techniques both for laboratory investigations and for in-plant measurements.

In this paper a new Contract Electric Resistance (CER) technique is described. The CER-technique has been used to determine in situ the electric resistance of films on metals during adsorption of water and anions, formation and destruction of oxides and hydrides, electroplating of metals[1-3] and to study the electric resistance of films on semiconductors. In some cases this method has been shown[1] to be more sensitive to adsorption and oxidation phenomena than e.g. scanning tunnelling microscopy or surface enhanced Raman spectroscopy, and it overcomes many of the problems encountered in applying the impedance measurement techniques. As an example of the applicability of the technique, results from an investigation of the oxidation behaviour of pure nickel and Inconel 600 in several simulated steam generator secondary side crevice water chemistries is discussed.

Contact Electric Resistance Technique

The Contact Electric Resistance (CER) method consists of accurate measurement of electric resistance between two periodically contacted metallic specimens. The measurement system is basically similar to the direct current potential drop (DCPD) technique used for measurement of crack length e.g. in corrosion fatigue tests. The CER method may be realized in two different ways: using a cyclically loaded (below corrosion fatigue crack growth threshold) single edge notched plate specimen with a fatigue precrack (Fig. 1a) or using two identical metallic samples periodically contacted in an electrolyte under potentiostatic control (Fig. 1b). The former method was used for stronger metals (Fe, Ni, Cu), and the latter method may be used for any metals including soft metals (Pb, Sn, Au) of which it is difficult to prepare the precracked specimen. Neither of the methods has any limitations connected with temperature or pressure of the environment.

In the first method[1,2], Fig. 1, the sample [1] of investigated metal (200 x 25 x 2 mm), with contacts (points AA) for measuring electric resistance of the central part of the sample, was coated with a chemically stable varnish, (except for an area of 0.5 to 1 cm^2 near the 3-4 mm long fatigue precrack. The sample was then placed in an electrochemical cell [2] under potentiostatic control [3] and fixed in electrically insulated grips of the Instron 1195 testing machine. During cyclic loading of the sample this machine provides an accuracy of 0.1 % in reproducibility of the maximum and minimum loads, which results in the reproducibility of the relative displacement of the contacting crack walls at the level of 10^{-9} m. A direct current (10 - 20 A) was passed through the sample from stabilized source [4] and variation of electric resistance of the sample during cyclic loading was measured by a double (Thompson) bridge [5] and continuously recorded by an amplifier [6] and a recorder [7]. Here, the precision of the direct current stabilizer and the double bridge employed for the measurement of electric resistance with the accuracy of up to 0.02 % and sensitivity of about 10^{-9} Ω are noteworthy.

The electrical analogue explaining the electric resistance variation of the sample with a crack at cyclic loading is given in Fig. 1c, where points AA indicate the points of current supply and switching of the double bridge. If there is no crack in the sample its electric resistance is equal to R_1. At maximum load of the cycle the crack is fully open and its walls do not contact each other, and the sample resistance increases by an amount of R_2 due to a corresponding decrease of its cross-sectional area. At minimum load the crack walls will contact each other, which is equivalent to shunting of the R_2-resistance by some effective constant electric resistance of R_3 and by contact electric resistance between the crack walls, R. For two separate metallic specimens (Fig. 1b) electric resistance R_3 is equal to the electric resistance of the connecting wires between contacting surfaces and the electric resistance of a resistance element, R_2. For the precracked sample the contact resistance R is equal to electric resistance of the successive layers: metal-film-electrolyte-film-metal between the crack walls. Thus, during cyclic loading the sample electric resistance changes from $R_1 + R_2$ at the maximum load to $R_1+[R_2\cdot(R_3+R)/(R_2+R_3+R)]$ at the minimum load. Load level is chosen so that the crack does not grow. The variation of the sample electric resistance during each loading cycle ΔR_1 is determined by the expression (1) and the contact electric resistance measured at the minimum load of the cycle R by the expression (2):

$$\Delta R_1 = R_2^2 / (R_2 + R_3 + R) , \qquad (1)$$

$$R = (R_2^2 / \Delta R_1) - R_2 - R_3 . \qquad (2)$$

These equations are valid also for periodically contacted separate specimens (Fig. 1b). The method applying separate specimens differs from that applying a precracked specimen by using an additional shunting electric resistance R_2 which is an analog of the electric resistance R_2 of precracked specimens and has a value of about 0.05 - 100 mΩ depending on the metal and/or oxide studied.

The reproducibility of relative displacements of cyclically contacting surfaces has been maintained at the level of 1 nm for both methods. For separate specimen this accuracy has been reached by use of a specially designed combination of soft and stiff springs loaded by a precise step motor. The design for high temperature applications up to 300 °C is shown in Fig. 2a. Two stiff frames are fixed on the autoclave head [1]. The first frame [2] supports the step motor [3] with the pull rod [4] passing into the autoclave volume through a seal [5]. The second frame [6] supports the special designed stiff spring [7]. Insulating holders [8] with specimens [9] are fixed in the stiff spring by screws. Connecting wires [10] pass through the autoclave head and are connected to the electric resistance R_2 and to the double bridge (Fig. 1b). The stiff spring [7] is cyclically loaded by the step motor [3] through the soft spring [11]. Such a loading system eliminates the effects of friction and the high internal autoclave pressure upon the deformation of both springs and the replacement of contacting surfaces of the samples. Calibration of the system has shown that each step of the step motor resulted in displacement of the contacting surfaces by about 1 nm.

All the components of the CER autoclave unit are made of stainless steel AISI 316, except the specimen holders (Fig. 2b), which are made of Zircaloy 4 oxidized at 550 °C for 48 h in air. In Fig. 2a and b some vital dimensions are shown, which make it possible to have a clear impression of the stiffness of all structural elements of the high temperature CER unit.

The experiments were performed first by measuring electric resistance of samples with a fatigue precrack in alkaline solutions of 0.1 - 1 M KOH at the free corrosion potential. Cyclic loading with a frequency of about 0.2 Hz and zero stress ratio (the ratio of minimum and maximum loads) was used. Fig. 3 represents the general behaviour of all investigated metals and alloys in terms of electrochemical potential dependence of the electric resistance of either samples with fatigue precrack or separated samples at any temperatures investigated in the range of 20 - 300 °C. The symbols referred to in the following are explained in Fig. 3. From the beginning of the cyclic loading, some time (10 - 30 min) is necessary for the stabilization of ΔR_1-values at the free corrosion potential E_{oc}. After this stabilization at moment t_1, the potential is potentiostatically changed to E_{RD} (normally from -1.1 V_{SHE} to -1.5 V_{SHE}), which is negative to the hydroxide equilibrium potential of the corresponding metal. During the first loading cycles, ΔR_1 sharply increases and then stabilizes after 5 - 20 min. Furthermore, the ΔR_1 dependence on potential was studied by varying the potential stepwise in 0.1 V increments after an exposure of 2 - 5 min at each potential. The potential shift towards the negative direction did not lead to any further change of ΔR_1. The same was true for the potential increase up to a certain value for each metal. The further increase of potential by 0.1 V at the moment t_2 induced a decrease of ΔR_1. Generally, this decrease of ΔR_1 occurred directly after switching the potential E_{ox1} (close to the hydroxide formation potential for each metal) and was gradually attenuating. The further increase of potential at the moments t_3 (E_{ox2}) and t_4 (E_{ox3}) lead to a decreasing ΔR_1 down to considerably lower values than the initial value at the free corrosion potential. The cathodic polarization at the moment t_5 to the potential E_{RD} causes an increase of ΔR_1 up to the previous maximum value. It seems that the variation of ΔR_1 in the potential region E_{ox1} - E_{ox3} reflects the kinetics of

formation and growth of films on crack walls at each potential while at the potential E_{RD} the kinetics of film reduction is observed.

The contact electric resistance (R) is independent of the ionic electrolyte conductivity, but is defined by electronic conductivity between the contacting surfaces. R is assumed to be zero at the most complete reduction of the films on the contacting surfaces during cathodic polarization. Any increase in the R obtained by polarization to more positive potentials is due to an increase of the electric resistance of the films on the contacting surfaces. The changes in the cyclic loading frequency (0.04 - 0.4 Hz) and direct current value through the specimens (0.03 - 30 A) do not have a noticeable effect on the dependence of the electric resistance on the potential. However, the changes in minimum and/or maximum loads or stress ratio of the cycling loading do have an effect on this dependence.

Although from equation (2) the film resistance R can be readily calculated, in the following several other equations are given, which help in understanding particularly the role of the resistances R_2 and R_3. As it is clear from Fig. 3, $\Delta R_{max} = \Delta R_1 + \Delta R_2$, where ΔR_1 is the difference between the maximum and minimum of the electric resistance of the sample during each loading cycle, and ΔR_2 is the difference between minimum electric resistance (when R = 0 at the most cathodic potential) and the minimum of the electric resistance of the sample during the particular loading cycle. Using this formula and the electric analog scheme in Fig. 1c, the following equations (3, 4, 5 and 6) may be arrived at. These equations are convenient in calculating the contact electric resistance, R, and to evaluate the optimum values of the resistances R_2 and R_3 in dependence upon the main target of the investigation. These equations also help in choosing between precracked and separated specimens (Fig. 1a, b) in particular cases. Both R_2 and R_3 are kept constant during each experiment. For R_3 one arrives at an equation,

$$R_3 = R_2 \cdot (R_2 - \Delta R_{max})/\Delta R_{max} = \text{const.} \tag{3}$$

and for film resistance R

$$R = (R_2 + R_3) \cdot \Delta R_2/\Delta R_1 = (R_2^2 \cdot \Delta R_2)/(\Delta R_{max} \cdot \Delta R_1). \tag{4}$$

For very thin oxide and/or adsorption films $\Delta R_1 \rightarrow \Delta R_{max}$, and from equation (4) it follows:

$$R \cong (R_2/\Delta R_{max})^2 \cdot \Delta R_2. \tag{5}$$

This means that in order to reach the maximum sensitivity of the CER method (at the level of 10^{-9} Ω) it is necessary to diminish as much as possible the electric resistances R_2 and R_3. The best way to do this is to use the precracked specimens.

For very thick oxide films $\Delta R_2 \rightarrow \Delta R_{max}$ and the following holds:

$$R \cong R_2^2 / \Delta R_1 \tag{6}$$

Thus the maximum film resistance that can be measured depends on R_2. By using separate specimens R_2 can be chosen to be between 0.05 - 100 mΩ. The use of either a precracked specimen or separate specimens provides the possibility to measure in situ the films resistivity for any metallic material from 10^{-9} up to 10^3 Ω.

Applications of the CER method

As an example of the measurement of extremely low electric resistance of the films using precracked specimens, Fig. 4 shows the potential dependence of the films on silver in alkaline electrolytes at room temperature. Four potential regions (I - IV) with different characteristics can be seen. In the first region ($E < -1.1$ V) intensive hydrogen evolution takes place, as well as adsorption and absorption of hydrogen. Adsorption of water and cations is also possible, but at KOH concentrations lower than 3 M, the electric resistance of the films does not exceed the sensitivity of measurements (curves 1 - 5). In the case of metals such as Ni, Sb, and Pb, in the first potential region there is some increase of the electric resistance connected with the hydride formation[1,2].

In the second potential region $-1.1\ V < E < -0.55$ V, R increases with the potential independently of pH-value. Possibly, in this region R is defined by the processes of water interaction with the Ag-surface, while in the potential region III R increases with the hydroxyl-ion concentration, reflecting their adsorption on Ag-surface. The higher the pH-value is, the higher R is for any potential in the potential region III. It was shown[1,2] that hydroxyl-ions do not adsorb on Ag at potentials more negative than -0.6 V, which corresponds to the beginning of the third region. Smooth increase of R in the potential region III (Fig. 4) is replaced by sharp increase of R, when the potentials of the beginning of the region IV are reached. For Ag, Cu, Fe, Ni, Zn, Cd and other six investigated pure metals it was experimentally proven[1,2] that these potentials were very close (within ± 0.02 V) to the equilibrium potentials of hydroxide formation of corresponding metals in alkaline electrolytes as shown in Fig. 5. The possible application of the CER method connected with these examples are the following: in situ investigations of the interaction of the metals and alloys with solvents, hydride and oxide formation and destruction depending upon the potential, estimation of the oxidation potentials of the alloys at room and high temperatures, investigation of anions and/or inhibitors adsorption in dependence upon the potential.

The following examples demonstrate the application of the CER method in high temperature and high pressure conditions using separate specimens of nickel and Inconel 600 (Figs. 6 to 9). The surface film resistance of Inconel 600 in a simulated steam generator crevice environment is shown in Fig. 6. The main result of this experiment was that there is no stable film on the surface of Inconel 600 in this 1 M caustic environment at 300 °C at open circuit conditions. However, when polarized anodically about 0.14 V, a passive film forms on the surface. This result in an accord with the result of Lumsden[4] for the same material in 50 % NaOH at 320 °C. He found that there is no stable film at open circuit conditions, but when polarized anodically about 0.15 V, a passive film forms on the surface. He also found that IGSCC occurred only above the potential at which the film formation first took place. Fig. 7 shows the kinetics of repassivation of nickel in 1M NaOH with boric acid. Both nickel and Inconel 600 have stable passive films at 300 °C in the presence of boric acid at open circuit potential.

Figure 8 shows a comparison of results of the passivation rates of Inconel 600 and pure nickel in 1 M NaOH presented as an Arrhenius plot. From this figure it is seen that the activation energy for repassivation of the both materials is about the same, roughly 10 $kcal*mol^{-1}$. However, the repassivation rate of Inconel 600 is two orders of magnitude higher than that of pure nickel. Based on the results we conclude that both the oxidation behaviour (equilibrium potentials and growth kinetics) and the electric resistance of the oxides on pure

nickel and Inconel 600 are different, and thus pure nickel should not be considered as a modelling material for Inconel 600.

Hydrogen is proposed to have a detrimental effect on IGSCC of Inconel 600 in PWR primary water. Hydrogen shifts the open circuit potential of the alloy in the negative direction, possibly resulting in changes in passive film properties and/or oxidation kinetics. In this work it was found that hydrogen overpressure retarded the oxidation of Ni and Inconel 600 only slightly in all the investigated conditions, and never completely prevented oxidation, which depended mainly upon the electrochemical potential (Fig. 9). However, at higher temperature, the addition of hydrogen changes the open circuit potential to such a level that the oxide films were reduced. At temperatures above about 250 °C the open circuit potential decreased even without hydrogen addition to a level at which oxides grown under potentiostatic control at higher potentials were reduced when open circuit potential was applied.

Discussion

Because surface film stability is so important a factor with regard to occurrence of stress corrosion cracking (SCC), factors that affect the surface films can have strong influences on the occurrence and rate of SCC. A major focus for both primary and secondary side SCC of PWR now involves investigation of the effects of elements that tend to be incorporated into and stabilize the oxide films that form on alloy 600. The CER technique provides in situ information on the stability and kinetics of changes of surface films. The technique has already been used to investigate the effect of candidate inhibitors on the surface film resistance of alloy 600 in PWR secondary side crevice environments.

In highly reducing environments, such as PWR primary water and BWR water with hydrogen water chemistry, the hydrogen oxidation-reduction reaction is the major electrochemical reaction occurring on the metal surfaces. This reaction, with a high exchange current density, fixes the corrosion potential to the potential of the reversible hydrogen electrode, RHE. Any electrochemical measurement, based on the measurement of current, carried out close to the corrosion potential is severely disturbed by the hydrogen reaction. However, the CER technique, which is based on direct measurement of the contact electric resistance of the surface film, can be reliably used even in these reducing environments.

The CER equipment shown in Fig. 2 is designed for laboratory use. For plant monitoring purposes another model has been developed, which has a 60 mm external diameter. From the point of view of a power plant engineer, reasons for using the CER equipment for monitoring purposes are equal to reasons for using electrochemical monitoring equipment. From our experience on high temperature water chemistry measurements at Loviisa PWR primary loop, the high temperature in situ measurement techniques have proved to be most valuable during transients and shutdown or start up periods.

The CER technique can be used also in non-aqueous environments, such as dry steam or exhaust gas. The equipment contains no aggressive chemical species. The CER equipment is commercially available from Cormet Ltd, Finland.

Conclusions

The new Contact Electric Resistance (CER) method for in situ investigation of the metals in electrolytes was described in details. The main applications of this method at room and high temperatures were discussed. Experimental data was presented for demonstration of the sensitivity and possible applications of the CER method.

Acknowledgements

This work was carried out at the Technical Research Centre of Finland (VTT) and was funded by the Ministry of Trade and Industry in Finland through the Nuclear Power Plant Structural Integrity Research Programme. Additional funding from the Academy of Science of Finland is acknowledged.

References

1. V. A. Marichev, Surface Science, 250 7 (1991): p. 220.

2. V. A. Marichev, Soviet Material Sci., 26 1 (1990): p. 8.

3. T. Saario, V. A. Marichev and H. Hänninen, Proceedings of the 12th Scandinavian Corrosion Congress and EUROCORR'92. Ed. P. J. Tunturi. Fincorr, 2 (1992): p. 169.

4. J. B. Lumsden, EPRI, IGA/SCC Workshop. San Antonio, TX, December 8 - 10 (1992).

metåå/rap2/592k.tjs

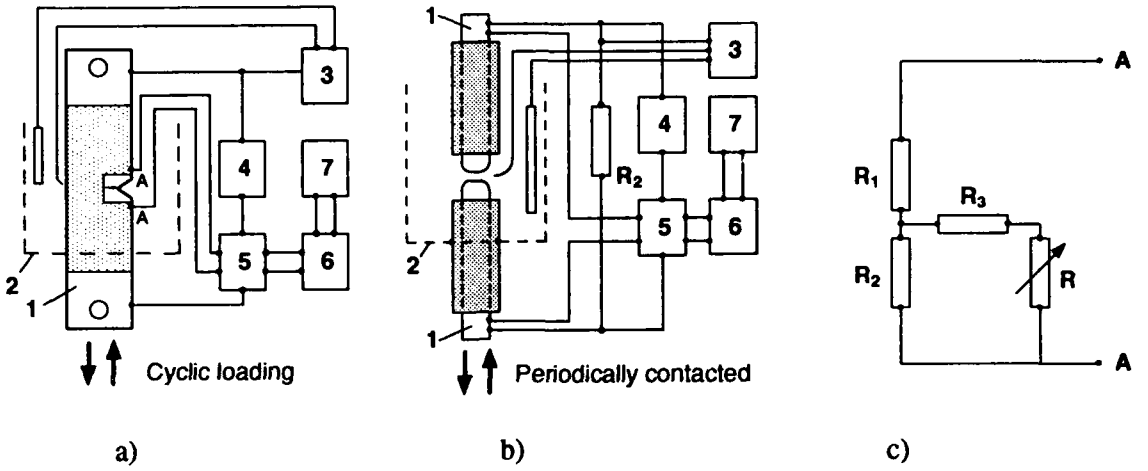

Fig. 1. Scheme for measurement of the Contact Electric Resistance (CER) of the sample with a fatigue precrack (a) and two identical periodically contacted samples (b). The electrical analog of the CER of the samples in both schemes (c). [1] Sample, [2] electrochemical cell, [3] potentiostat Wenking Model LB 81 M, [4] direct current source Hewlett Packard 6033A, [5] double bridge P329, [6] dc amplifier Yokogawa 3131, [7] recorder Yokogawa LR 4220.

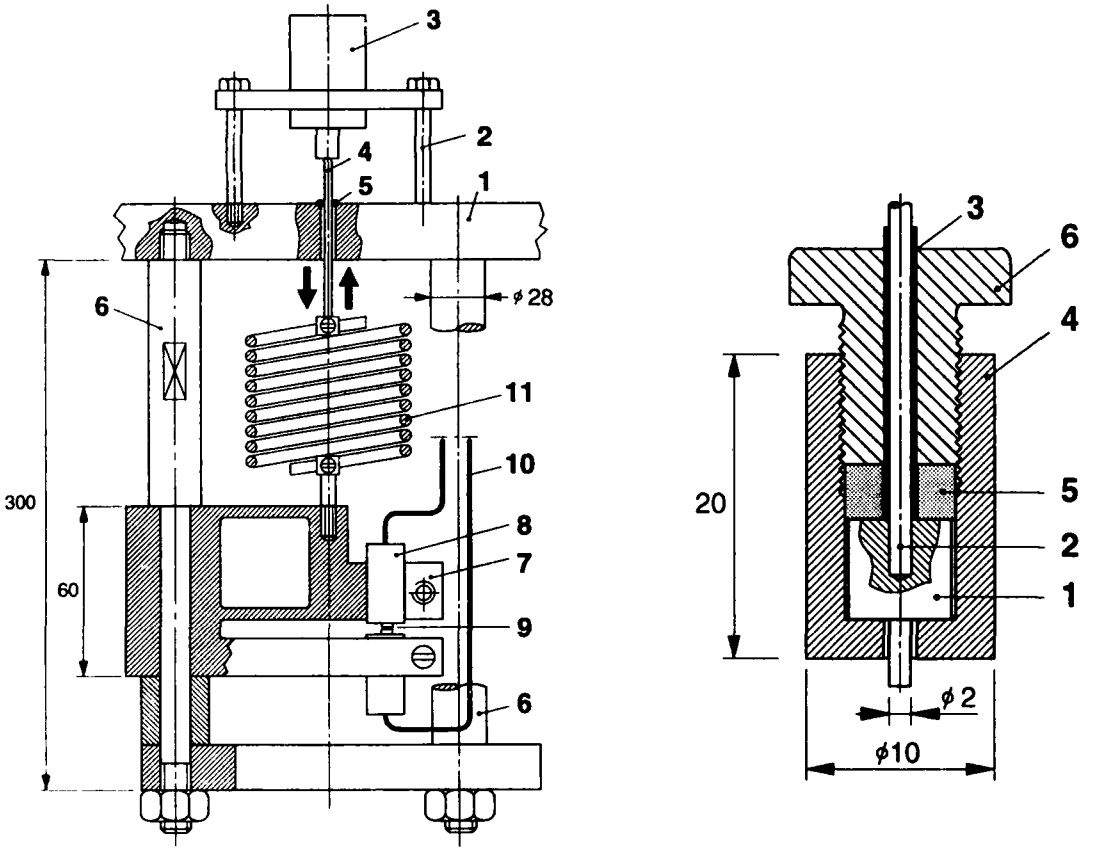

Fig. 2. Scheme for measurement of the CER at high temperatures and pressures (a). [1] autoclave head, [2] supporting frame, [3] step motor, [4] pull rod, [5] seal, [6] supporting frame, [7] stiff spring, [8] specimen holder, [9] specimen, [10] connecting wires, [11] soft spring. Specimen holder with fixed specimen (b). [1] specimen, [2] silver connecting wire, [3] insulation, [4] Zr holder, [5] Zr-ring, [6] Zr screw.

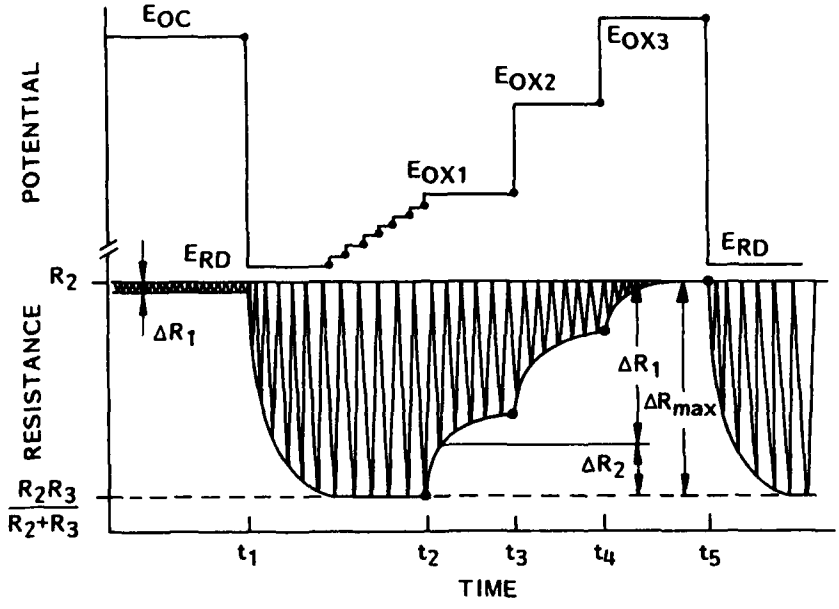

Fig. 3. The schematic potential-time-dependence of electric resistance of the samples. E_{RD} -the potential during reduction of the film, E_{ox} - the potentials during oxidation of the sample. Explanations are in the text.

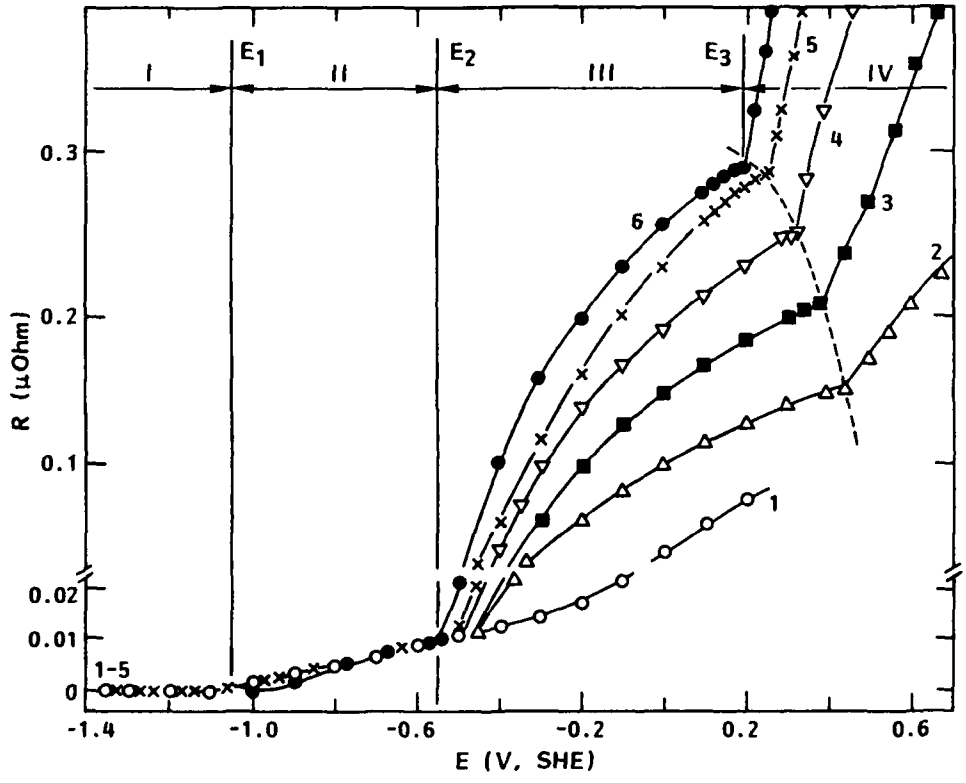

Fig. 4. The potential dependence of the film electric resistance on the crack walls of a silver specimen in KOH solutions: (1) pH 7, (2) 0.001, (3) 0.01, (4) 0.1, (5) 1.0, (6) 10 M KOH. Stress ratio = 0.3.

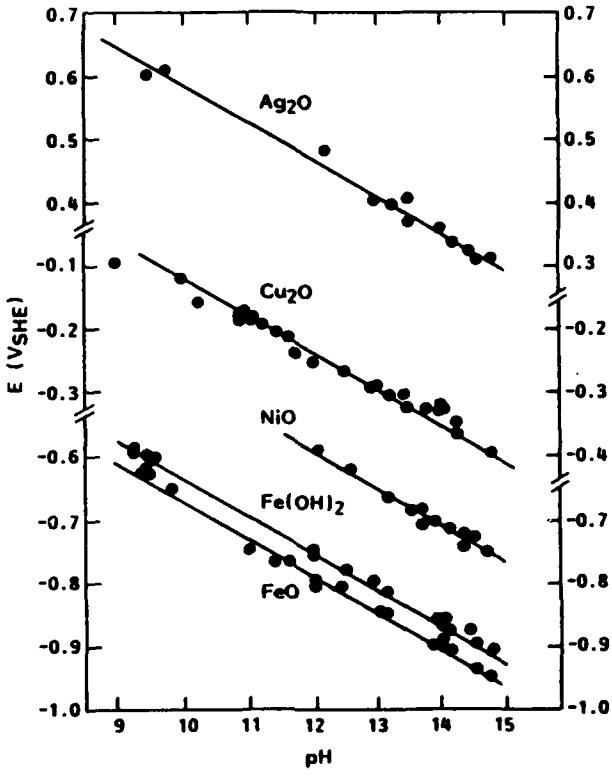

Fig. 5. Oxidation potentials in alkaline electrolytes of Ag, Cu, Ni and Fe measured by the CER-method (black points) and theoretical equilibrium oxidation potentials for the same metals (the lines) at room temperature.

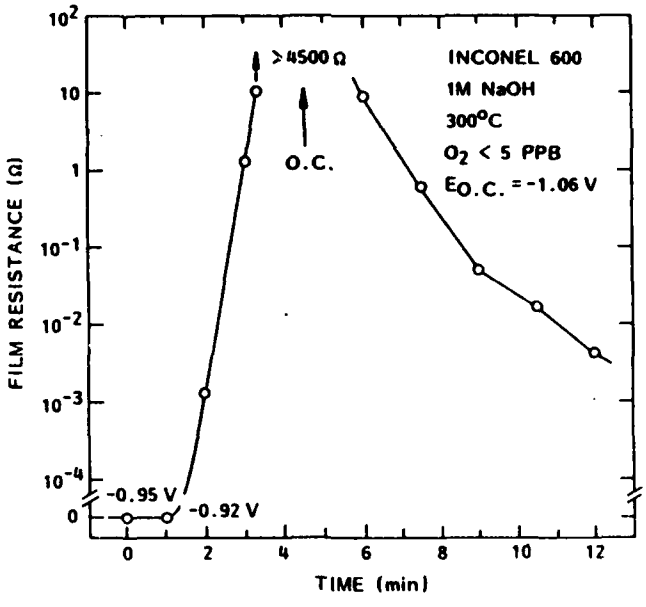

Fig. 6. The electric resistance of the surface film on Inconel 600 as a function of time at 300 °C in 1M NaOH solution. The specimen was first polarized to -1.0 V_{SHE} to reduce the films, then to -0.95 V_{SHE} with no increase in the electric resistance and then at time 1 minute to -0.92 VSHE. At this potential the resistance starts to grow and increases to more than 4.5 kΩ in 3 minutes (4.5 kΩ was the upper limit for this run). After switching the polarization off at time 4.5 minutes (marked by arrow + O.C.), reduction starts and the resistance falls down to $3*10^{-3}$ Ω in 8 minutes. After switching off the polarization the open circuit potential stabilizes very quickly to -1.06 V_{SHE}.

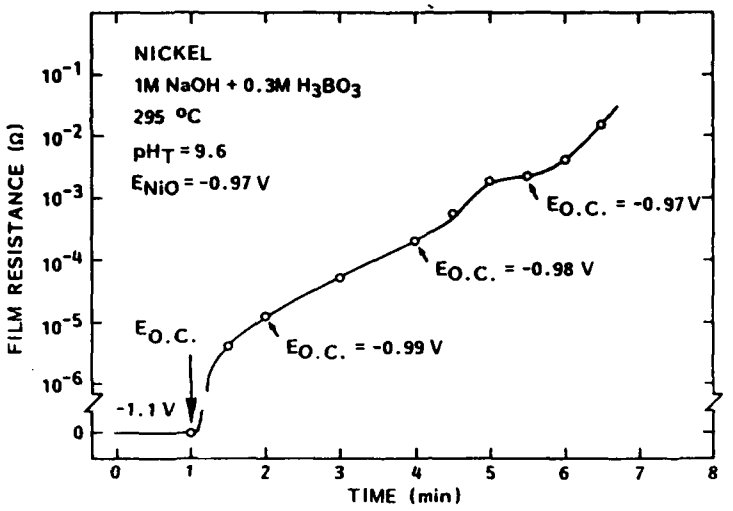

Fig. 7. The electric resistance of the surface film on Ni as a function of time at 295 °C in 1M NaOH + 0.3M H_3BO_3 solution. The specimen was first polarized to -1.1 V_{SHE} to reduce the films. At time 1 minute polarization was switched off. Oxidation starts and the film resistance increases to $1.5*10^{-2}$ Ω in 5.5 minutes.

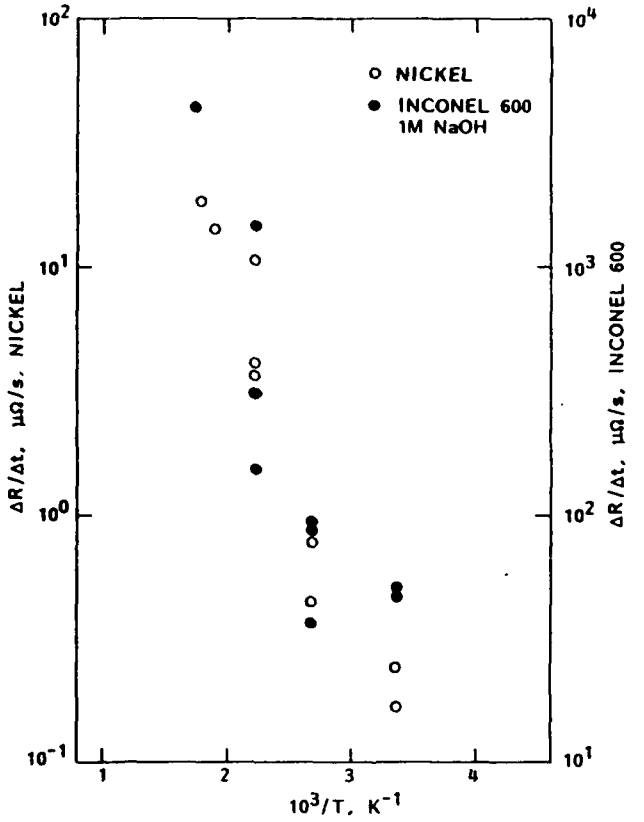

Fig. 8. The rate of change of the surface film electric resistance as a function of T^{-1}. The rate was measured in the following way. After reducing the previous films by cathodic polarization the potential was increased (to anodic direction) by steps of 25 mV. The rate for the potential at which the absolute resistance increased steadily was taken as the value for this figure. Thus the external driving force for oxidation at different temperatures was roughly equal. Note that the absolute values for Alloy 600 are roughly two orders of magnitude higher than those for pure nickel. The apparent activation energy is 10 kcal/mol for both materials. This activation energy is considered to represent the growth of the first monolayers of the surface film.

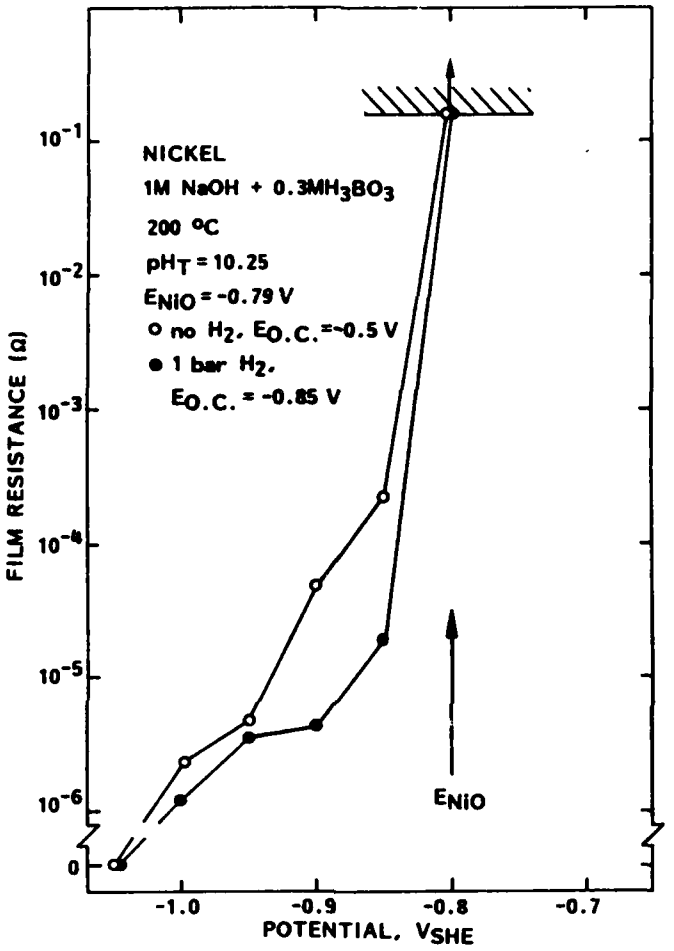

Fig. 9. The electric resistance of the surface film on Ni as a function of the electrochemical potential at 200 °C in 1M NaOH + 0.3M H_3BO_3 solution. Open circles denote the run without hydrogen, closed circles denote 1 bar hydrogen overpressure. The open circuit potentials were -0.5 V_{SHE} without hydrogen and -0.85 V_{SHE} with hydrogen. Hydrogen overpressure is seen to change the potential at which oxidation starts with roughly 50 mV (comparison based on the level 10^{-4} Ω).